

Technical Documentation for the Framework for Evaluating Damages and Impacts (FrEDI)

APPENDICES

CONTENTS

APPENDIX A INFORMATION QUALITY AND PEER REVIEW PROCEDURES.....	A-1
A.1 Ensuring Information Quality.....	A-1
A.2 Consideration of Assessment Factors	A-3
A.3 Review Process for the 2021 Technical Documentation	A-6
Public Review Period.....	A-6
Expert Peer Review	A-6
A.4 Review Process for the 2024 Technical Documentation	A-7
Public Review Period.....	A-8
Expert External Peer Review	A-8
A.5 Review Process for the Supplement to the Technical Documentation	A-11
Public Review Period.....	A-12
Expert External Peer Review	A-12
APPENDIX B DETAILS OF SECTORAL IMPACT STUDIES.....	B-1
B.1 Sectoral Impact Category Data Overview	B-2
B.2 Health Sectors.....	B-5
Climate-Driven Changes in Air Quality	B-5
Extreme Temperature	B-14
CIL Temperature-Related Mortality	B-19
ATS Temperature-Related Mortality	B-23
Southwest Dust.....	B-28
Valley Fever.....	B-34
Wildfire	B-38

CIL Crime	B-43
Vibriosis.....	B-47
Suicide.....	B-50
Lyme Disease	B-54
B.3 Infrastructure Sectors	B-57
Coastal Properties.....	B-57
Transportation Impacts from High Tide Flooding	B-60
Rail	B-63
Roads	B-66
Asphalt Roads	B-70
Urban Drainage	B-73
Inland Flooding	B-76
Hurricane Wind Damage	B-79
B.4 Electricity Sectors.....	B-83
Electricity Demand and Supply.....	B-83
Electricity Transmission and Distribution Infrastructure	B-86
B.5 Ecosystems and Recreation Sectors.....	B-90
Water Quality.....	B-90
Outdoor Recreation	B-93
Winter Recreation.....	B-98
Marine Fisheries.....	B-102
Marsh Migration	B-105
B.6 Labor and Learning Sector	B-108
Labor	B-108
Learning Loss.....	B-111
B.7 Agriculture Sector	B-116
CIL Agriculture.....	B-116
Forestry Loss	B-120
APPENDIX C IMPACTS-BY-DEGREE AND TEMPERATURE BINNING METHODOLOGY	C-1
C.1 Impacts-By-Degree	C-1
C.1 Sensitivity to GHG emissions scenarios.....	C-5
C.2 Sensitivity to GCM selection and CMIP6 Recommendations	C-8
GCM Selection Criteria Details	C-9
Model Analysis Summary	C-13
Additional Recommendations for Using GCM Data in U.S. Climate Impact Analyses	C-15
APPENDIX D METHODS DETAILS.....	D-1
D.1 Global to CONUS Temperature Translation	D-1
D.2 Calculation of global mean sea level.....	D-2
APPENDIX E SOCIAL VULNERABILITY MODULE	E-1

E.1 Overview.....	E-1
E.2 Features of the module.....	E-1
E.3 Approach.....	E-3
E.4 Disproportionality, difference in risk calculation.....	E-4
E.5 Calculating impacts and rates by population groups.....	E-6
E.6 Demographic data.....	E-7
E.7 Outputs and Visualization	E-7
E.8 Comparison of FrEDI-SV to Underlying EPA (2021) SV Report.....	E-9
E.9 Guidance on interpreting results	E-11

APPENDIX F | CONCENTRATION-DRIVEN MODULE F-1

F.1 Overview and Background	F-1
F.2 Approach.....	F-2
F.3 Module Details and Underlying Data	F-3
Methane-Ozone Health.....	F-3
Methane Ozone Health Underlying Datasets	F-6
Methane Ozone Health - Additional Function Details	F-8
F.4 Running FrEDI-GHG	F-8
Inputs	F-8
Runtime Processes	F-10
F.4 Limitations and Uncertainty	F-14
F.5 Comparison of FrEDI-GHG to Underlying Studies.....	F-14
F.5 Guidance on Interpreting Results.....	F-16
Streamlined Policy Benefits Calculation	F-16

APPENDIX G | UPDATE REVISION LOG G-1

APPENDIX A | INFORMATION QUALITY AND PEER REVIEW PROCEDURES

A.1 Ensuring Information Quality

The FrEDI Technical Documentation, framework, underlying analyses, and associated R package were developed in accordance with EPA's *Guidelines for Ensuring and Maximizing the Quality, Objectivity, Utility, and Integrity of Information Disseminated by the Environmental Protection Agency*,¹ which follows Office of Management and Budget (OMB) guidelines² and implements the Information Quality Act (IQA) (Section 515 of Public Law 106–554).³

In accordance with OMB definitions, EPA defines the basic standard of information “quality” by its objectivity, integrity, utility, and transparency. For products meeting a higher standard of quality, like this product, the Agency requires an appropriate level of transparency regarding data and methods to facilitate the reproducibility of information by qualified third parties. The EPA uses various established Agency processes (e.g., the Quality System, peer review requirements and processes) to ensure the appropriate level of objectivity, utility, integrity, and transparency for its products, based on the intended use of the information and the resources available. Sections below describe how the technical documentation and associated R code meet each requirement.

Objectivity focuses on whether the disseminated information is being presented in an accurate, clear, complete, and unbiased manner, and as a matter of substance, is accurate, reliable, and unbiased. The technical documentation and associated R code meet this standard for objectivity, due to activities described in the following:

- a. The information disseminated is determined to be complete, accurate, and reliable based on internal quality control measures adopted by the expert modeling teams. This includes quality checks throughout the chain of analytic steps, including developing and processing climate projections, calibrating and validating the sectoral impact models, and checking data to ensure that no errors occur in the process to compile and summarize results. The FrEDI R code package also

¹ EPA, 2002: Guidelines for ensuring and maximizing the quality, objectivity, utility, and integrity of information disseminated by the Environmental Protection Agency. United States Environmental Protection Agency, EPA/260R-02-008. Available online at https://www.epa.gov/sites/default/files/2020-02/documents/epa-info-quality-guidelines_pdf_version.pdf.

² OMB, 2002: Office of Management and Budget Information Quality Guidelines. Executive Office of the President, Office of Management and Budget. Available online at https://www.whitehouse.gov/wp-content/uploads/legacy_drupal_files/omb/assets/OMB/inforeg/iqg_oct2002.pdf.

³ The IQA requires the Office of Management and Budget and federal agencies to issue guidelines that “ensur[e] and maximize[e] the quality, objectivity, utility, and integrity of information (including statistical information) disseminated by Federal agencies” (Public Law 106-554; 44 U.S.C. 3516, note). The IQA does not impose its own standard of “quality” on agency information; instead, it requires only that an agency “issue guidelines” ensuring data quality. Following guidelines issued by the Office of Management and Budget, EPA released its own guidelines to implement the IQA: “Guidelines for Ensuring and Maximizing the Quality, Objectivity, Utility, and Integrity of Information Disseminated by the Environmental Protection Agency.”

includes a series of automatic quality control tests to ensure the code runs as expected and to flag changes to the FrEDI outputs relative to a benchmark run to assist in additional quality control review.

- b. The information disseminated is determined to be clear, complete, and unbiased based on multiple rounds of independent review. Consistent with guidelines described in EPA's Peer Review Handbook,⁴ the underlying sectoral modeling methodologies are peer-reviewed through scientific journal publication processes. Citations for these publications can be found throughout the main technical documentation and its appendices. In addition, aspects of the FrEDI technical documentation and associated R package have also been subject to external journal publication processes (Sarofim et al., 2021, Hartin et al., 2023).
- c. The FrEDI technical documentation and associated R code have been subject to both public review and external peer review. See Sections A.3-A.5 for details about the peer and public reviews conducted since 2021.

Integrity refers to security of information, such as the protection of information from unauthorized access or revision, to ensure that the information is not compromised through corruption or falsification. The technical documentation, framework, R code, and underlying analyses meet the standard for integrity due to the strategic steps taken to ensure that the data and information remained secure. These steps included the use of password protected data storage repositories, password protected data transfer technology, and multiple layers of data validation checks to ensure that the integrity was not compromised.

Utility is the usefulness of the information to the intended users. The technical documentation, framework, R code, and underlying analyses meet the standard for utility because the information disseminated provides insights (technical methods for quantifying physical and economic impacts) regarding the potential magnitude of the impacts of climate change. Understanding the risks posed by climate change can inform broader assessment reports and policy decisions designed to address these risks. See section 1.2 of the main technical documentation for a discussion of other example applications and intended uses.

Transparency ensures access to and description of (1) the source of the data, (2) the various assumptions employed, (3) the analytic methods applied, and (4) the statistical procedures used. The report and its underlying analyses meet the standard for transparency for the following reasons:

- a. The underlying datasets, sectoral impact models, and the methods supporting the framework and associated R package have been published with open access in the peer-reviewed scientific literature and are cited throughout the report. These papers, along with their online supplementary materials, provide detailed information on the sources of data used, assumptions employed, the analytic and statistical methods applied, and important limitations regarding the approaches and/or how the results should be interpreted.

⁴ EPA, 2015: Peer Review Handbook, 4th Edition, 2015. United States Environmental Protection Agency, Programs of the Office of the Science Advisor.

- b. Appendix B for this Technical Documentation provides details on how results and output from each sectoral impact model (or impacts study) are formatted and adapted for usage in the framework and R code. This Appendix contains descriptions of the methodologies used in estimating impacts, assumptions used, and citations to the underlying literature where the reader can go for more information.
- c. The R package for FrEDI has been posted as a public repository on the USEPA GitHub website. Updates to the FrEDI R code are published as tagged releases, accompanied by release notes that summarize each update. See <https://www.github.com/USEPA/FrEDI>. Additional documentation on the R package components, as well as general information about downloading and running the FrEDI R package are posted on the following website: <https://usepa.github.io/FrEDI>.
- d. Both the 2021 and 2024 versions of the Technical Documentation were subject to a public comment period to ensure interested stakeholders had a chance to review and provide input on the framework and tool methods.
- e. Responses to all comments received during both the 2021 and 2024 public comment periods are publicly posted. See <https://cfpub.epa.gov/si/>. Search using the report title or 'FrEDI'.
- f. Responses to all comments received during the 2021, 2024, and 2025 independent, expert peer reviews have been posted on EPA's Science Inventory. See <https://cfpub.epa.gov/si/>. Search using the report title or 'FrEDI'. During their review period, when applicable, expert peer reviewers were provided a copy of all comments received from the public comment period.

A.2 Consideration of Assessment Factors

When evaluating the quality, objectivity, and relevance of scientific and technical information, the considerations that EPA takes into account can be characterized by five general assessment factors, as found in *A Summary of General Assessment Factors for Evaluating the Quality of Scientific and Technical Information, and the Guidance for Evaluating and Documenting the Quality of Existing Scientific and Technical Information*.⁵ The following section lays out how the assessment factors are considered to determine whether models and data in the technical documentation, framework, R package, and underlying analyses are acceptable for their intended use.

⁵ USEPA. 2003. *A Summary of General Assessment Factors for Evaluating the Quality of Scientific and Technical Information, and the Guidance for Evaluating and Documenting the Quality of Existing Scientific and Technical Information*. Science Policy Council U.S. Environmental Protection Agency Washington, DC. EPA 100/B-03/001

TABLE A-1. SUMMARY OF QUALITY ASSESSMENT FACTORS

Factor	Description	How the Factor was Considered
Soundness	The extent to which the scientific and technical procedures, measures, methods or models employed to generate the information are reasonable for, and consistent with, the intended application.	<ul style="list-style-type: none"> • Used publicly available (to the maximum extent practicable) data, reviewed for quality and accuracy with complete metadata available. • Used data included in peer-reviewed publications. Ensured evaluation of the scientific and technical procedures, measures, and methods employed to generate estimates produced by sectoral impact models. • Considered the capabilities of integrated assessment, simple climate, and sectoral impacts models to examine changes in physical effects, economic damages, and changes in risk from climate change in a manner consistent with sound scientific theory and accepted approaches. • Considered the extent to which underlying models and data had been previously applied in projects of similar scope, such as the Climate Change Impacts and Risk Analysis (CIRA) project. For example, the BenMAP model has been used in similar climate and health impact analyses, and the labor analysis has been employed in other multi-sector modeling projects (e.g., Hsiang et al. 2017). • Considered whether the data and code are available, made available by EPA, or determined to not be feasible as it is claimed as proprietary by a non-federal business. • Selected sectoral impacts models with the following criteria: sufficient understanding of how climate change affects the sector; the existence of data to support the methodologies; availability of modeling applications that could be applied in the FrEDI framework; based on peer reviewed literature and datasets; and the economic, iconic, or cultural significance of impacts and damages in the sector to the U.S.
Applicability and Utility	The extent to which the information is relevant for the Agency's intended use.	<ul style="list-style-type: none"> • Ensured that FrEDI uses applicable and relevant inputs and considers the capabilities of the integrated assessment, simple climate model, and sectoral impacts models to examine changes in physical effects, economic damages, and risk associated with climate change. • Ensured that FrEDI and its underlying analyses are relevant to their intended use so that the information disseminated provides insights and methods for quantifying the physical and economic impacts of climate change at national, regional, and state levels. • Ensured sectoral impacts models are reasonable for, and consistent with, the intended application by being sufficiently flexible to ensure consistency in inputs and monetizing physical impacts. • Ensured that models have been applied in peer-reviewed, published studies.
Clarity and Completeness	The degree of clarity and completeness with which the data, assumptions, methods, quality assurance, sponsoring organizations and analyses employed to generate the information are documented.	<ul style="list-style-type: none"> • Ensured use of clear and complete inputs by considering the extent to which sectoral impacts models documented their key methods, assumptions, parameter values, limitations, sponsoring organizations/author affiliations, and funding information. • Ensured publications clearly and comprehensively describe analytic methods used and how they apply and build off existing bodies of research and underlying scientific and/or economic theories.

Factor	Description	How the Factor was Considered
Uncertainty and Variability	The extent to which the variability and uncertainty (quantitative and qualitative) in the information or in the procedures, measures, methods or models are evaluated and characterized.	<ul style="list-style-type: none"> • Ensured inputs that appropriately characterize uncertainty and variability by considering the capabilities of sectoral impacts models to evaluate and characterize key sources of variability and uncertainty. Results of these analyses are described in the underlying journal articles. • Reviewed the model documentation and peer-reviewed publications to determine if a model is sufficiently flexible and capable of evaluating important sources of uncertainty for climate change impacts analysis. • Documented outcomes of sensitivity and uncertainty analyses, where applicable, in the presentation of results using ranges and confidence intervals. • Addressed key sources of uncertainty by developing a flexible framework, as described in Section 2 of the Main Text.
Evaluation and Review	The extent of independent verification, validation and peer review of the information or of the procedures, measures, methods or models.	<ul style="list-style-type: none"> • Ensured use of independently verified and validated inputs by considering the extent to which models have been independently peer reviewed. • Reviewed the documentation associated with each model and determined if they have been independently peer-reviewed and published in scientific journals with procedures to ensure that the methods are technically supportable, properly documented, and consistent with established quality criteria. • Used scenarios and projections that have been independently verified and validated (e.g., scenarios and projections developed for the IPCC and its assessments, and then downscaled for the U.S. National Climate Assessment).

A.3 Review Process for the 2021 Technical Documentation

Consistent with guidelines described in EPA's Peer Review Handbook,^{6,7} the 2021 Technical Documentation was subject to a public review comment period, and an independent, external expert peer review that concluded with the publication of the original Technical Documentation in October 2021. The peer and public review documentation is available at [EPA's Science Inventory](#).

The 2021 Technical Documentation was subject to a public comment period to ensure that the information summarized by EPA was technically supported, competently performed, properly documented, consistent with established quality criteria, and communicated clearly. This public review period was also intended to provide feedback and comments on the framework's utility. Similarly, the purpose of the expert peer review by independent, qualified, and objective experts was to ensure that the information summarized by EPA was technically supported, competently performed, properly documented, consistent with established quality criteria, and communicated clearly. The sectoral impact models underlying the technical documentation, as well as the temperature binning approach used in the FrEDI framework were previously peer reviewed and published in the research literature.

Public Review Period

A 30-day public comment period was held from April 15th through May 17th, 2021. All comments received were carefully reviewed, considered, and responded to.

Expert Peer Review

The expert review was managed by a contractor (ICF International) under the direction of a designated independent EPA peer review leader, who prepared a peer review plan, the scope of work for the review contract, and the charge for the reviewers. Importantly, the EPA peer review leader played no role in producing any portion of the report. Reviewers worked individually (i.e., without contact with other reviewers, colleagues, or EPA) to prepare written comments in response to the charge questions. The reviewers were also provided with the public review comments for informational purposes.

The contractor identified, screened, and selected five reviewers who had no conflict of interest in performing the review, and who collectively met the technical selection criteria provided by EPA.

The peer review charge directed reviewers to provide responses to the following questions during the main review:

⁶ EPA, 2015 (see footnote 4)

⁷ EPA has determined that the 2021 Technical Documentation report fell under the classification of "influential scientific information," as defined by OMB and further described in the EPA Peer Review Handbook. The 2021 Documentation was for science dissemination and communication purposes only, and does not reflect analysis of nor recommendations regarding any particular policy.

1. Does the introductory chapter clearly explain the purpose of the report and provide appropriate context for the rest of the documentation? If not, please provide recommendations for improvement.
2. The report has been written for an educated and semi-technical audience. Are the writing level and graphics appropriate for these audiences?
3. Does the report adequately explain the overall analytic framework of the temperature binning approach?
4. Do the text, figures, and tables clearly communicate the framework's structure and design? Are the requirements for input data, and the options for output/results summaries, clearly stated?
5. Does the report clearly convey both the conceptual basis for temperature binning and the specific data processing and analytic steps taken to execute the concept? Is it clear how both the EPA-sponsored CIRA sector studies, and other non-CIRA studies, can be incorporated in the framework?
6. Is the sector-specific approach to account for the role of socioeconomic driver data clear? Is it reasonable and well-supported?
7. Is the approach to estimating sector-specific and aggregate economic impact (damages) of specified temperature trajectories reasonable and suitable for the stated purposes?
8. Does the report adequately inform the reader about how uncertainty is addressed in the framework, including how results should be interpreted and used given the limitations?
9. Has EPA objectively used, applied, and documented the underlying data of the temperature binning framework? Has the Agency appropriately described the sensitivity of the findings to analytic assumptions?
10. Is the draft technical documentation report missing important information based on your review of the report?
11. Report Format: Please comment on whether any aspects of the layout help or hinder the reader to understand the content and key messages of the report.

A.4 Review Process for the 2024 Technical Documentation

Consistent with guidelines described in EPA's Peer Review Handbook,^{8,9} the 2024 Technical Documentation was subject to a public review comment period, and an independent, external expert peer review that concluded with the publication of the 2024 Technical Documentation in August 2024. The peer and public review documentation is available at [EPA's Science Inventory](#). Reviewers were charged with focusing on the updates to the FrEDI Technical Documentation and associated R package since the 2021 publication. Key aspects included the addition of several new sectoral impact categories, additional state-level impact calculations, and two modules for extending the default FrEDI framework: one module to extend FrEDI to calculate impacts through 2300 and a second Social Vulnerability module that extended the dimensionality

⁸ EPA, 2015 (see footnote 4)

⁹ EPA has determined that the 2024 report falls under the classification of "influential scientific information," as defined by OMB and further described in the EPA Peer Review Handbook. This product is for science dissemination and communication purposes only, and does not reflect analysis of nor recommendations regarding any particular policy.

of FrEDI to provide a distributional analysis of climate change impacts to different population groups within the U.S. through 2100.

Public Review Period

A 60-day public comment period was held from February 23rd through April 24th, 2024. All comments received were carefully reviewed, considered, and responded to.

Expert External Peer Review

The expert review was managed by a contractor (ICF International) under the direction of a designated independent EPA peer review leader, who prepared a peer review plan, the scope of work for the review contract, and the charge for the reviewers. Importantly, the EPA peer review leader played no role in producing any portion of the report. Reviewers worked individually (i.e., without contact with other reviewers, colleagues, or EPA) to prepare written comments in response to the charge questions.

The contractor identified, screened, and selected four reviewers who had no conflict of interest in performing the review, and who collectively met the technical selection criteria provided by EPA.

The peer review charge directed reviewers to provide responses to the following questions during the main review:

General FrEDI

Consistent with the guidelines described in EPA's Peer Review Handbook, the FrEDI Technical Documentation and accompanying R package were subject to a public review comment period and an independent, external expert peer review in 2021. Since the 2021 Report, seven peer-reviewed sectoral impact studies have been pre-processed and implemented into FrEDI's analytical framework. FrEDI's pre-processing and run-time steps have also been updated to output FrEDI data for 48 U.S. states, in addition to regional and national totals. Lastly, additional features have been implemented into the FrEDI R package that extend FrEDI calculations past the year 2100 and incorporate calculations of differential climate change risks across U.S. demographics. The updated 2024 Technical Documentation describes the underlying FrEDI framework, which remains unchanged since the 2021 review, but now also provides additional methodological information on the standard approach for incorporating new impacts, the process for generating FrEDI results at finer geographic scales, and updated Appendices describing new sectoral studies. The following questions are related to these general topics.

1. Has EPA clearly used, applied, and documented the data underlying FrEDI and does the Technical Documentation adequately explain how these data are used in the FrEDI framework?
2. The Technical Documentation (Main Text and Appendix B) describe how data from sectoral impact studies have been processed to develop state-level damage functions for use in FrEDI.
 - a. Does the Technical Documentation clearly convey the conceptual basis and pre-processing steps used to develop impact-by-degree damage functions at the state-level and how these

- functions are used within FrEDI to project climate change impacts at the state, regional, and national geographic scales?
- b. Are the projected state-level climate change impacts clearly illustrated in Chapter 3? If not, are there alternative approaches for presenting the state-specific impact data that would improve the communication of future climate change impacts to each U.S. state?
 - 3. Seven impact sector studies (CIL agriculture, CIL temperature-related mortality, ATS temperature-related mortality, marine fisheries, CIL crime, suicide, vibriosis)¹⁰ have been incorporated into FrEDI since the 2021 peer-review.
 - a. In Chapter 2 and Appendix B, has EPA clearly used, applied, and documented the data underlying these new sectoral studies and adequately explained how this information was pre-processed for use in the FrEDI R code?
 - b. Does Chapter 2 clearly and sufficiently describe the conceptual basis and methodological process for the ongoing and long-term incorporation of additional impact studies and capabilities into future versions of the FrEDI R package? If not, please describe any additional information needed to clarify this approach or additional information EPA should consider documenting when incorporating new impacts into FrEDI.
 - 4. Are there additional categories of damages that are currently missing that EPA should consider for inclusion as damage functions within the FrEDI framework? If so, please mention any specific peer reviewed literature that could be used to inform the modeling of these additional impacts.
 - 5. Peer-reviewed sectoral impact studies are pre-processed to generate national, region, and state-specific ‘impact-by-degree’ damage functions for use in FrEDI. As described in Chapter 2, each damage function is linearly extrapolated to higher degrees of warming than originally considered in each underlying study, so that FrEDI can be extended to assess impacts over a broader range of temperatures (and impacts in years past 2100¹¹). Other climate impact applications similarly extend information from peer-reviewed impacts studies to project damages across large temperature ranges (e.g., Rennert et al., 2021).
 - 6. Does EPA clearly describe the current approach used to extrapolate sectoral damage functions to temperature above the ranges provided by the underlying study data?
 - 7. Are there alternative and superior approaches that EPA should consider for extrapolating damage functions to warmer temperatures? If so, please describe the advantages (and any potential drawbacks) of these alternative extrapolation approaches.
 - 8. The FrEDI R package includes the ‘social vulnerability’ or ‘SV’ module for estimating several impact metrics, including future climate change impact rates across different demographics. The data and methods underlying this module are based on EPA’s recent report on [Climate Change and Social Vulnerability in the United States](#), which was itself peer-reviewed prior to the report’s release in 2021. Do you have specific recommendations that EPA should consider as long-term improvements to the

¹⁰ CIL –studies conducted by the Climate Impacts Lab, ATS –studies led by the American Thoracic Society.

¹¹ See Hartin et al. (2023) for an application of this approach to scenarios through the year 2300.

- FrEDI SV module (e.g., different metrics, assumptions, analyses, etc.). If so, please describe the advantages (and any potential drawbacks) of any recommended changes or additions.
9. Are there additional graphics or text that should be added to the Technical Documentation to improve the clarity of the methodological descriptions in Chapter 2 or Appendix B?

FrEDI Analytical Applications

Quantitative evidence of climate change and its impacts over time is a critical input to decision-making and policy development. In addition to the total magnitude of change, impact analyses that disaggregate impacts to finer sectoral and spatial scales also provide unique understanding and insight into how climate change risks may be experienced differently across the United States. For example, the impacts of climate change occurring in a particular region or community will be determined by local sensitivities to physical climate stressors (e.g., heat, wildfire, flooding), as well as the ability or capacity of each community to adapt. Chapter 1 provides an overview of how FrEDI can be applied to these types of analyses. Chapter 3 further provides extended examples of how FrEDI output can be used to quantitatively project impacts of climate change and their distribution across U.S. states, sectors, and populations.

The first application in Chapter 3 presents impacts for an example warming scenario while the second presents changes in impacts under a hypothetical warming mitigation scenario. This second mitigation scenario is designed to illustrate an assessment of the climate-related benefits to the U.S. associated with a hypothetical GHG emissions regulatory action. This information is relevant to regulatory cost-benefit analyses, for example, as stated by OMB Circular A-4 (2003)¹², “The benefits and costs of a regulation are ultimately experienced by people. For some regulations, different groups of people may be impacted differently. Distributional analysis, whether quantitative or qualitative, can help illustrate these effects.” In addition, EPA’s Science Advisory Board (SAB) on a recent Agency rule¹³ also recognized that “The differential benefits of reduced greenhouse gas emissions are not captured by the average social cost of carbon value and therefore additional consideration of the distributional effects of reducing greenhouse gas emissions is warranted” and that “the EPA should utilize … the EPA CIRA program [precursor to FrEDI] for information on the disproportionate health impacts of climate change and consider greenhouse gas implications from the proposed rule.”

The following questions are related to both FrEDI applications presented in Chapter 3.

10. Does Chapter 3 clearly inform the reader how FrEDI output can be used to quantify ‘baseline’ climate change impacts to the U.S. that are associated with a single emissions (or temperature) scenario? If not, what additional documentation should EPA consider adding to this Chapter?
11. Does Chapter 3 clearly describe how FrEDI can be applied within a broader analytical workflow to quantify the climate change-related benefits to the U.S. that are associated with a marginal change in GHG emissions (or temperature)? If not, what additional documentation should EPA consider adding to this Chapter?

¹² Circular No. A-4, Nov. 9, 2023 (<https://www.whitehouse.gov/wp-content/uploads/2023/11/CircularA-4.pdf>)

¹³ EPA Science Advisory Board Letter to Administrator Regan, Final Science Advisory Board Regulatory Review Report of Science Supporting EPA Decisions for the Proposed Rule: Control of Air Pollution from New Motor Vehicles: Heavy-Duty Engine and Vehicle Standards (RIN 2060-AU41), EPA-SAB-23-001, December 15th, 2022.

12. Do the figures and text in Chapter 3 clearly illustrate how FrEDI can be used to assess and communicate disaggregated climate change impacts and climate-related benefits across FrEDI's multiple impact category sectors, spatial scales, and population groups? Are there alternative graphics and/or clarifying text that EPA should consider adding to this Chapter to more clearly illustrate or communicate how climate-related impacts or benefits will be experienced by different groups across the U.S.?
13. Chapter 3 also describes the application of the FrEDI SV module to assess the relative risk of climate change impacts across different population groups of concern and how relative risks may change under a hypothetical mitigation scenario. In order to effectively assess the change in disproportionate climate-related impacts in a hypothetical mitigation scenario, the FrEDI SV analysis should provide information that addresses the following questions:
 - a. Are there potential Environmental Justice (EJ) concerns¹⁴ associated with future climate change under a baseline scenario?
 - b. Are there potential EJ concerns associated with future climate change, under a specific GHG emissions reduction scenario?
 - c. Are the potential EJ concerns exacerbated, mitigated, or unchanged when GHG emissions are reduced compared to the baseline scenario?
14. To what extent does the SV analysis in Chapter 3 describe and illustrate how FrEDI output can be applied to address these three questions? Are there alternative and superior approaches to presenting FrEDI output that EPA should consider including to more clearly address these three questions? If so, please describe the advantage (and potential drawbacks) of any alternative approaches.

A.5 Review Process for the Supplement to the Technical Documentation

Consistent with guidelines described in EPA's Peer Review Handbook,¹⁵ the Supplement to the FrEDI Technical Documentation, describing the Concentration-Driven module, was subject to an independent, external expert peer review. The review documentation is available upon request. Reviewers were charged with focusing on the updates to the FrEDI Technical Documentation associated with the new module and not a re-review of any existing content was previously peer-reviewed in 2024. Key aspects include a description of the module inputs, runtime processes, process for future updates, and how to interpret and combine the results with FrEDI's main temperature- and sea level rise-driven impacts to clearly communicate the broad range of climate and concentration impacts to the American public.

¹⁴ defined as "disproportionate impacts on minority populations, low-income populations, and/or indigenous peoples that may exist prior to or that may be created by the proposed regulatory action". EPA *Technical Guidance for Assessing Environmental Justice in Regulatory Analyses*, 2016.

¹⁵ EPA, 2015 (see footnote 4)

Public Review Period

Given that the FrEDI Technical Documentation was peer-reviewed and received public comment in 2024, and that the description of the concentration-driven module was a technical supplement to the 2024 FrEDI Technical Documentation, public comment was not solicited on the Concentration-Driven Module Report.

Expert External Peer Review

The expert review was managed by a contractor (Abt Global) under the direction of a designated independent EPA peer review leader, who prepared a peer review plan, the scope of work for the review contract, and the charge for the reviewers. Importantly, the EPA peer review leader played no role in producing any portion of the report. Reviewers worked individually (i.e., without contact with other reviewers, colleagues, or EPA) to prepare written comments in response to the charge questions.

The contractor identified, screened, and selected two reviewers who had no conflict of interest in performing the review, and who collectively met the technical selection criteria provided by EPA.

The peer review charge directed reviewers to provide responses to the following questions:

1. Has EPA clearly used, applied, and documented the data and conceptual basis underlying the FrEDI concentration-driven module? If not, are there additional graphics or text that should be added to the Report to improve the clarity of the descriptions of the underlying module methodology?
2. Does the Report clearly inform the reader how output from the Concentration-Driven module can be combined with the output from other FrEDI modules to quantify the combined impacts associated with both climate change and concentration-driven impacts? If not, what additional documentation should EPA consider adding to the Report?
3. Does the report adequately inform the reader about how uncertainty is addressed in the module, including how results should be interpreted and used given the limitations?
4. Does the Report clearly and sufficiently describe the conceptual basis and methodological process for the ongoing and long-term incorporation of additional concentration-driven impact studies into future versions of the FrEDI R package? If not, please describe any additional information needed to clarify this approach or additional information EPA should consider documenting when incorporating new concentration-driven impacts into FrEDI.
5. Are there additional concentration-driven impacts that are currently missing that EPA should consider for incorporation into this FrEDI module (e.g., methane-ozone impacts on agriculture)? Do you have specific recommendations that EPA should consider as long-term improvements to the FrEDI Concentration-Driven module (e.g., different metrics, assumptions, analyses, etc.). If so, please describe the advantages (and any potential drawbacks) of any recommended changes or additions.

APPENDIX B | DETAILS OF SECTORAL IMPACT STUDIES

B.2 Health Sectors	B-5
Climate-Driven Changes in Air Quality	B-5
Extreme Temperature	B-14
CIL Temperature-Related Mortality	B-19
ATS Temperature-Related Mortality	B-23
Southwest Dust	B-28
Valley Fever	B-34
Wildfire	B-38
CIL Crime	B-43
Vibriosis	B-47
Suicide	B-50
Lyme Disease	B-54
B.3 Infrastructure Sectors	B-57
Coastal Properties	B-57
Transportation Impacts from High Tide Flooding	B-60
Rail	B-63
Roads	B-66
Asphalt Roads	B-70
Urban Drainage	B-73
Inland Flooding	B-76
Hurricane Wind Damage	B-79
B.4 Electricity Sectors	B-83
Electricity Demand and Supply	B-83
Electricity Transmission and Distribution Infrastructure	B-86
B.5 Ecosystems and Recreation Sectors	B-90
Water Quality	B-90
Outdoor Recreation	B-93
Winter Recreation	B-98
Marine Fisheries	B-102
Marsh Migration	B-105
B.6 Labor and Learning Sector	B-108
Labor	B-108
Learning Loss	B-111
B.7 Agriculture Sector	B-116
CIL Agriculture	B-116
Forestry Loss	B-120

B.1 Sectoral Impact Category Data Overview

This appendix provides additional detail on the sectoral impact studies included in the FrEDI framework. The main advantage of FrEDI is that it offers the unique flexibility to incorporate a broad range of peer-reviewed climate impact studies into a common analytical framework, as implemented by the FrEDI R code. While details of each study vary, there is a series of similar steps used to pre-process and format the results from each study into the impact-by-degree damage functions that are used in FrEDI. Common pre-processing steps often include: 1) the (dis)aggregation of underlying study impact data to the state level, 2) the isolation of climate-driven impacts by subtracting baseline impacts, and 3) binning the annual impacts (or impact rates) by temperature for each available GCM (temperature binning discussed in Appendix C) to calculate the final by-degree damage functions that are then used when the FrEDI R code is run.

Consistent with Section 3 in the Main Documentation, individual impact sectors in this Appendix are organized and grouped into six aggregate categories: Health, Infrastructure, Electricity, Ecosystems & Recreation, Labor, and Agriculture. **Table B-1** lists each individual impact sector by aggregate group, summarizes the geographic coverage of each impact within the Contiguous U.S. (CONUS), and lists the GCMs used in the underlying sectoral impact models that form the basis of FrEDI's damage functions. Main text **Table 1** (impact types, socioeconomic drivers, adaptation scenarios), **Table 4** (links to population and GDP inputs), **Table 5** (time dependent scalars), and **Table 3** (valuation measures) also provide summarized information about the impact sectors.

TABLE B-1. REGIONAL COVERAGE AND GCMS USED BY SECTOR

		Regional Coverage ^a							CMIP5 GCMs Used							
		Midwest	Northeast	Northern Plains	Northwest	Southeast	Southern Plains	Southwest	CanESM2	CCSM4	GFDL-CM3	GISS-E2-R	HadGEM2- ES	MIROC5	Other	SLR Scenarios
Health	Climate-Driven Changes in Air Quality															
	Extreme Temperature															
	CIL Temperature-Related Mortality															
	ATS Temperature-Related Mortality															
	Southwest Dust															
	Valley Fever															
	Wildfire															
	CIL Crime															
	Vibriosis															
	Suicide															
	Lyme Disease															
Infrastructure	Coastal Properties															
	Transportation Impacts from HTF															
	Rail															
	Roads															
	Asphalt Roads															b
	Urban Drainage															
	Inland Flooding															c
Electricity	Hurricane Wind Damage															d
	Electricity Demand and Supply															
	Electricity Transmission and Distribution															
Ecosystems and Recreation	Water Quality															
	Outdoor Recreation															
	Winter Recreation															
	Marine Fisheries															
	Marsh Migration															
Labor and Learning	Labor															
Agriculture	Learning Loss															
Agriculture	CIL Agriculture															
	Forestry Loss															

a. Sectors listed for a specific NCA region do not necessarily include non-zero impacts for all states within that region. See the tables in the sector-specific sections below for details on states with non-zero impacts.

b. Asphalt Roads, a study not designed within the CIRA framework, utilized three CMIP5 GCMs in common with the CIRA2.0 set of scenarios (CanESM2, CCSM4, MIROC5) however, the climate data used in the underlying study was bias corrected and downscaled using a different process than the method used in CIRA. Therefore, although the GCMs are the same, the integer degree arrival times differ slightly for this sector.

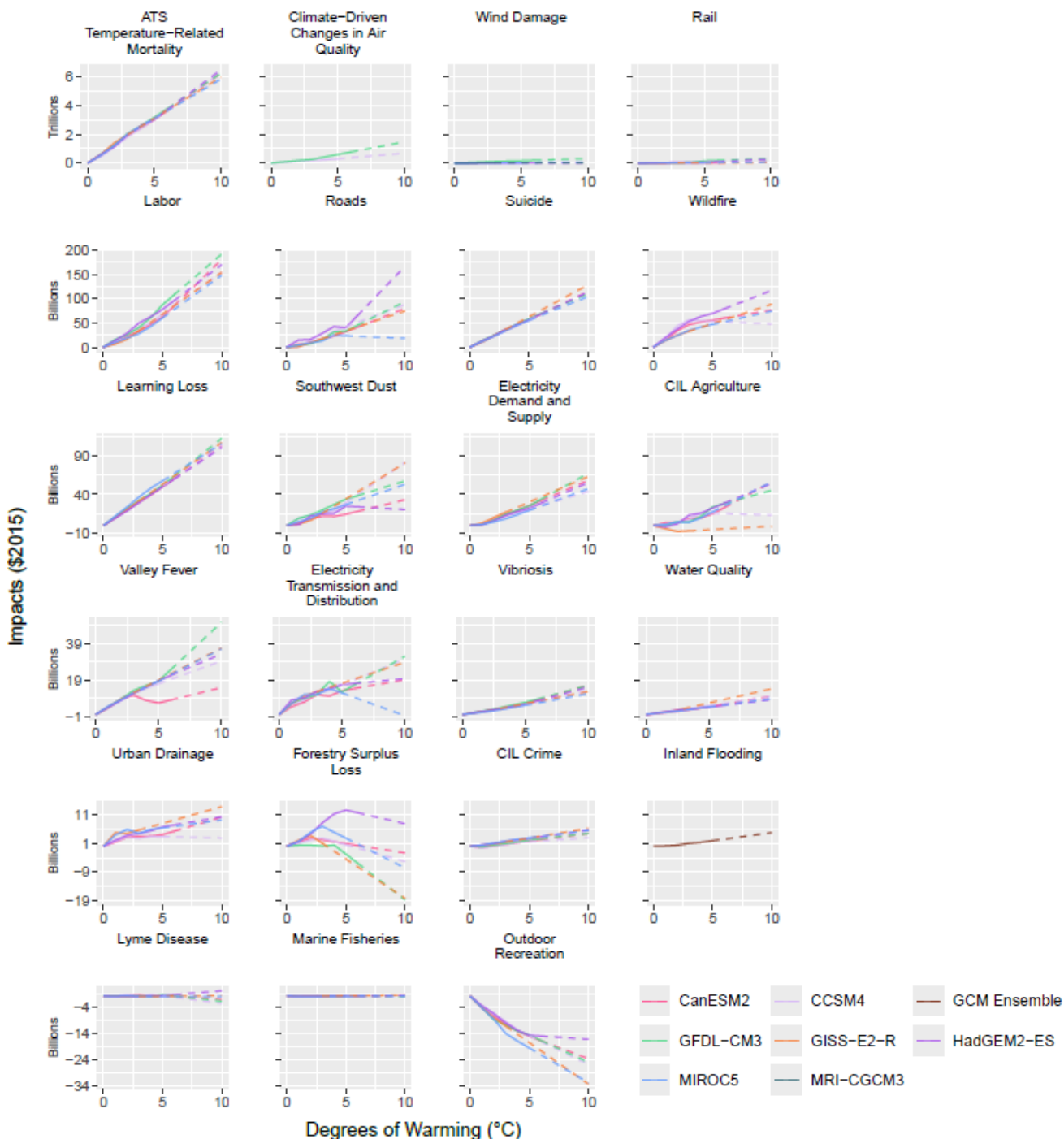
c. The Inland Flooding sector used an ensemble of 14 CMIP5 GCMs (list provided in detailed write-up below), which includes four of the six CMIP5 GCMs from the CIRA2.0 set of scenarios (CanESM2, GFDL-CM3, HadGEM2-ES, MIROC5). The authors estimated arrival times and provided estimates of impacts by degree of warming for the mean of 14 CMIP5 GCM results.

d. The Hurricane Wind sector uses four of the six standard CIRA CMIP5 GCMs (CCSM4, GFDL-CM3, HadGEM2-ES, MIROC5) and MRI-CGCM3 to follow the underlying literature Marsooli et al. (2019). Similar to Asphalt Roads, the climate data used in the Hurricane Winds study was bias corrected and downscaled using a different process than the method used in CIRA. Therefore, although the CMIP5 GCMs are the same, the integer degree arrival times differ slightly for this sector. Unlike Marsooli et al. (2019), FrEDI does not include MPI5 due to data availability constraints.

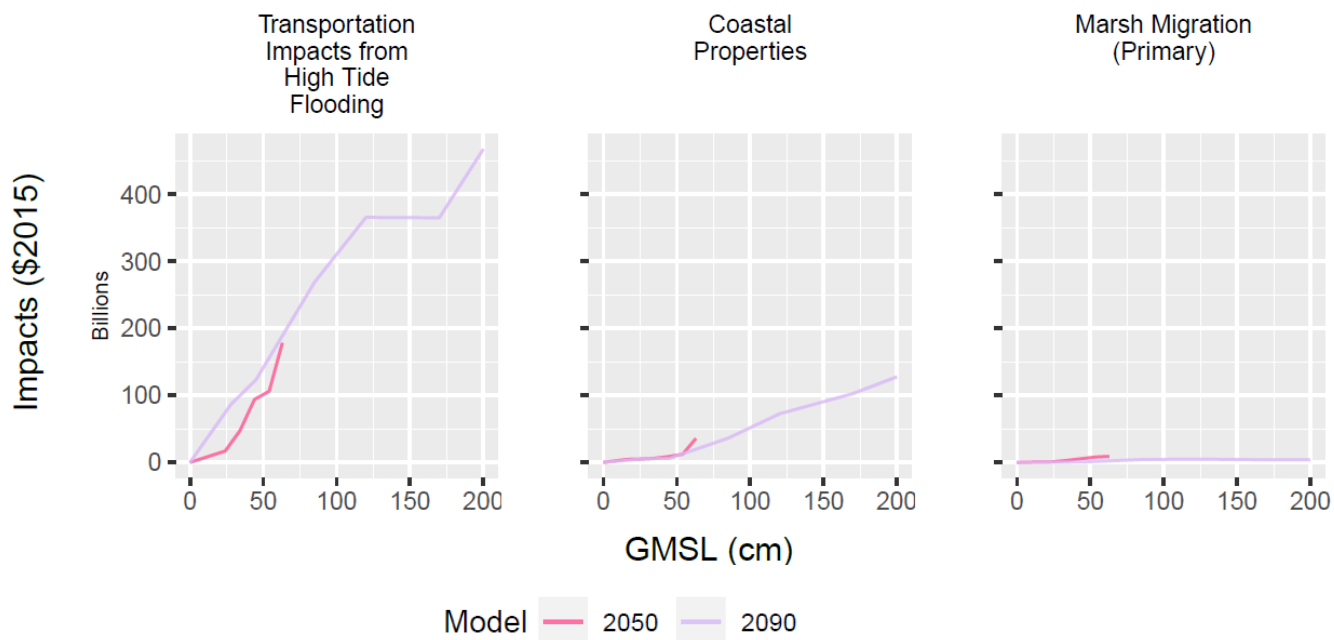
Figure B-1 and **Figure B-2** present the monetized sectoral damages in FrEDI; damages are presented by degree of CONUS warming for each temperature-driven impact category sector in Figure B-1 and by centimeter of Global Mean Sea Level (GMSL) rise for each sea level rise (SLR)-driven sector in Figure B-2. These results (for illustrative purposes only) are calculated using the default socioeconomic inputs for 2090. These figures illustrate the relative magnitude of damages in each impact sector, by GCM, and the final shape of the CONUS damage functions (i.e. the sum of all state-level damages functions) after valuation scalars have been applied. The GCMs in each underlying study do not all reach the same level of future warming. Therefore, FrEDI's sector-specific damage functions are derived from a piece-wise linear fit between integer degrees of warming for the range of warming degrees available from each GCM (e.g., shown by solid lines in Figure B-1 and each impact-by-degree figure in this Appendix), and are linearly extrapolated (as described in Section 2.3 of the Main Documentation) to higher levels of warming (shown by dashed lines in each impact-by-degree figure).

Application of the FrEDI framework is not limited to the current impact sectors. New sectors that meet the requirements outlined in Section 2 of the Main Documentation can be added to the framework. This appendix will be updated as additional sectoral studies, and their functions are incorporated into FrEDI.

FIGURE B-1. TOTAL CONUS ECONOMIC IMPACTS BY DEGREE OF WARMING IN 2090, BY SECTOR FOR DEFAULT TEMPERATURE-DRIVEN SECTORS



Impacts by CONUS degree of warming (Celsius) relative to the 1986-2005 average baseline, under default 2090 socioeconomic conditions, in trillions (top row) and billions (remaining rows) of 2015\$ for the default temperature-driven FrEDI sectors, variants, and adaptation options (see Section 2.2 of the Main Text). Each line represents the GCMs available in each underlying study; dashed lines represent extrapolations above available integer degrees. Sectors are ordered by the magnitude of their average impacts at 5-degrees. Not all sectors include estimates for all models listed in the legend (see Table B-1). Note that the y-axis scales vary by row. Figure produced using results from FrEDI v5.0

FIGURE B-2. TOTAL CONUS ECONOMIC IMPACTS, BY CENTIMETER OF GMSL FOR SLR-DRIVEN SECTORS

Impacts by centimeter of GMSL rise relative to a year 2000 baseline, in billions of 2015\$, for default sectors, variants, and adaptation options (See Section 2.2 of the Main Text). The two lines represent the damages associated with the GMSL rise for each of six GMSL rise scenarios from Sweet et al. (2017), used in the underlying damage studies, in 2050 (pink line) and 2090 (purple line). Note that the 2050 series stops at 63cm of GMSL rise, which is the largest magnitude of GMSL rise projected across the six Sweet et al. (2017) scenarios by mid-century. Figure produced using results from FrEDI v5.0.

For each sectoral impact category, the following sections include a description of the impacts considered, a reference to the underlying impact sector study, a description of the pre-processing steps used to derive sectoral damage functions, details about implementation into the FrEDI R code, and discussion of any limitations. To show GCM variability, impacts-by-degree of warming are shown for the GCMs used in each underlying study. As of FrEDI v5.0, all GCM data used in the underlying studies are from the 5th Coupled Model Intercomparison project (CMIP5), unless otherwise noted. In addition, for sectors that are projected to scale with temperature (or SLR) and socioeconomic conditions (i.e., population and GDP), impacts-by-degree are also provided for two example socioeconomic scenarios (e.g., 2010 and 2090) to illustrate the sensitivity of the impacts to changes in socioeconomics.

B.2 Health Sectors

Climate-Driven Changes in Air Quality

Summary

This sector estimates mortality for all ages, incidence of childhood asthma, childhood emergency department (ED) visits, and school loss days associated with climate-driven changes in air quality in the CONUS; specifically, concentrations of ozone (O_3) and fine particulate matter ($PM_{2.5}$).

This analysis uses air quality surfaces (i.e., concentrations in response to changes in meteorology) in combination with a) concentration-response functions employed by Fann et al. (2021) to quantify future $PM_{2.5}$ - and O_3 -attributable premature mortality, and b) with morbidity concentration-response functions from EPA (2023)^{16,17} to quantify new childhood asthma cases, childhood ED visits, and school loss days. Air quality concentration changes are driven by changes in meteorology only and do not reflect time-varying changes in pollutant precursor emissions.

Mortality is monetized using the value of a statistical life (VSL). In this context, VSL refers to an individual's willingness to pay for a small reduction in the risk of their own premature death within each future year, calculated as the population average for each country. Future estimates of VSL are calculated each year following Eq. B-1 by referencing the EPA 1990¹⁸ VSL for the U.S. (adjusted for income growth and inflation to \$9.8 million in 2015 dollars¹⁹) and scaling relative to U.S. income (represented by GDP per capita) in

UNDERLYING DATA SOURCES AND LITERATURE

Fann, N. L., Nolte, C. G., Sarofim, M. C., Martinich, J., & Nassikas, N.J. (2021). Associations between simulated future changes in climate, air quality, and human health. *JAMA Network Open*, 4(1).

<https://doi.org/10.1001/jamanetworkopen.2020.32064>

EPA (2023). Climate Change and Children's Health and Well-Being in the United States. U.S. Environmental Protection Agency, EPA 430-R-23-001.

<https://www.epa.gov/cira/climate-change-and-childrens-health-and-well-being-united-states-report>

¹⁶ Morbidity functions from: Tetreault, L.F., Doucet, M., Gamache, P., Fournier, M., Brand, A., Kosatsky, T. and Smargiassi, A., 2016. Childhood exposure to ambient air pollutants and the onset of asthma: an administrative cohort study in Québec. *Environmental Health Perspectives*, 124(8); Gilliland, F.D., Berhane, K., Rappaport, E.B., Thomas, D.C., Avol, E., Gauderman, W.J., London, S.J., Margolis, H.G., McConnell, R., Islam, K.T. and Peters, J.M., 2001. The effects of ambient air pollution on school absenteeism due to respiratory illnesses. *Epidemiology*; Alhanti, B.A., Chang, H.H., Winquist, A., Mulholland, J.A., Darrow, L.A. and Sarnat, S.E., 2016. Ambient air pollution and emergency department visits for asthma: a multi-city assessment of effect modification by age. *Journal of Exposure Science & Environmental Epidemiology*, 26(2); Mar, T.F. and Koenig, J.Q., 2009. Relationship between visits to emergency departments for asthma and O_3 exposure in greater Seattle, Washington. *Annals of Allergy, Asthma & Immunology*, 103(6).

¹⁷ Damages from new childhood asthma cases and childhood ED visits are fully additive; there is no overlap between the populations considered or the endpoints themselves. The childhood asthma ED visits are estimated for the child population with current prevalence of chronic asthma. The new childhood asthma cases are additional changes to the current prevalence and so constitute new chronic childhood onset asthma over and above current prevalence levels.

¹⁸ U.S. Environmental Protection Agency. (2010). Guidelines for preparing economic analyses. Appendix B. Retrieved from <https://www.epa.gov/environmental-economics/guidelines-preparing-economic-analyses>

¹⁹ U.S. Environmental Protection Agency (EPA). (2023). Supplementary Material for the Regulatory Impact Analysis for the Final Rulemaking, "Standards of performance for new, reconstructed, and modified sources and emissions guidelines for

2010. Income elasticity (ϵ) is a user-defined parameter but is set to 1 as default, following Hammitt and Robinson (2011)²⁰ and Rennert et al. (2022), such that projected changes in VSL are proportional to average national income. Due to limited availability of socioeconomic projections, we approximate future changes in income as national GDP per capita, consistent with previous similar studies, using user input (or FrEDI default) projections of U.S. GDP and population.

Morbidity endpoints (incidence of childhood asthma, childhood ED visits, and school loss days) are monetized using U.S. EPA's Benefits Mapping and Analysis Program (BenMAP), which estimates human health impacts and economic value of air quality changes in the atmosphere. For incidence of childhood asthma, valuation in BenMAP is derived from Appéré et al. (2024)²¹, which estimates the mean value of a statistical case of childhood asthma using a marginal willingness to pay per year over a ten-year period. This value reflects the amount a parent is willing to pay to reduce the risk of their child developing a new case of chronic asthma. The mean value of a statistical case of asthma we apply in FrEDI is the U.S.-specific recommended value of \$637,041 (in 2015\$), which is scaled each year with the change in GDP per capita relative to 2010, and an income elasticity of 0.06. For childhood ED visits, valuation in BenMAP is averaged across two studies, for the cost per ED visit due to asthma: Smith et al. (1997)²² and Stanford et al. (1999).²³ Smith et al. (1997) report the average cost per visit to the hospital for treating asthma, for the approximate 1.2 million asthma-related visits in 1987 to get a cost of \$533.69 (in 2015\$). Stanford et al. (1999) builds on Smith et al. (1997) to consider costs or charges by the patient and/or third-party payer for asthma treatments in the ED. The average value used in FrEDI is \$490.11 (2015\$) per ED visit. The valuation used here is consistent with the process of EPA's 2023 report, *Climate Change and Children's Health and Well-Being in the United States* (EPA, 2023; henceforth referred to as the Children's Health Report)—the source of our data—as well as two other CIRA sector studies (Wildfire and Southwest Dust) which averaged the two values.²⁴ ED visit valuation is not scaled with GDP per capita or income elasticity.

Finally, for school loss, valuation in BenMAP is the loss of wages due to an adult caregiver staying home to take care of a sick child. Working caregiver costs are compiled using employers' average cost of wages

existing sources: Oil and natural gas sector climate review, Supplementary Material for the Regulatory Impact Analysis", EPA Report on the Social Cost of Greenhouse Gases: Incorporating Recent Scientific Advances, Retrieved from https://www.epa.gov/system/files/documents/2023-12/epa_scghg_2023_report_final.pdf

²⁰ Hammitt, J. K., & Robinson, L. A. (2011). The income elasticity of the value per statistical life: transferring estimates between high and low income populations. *Journal of Benefit-Cost Analysis*, 2(1); Rennert, K., Errickson, F., Prest, B. C., Rennels, L., Newell, R. G., Pizer, W., et al. (2022). Comprehensive evidence implies a higher social cost of CO₂. *Nature*, 610(7933), 687-692.

²¹Appéré G, Dussaux D, Krupnick A, Travers M. (2024) Valuing a Reduction in the Risk and Severity of Asthma: A Large Scale Multi-Country Stated Preference Approach. *Journal of Benefit-Cost Analysis*. 15(1):14-86. doi:10.1017/bca.2024.4

²² Smith, D. H., D. C. Malone, K. A. Lawson, L. J. Okamoto, C. Battista and W. B. Saunders. 1997. A national estimate of the economic costs of asthma. *Am J Respir Crit Care Med*. Vol. 156 (3 Pt 1): 787-93.

²³ Stanford, R., T. McLaughlin and L. J. Okamoto. 1999. The cost of asthma in the emergency department and hospital. *Am J Respir Crit Care Med*. Vol. 160 (1): 211-5.

²⁴ BenMAP manual (2023) and technical support document (2024) (<https://www.epa.gov/benmap/benmap-ce-manual-and-appendices>) suggest that the costs incurred by the hospital are likely the better measure of visit cost, but for consistency with other CIRA work we average the two values.

including overhead costs and fringe benefits, and non-working caregiver costs are from the opportunity cost of their time calculated as the average take home pay (Chetty et al., 2024²⁵; Liu et al., 2021²⁶). The probability that a parent is working uses the employment population ratio of 77.2 percent resulting in an average caregiver cost of \$305 (in 2015\$) per school loss day due to loss wages (U.S. Bureau of Labor Statistics, 2021b).²⁷ This value is scaled with the change of GDP per capita relative to 2010.

Following Fann et al., (2021), FrEDI also includes two variants for the mortality endpoint only: concentration changes using a 2011 emissions dataset that estimates unrestricted pollution burden from all sources as of that year, and concentration changes using a 2040 emissions dataset that accounts for the implementation of a suite of regulatory policies on stationary and mobile emissions sources.²⁸ These variants were included to assess the sensitivity of the projected climate-driven changes to changes in pollutant precursor emissions (e.g., nitrogen oxides, sulfur dioxide, carbonaceous aerosol, ammonia, etc.).

TABLE B-2. INPUT DATA CHARACTERISTICS: CLIMATE DRIVEN CHANGES IN AIR QUALITY

Data Features	Climate-Driven Changes in Air Quality Attributes
Evaluated Impacts	<ul style="list-style-type: none"> Mortality: premature deaths from O₃ and PM_{2.5} (physical) and value of premature deaths, O₃ and PM_{2.5} (economic) Morbidity: New cases of childhood asthma from O₃ and PM_{2.5} (physical) and value of new cases of childhood asthma (economic) Morbidity: Childhood ED visits from O₃ and PM_{2.5} (physical) and value per visit (economic) Morbidity: School loss days per capita from O₃ (physical) and value of school loss days, O₃ (economic)
Variants	<ul style="list-style-type: none"> 2011 Air Pollutant Emissions Level 2040 Air Pollutant Emissions Level^a
Data Shape	<ul style="list-style-type: none"> Four eras Two CMIP5 GCMs (CCSM4 and GFDL-CM3) 26-km grid cell State level (mortality) County level (morbidity impacts) Two pollutants (O₃ and PM_{2.5})^b
Model Type ²⁹	<ul style="list-style-type: none"> Simulation and Empirical

²⁵ Chetty, R., Friedman, J. N., & Rockoff, J. E. (2014). Measuring the Impacts of Teachers II: Teacher Value-Added and Student Outcomes in Adulthood. *American Economic Review*, 104(9), 2633–2679. <https://doi.org/10.1257/aer.104.9.2633>.

²⁶ Liu, J., Lee, M., & Gershenson, S. (2021). The short- and long-run impacts of secondary school absences. *Journal of Public Economics*, 199, 104441. <https://doi.org/10.1016/j.jpubeco.2021.104441>.

²⁷ US Bureau of Labor Statistics Employment Characteristics of Families, 2021, Table 5.

²⁸ Morbidity endpoints (i.e. all impact types except mortality) are only available for the 2011 emissions inventory variant.

²⁹ The term "empirical" model is used to refer to a statistically estimated relationship between a climate stressor (such as temperature) and a physical or economic impact outcome, based on historical data. Epidemiological and most econometric analyses both fit this model type. The term "simulation" model is used to refer to a process-based or engineering model of a system which uses physical, ecological, or physics-based relationships to model a system of interacting elements which may be influenced by climate or weather variables, such as temperature or precipitation. Simulation models may include or be constructed from certain types of process-based crop yield, air quality, or water quality models; engineering models such as fragility curves; or ecosystem models such as thermally available habitat relationships. Some sector studies may

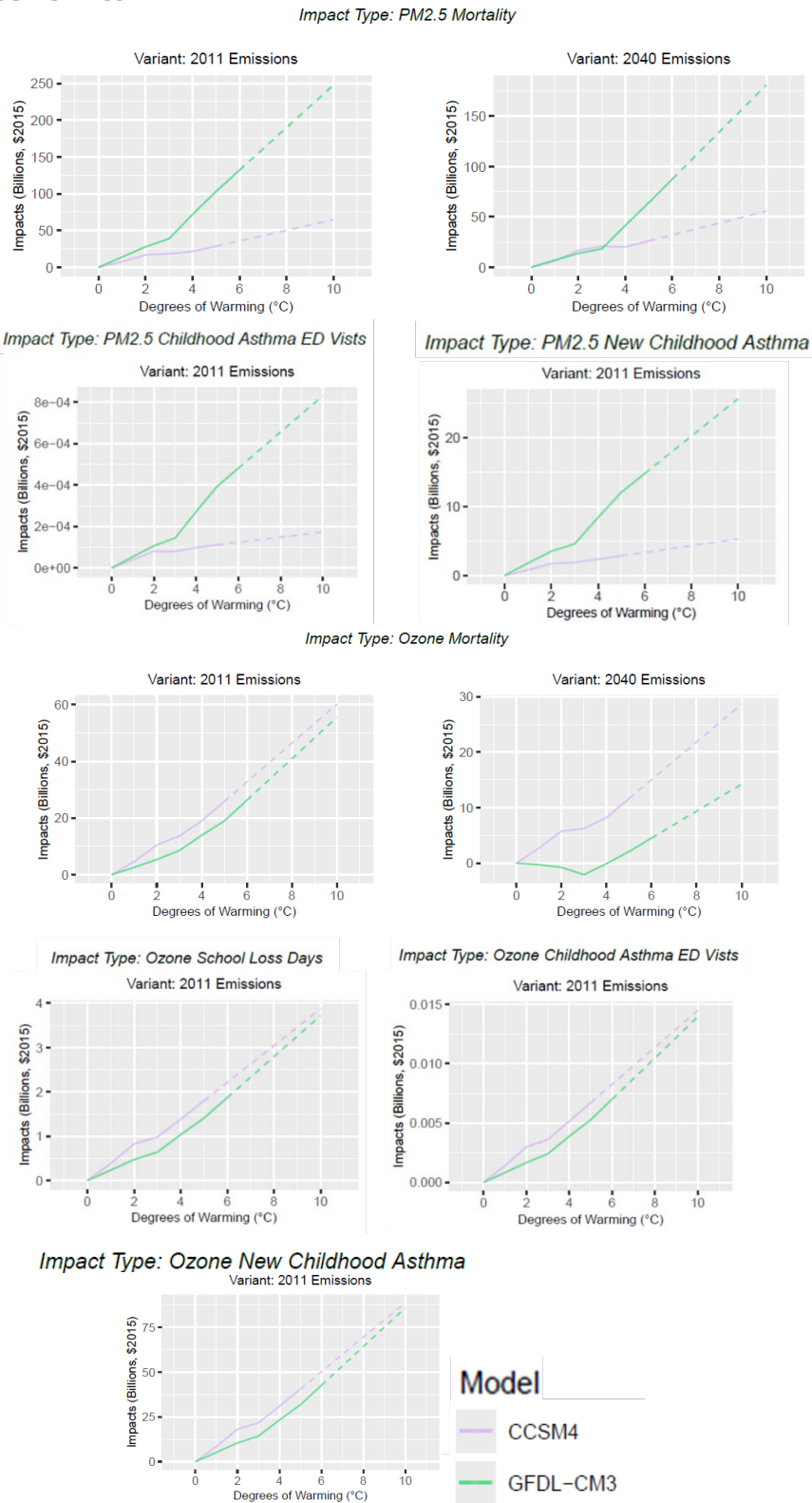
Data Features	Climate-Driven Changes in Air Quality Attributes
Runs Provided	<ul style="list-style-type: none"> With climate change and population growth With climate change and no population growth^c
Additional Data	<ul style="list-style-type: none"> None
Regions and States with Impacts	<ul style="list-style-type: none"> All CONUS regions and states
	<ul style="list-style-type: none"> 2040 Air Pollutant Emissions Level is only available for the Mortality impact. <ul style="list-style-type: none"> School loss days are only measured for O₃ (not PM_{2.5}). 'No population growth' runs are only available for morbidity impacts.

For illustrative purposes, **Figure B-3** shows plots of resulting impacts by temperature degree for PM_{2.5} and O₃, calculated using 2010 (A) and 2090 (B) socioeconomics (the end points of socioeconomics), for the default emission inventory variant.

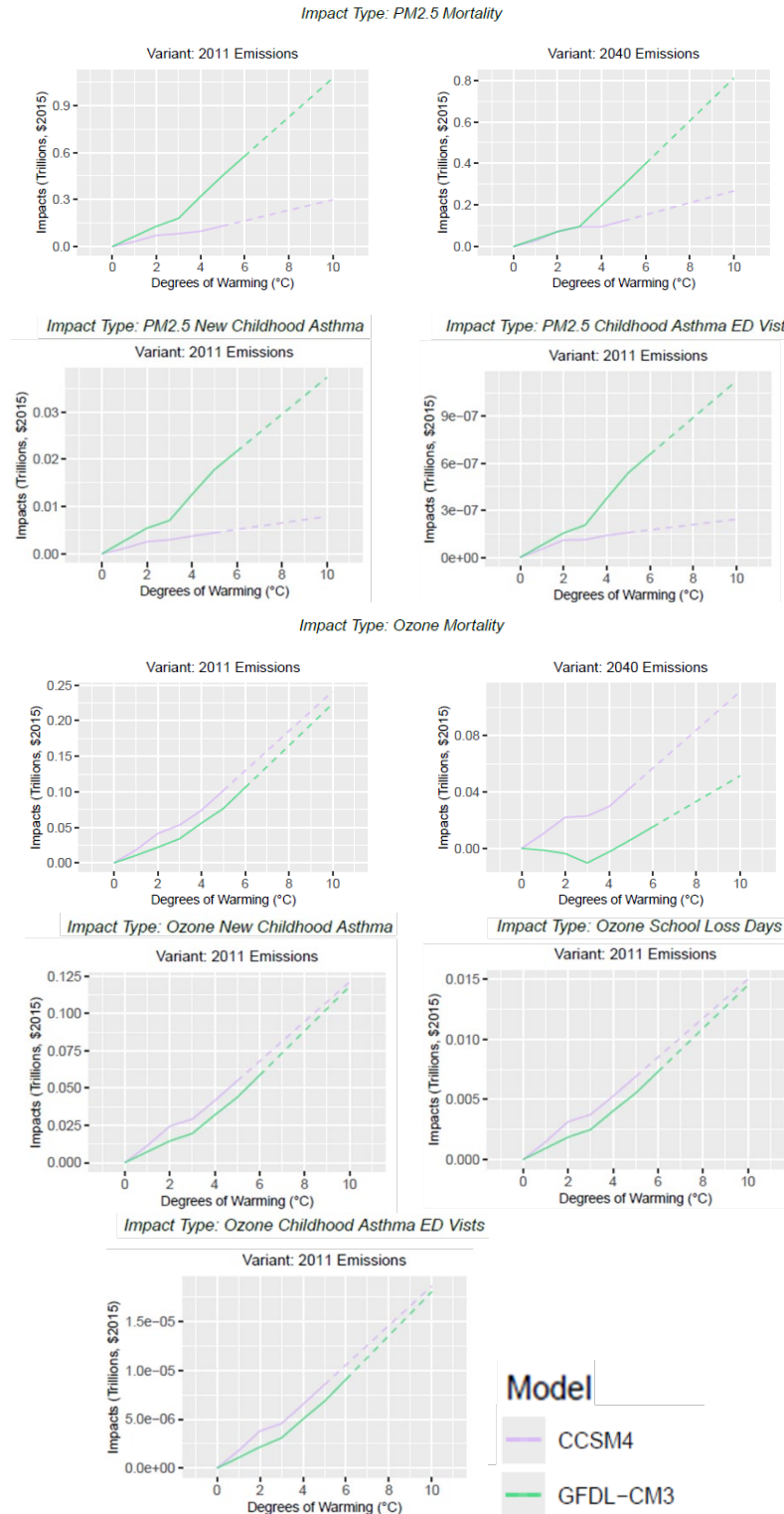
combine use of both models, such as the air quality sector, which incorporates a process-based simulation of air quality with epidemiological functions for health effects estimation. These models are used in simulation exercises within FrEDI as they are applied to future climatic conditions through 2100 or 2300.

FIGURE B-3. AIR QUALITY IMPACTS BY TEMPERATURE BIN DEGREE

A. 2010 SOCIOECONOMICS



B. 2090 SOCIOECONOMICS



Total impacts (trillions of 2015\$) by degree ($^{\circ}\text{C}$) for each impact type and variant (mortality only) for two socioeconomic snapshots (2010 and 2090 default scenarios). Extrapolated portions shown with a dashed line. Note y-axis varies by plot.

Processing steps

Processing steps are illustrated in **Figure B-4**.

Pre-Processing Mortality: The mortality impact is processed differently than the morbidity impacts because of differences in the input data (namely, the morbidity impacts input data includes a run with no population growth). For the mortality impact, to derive impact-by-degree-damage functions, EPA's BenMAP – Community Edition (BenMAP-CE³⁰) is first used to generate total mortality results using the same data inputs as from Fann et al. (2021). For example, the air quality exposure data (for each 36-km CONUS grid cell) was provided by study authors by era, GCM, pollutant ($O_3/PM_{2.5}$), and emissions inventory (2011/2040). This exposure data is available for four eras (2030, 2050, 2075, 2095), derived from two CMIP5 climate models (CCSM4 and GFDL-CM3). Concentration-response functions used within BenMAP-CE to derive mortality counts from air pollutant exposure levels are also the same as those used in Fann et al. (2021), which are based on risk model information for those age 30-99 for $PM_{2.5}$ and those age 0-99 for O_3 . Therefore, to derive total mortality estimates for FrEDI (1st pre-processing step in the mortality diagram in **Figure B-4**), BenMAP-CE was used with these study data inputs to derive mortality impacts at the state level for each era, GCM, pollutant, and emissions inventory scenario.

In the second pre-processing step for mortality (second box in **Figure B-4**), total mortality is divided by dynamic state population from the Integrated Climate and Land Use Scenarios, v2 (ICLUSv2) dataset³¹, to acquire per capita mortality estimates for each era and state. The original exposure levels provided in Fann et al., (2021) already account for baseline mortality rates and therefore no additional processing was needed to isolate climate impacts for use in FrEDI. In the last pre-processing step (fourth box in **Figure B-4**), era-level per capita mortality impacts are assigned to the central year of the era (i.e., 2030, 2050, 2075, and 2095), and impacts for remaining years are derived by interpolating linearly between central era years. Finally, to bin the results by temperature degree and derive impact-by-degree functions, the yearly per capita impacts for each pollutant impact type ($O_3/PM_{2.5}$) are averaged across the 11-year windows where each GCM reaches each integer degree of CONUS warming relative to the baseline

Pre-processing Morbidity: For the childhood-specific morbidity impacts, these follow similar pre-processing steps as the total population mortality impact. Childhood-specific impacts were estimated in EPA (2023) based on the air quality results of Fann et al. (2021) by era, county, GCM, pollutant ($O_3/PM_{2.5}$), and impact (new incidence of childhood asthma, childhood ED visits, and school loss days). This set of impacts only uses the 2011 emissions inventory. Like the mortality impact, exposure data is available for four eras (2030, 2050, 2075, 2095), derived from two CMIP5 climate models (CCSM4 and GFDL-CM3). Incidence of childhood asthma uses risk model information for those age 0-17 for both O_3 and $PM_{2.5}$, childhood ED visits

³⁰ Sacks JD, Lloyd JM, Zhu Y, et al. The Environmental Benefits Mapping and Analysis Program—Community Edition (BenMAP-CE): a tool to estimate the health and economic benefits of reducing air pollution. Environ Model Softw. 2018;104:118-129. doi:10.1016/j.envsoft.2018.02.009

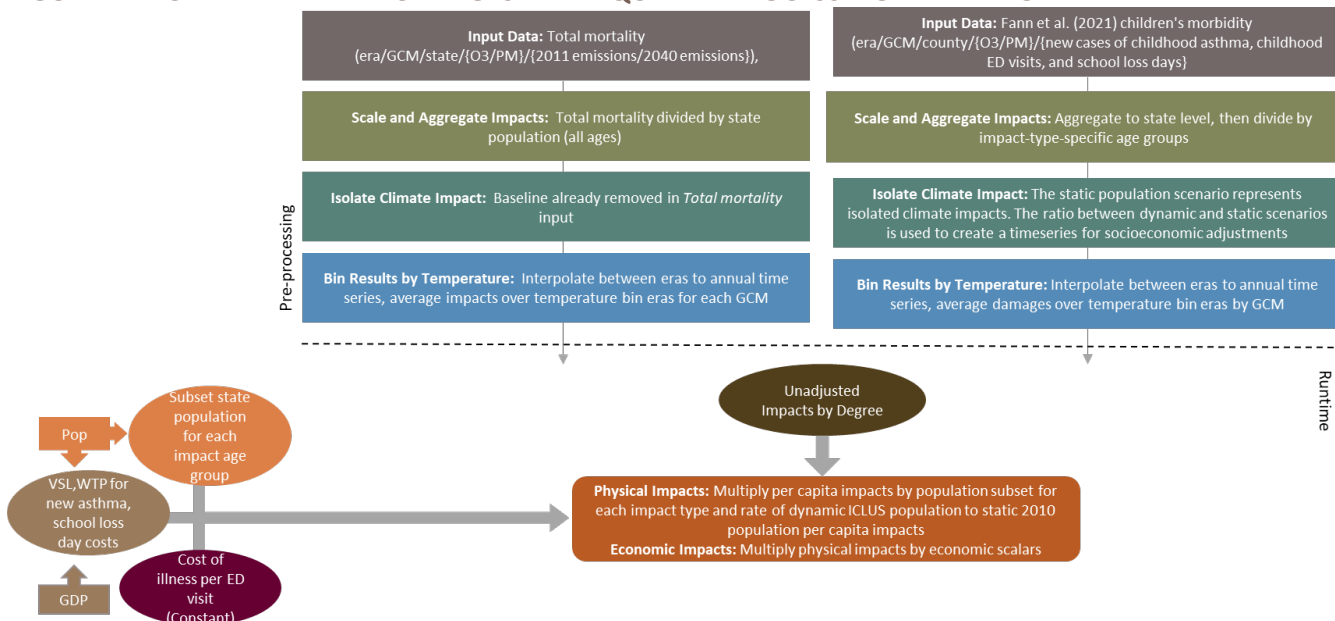
³¹ Bierwagen, B., Theobald, D.M., Pyke, A., Choate, A.P., Thomas, J.V., Morefield, P., 2010. 2010: National housing and impervious surface scenarios for integrated climate impact assessments. Proc. Natl. Acad. Sci. 107; EPA, 2017. Updates to the Demographic and Spatial Allocation Models to Produce Integrated Climate and Land Use Scenarios (ICLUS) (Version 2)

uses information for those age 0-17 for O₃ and 0-18 for PM_{2.5}, and school loss days use information for those age 5-17 for O₃. As shown in **Figure B-4**, total number of cases at the county level are provided for each era, GCM, pollutant, and impact for two population scenarios (dynamic and static populations). The number of cases and county-level population for each year in each population scenario are interpolated to get an annual timeseries before summing to the state level and dividing by population to get impact rates. We then temperature bin the results associated with the static 2010 population.

We generate a scalar that takes the ratio of impact rates in the dynamic population scenario to the static 2010 population rate to represent demographic changes on the projected impact rates for morbidity. This accounts for implicit assumptions about how the relative weights of each age bins change over time. We also create a scalar of the ratio of the relevant population for each morbidity endpoint³² compared to the total population by year and state using the ICLUSv2 projections, which is the basis of FrEDI's default population scenario and the morbidity analyses.

Scaled impacts are checked for consistency against the Children's Health Report, which runs a similar analysis for number of cases by degree.

FIGURE B-4. CLIMATE-DRIVEN CHANGES IN AIR QUALITY PROCESSING FRAMEWORK



Runtime: When FrEDI is run, the pre-processed by-degree per capita impacts are then applied to the input temperature scenario to calculate the unadjusted annual per capita impacts based on the level of warming in each year of the input scenario. The total annual physical counts are then calculated by applying these annual per capita rates, to the input population scenario multiplied by the proportion of total population

³² Relevant populations are age 0 to 17 for ED visits - O₃, new childhood asthma – O₃ and PM_{2.5}; age 0 to 18 for ED visits – PM_{2.5}; and age 5 to 18 for school loss days.

affected by each impact (e.g. new childhood asthma is only applied to the proportion of the total population that are children). For morbidity impacts, populations are adjusted to account for changes in population demographics overtime.

Lastly, physical impacts are monetized. Annual mortality counts are monetized using the VSL, calculated at runtime from input GDP per capita. VSL is adjusted for changes in GDP per capita using an income elasticity function³³ (Eq. B-1):

$$VSL_t = VSL_{2010} \times \left(\frac{GDPcap_t}{GDPcap_{2010}} \right)^{\text{elasticity}} \quad (\text{Equation B-1})$$

Morbidity impacts apply the values as described in the summary section. The value of incidence of childhood asthma are scaled with changes in GDP per capita relative to 2010, and a different income elasticity specific to childhood asthma valuation (0.06); childhood ED visits apply a constant value over time to each visit; and school loss days lost wages are scaled with GDP per capita relative to 2010.

Limitations and Assumptions

- PM_{2.5}-attributable premature mortality is quantified for those age 30 and older. Assuming zero impacts for those under 30 underestimates the risk of premature mortality experienced by this age group. This also assumes that age demographics remain proportional over the century.
- This analysis quantifies ED visits associated with O₃, and new childhood asthma associated with PM_{2.5} for those age 0-17 as well as ED visits associated with PM_{2.5} for those age 0-18, assuming the impacts for those over the included ages to be zero. Doing so underestimates the risk of morbidity experienced by the total population and misses out on quantifying other morbidity endpoints (e.g., hospital admissions and outpatient visits for respiratory diseases and cardiovascular conditions).
- School loss days are only quantified for parents with children ages 5-18; this underestimates the impact for parents with children age under 5.
- There is limited epidemiological literature specifically on children's health effects of air pollution. This analysis relies on standard health functions used by the U.S. EPA for regulatory impacts analyses that are relevant to children. Children are likely to experience additional morbidity and mortality effects that are not quantified by this analysis.
- A broader literature exists on the effects of air quality on morbidity, but was not included in the underlying study and so is omitted here. Some of those morbidity impacts are considered in other FrEDI impacts, such as the Wildfire and Southwest Dust categories but were not included here. This analysis therefore underestimates the full effect of air quality on health outcomes.
- Respiratory health may degrade for other climate-related reasons – the combined effect of multiple stressors may be larger than individual impacts. The health effects presented for this impact are associated with changes in air quality linked with exposure to O₃ and PM_{2.5}. Respiratory health is

³³ This is a generic elasticity function that can be used in a time-series fashion, as used here, or for cross-sectional benefits transfers, as in the example in Masterman and Viscusi (2018), "The Income Elasticity of Global Values of a Statistical Life: Stated Preference Evidence", Journal of Benefit-Cost Analysis, 9(3):407-434. The current default elasticity is 1.0 but can be set by the user as an input to the R code.

- likely to worsen among individuals exposed to air pollution for other climate-induced reasons, including changes and shifts in plant pollen production, that also affect respiratory health.
- For further discussion of the limitations and assumptions in the underlying sectoral modeling approaches, see Fann et al. (2021) and EPA (2023).

Extreme Temperature

Summary

This sector estimates the impact of extreme temperature on premature mortality in 49 major U.S. cities. In the 2010 Census, these 49 cities accounted for 91.3 million of the total U.S. population of 309.3 million, or nearly 30 percent. Economic damages are based on extreme heat and cold mortality rates, monetized by applying GDP per capita-adjusted VSLs. Note: there are multiple study options for quantifying temperature-related mortality in FrEDI; other study options are explained in the following sections, “CIL Temperature-Related Mortality” and “ATS Temperature-Related Mortality.” The default for FrEDI is the ATS Temperature-Related Mortality, which represents the broadest consensus among the three options regarding the relevant temperature response function, from a diverse group of co-authors, and is also used in other frameworks similar to FrEDI (e.g., the GIVE framework³⁴).

This “Extreme Temperature” study is unique from the other two temperature-health impact studies in FrEDI because it is based on geographically differentiated city-specific response functions, using a daily event-based approach which is indexed to historical patterns and temperature anomalies for both high and low temperatures. Extremely hot days are defined as those with a daily minimum temperature warmer than 99 percent of the days in the reference period (1989-2000) and that are at least 20°C (68°F). Extremely cold days are defined as those with a daily maximum temperature colder than 99 percent of the days in the reference period (1989-2000) and do not exceed 10°C (50°F). As a result, and consistent with the other two studies, the Mills et al. (2014) study explicitly considers changes in both warm season and cold season effects, but this study also provides differentiated estimates rather than a net estimate. The Mills et al. (2014) study as implemented in FrEDI also includes a ‘with adaptation’ variant that does not reflect a benefit-cost calculation but an assumption that U.S. cities will gradually adapt to a hotter environment

UNDERLYING DATA SOURCES AND LITERATURE

Mills, D., Schwartz, J., Lee, M., Sarofim, M., Jones, R., Lawson, M., Duckworth, M., & Deck, L. (2014). Climate Change Impacts on Extreme Temperature Mortality in Select Metropolitan Areas in the United States. *Climatic Change*, 131, 83-95. <https://doi.org/10.1007/s10584-014-1154-8>

U.S. EPA. (2017). “Multi-Model Framework for Quantitative Sectoral Impacts Analysis: A Technical Report for the Fourth National Climate Assessment.” (EPA 430-R-17-001) <https://www.epa.gov/cira/multi-model-framework-quantitative-sectoral-impacts-analysis>

³⁴ Rennert, K., Errickson, F., Prest, B. C., Rennels, L., Newell, R. G., Pizer, W., Kingdon, C., Wingenroth, J., Cooke, R., Parthum, B., Smith, D., Cromar, K., Diaz, D., Moore, F. C., Müller, U. K., Plevin, R. J., Raftery, A. E., Ševčíková, H., Sheets, H., ... Anthoff, D. (2022). Comprehensive evidence implies a higher social cost of CO₂. *Nature*, 610(7933), 687–692.

<https://doi.org/10.1038/s41586-022-05224-9>

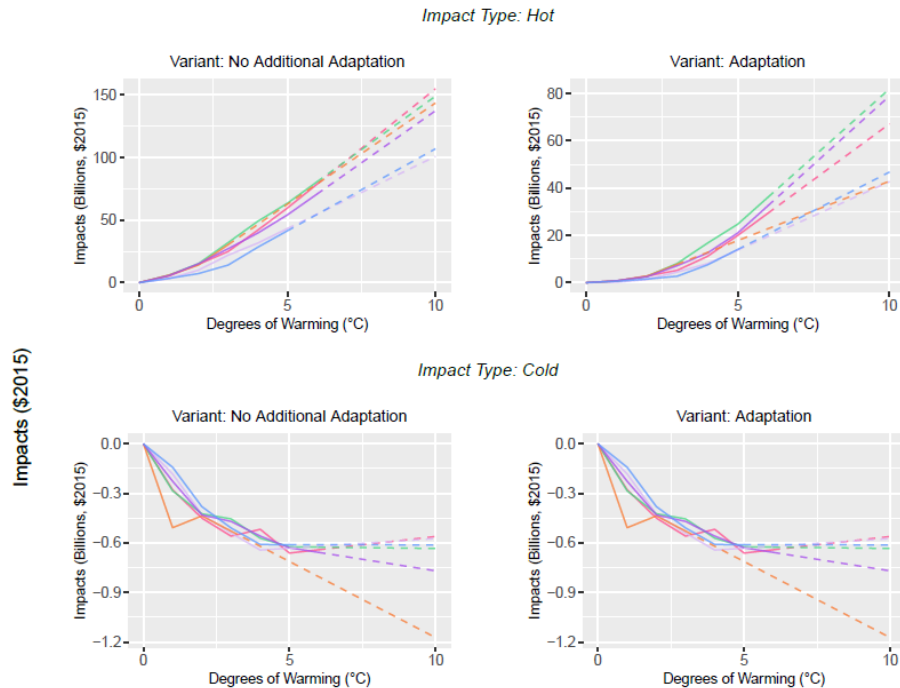
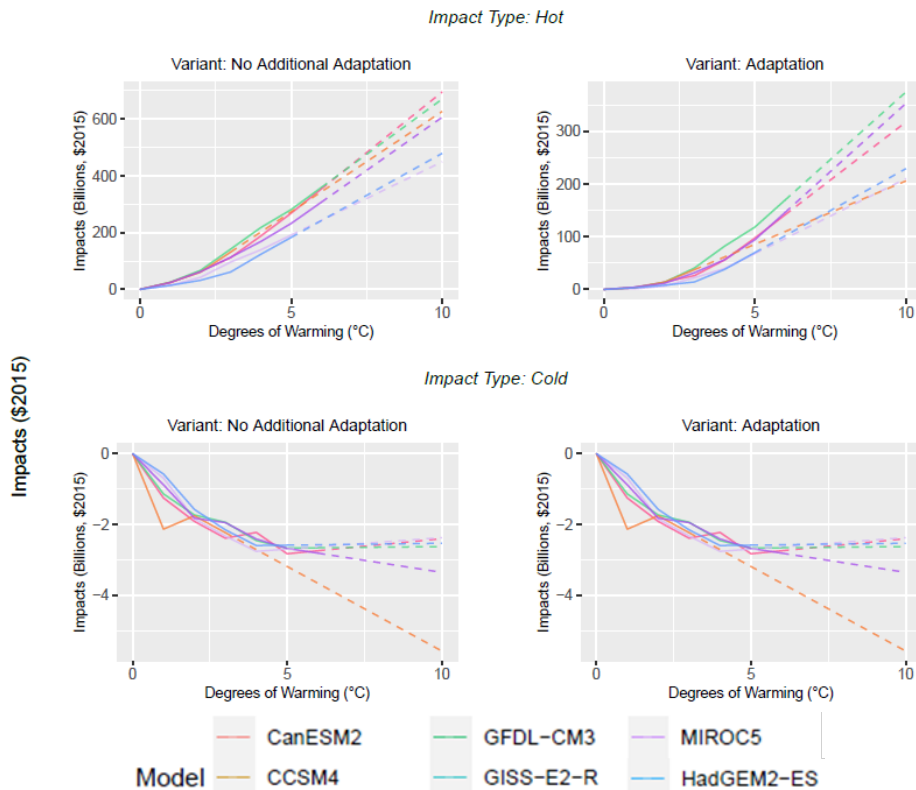
through physical acclimatization of their residents, infrastructure replacement with more heat suitable shading and air conditioning, and behavioral changes, so that the stressor-response will look like that of the current Dallas context.³⁵ The original Mills et al. (2014) spatial and population domain, however, is limited to 33 cities, which was expanded in EPA (2017) to include 49 cities, so it accounts for exposures to roughly one-third of the total U.S. population.

TABLE B-3. INCOMING DATA CHARACTERISTICS: EXTREME TEMPERATURE

Data Features	Extreme Temperature Attributes
Evaluated Impacts	<ul style="list-style-type: none"> Mortality: premature deaths associated with extreme temperature per capita (physical) and value of premature deaths (economic)
Variants	<ul style="list-style-type: none"> Adaptation No additional adaptation
Data Shape	<ul style="list-style-type: none"> Degree Six GCMs (standard CIRA set) Two variants Two impact years City level
Model Type	<ul style="list-style-type: none"> Empirical
Runs Provided	<ul style="list-style-type: none"> 2010 population with climate change 2090 population with climate change
Additional Data	<ul style="list-style-type: none"> Baseline mortality by state
Regions and States with Impacts	<ul style="list-style-type: none"> Midwest (excluding IA) Northeast (excluding DE, ME, NH, RI, VT, WV) Northwest (excluding ID) Southeast (excluding AR, KY, MS, SC, VA) Southern Plains (excluding KS) Southwest (excluding NV)

For illustrative purposes, **Figure B-5** shows the resulting damages by degree of warming for both the extreme heat and cold related mortality variants (top and bottom panels), both adaptation scenarios (left and right plots), and six GCMs, calculated using 2010 (panel A) and 2090 (panel B) socioeconomics (i.e., the endpoints of the socioeconomic scenarios).

³⁵ The adaptation scenario was considered in Mills et al. (2014) and U.S. EPA. (2017). More refined adaptation scenarios for this sector, including the costs and efficacy of increased air conditioning market penetration, are the subject of active and ongoing research. Some research has found the efficacy of cooling centers can be high in preventing extreme heat mortality, but surveys and current experience suggest that many residents are unwilling to use formal cooling centers. For at least some of the cities evaluated in Mills et al. (2014), the empirical data reflects the availability, if not the widespread use, of cooling centers to residents.

FIGURE B-5. EXTREME TEMPERATURE IMPACTS BY TEMPERATURE BIN DEGREE
A. 2010 SOCIOECONOMICS

B. 2090 SOCIOECONOMICS


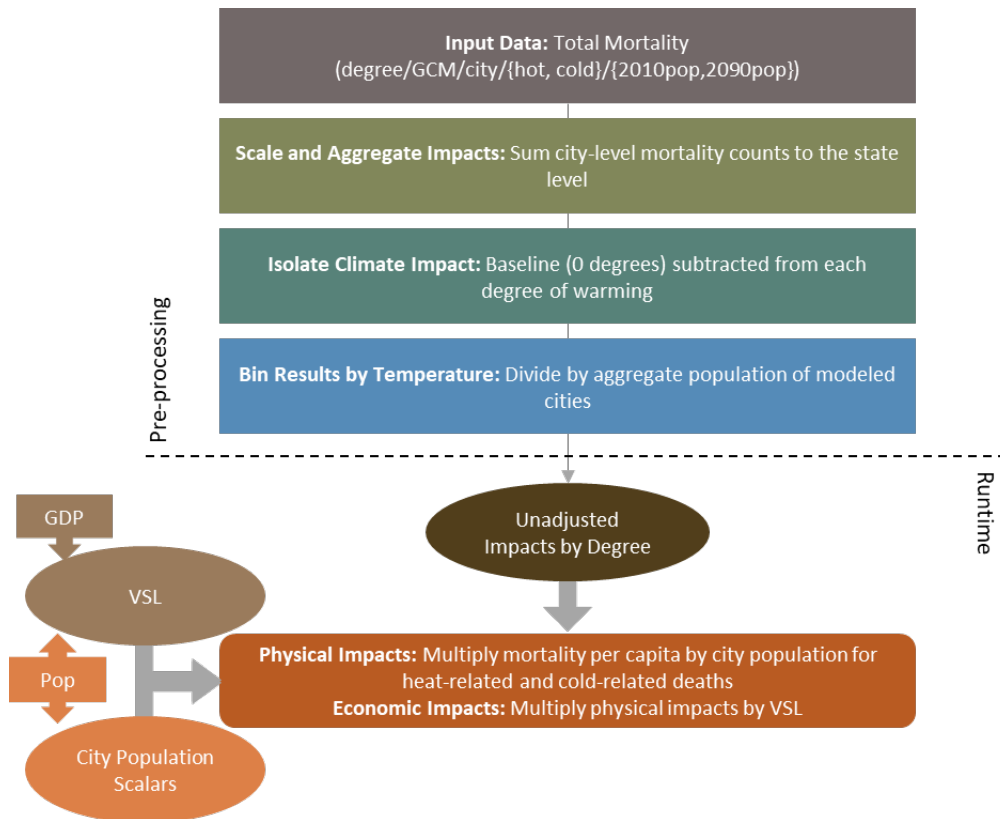
Total impacts (\$billions of 2015\$) by degree ($^{\circ}\text{C}$) for each impact type and variant for two socioeconomic snapshots (2010 and 2090 default scenarios). Extrapolated portions are shown with a dashed line. Note y-axis scales vary by plot.

Processing steps

Processing steps are shown in **Figure B-6**.

Pre-processing: Total mortality data are provided by the study authors by *degree, GCM, city, damage type (heat/cold mortality), and base population (2010/2090)*. These original city-level mortality counts are then summed to counts for each CONUS state. In the next pre-processing step, the incremental impacts of climate change are isolated by subtracting baseline mortality counts from the counts in each degree bin. The original model in Mills et al. (2014) was run under two constant population assumptions: 2010 and 2090 estimates from ICLUSv2³⁶, which vary in total population and the distribution of population across modeled cities. In the third pre-processing step, state mortality counts from the two population scenarios (and for hot and cold impacts and two adaptation scenarios) are divided by population for the modeled cities in each state to obtain a mortality per capita estimate for each population scenario (2010/2090) by state, GCM, adaptation variant, and extreme heat and cold impact type. The last step is to calculate a population scalar to account for the fraction of each state's population living in the 49 study cities, by taking the ratio of the modeled city population to the total state population from ICLUSv2 (i.e., FrEDI default population scenario) for each state in 2010 and 2090.

FIGURE B-6. EXTREME TEMPERATURE DATA PROCESSING FRAMEWORK



³⁶ Bierwagen et al., 2010; ICLUSv2, 2017 (see footnote 31)

Runtime: When FrEDI is run, the pre-processed, by-degree per capita mortality functions are applied to the input temperature scenario to calculate the unadjusted annual per capita impacts based on the level of warming in each year of the input scenario. The total annual physical mortality counts are then calculated by applying these annual per capita rates to the input population scenario. State population inputs are translated to city populations using the population scalars derived from the ICLUSv2 population scenarios in 2010 and 2090 and interpolated for years in between. Lastly, annual mortality counts are monetized using the VSL, calculated at runtime from input GDP per capita (Eq. B-1).

Limitations and Assumptions

- National per capita averages are based on the total population of modeled cities with extreme heat and cold impacts. There are certain cities in the Southeast (Atlanta, Broward-Ft. Lauderdale, Miami, and Orlando), Southern Plains (Austin and Dallas), and Southwest (Albuquerque, Los Angeles, Phoenix, and San Diego) regions that are modeled for adaptation to heat but are not modeled for adaptation to extreme cold. It is assumed that these cities have minimal extreme cold damages, and therefore their populations are included in the denominator as part of the total population over which cold damages are averaged.
- This analysis only considers health impacts to individuals living in 49 cities within the CONUS and therefore omits a large fraction of the population vulnerable to extreme temperatures.
- Cities that only experienced extreme cold in the historic period, notably those in the Northwest region, do not show an increase in extreme-temperature related mortality in this analysis. This result is an artifact of the methodology, which relies on observed temperature thresholds based on a historic period. With increased temperatures, it is likely that many of these Northwestern cities could experience heat-related mortality as well, which might be reflected if a different impact estimation methodology had been applied.
- This analysis does not include morbidity outcomes. While the valuation of mortality far outweighs morbidity outcomes, morbidity is a common outcome associated with extreme heat and cold.
- For further discussion of the limitations and assumptions in the underlying sectoral model, please see Mills et al. (2014) and U.S.EPA (2017).

CIL Temperature-Related Mortality

Summary

This sector estimates the impact of climate-driven temperature changes on premature mortality across all of CONUS. Note: there are multiple study options for quantifying temperature-related mortality in FrEDI. The default for FrEDI is the ATS Temperature-Related Mortality, which represents the broadest consensus among the three options regarding the relevant temperature response function, from a diverse group of co-authors, and is also used in other frameworks similar to FrEDI (e.g., the GIVE framework³⁷).

UNDERLYING DATA SOURCES AND LITERATURE

Deschênes, O., Greenstone, M. (2011). Climate Change, Mortality, and Adaptation: Evidence from Annual Fluctuations in Weather in the US. *American Economic Journal: Applied Economics* 3(4): 152–185. <https://doi.org/10.1257/app.3.4.152>

Barreca, A., Clay, K., Deschênes, O., Greenstone, M., Shapiro, J. S. (2016). Adapting to Climate Change: The Remarkable Decline in the US Temperature-Mortality Relationship over the Twentieth Century. *J. Polit. Econ.* 124, 105–159. <https://doi.org/10.1086/684582>

Hsiang, S., Kopp, R., Jina, A., Rising, J., Delgado, M., Mohan, S., Rasmussen, D. J., Muir-Wood, R., Wilson, P., Oppenheimer, M., Larsen, K., Houser, T. (2017) Estimating economic damage from climate change in the United States *Science* 356: 1362–1369. <https://www.doi.org/10.1126/science.aal4369>

The Climate Impact Lab (CIL) Temperature-Related Mortality estimates rely on the development of a function linking extreme temperatures to excess mortality rates, using a method first established in Deschenes and Greenstone (2011), updated in Barreca et al. (2016), and refined to develop projections of future impacts by GCM and RCP through the 21st century in Hsiang et al. (2017). This CIL Temperature-related Mortality estimate provides two improvements over the Mills et al., (2014) Extreme Temperature option. First, the CIL estimate provides full coverage of all CONUS locations and populations, and as a result this work addresses temperature-related mortality for a population approximately three times larger than the Mills et al. (2014) work. Second, the estimates include uncertainty measures, important for this largest of the economic impact categories in FrEDI. It is in many ways comparable to the ATS Temperature-Related Mortality estimate, but likely reflects a somewhat older empirical basis for the mortality function than the ATS study team relied on.

Economic damages are based on the net effect of extreme heat and cold mortality rates, monetized by applying the VSL. Although the original Hsiang et al. (2017) application held VSL constant through time, the VSL used in FrEDI changes as a function of annual per capita income. As shown in Hsiang et al. (2017), consideration of the net effect of changes in both cold and heat related mortality results in a net increase in mortality rates attributed to temperature changes in southern areas of CONUS, and a net decrease in mortality rates in northern areas of CONUS. As in Hsiang et al. (2017), we rely on the premature mortality estimates dose response function derived from survival function components of the Deschenes and Greenstone (2011) paper (i.e., the mortality dose response function with respect to temperature) and apply a VSL consistent with the FrEDI framework (Eq. B-1). The willingness-to-pay valuation component in Deschenes and Greenstone (2011) was not adopted for this work.

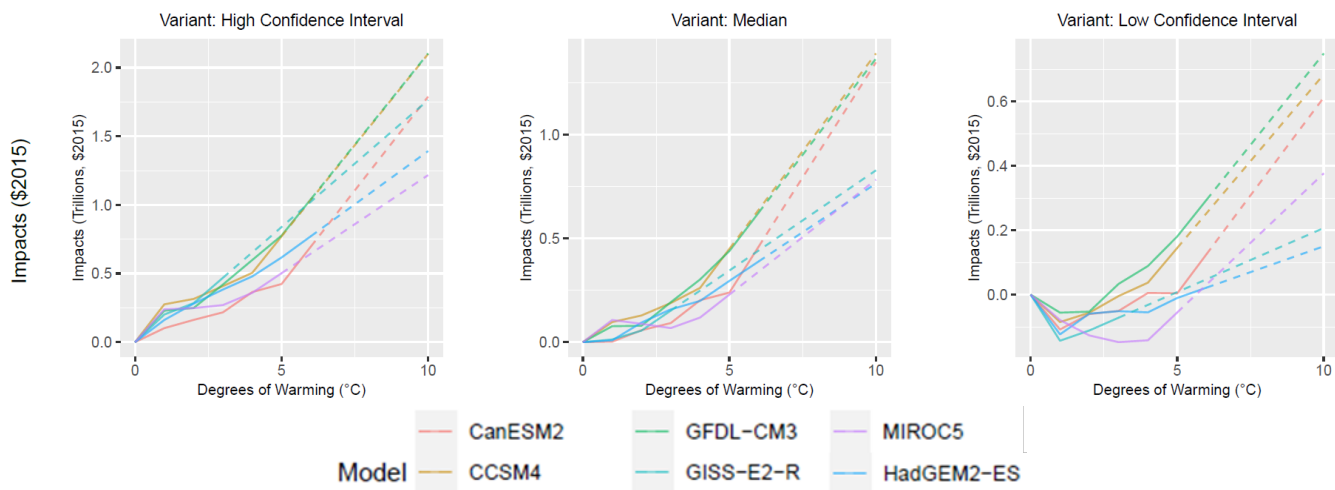
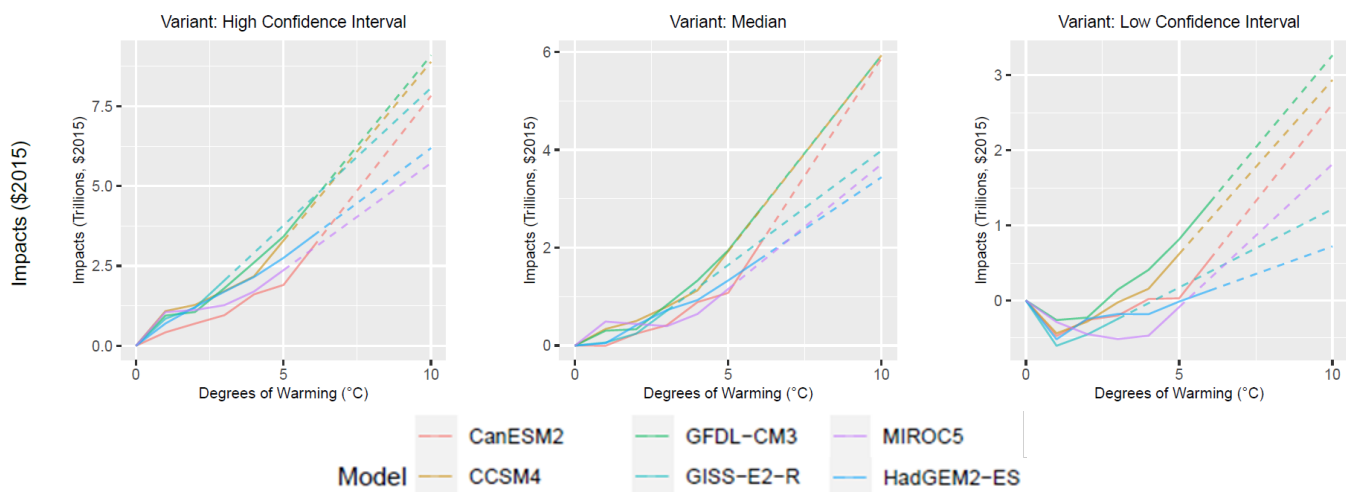
³⁷ Rennert et al., (2022) (see footnote 34)

To date, the CIL study authors have shared data for the “without additional adaptation” scenario, which is currently included in FrEDI. FrEDI results from this sector study therefore reflect damages when considering current rates of air conditioning penetration. We anticipate that future revisions of FrEDI could incorporate a “with adaptation” variant from this sector study, based in part on the findings of Barreca et al. (2016) that show a large impact of air conditioning in reducing the rate of heat-related mortality in the historical (1900–2004) period, with extensions to forecast air conditioning penetration rates. The CIL study authors also shared results from uncertainty modeling in the underlying work, which were used to develop two additional damage functions for FrEDI that reflect the 90 percent confidence interval of the damages. Therefore, physical and economic damages from this study in FrEDI are available for the low and high end of the confidence interval (5th and 95th percentile values) as well as a central estimate which corresponds to the median result (50th percentile).

TABLE B-4. INCOMING DATA CHARACTERISTICS: CIL TEMPERATURE-RELATED MORTALITY

Data Features	CIL Temperature-Related Mortality Attributes
Evaluated Impacts	<ul style="list-style-type: none"> Mortality: temperature-related premature deaths per capita (physical) and value of premature deaths (economic)
Variants	<ul style="list-style-type: none"> Median Low confidence interval High confidence interval
Data Shape	<ul style="list-style-type: none"> Year Six GCMs (standard CIRA set) Three variants State level
Model Type	<ul style="list-style-type: none"> Empirical
Runs Provided	<ul style="list-style-type: none"> Without socioeconomic growth and with climate change
Additional Data	<ul style="list-style-type: none"> Baseline mortality by state
Regions and States with Impacts	<ul style="list-style-type: none"> All CONUS regions and states

For illustrative purposes, **Figure B-7** shows a summary of the damages by degree of warming for the median and low and high confidence intervals, by GCM and for both 2010 (panel A) and 2090 (panel B) socioeconomics (i.e., the endpoints of the socioeconomic scenarios).

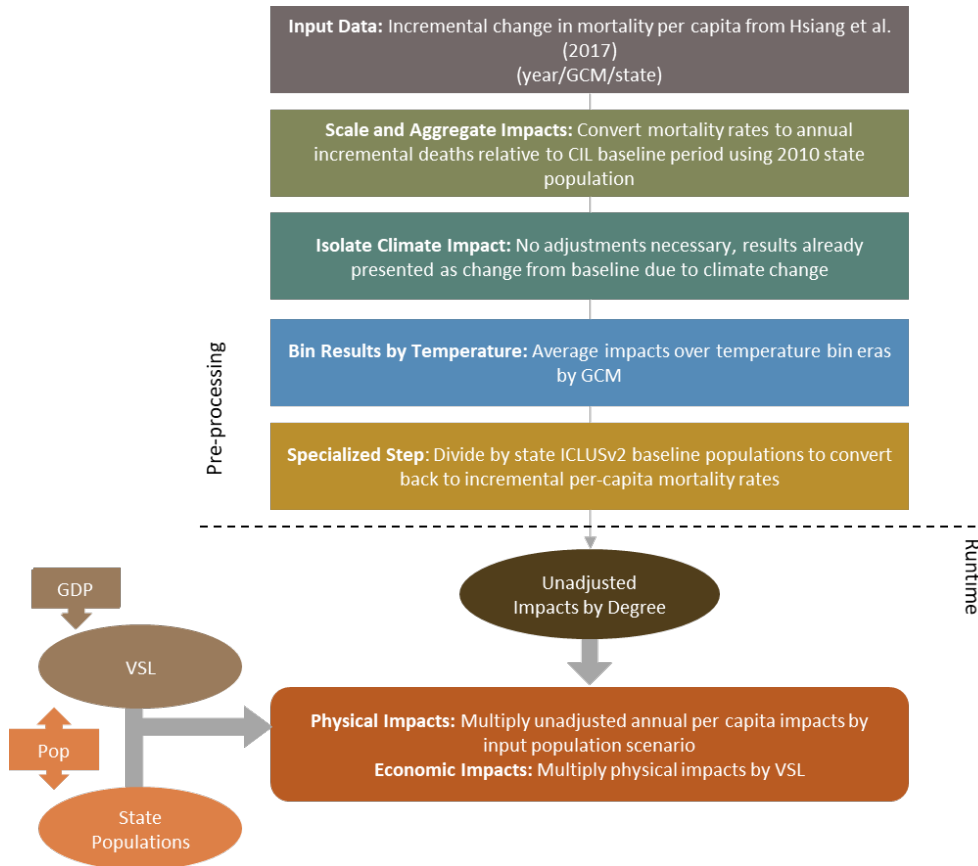
FIGURE B-7. CIL TEMPERATURE-RELATED IMPACTS BY TEMPERATURE BIN DEGREE**A. 2010 SOCIOECONOMICS****B. 2090 SOCIOECONOMICS**

Total impacts (trillions of 2015\$) by degree (°C) for each variant for two socioeconomic snapshots (2010 and 2090 default scenarios). Extrapolated portions are shown with a dashed line. Note y-axis scales vary by plot.

Processing steps

Processing steps are shown in **Figure B-8**.

Pre-processing: The Hsiang et al. (2017) study authors provided data on the incremental net change in per capita mortality under the RCP 8.5 scenario, by GCM, year, and state. These results reflect a single base socioeconomic scenario in 2012. Results are converted to annual incremental deaths due to temperature increases projected with climate change. The incoming results represent excess deaths due to temperature increases projected with climate change so no adjustment for the baseline is necessary. These data are then binned by degree by averaging across the 11-year windows where each GCM reaches each integer degree of CONUS warming relative to the baseline. Finally, total deaths are converted back to mortality rates, the scaled damage entered into FrEDI, using the ICLUSv2 populations.

FIGURE B-8. CIL TEMPERATURE-RELATED MORTALITY DATA PROCESSING FRAMEWORK

Runtime: When FrEDI is run, the pre-processed by-degree per capita mortality functions are then applied to the input temperature scenario to calculate the unadjusted annual per capita impacts based on the level of warming in each year of the input scenario. The total annual physical mortality counts are then calculated by applying these annual per capita rates to the input population scenario. Lastly, annual mortality counts are monetized using the VSL, calculated at runtime from input GDP per capita (Eq. B-1).

Limitations and Assumptions

- The estimates included in FrEDI reflect a scenario of current air conditioning penetration rates, without expansion of air conditioning to mitigate health risks, consistent with the results initially shared by the study authors. When results that reflect additional adaptation effort are shared, results for enhanced adaptation will be incorporated in future revisions of the tool.
- The underlying studies focus on extreme temperature mortality impacts, and as noted in Deschenes and Greenstone (2011) excludes impacts of extreme temperature on morbidity, so likely underestimates the full effect of temperature on health.
- The Hsiang et al. (2017) work includes adjustments to climate damages associated with general equilibrium impacts. While the general equilibrium effects estimate in that paper shows a lower economic impact for mortality when compared to the direct impact included in FrEDI, as the authors note, the general equilibrium approach omits the large component of willingness to pay to

avoid mortality risk that is captured in the VSL. For this reason, as in the underlying study, we omit the general equilibrium adjustment for mortality impacts.

- The potentially broad scope of the mortality impact linked to temperature increases in the Hsiang et al. (2017) mortality analysis introduces the potential for overlap with some other sectoral results that associate temperature increases with mortality, most notably the Suicide sector. The reader is referred to Section 2.2, under the header Aggregation of Sectoral Impacts, for guidance on interpreting applications of FrEDI that include both of these sectors.
- For further discussion of the limitations and assumptions in the underlying sectoral model, please see Deschenes and Greenstone (2011) and Hsiang et al. (2017).

ATS Temperature-Related Mortality

Summary

This sector estimates the impact of climate-driven change in temperature on premature mortality across all the CONUS. Note: there are multiple study options for quantifying temperature-related mortality in FrEDI. The default for FrEDI is this ATS Temperature-Related Mortality study. The main advantage of this study is that represents the broadest consensus among the three options regarding the relevant temperature response function, from a diverse group of co-authors, and is also used in other frameworks similar to FrEDI (e.g., the GIVE framework³⁸). In

addition, the ATS Temperature-Related Mortality estimates provide a direct means for the FrEDI project team to apply as inputs the same county-level baseline and projected mortality rates used in other FrEDI studies, such as the Air Quality and other health sector studies.

The American Thoracic Society (ATS) Temperature-Related Mortality study developed a mortality impact function using meta-analysis of seven previously published U.S. studies of the connection between temperature change and excess mortality rates, as well as other non-U.S. studies for results in other countries. The result of the meta-analysis is a set of globally applicable, region-specific impact functions calibrated to changes in average annual temperature. Based on guidance from the lead study author, we interpret the relevant average annual temperature to be a locally experienced exposure (i.e., CONUS temperature), which is also consistent with the relevant exposure metric applied in the seven U.S. studies to which the USA region results are calibrated. For this work, we rely on the estimates for the USA region

UNDERLYING DATA SOURCES AND LITERATURE

Cromar, K. R., Anenberg, S. C., Balmes, J. R., Fawcett, A. A., Ghazipura, M., Gohlke, J. M., Hashizume, M., Howard, P., Lavigne, E., Levy, K., Madrigano, J., Martinich, J. A., Mordecai, E. A., Rice, M. B., Saha, S., Scovronick, N. C., Sekercioğlu, F., Svendsen, E. R., Zaitchik, B. F., & Ewart, G. (2022). Global Health Impacts for Economic Models of Climate Change: A Systematic Review and Meta-Analysis. *Annals of the American Thoracic Society*, 19(7), 1203–1212.

<https://doi.org/10.1513/AnnalsATS.202110-1193OC>

Rennert, K., Errickson, F., Prest, B. C., Rennels, L., Newell, R. G., Pizer, W., Kingdon, C., Wingrenroth, J., Cooke, R., Parthum, B., Smith, D., Cromar, K., Diaz, D., Moore, F. C., Müller, U. K., Plevin, R. J., Raftery, A. E., Ševčíková, H., Sheets, H., ... Anthoff, D. (2022). Comprehensive evidence implies a higher social cost of CO₂. *Nature*, 610(7933), 687–692. <https://doi.org/10.1038/s41586-022-05224-9>

³⁸ Rennert et al., (2022) (see footnote 34)

only. This interpretation of the ATS study largely mirrors that used in the open-source Greenhouse Gas Impact Value Estimator (GIVE) model described in Rennert et al. (2022).

As recommended by the study's lead author, we apply an aggregated net function that reflects both reductions in cold-related mortality and increases in heat-related mortality as temperatures increase.³⁹ To provide the state-level estimates for FrEDI, we then applied the ATS study USA region relative mortality risk function at county scale using county-level baseline and projected all-cause mortality risk estimates from BenMAP and county level baseline and projected populations from ICLUS V2 (that is, the same input data used for other mortality functions applied in FrEDI). The county level mortality estimates were then aggregated to state-level.

Economic damages are based on the net effect of heat and cold-related mortality rates, monetized by applying the VSL. The original work did not attempt to project damages for any climate scenarios, or attempt valuation, but the VSL in FrEDI is applied as a function of per capita income (Eq. B-1).

The ATS study also provides a standard error on the impact function relative risk coefficient, which was used to develop two additional damage functions that represent a 90 percent confidence interval around the excess risk parameter. As a result, the final physical and economic impacts from this sector study in FrEDI are available for the low and high end of the confidence interval (5th and 95th percentile values) as well as a central estimate which corresponds to the mean result.

TABLE B-5. INCOMING DATA CHARACTERISTICS: ATS TEMPERATURE-RELATED MORTALITY

Data Features	ATS Temperature-Related Mortality Attributes
Evaluated Impacts	<ul style="list-style-type: none"> Mortality: temperature-related premature deaths (physical) and value of premature deaths (economic)^a
Variants	<ul style="list-style-type: none"> Mean estimate High confidence interval Low confidence interval
Data Shape	<ul style="list-style-type: none"> Integer degree (1-6°C) Six GCMs (standard CIRA set) County level
Model Type	<ul style="list-style-type: none"> Empirical
Runs Provided	<ul style="list-style-type: none"> With socioeconomic growth and with climate change
Additional Data	<ul style="list-style-type: none"> None
Regions and States with Impacts	<ul style="list-style-type: none"> All CONUS regions and states

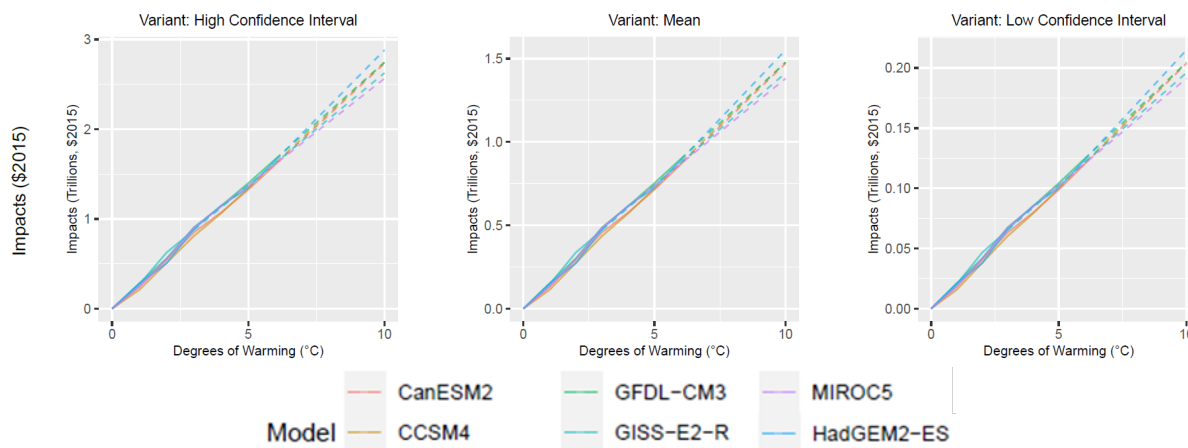
a. The underlying studies provide a mean and 90 percent confidence interval beta coefficient for excess relative risk associated with temperature changes (see Eq. 2). FrEDI pre-processing steps develop the projected county level mortality rates for each GCM, consistent with the data shape stated in this table.

³⁹ See Table 3 in Cromar et al. (2022) – the value used is the mean estimate for the USA and Canada region. The table shows a mean beta value of 0.0046 (0.46%) – as confirmed by the study lead author, we use the value reported in the Supplemental Information of Rennert et al. (2022) of 0.464%.

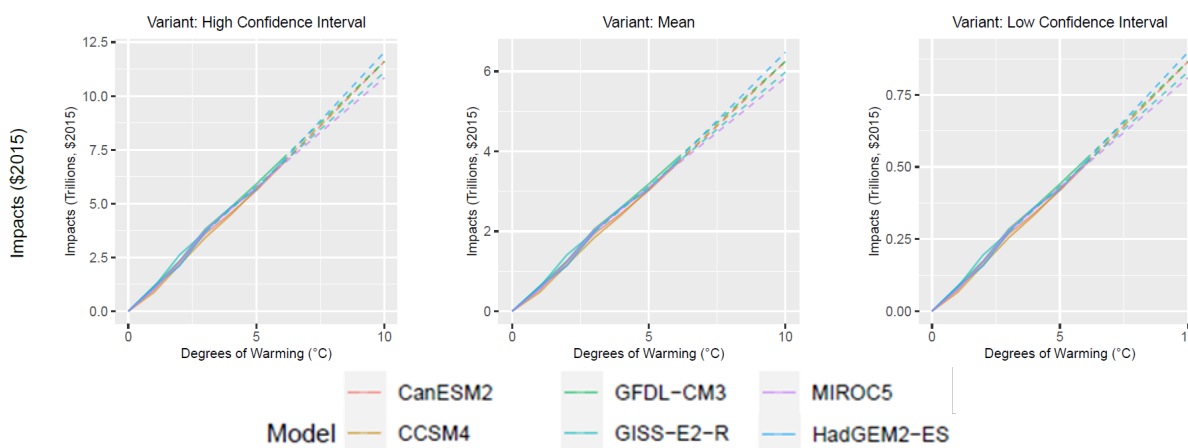
For illustrative purposes, **Figure B-9** shows the resulting damages by degree of warming for the mean and high and low confidence intervals, by GCM, calculated using 2010 (panel A) and 2090 (panel B) socioeconomic scenarios (i.e., the endpoints of the socioeconomic scenarios).

FIGURE B-9. ATS TEMPERATURE-RELATED IMPACTS BY TEMPERATURE BIN DEGREE

A. 2010 SOCIOECONOMICS



B. 2090 SOCIOECONOMICS



Total impacts (trillions of 2015\$) by degree (°C) for each variant for two socioeconomic snapshots (2010 and 2090 default scenarios). Extrapolated portions are shown with a dashed line. Note y-axis scales vary by plot.

Processing steps

Processing steps are shown in **Figure B-10**.

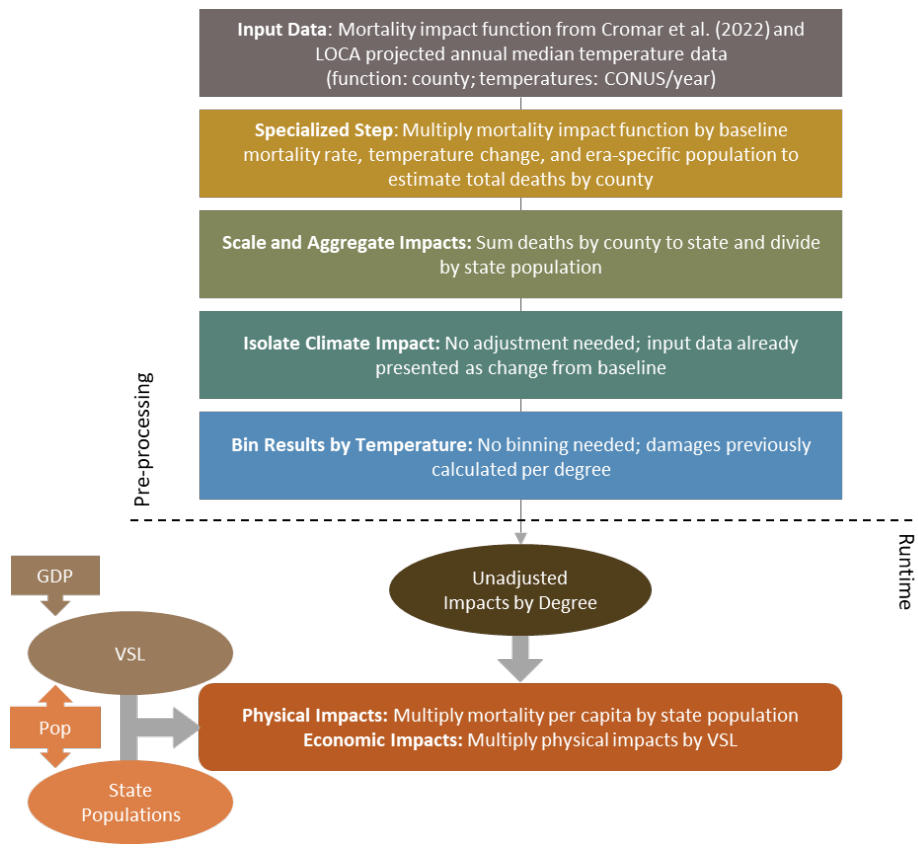
Pre-processing: Unlike most sectoral impacts where the underlying study provides either damages by degree or a trajectory of damages over time, the input ‘data’ from Cromar et al. (2022) are relative excess risk functions. Specifically, FrEDI uses the U.S.-specific relative risk functions (Eq B-2) for incremental annual mortality associated with the net effect of heat and cold-related mortality for each incremental change in annual average temperature ($\beta = 0.464\%$, from Table 3 of Cromar et al. 2022), and the standard errors of estimation for these functions.

$$\Delta Y = (1 - e^{-\beta \Delta Temp}) * Y_0 * Pop \quad (\text{Equation B-2})$$

Where $\Delta Temp$ is the temperature change; Y_0 is the baseline mortality rate (at county scale); Pop is the county level population; β is as stated above, taken from the underlying study; and ΔY is the change in mortality rate.

Therefore, in the first and second pre-processing steps, the relative risk function is used with annual county-level mean temperatures (relative to the 1986-2005 baseline) for each temperature bin and GCM, county-level baseline mortality rates forecasted through the 21st century from EPA's BenMAP model⁴⁰, and default county-level populations from ICLUSv2⁴¹ to calculate the net change in county-level mortality by degree and by GCM. The by-degree total county-level mortality counts are then aggregated to the state level, and converted to mortality rates (i.e., mortality per capita) by degree by dividing by the ICLUSv2 state population for each era of GCM integer degree of warming. This sector does not utilize any sector-specific scalars beyond FrEDI GDP and population inputs. Therefore, no scalar extensions are necessary to run the 2300 extension module.

FIGURE B-10. ATS TEMPERATURE-RELATED MORTALITY DATA PROCESSING FRAMEWORK



⁴⁰ EPA 2022, Environmental Benefits Mapping and Analysis Program – Community Edition, User’s Manual. January 2022, Updated for BenMAP-CE Version 1.5.8. Available at: https://www.epa.gov/sites/default/files/2015-04/documents/benmap-ce_user_manual_march_2015.pdf

⁴¹ Bierwagen, et al., 2010; ICLUSv2, 2017 (see footnote 31)

Runtime: When FrEDI is run, the pre-processed by-degree per capita mortality functions are then applied to the input temperature scenario to calculate the unadjusted annual per capita impacts based on the level of warming in each year of the input scenario. The total annual physical mortality counts are then calculated by applying these annual per capita rates to the input population scenario. Lastly, annual mortality counts are monetized using the VSL, calculated at runtime from input GDP per capita (Eq. B-1). In addition to the mean results, this sector includes additional variants that reflect the 5th and 95th percentile results for the net impacts of cold and heat mortality. These estimates reflect statistical estimation uncertainty in the underlying Cromar et al. (2022) study, reported as the standard error on the health impact function relative risk result (see underlying study, Table 3 for detail).

Limitations and Assumptions

- The estimates added to the FrEDI tool for this revision do not incorporate adaptations to temperature changes beyond measures reflected in current practices, as established in the seven underlying studies of the Cromar et al. (2022) meta-analysis.
- The underlying studies focus on extreme temperature mortality impacts, and exclude impacts of extreme temperature on morbidity; therefore, the Cromar et al. (2022) meta-analysis likely underestimates the full effect of temperature on health (e.g., it does not capture ED visits, hospitalizations, outpatient visits for heat-related illnesses, or occupational injuries and illnesses). For additional details on the specific meta-analytic techniques applied, please contact the Cromar et al. (2022) study authors.
- The potentially broad scope of the mortality impact linked to temperature increases in the Cromar et al. (2022) meta-analysis introduces the potential for overlap with some other sectoral results that associate temperature increases with mortality, most notably the Suicide sector. The reader is referred to Section 2.2, under the header Aggregation of Sectoral Impacts, for guidance on interpreting applications of FrEDI that include both of these sectors.
- For further discussion of the limitations and assumptions in the underlying sectoral model, please see Cromar et al. (2022).

Southwest Dust

Summary

This sector estimates the health burden and associated economic value resulting from changes in exposure to fine and coarse airborne dust projected with climate change in the Southwest.

Damages are based on Achakulwisut et al. (2019) which relies on changes in mortality outcomes from Krewski et al. (2009)⁴² and multiple morbidity outcomes associated with increased Southwest dust exposure. These

morbidity outcomes include cardiovascular hospitalizations (less acute myocardial infarction) from Zanobetti et al. (2009)⁴³, non-fatal acute myocardial infarction hospitalizations from Peters et al. (2001)⁴⁴, respiratory hospitalizations from Zanobetti et al. (2009), and emergency department visits for asthma from Malig et al. (2013)⁴⁵. The premature mortality impact is valued using the VSL and the morbidity impacts are monetized using the same cost-of-illness estimates from BenMAP-CE as those used in Achakulwisut et al. (2019) (i.e., direct costs and indirect loss of income for hospitalizations and direct costs of emergency department visits).

New onset of childhood asthma is also included as a morbidity endpoint, following the results of EPA (2023), which relied on morbidity functions from Tetreault et al. (2016).^{46,47} As described in the Air Quality section above, valuation for this endpoint is derived from Appéré et al. (2024),⁴⁸ which estimates the mean value of a statistical case of childhood asthma using a marginal willingness to pay per year over a ten year

UNDERLYING DATA SOURCES AND LITERATURE

Achakulwisut, P., Anenberg, S. C., Neumann, J. E., Penn, S. L., Weiss, N., Crimmins, A., Fann, N., Martinich, J., Roman, H. A., & Mickley, L. J. (2019). Effects of increasing aridity on ambient dust and public health in the U.S. southwest under climate change. *GeoHealth*, 3(5), 127-144.
<https://doi.org/10.1029/2019GH000187>

EPA. (2023). Climate Change and Children's Health and Well-Being in the United States. U.S. Environmental Protection Agency, EPA 430-R-23-001. <https://www.epa.gov/cira/climate-change-and-childrens-health-and-well-being-united-states-report>

⁴² Krewski, D., Jerrett, M., Burnett, R. T., Ma, R., Hughes, E., Shi, Y., et al. (2009). Extended follow-up and spatial analysis of the American Cancer Society study linking particulate air pollution and mortality. Research Report (Health Effects Institute), (140), 5-36. <https://pubmed.ncbi.nlm.nih.gov/19627030/>

⁴³ Zanobetti, A., Franklin, M., Koutrakis, P., & Schwartz, J. (2009). Fine particulate air pollution and its components in association with cause-specific emergency admissions. *Environmental Health: A Global Access Science Source*, 8(1). <https://doi.org/10.1186/1476-069X-8-58>

⁴⁴ Peters, A., Dockery, D. W., Muller, J. E., & Mittleman, M. A. (2001). Increased particulate air pollution and the triggering of myocardial infarction. *Circulation*, 103(23), 2810–2815. <https://doi.org/10.1161/01.CIR.103.23.2810>

⁴⁵ Malig, B. J., Green, S., Basu, R., & Broadwin, R. (2013). Coarse particles and respiratory emergency department visits in California. *American Journal of Epidemiology*, 178(1), 58–69. <https://doi.org/10.1093/aje/kws451>

⁴⁶ Tetreault, L.F., Doucet, M., Gamache, P., Fournier, M., Brand, A., Kosatsky, T. and Smargiassi, A., 2016. Childhood exposure to ambient air pollutants and the onset of asthma: an administrative cohort study in Québec. *Environmental Health Perspectives*, 124(8), pp.1276-1282

⁴⁷ Damages from new childhood asthma cases and childhood ED visits are fully additive; there is no overlap between the populations considered or the endpoints themselves. The childhood asthma ED visits are estimated for the child population with current prevalence of chronic asthma. The new childhood asthma cases are additional changes to the current prevalence and so constitute new chronic childhood onset asthma over and above current prevalence levels.

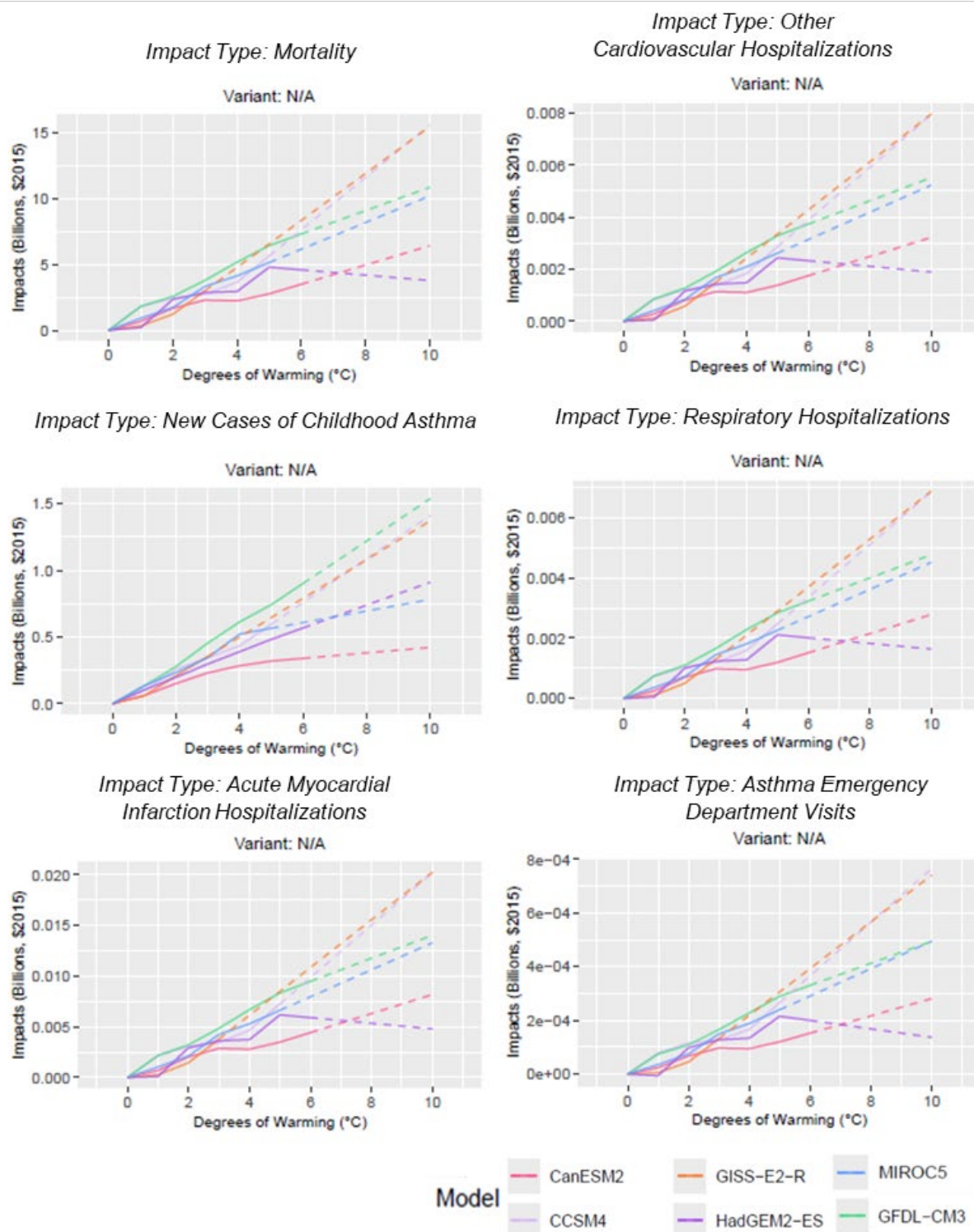
⁴⁸ Appéré et al., 2024 (see footnote 21)

period. This value reflects a parent's willingness to pay to reduce the risk of their child developing a new case of chronic asthma. In FrEDI we use the U.S. specific recommended value of \$637,041 (in 2015\$), which is scaled with the change of GDP per capita relative to 2010, and a 0.06 income elasticity.

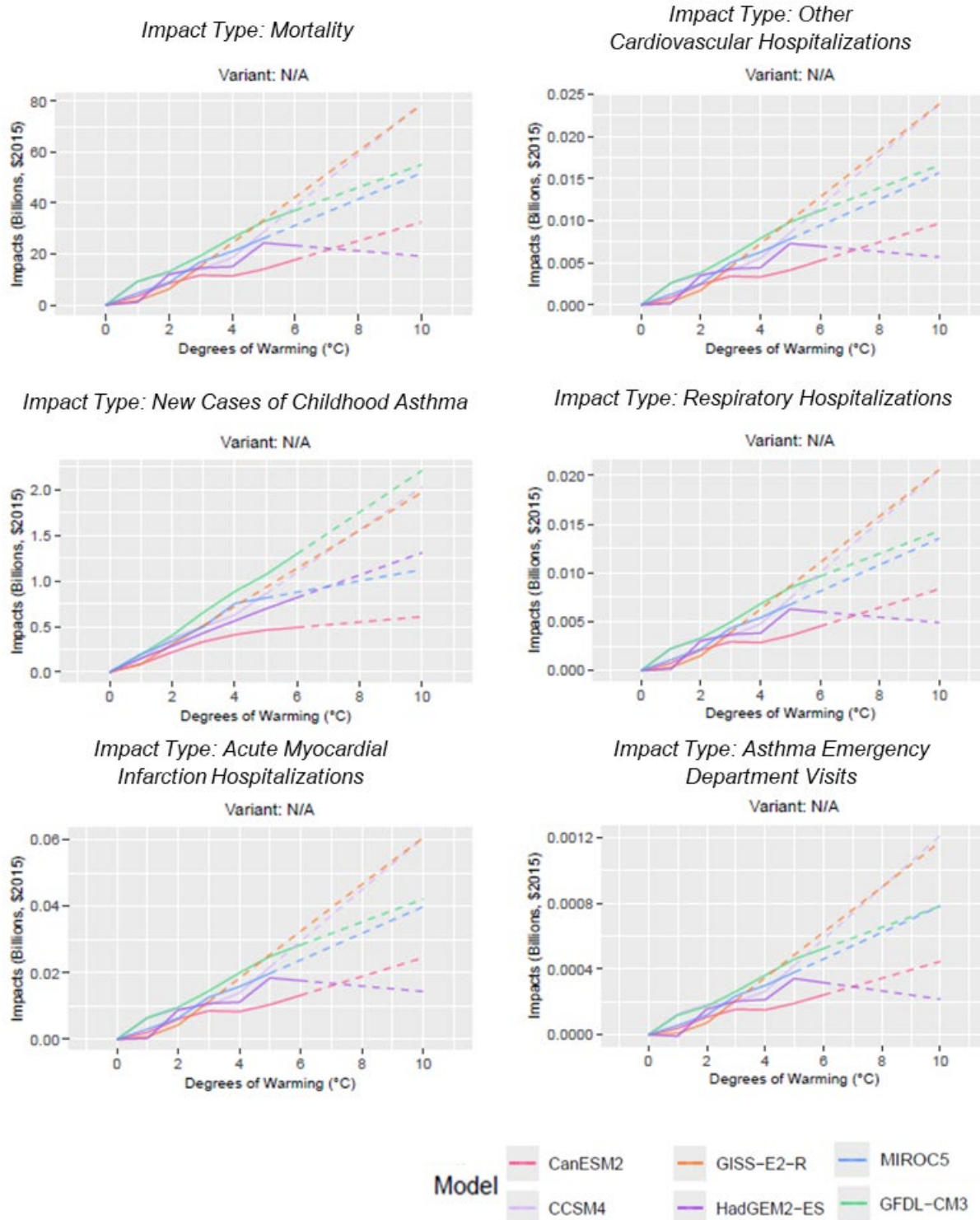
TABLE B-6. INCOMING DATA CHARACTERISTICS: SOUTHWEST DUST

Data Features	Southwest Dust Attributes
Evaluated Impacts	<ul style="list-style-type: none"> Mortality: premature deaths from Southwest Dust (physical) and value of premature deaths (economic) Respiratory hospitalizations from Southwest Dust (physical) and hospitalization costs (economic) Acute myocardial infarction hospitalizations from Southwest Dust (physical) and hospitalizations costs (economic) Other cardiovascular hospitalizations from Southwest Dust (physical) and hospitalization costs (economic) Asthma emergency department visits from Southwest Dust (physical) and emergency department visit costs (economic) New cases of childhood asthma from Southwest Dust per capita (physical) and value of new cases (economic)
Variants	<ul style="list-style-type: none"> No additional adaptation
Data Shape	<ul style="list-style-type: none"> Year (2050 and 2090) (all impacts but new childhood asthma) Annual (new childhood asthma only) Six GCMs (standard CIRA set) Four-state region (AZ, CO, NM, UT)
Model Type	<ul style="list-style-type: none"> Empirical
Runs Provided	<ul style="list-style-type: none"> Without socioeconomic growth and with climate change (Childhood Asthma Incidence) With socioeconomic growth and with climate change (All endpoints)
Additional Data	<ul style="list-style-type: none"> Age-stratified ICCLUSv2 population data
Regions and States with Impacts	<ul style="list-style-type: none"> Southwest (excluding CA, NV)

For illustrative purposes, **Figure B-11** shows the resulting damages by degree of warming for each of the six health endpoints (or impact types) by GCM, calculated using 2010 (panel A) and 2090 (panel B) socioeconomics (i.e., the endpoints of the socioeconomic scenarios).

FIGURE B-11. SOUTHWEST DUST IMPACTS BY TEMPERATURE BIN DEGREE**A. 2010 SOCIOECONOMICS**

B. 2090 SOCIOECONOMICS



Total impacts (billions of 2015\$) by degree ($^{\circ}\text{C}$) for each impact type for two socioeconomic snapshots (2010 and 2090 default scenarios). Extrapolated portions are shown with a dashed line. Note y-axis scales vary by plot.

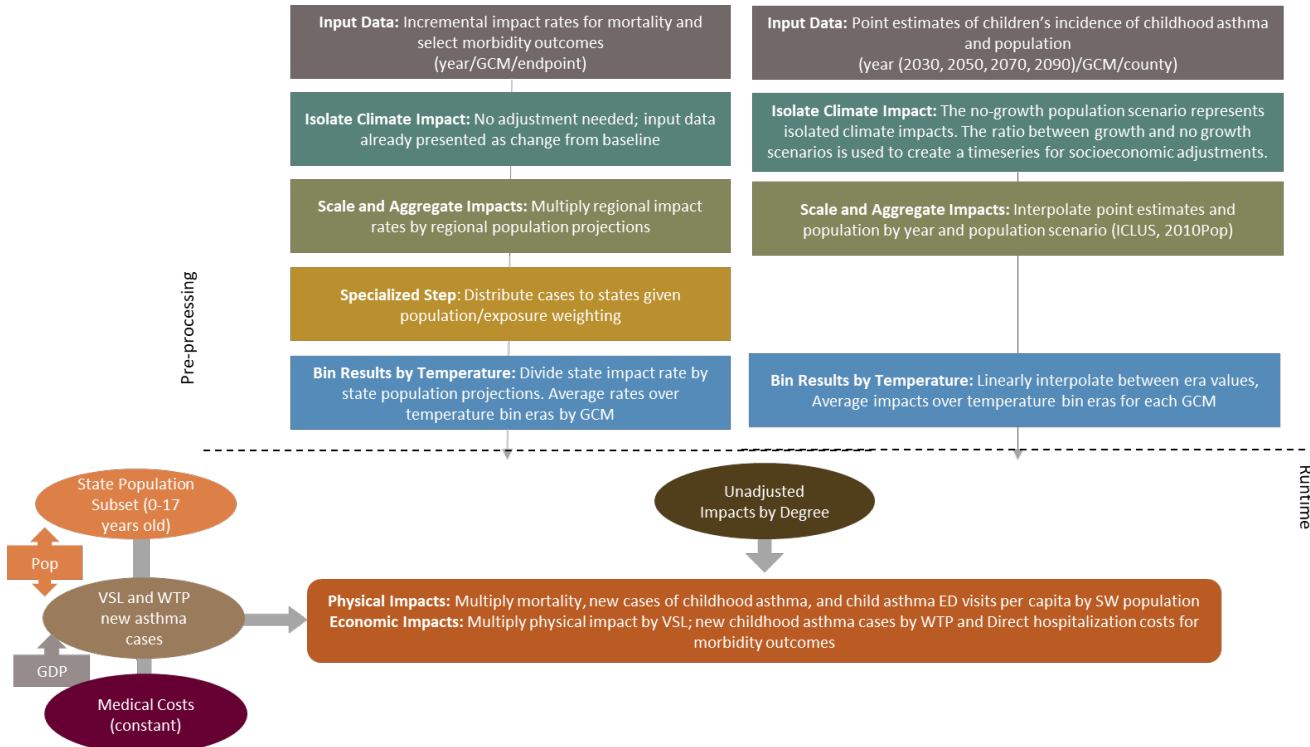
Processing steps

Processing steps are illustrated in **Figure B-12**.

Pre-processing: Input data from Achakulwisut et al. (2019) is presented as annual changes in the rates of health impacts relative to baseline levels for affected populations — for example, changes in the cardiovascular hospitalizations per capita for individuals 65 and older. These results already account for baseline rates, so no additional processing is needed to isolate climate impacts for use in FrEDI. These regional results reflect impacts across AZ, NM, CO, and UT. We use age-stratified annual ICLUSv2 population data from BenMAP to calculate state-specific scalars representing the proportion of the population 0 to 17 years old, 30 and older, and 65 and older. These scalars are included in FrEDI to ensure that calculated impact rates are applied only to the affected fraction of the population for each health endpoint. Results are first converted to case counts by multiplying incremental impact rates by annual ICLUSv2⁴⁹ regional affected populations specific to each health endpoint. Regional cases are then distributed to states using population-weighted exposure to particulate matter. State incremental impact rates are derived by dividing case counts by annual ICLUSv2 state affected populations specific to each health endpoint from BenMAP. The last pre-processing step is to bin the incremental incidence rates by degree of CONUS temperature change for each GCM by averaging across the 11-year windows centered on GCM arrival years.

For incidence of childhood asthma, the EPA (2023) Children’s Health Report authors apply the dose response function of childhood exposure to ambient air pollutants from Tetreault et al. (2016) in BenMAP to provide data by year (2030, 2050, 2070, 2090), GCM, and county. The authors provide two sets of results: a changing population scenario, based on ICLUSv2 population projections, and a static 2010 population scenario. In the first pre-processing step, the child population (0-17 years-old) and incremental incidence of childhood asthma cases are interpolated between 1995 (baseline year), 2030, 2050, 2070, and 2090 and extrapolated from 2090 to 2096 given the rate of change from 2070 to 2090 to develop annual projections. In the next step, incremental cases are divided by the child population to estimate impact rates. To isolate changes in population distributions, the static and ICLUS population scenarios are averaged across GCMs, and the ICLUS scenario is divided by the static scenario to develop a state- and year-specific scalar. GCM-specific static impact rates are temperature binned across GCM-specific 11-year windows to derive per capita childhood asthma incidence per state per degree for input into FrEDI. Finally, an annual state-level population scalar is developed to estimate the share of the total population in the 0–17-year age range using state-level ICLUSv2 population data from BenMAP. Incidence of childhood asthma is scaled with changes in GDP per capita relative to 2010 and income elasticity of 0.06 from the underlying study.

⁴⁹ Bierwagen, et al., 2010; ICLUSv2, 2017 (see footnote 31)

FIGURE B-12. SOUTHWEST DATA PROCESSING FRAMEWORK

Runtime: When FrEDI is run, the pre-processed by-degree per capita impact rates for each health endpoint are applied to the input temperature scenario to calculate unadjusted annual per capita impacts based on the level of warming in each year of the input scenario. Total annual cases are then estimated by applying these annual per capita rates to the input population scenario using the endpoint-specific population proportion scalars. Lastly, physical impacts are adjusted for future population distributions and monetized by multiplying these impacts by average medical costs. Morbidity endpoint medical costs are variable across health impacts and constant over time. Annual mortality counts are monetized using the VSL, calculated at runtime from input GDP per capita (Eq. B-1).

Limitations and Assumptions

- While dust exposures are known to be large in the southwestern U.S., this analysis does not consider health effects from inhalation of airborne coarse and fine dust in other regions of the U.S.
- Consistent with standard EPA practice, real healthcare costs are assumed constant over time in this analysis. There is some evidence, however, that healthcare costs have risen faster than the overall rate of inflation in the recent past – if that trend were to hold true in the future, this assumption would lead to an underestimation in the valuation component of this analysis.
- This sector relies on population for a section of the Southwest region (Arizona, Colorado, New Mexico, Utah) to calculate damages across impact types. The scaling of damages by this population allows for custom inputs of socioeconomic estimates, and FrEDI applies state-level changes in age structure over time based on age-stratified population projections from ICLUS.

- Additional limitations apply to the scope of morbidity impacts associated with the air pollutants considered in this study – that is, not all possible morbidity impacts for all possible affected age groups are considered here. See the Air Quality sector section above for more details.
- For further discussion of the limitations and assumptions in the underlying sectoral model, see Achakulwiset et al. (2019). For further information on child endpoints, see EPA (2023).

Valley Fever

Summary

This sector estimates the health burden and economic value associated with climate change-related Valley fever incidence. Valley fever is a prevalent disease in the hot and dry Southwest region of the U.S. but is expected to expand in geographic scope with warming. Therefore, this analysis quantifies Valley fever impacts across the CONUS, with most of the burden in the Southwest.

UNDERLYING DATA SOURCES AND LITERATURE

Gorris, M. E., Neumann, J. E., Kinney, P. L., Sheahan, M., & Sarofim, M. C. (2020). Economic Valuation of Coccidioidomycosis (Valley Fever) Projections in the United States in Response to Climate Change. *Weather, Climate, and Society*, 13(1), 107-123. <https://doi.org/10.1175/WCAS-D-20-0036.1>

Impacts are based on the change in number of Valley fever cases and the probability of a range of outcomes from Gorris et al. (2020) including hospitalization, physicians visit, emergency department visits, and death. Gorris et al. (2020) value these outcomes using direct hospitalization costs, costs of emergency department visits, costs of physician visits, indirect cost of lost productivity from hospitalization, and the VSL (for premature mortality).

TABLE B-7. INCOMING DATA CHARACTERISTICS: VALLEY FEVER

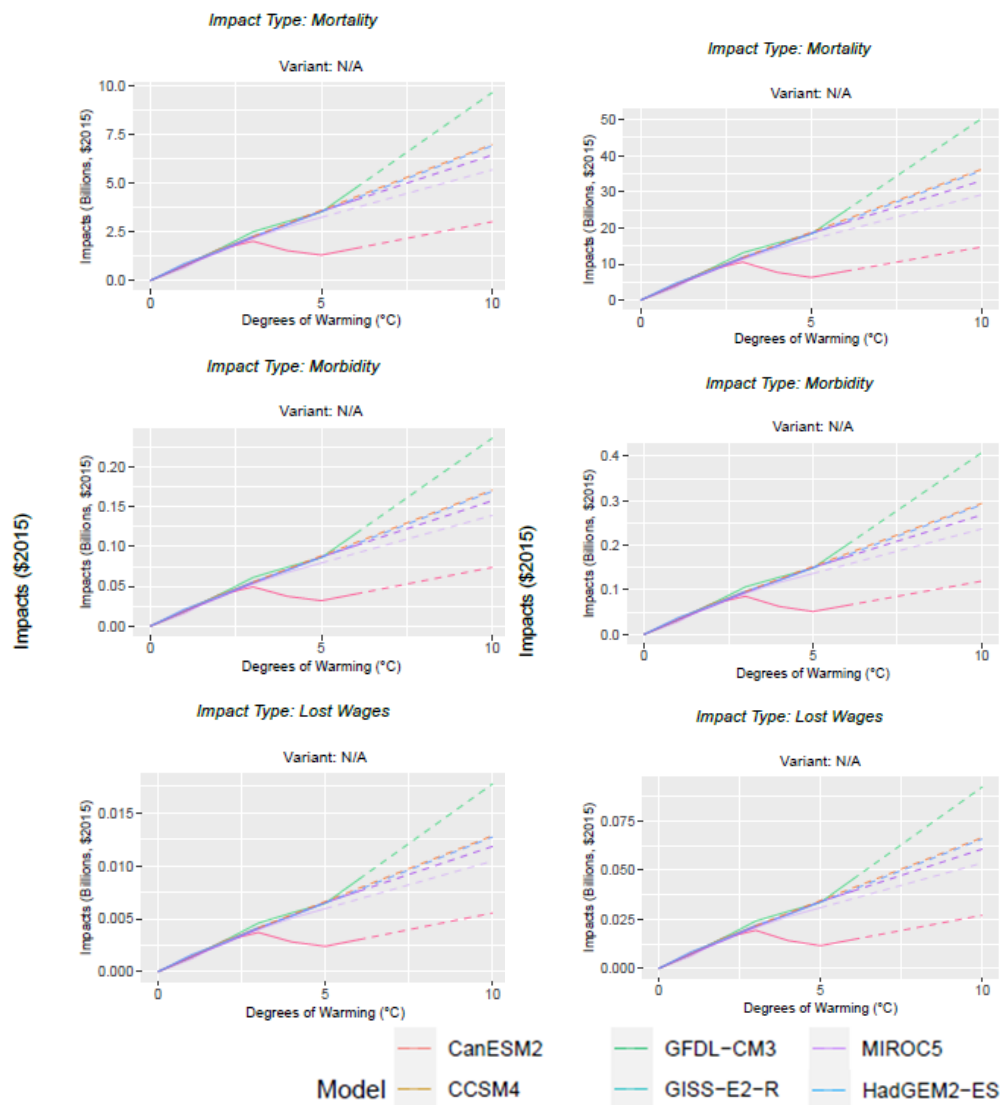
Data Features	Valley Fever Attributes
Evaluated Impacts	<ul style="list-style-type: none"> • Mortality: premature deaths from Valley fever (physical) and value of premature deaths (economic) • Morbidity: value of Valley fever cases (economic) • Productivity losses: lost wages during hospitalization (economic)
Variants	<ul style="list-style-type: none"> • No additional adaptation
Data Shape	<ul style="list-style-type: none"> • Annual • Six CMIP5 GCMs (standard CIRA set) • State level
Model Type	<ul style="list-style-type: none"> • Empirical
Runs Provided	<ul style="list-style-type: none"> • With climate change population growth, historical baseline Valley fever rates
Additional Data	<ul style="list-style-type: none"> • None
Regions and States with Impacts	<ul style="list-style-type: none"> • Midwest (excluding IL, IN, MI, MO, OH, WI) • Northern Plains • Northwest • Southern Plains • Southwest

For illustrative purposes, **Figure B-13** shows the resulting damages by degree of warming for mortality, all morbidity, and lost wage end points, by GCM, calculated using 2010 (panel A) and 2090 (panel B) socioeconomic scenarios (i.e., the endpoints of the socioeconomic scenarios).

FIGURE B-13. VALLEY FEVER IMPACTS BY TEMPERATURE BIN DEGREE

A. 2010 SOCIOECONOMICS

B. 2090 SOCIOECONOMICS



Total impacts (billions of 2015\$) by degree ($^{\circ}\text{C}$) for each impact type for two socioeconomic snapshots (2010 and 2090 default scenarios). Extrapolated portions are shown with a dashed line. Note y-axis scales vary by plot.

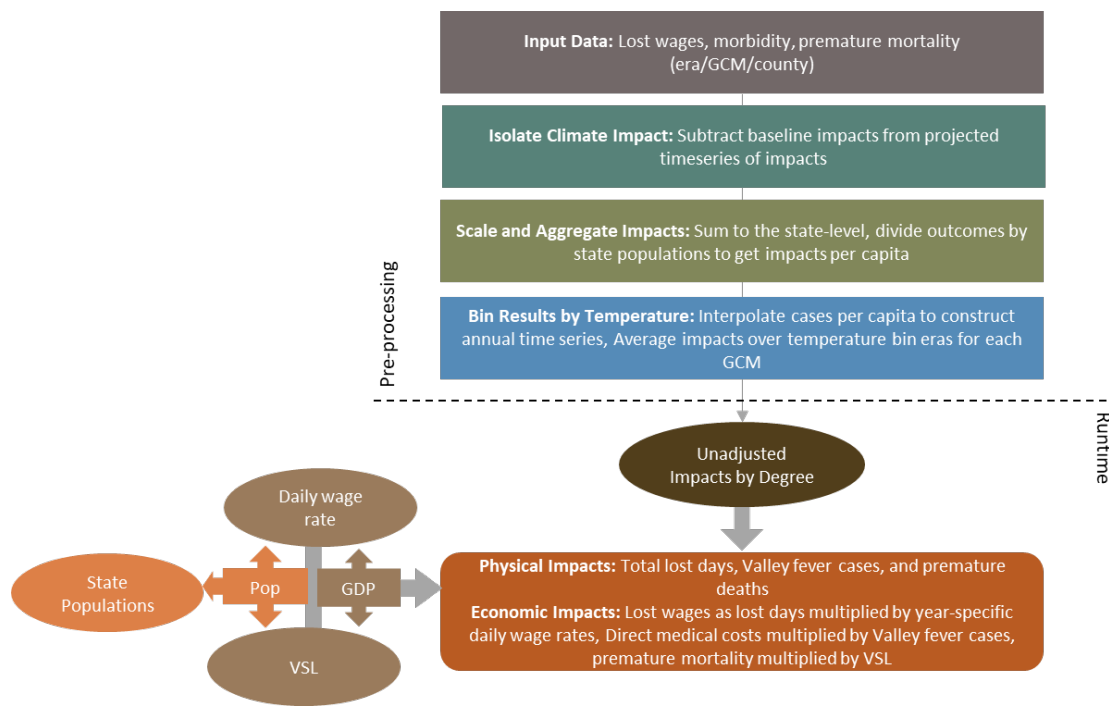
Processing steps

Processing steps are illustrated in **Figure B-14**.

Pre-processing: The Gorris et al. (2020) study authors provided the projected number of Valley fever cases at the county-level for 10-year eras centered on the years 2030, 2050, 2070, and 2090, for six CMIP5 GCMs.

In the first pre-processing step, the impacts from climate change are isolated by subtracting the baseline Valley fever rates by county, for those Southwest counties that met an endemicity threshold for Valley fever in the baseline period (112 Southwest counties out of 216). A baseline of zero is assumed for all other counties with projected incidence.⁵⁰ To ensure that changes in Valley fever rates are relative to the FrEDI baseline (e.g., 1986-2005), the baseline rates used in this pre-processing step are based on results derived from LOCA weather data instead of the baseline used in the underlying study.⁵¹ In the next pre-processing step, the number of cases in each county are summed to the state level, resulting in total counts of Valley fever cases per state. These total impacts are then divided by dynamic ICLUSv2⁵² state population to calculate the cases per capita for each era, GCM, and state. Lastly, cases per capita for each era are interpolated to construct an annual timeseries of cases per capita, which are then binned by degree of CONUS temperature change for each GCM by averaging across the 11-year windows where each GCM reaches each integer degree of CONUS warming relative to the baseline.

FIGURE B-14. VALLEY FEVER PROCESSING FRAMEWORK



⁵⁰ Climate-attributed excess cases are estimated by comparing modeled future climate to the model baseline, using the two-stage approach developed in the paper. Incidence is only calculated in counties that meet an endemicity threshold. Therefore, there are two ways that cases can be attributed to climate change: 1. Endemicity thresholds are met in both the baseline and future climate, and so excess cases are the difference between the calculated incidence in future minus baseline; 2. Climate change causes a county to cross the endemicity threshold, in which all future cases are attributed to climate change. This approach is consistent with the current understanding of Valley fever incidence, which is that the fungus must first be established in the soil before a case attributed to exposure in the county can be inferred.

⁵¹ Baseline Valley fever rates from the Gorris et al., (2020) study are from the Precipitation-Elevation Regressions on Independent Slopes Model (PRISM). The PRISM baseline provides total regional incidence but does temporally align with the FrEDI baseline period and therefore impacts are re-based during this pre-processing stage.

⁵² Bierwagen et al., 2010; ICLUSv2, 2017 (see footnote 31)

Runtime: When FrEDI is run, the pre-processed by-degree per capita impact functions for each endpoint are then applied to the input temperature scenario and weighted by the occurrence rates of each to calculate the unadjusted annual per capita impacts based on the level of warming in each year of the input scenario. For example, based on literature cited in Gorris et al. (2019)⁵³, morbidity outcomes are expected to occur in 96 percent of Valley fever cases. The annual totals for each endpoint are then calculated by applying these annual per capita rates to the input population scenario. Lastly, direct morbidity impacts (direct hospitalization, emergency room visit with discharge, emergency room visit with hospitalization, and physician visit) are monetized based on a weighted-average morbidity outcome, with the weights based on the probability of a Valley fever case resulting in any of a range of four morbidity outcomes of varying severity, applied to the cost of illness value for each of the four mutually exclusive outcomes. Lost productivity costs in the form of lost wages associated with hospitalizations are monetized using the probability (or weight) of outcome and wage rate, scaled by user-input GDP per capita.⁵⁴ Mortality is also expected to occur in four percent of Valley fever cases and these physical impacts are monetized using the VSL, calculated at runtime from input GDP per capita (Eq. B-1).

Limitations and Assumptions

- This analysis assumes a baseline of zero cases for counties that did not meet the endemicity threshold in the Southwest region during the baseline period and all counties with projected Valley fever cases outside of the Southwest region.
- Consistent with standard EPA practice, real healthcare costs are assumed constant over time in this analysis. There is some evidence, however, that healthcare costs have risen faster than the overall rate of inflation in the recent past – if that trend were to hold true in the future, this assumption would lead to an underestimation bias in the valuation component of this analysis.
- For further discussion of the limitations and assumptions in the underlying sectoral model, see Gorris et al. (2020).

⁵³ Gorris, M. E., K. K. Treseder, C. S. Zender, and J. T. Randerson, 2019: Expansion of coccidioidomycosis endemic regions in the United States in response to climate change. *GeoHealth*, 3, 10, 308–327, <https://doi.org/10.1029/2019GH000209>; Agency for Healthcare Research and Quality, 2019, Healthcare Cost and Utilization Project (HCUPnet), <https://datatools.ahrq.gov/hcupnet/>.

⁵⁴ As described in Gorris et al. (2022), available data sources suggest that 19% of valley fever cases will result in direct hospitalization, 8% in emergency room visits followed by discharge, 26% in emergency room visits followed by admittance to the hospital, 43% in physician visits, and 4% in death (where valley fever is either the primary or secondary contributor). These are the weights used in the weighted-average described here.

Wildfire

Summary

This sector estimates health impacts from wildfire emissions and response costs from wildfire suppression. Neumann et al. (2021) models change in wildfire activity for the western CONUS region. As such, response costs are limited to this area, but the health impacts of the PM_{2.5} from western wildfires are estimate across the CONUS (as PM_{2.5} typically travels eastward across CONUS).

Health impacts are based on the change in rates of a range of morbidity and mortality outcomes, which are monetized using direct hospitalization costs, costs of emergency department visits, lost productivity, and for mortality, the VSL. The morbidity impact in FrEDI represents a sum of multiple morbidity endpoints from Neumann et al., (2021), valued using the cost-of-illness estimate for each endpoint in BenMAP-CE (the tool used in the underlying study to calculate health outcomes), as well as from EPA (2023), which used the air quality results from Neumann et al. (2021) combined with an epidemiological function from Tetreault et al. (2016).^{55,56} As described in the Air Quality section above, valuation of incidence of childhood asthma in BenMAP is derived from Appéré et al. (2024), which estimates the mean value of a statistical case of childhood asthma using a marginal willingness to pay per year over a ten-year period, with a mean U.S. specific recommended value of \$637,041 (in 2015\$), which is scaled with the change of GDP per capita relative to 2010, and a 0.06 income elasticity. In addition, response costs are estimated based on average wildfire response costs per acre burned, by state from Neumann et al. (2020).

UNDERLYING DATA SOURCES AND LITERATURE

Neumann, J. E., Amend, M., Anenberg, S., Kinney, P. L., Sarofim, M., Martinich, J., Lukens, J., Xu, J., & Roman, H. (2021). Estimating PM_{2.5}-related premature mortality and morbidity associated with future wildfire emissions in the western US. Environmental Research Letters, 16(3).

<https://pubmed.ncbi.nlm.nih.gov/33868453/>

EPA. (2023). Climate Change and Children's Health and Well-Being in the United States. U.S. Environmental Protection Agency, EPA 430-R-23-001. <https://www.epa.gov/cira/climate-change-and-childrens-health-and-well-being-united-states-report>

TABLE B-8. INPUT DATA CHARACTERISTICS: WILDFIRE

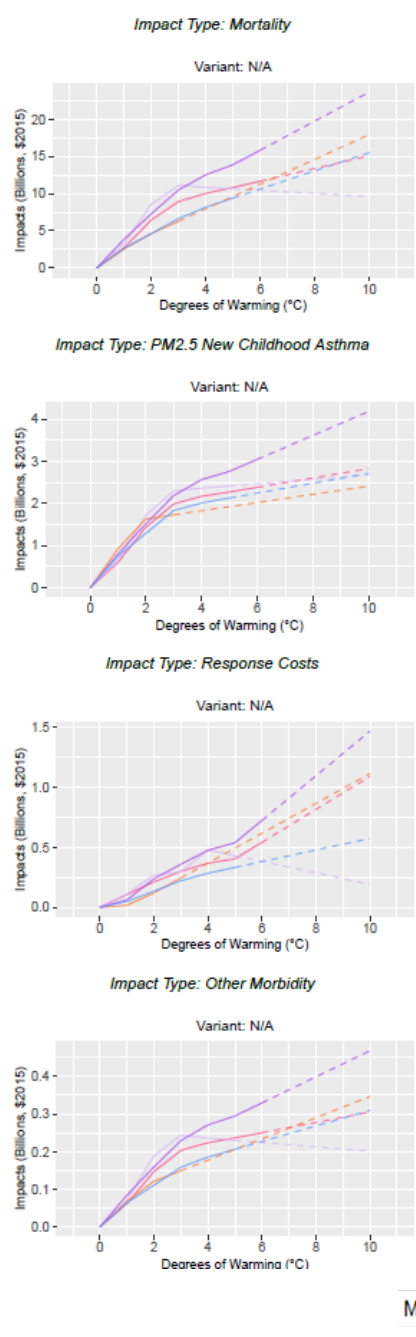
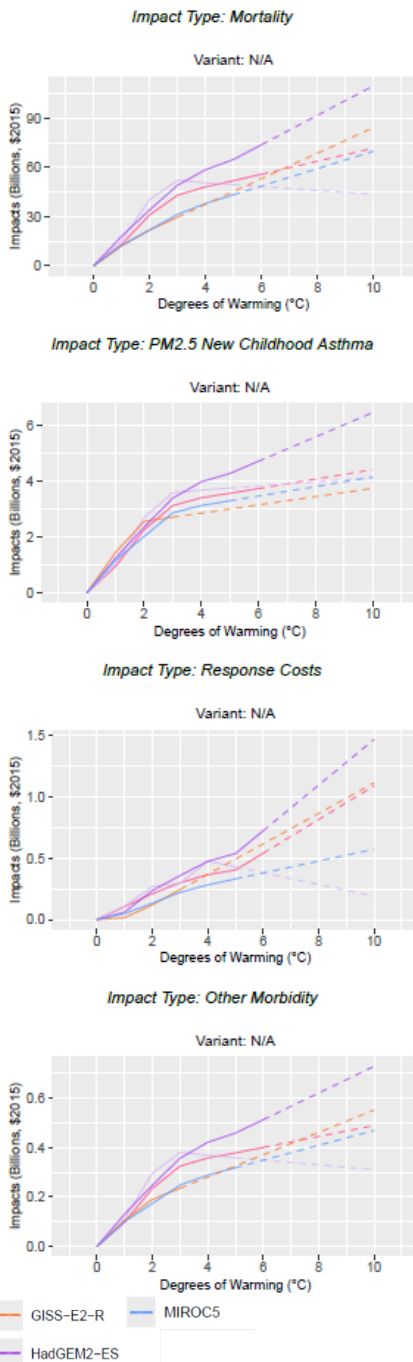
Data Features	Wildfire Attributes
Evaluated Impacts	<ul style="list-style-type: none"> Mortality: premature deaths from wildfire (physical) and value of premature deaths (economic) Morbidity: new cases of childhood asthma (physical and economic) and summed value of excess respiratory hospital admissions, nonfatal acute myocardial infarction cases, and asthma emergency department visits (economic) Response: acres burned by wildfire (physical) and response costs (economic)
Variants	<ul style="list-style-type: none"> No additional adaptation
Data Shape	<ul style="list-style-type: none"> Year (2050 and 2090) Annual (new childhood asthma only)

⁵⁵ Tetreault et al., (2016) (see footnote 46)

⁵⁶ Damages from new childhood asthma cases and childhood ED visits are fully additive (see footnote 47)

	<ul style="list-style-type: none">• Five GCMs (standard CIRA set, excluding GFDL)• State level for all estimates from Neumann et al. (2021)• County level for new cases of childhood asthma
Model Type	<ul style="list-style-type: none">• Empirical and Simulation
Runs Provided	<ul style="list-style-type: none">• With climate change, with and without population growth
Additional Data	<ul style="list-style-type: none">• None
Regions and States with Impacts	<ul style="list-style-type: none">• All CONUS regions and states^a
a. For the Response Costs impact type, data is not included for states in the Midwest, Northeast, and Southeast regions.	

For illustrative purposes, **Figure B-15** shows the resulting damages by degree of warming all mortality, response costs, and morbidity impact types by GCM, calculated using 2010 (panel A) and 2090 (panel B) socioeconomics (i.e., the endpoints of the socioeconomic scenarios).

FIGURE B-15. WILDFIRE IMPACTS BY TEMPERATURE BIN DEGREE
A. 2010 SOCIOECONOMICS

B. 2090 SOCIOECONOMICS


Total impacts (billions of 2015\$) by degree (°C) for each impact type for two socioeconomic snapshots (2010 and 2090 default scenarios). Extrapolated portions are shown with a dashed line. Note y-axis scales vary by plot.

Processing steps

Processing steps are illustrated in **Figure B-16**.

Pre-processing: Data for each impact type (mortality, morbidity, and response costs) are each processed separately. For mortality, the Neumann et al. (2021) study authors provided state-level mortality rates attributable to climate change-related changes in PM_{2.5} concentrations resulting from wildfires for two 10-year eras centered on 2050 and 2090 using five GCMs. This analysis considers mortality estimated using a concentration-response function based on risk model information specific to those age 30 and older. In the first pre-processing step, the excess health burden associated with climate-induced changes in wildfire activity is isolated by subtracting baseline mortality rates (i.e. “no additional wildfires”) from the projected mortality rate with wildfires. This technique allows identification of air quality and health effects associated solely with wildfire. In the next pre-processing step, the climate change-related mortality rate is then divided by dynamic ICLUSv2⁵⁷ state-level population for each era to calculate mortality per capita for each era/GCM/state scenario. Finally, an annual time series of mortality per capita is constructed by linearly interpolating between era values, and yearly impacts are binned by degree of CONUS temperature change for each GCM by averaging across the 11-year windows where each GCM reaches each integer degree of CONUS warming relative to the baseline.

For morbidity (not including new childhood asthma incidence), the Neumann et al. (2021) study authors provided state-level morbidity rates and valuation for the same 10-year eras centered on 2050 and 2090 using five GCMs. To represent this morbidity impact type in FrEDI, the valuation is summed across a set of health endpoints to determine one value associated with all morbidity impacts, representing cost of illness and lost productivity for each era/GCM/state scenario.⁵⁸ In the first pre-processing step, the baseline valuation is subtracted from the 2050 and 2090 projected valuation to isolate the impact of climate change on wildfire-related morbidity. In the following steps, the morbidity valuation for each era is then divided by state-level population, interpolated to construct an annual timeseries, and temperature binned by GCM-specific 11-year windows to generate state-level morbidity damages per capita by degree damage functions.

For incidence of childhood asthma, the Children’s Health Report (EPA, 2023) authors apply the dose response function of childhood exposure to ambient air pollutants from Tetreault et al. (2016), processed through BenMAP, to provide data by year (2050 and 2090), GCM, and county. The authors provide two sets of results: a dynamic population scenario, based on ICLUSv2 population projections, and a static 2010 population scenario. In the first pre-processing step, the child population (0-17 years-old) and incremental incidence of childhood asthma cases are interpolated between 1995 (baseline year), 2050, and 2090, and extrapolated from 2090 to 2096 given the rate of change from 2070 to 2090 to develop annual projections for each set of results. In the next step, incremental cases are divided by the child population to calculate incidence rates. Incidence rates are temperature binned per state across the GCM-specific 11-year windows to derive per capita incidence of childhood asthma cases per state per degree. The static population

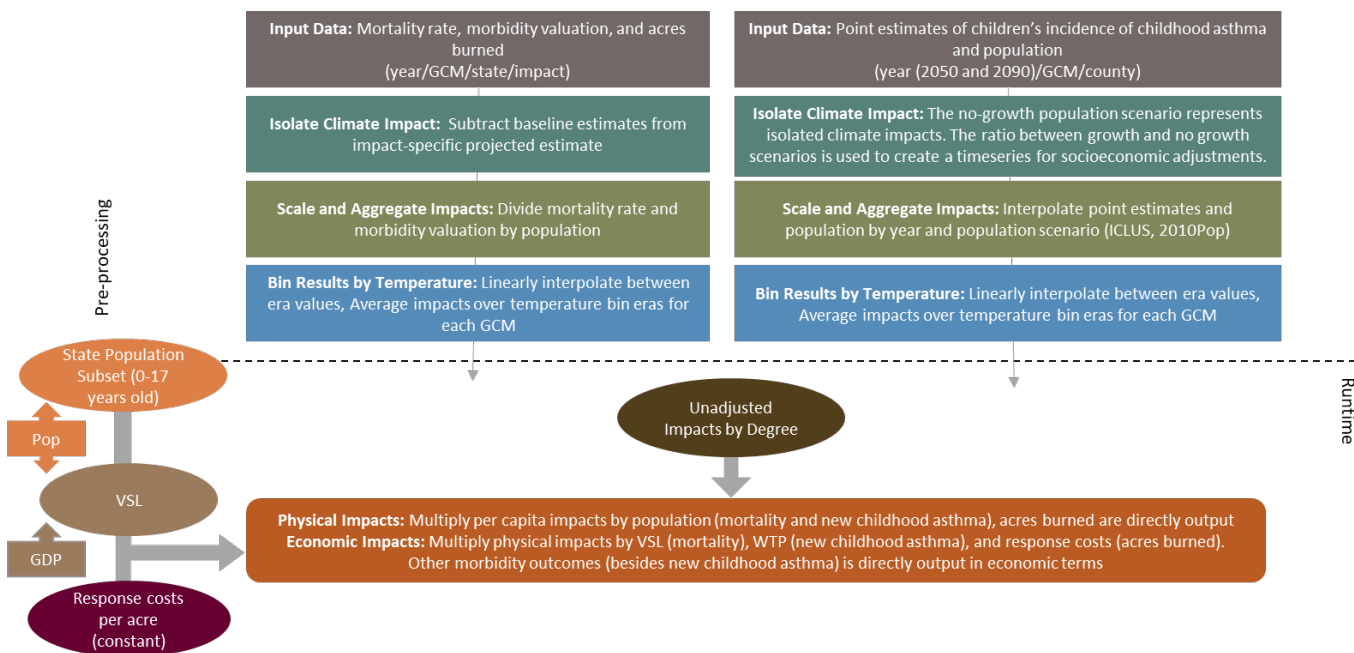
⁵⁷ Bierwagen et al., 2010; ICLUSv2, 2017 (see footnote 31)

⁵⁸ The full list of health endpoints from Neumann et al. (2021) includes acute bronchitis, nonfatal acute myocardial infarction, asthma exacerbation (cough, wheeze, shortness of breath), asthma ED visits, cardiovascular hospital admissions, asthma hospital admissions, chronic lung disease hospital admissions (less asthma), respiratory hospital admissions, lower respiratory symptoms, upper respiratory symptoms, work loss days, and minor restricted activity days.

scenario is inputted into FrEDI as the childhood asthma incidence scaled impact. The static and dynamic population scenarios are averaged across GCMs, and the dynamic population scenario is divided by the static scenario to develop a state-degree specific scalar to reflect changes in population distributions across space over time. Finally, a population scalar is input to subset the 0–17-year ages from the total population using state-level ICLUSv2 population data from BenMAP. New cases of childhood asthma are scaled with changes in GDP per capita relative to 2010, and income elasticity of 0.6 from the underlying study.

For the response costs, the Neumann et al. (2021) study authors provided data on the acres burned by year, GCM, and state (excluding states within the Midwest, Northeast, and Southeast regions). In the first pre-processing step, acres burned in the baseline are subtracted from the projected acres burned values. As this endpoint is not dependent on population, the next step temperature bins the acres burned per state across the GCM-specific 11-year windows to derive acres burned per state per degree damage functions. For this impact type, state-level response costs per acre from the original study are also input as an economic scalar in FrEDI. Response costs per acre remain constant throughout the century.

FIGURE B-16. WILDFIRE PROCESSING FRAMEWORK



Runtime: When FrEDI is run, the pre-processed by-degree per capita impact (morbidity and mortality) and acres burned functions are then applied to the input temperature scenario to calculate the unadjusted impacts based on the level of warming in each year of the input scenario. The total annual physical mortality counts, and the total value of morbidity damages are then calculated by applying these annual per capita rates to the input population scenario. For the new childhood asthma cases, total annual incidence rates are calculated by applying annual per capita rates that are adjusted to account for changes in population demographics over time, to the input population scenario multiplied by the proportion of total population affected by each impact (i.e., population age 0-17). Lastly, annual mortality counts are

monetized using the VSL, calculated at runtime from input GDP per capita (Eq. B-1); new asthma cases are monetized using the WTP, suppression costs are monetized by scaling the acres burned by the response cost per acre burned economic scalar, and non-new asthma case morbidity impacts are already valued. The willingness to pay (new asthma costs) are then multiplied by the WTP to produce economic impacts.

Limitations and Assumptions

- Mortality rates are quantified for those age 30+, and this analysis assumes the impacts for those under 30 to be zero. This underestimates the risk of premature mortality experienced by those under 30 and assumes that age demographics remain proportional over the century.
- Morbidity health endpoints are associated with various age distributions. Total valuation is divided by state population, assuming the health burden outside of included age ranges is zero.
- Consistent with standard EPA practice, real healthcare costs are assumed constant over time in this analysis. There is some evidence, however, that healthcare costs have risen faster than the overall rate of inflation in the recent past – if that trend were to hold true in the future, this assumption would lead to an underestimation bias in the valuation component of this analysis.
- Additional limitations apply to the scope of morbidity impacts associated with the air pollutants considered in this study – that is, not all possible morbidity impacts for all possible affected age groups are considered here. See the Air Quality sector section above for more details.
- For further discussion of the limitations and assumptions in the underlying sectoral model see Neumann et al. (2021) and EPA (2023).

CIL Crime

Summary

This sector estimates the impact of climate change on the rates of property and violent crime across all of CONUS.

The Climate Impact Lab (CIL) crime projections are drawn from a temperature response function derived

from Jacob, Lefgren, and Moretti (2007)⁵⁹, refined and calibrated to data from Ranson (2014)⁶⁰, and applied in Hsiang et al. (2017) to generate projected future climate impacts on crime occurrence by GCM and RCP through the 21st century.

UNDERLYING DATA SOURCES AND LITERATURE

Hsiang, S., Kopp, R., Jina, A., Rising, J., Delgado, M., Mohan, S., Rasmussen, D.J., Muir-Wood, R., Wilson, P., Oppenheimer, M., Larsen, K., and Houser T. (2017). Estimating economic damage from climate change in the United States, *Science*, 356, 1362–1369.

<https://www.doi.org/10.1126/science.aal4369>

While the empirical link between heat and criminal activity is well established in the literature, the theoretical explanation for this connection is still debated. Two principal theories are the routine activity

⁵⁹ Jacob, B., Lefgren, L., and Moretti, E. (2007). The dynamics of criminal behavior, *J. Hum. Resour.*, 42, 489–527.
<https://www.jstor.org/stable/40057316>

⁶⁰ Ranson, M. (2014). Crime, weather, and climate change, *J. Environ. Econ. Manage.*, 67, 274–302.
<https://doi.org/10.1016/j.jeem.2013.11.008>

theory, which suggests that heat and weather patterns affect individuals' decisions and movement patterns and by extension alter the frequency of crime opportunities, and the temperature-aggression hypothesis, which posits that higher temperatures induce aggression and impulsiveness.⁶¹

Data on costs of crime from Heaton (2010)⁶² and baseline crime rate data from Hsiang et al. (2017) are used to construct state-specific costs for two categories of crime: property (robbery, burglary, larceny, and motor vehicle theft) and violent (murder, rape, and assault). For each category, the cost of crime is calculated as a weighted average of the costs of the included crimes, using the per-state relative frequency of specific crime occurrence within each category as the weights, and the costs of each of the specific crimes. Cost of crime estimates from Heaton (2010) represent an average across three studies employing different methods of estimating the costs of crimes. Two of these studies use an accounting-based method wherein the individual costs of various outcomes of a crime are valued separately and their costs are summed (e.g., the cost of a robbery consists of the costs to individuals and to society of lost property, preventative measures, medical treatment, pain and suffering, and the criminal justice process). The third study relies on contingent valuation methods to estimate society's willingness to pay for avoided instances of each crime (Heaton, 2010).

The currently available results account for adaptation approaches only to the extent that they have been previously implemented within the studied populations. We anticipate that future revisions of FrEDI may incorporate a “with adaptation” variant that includes modelling of projected future adaptations.

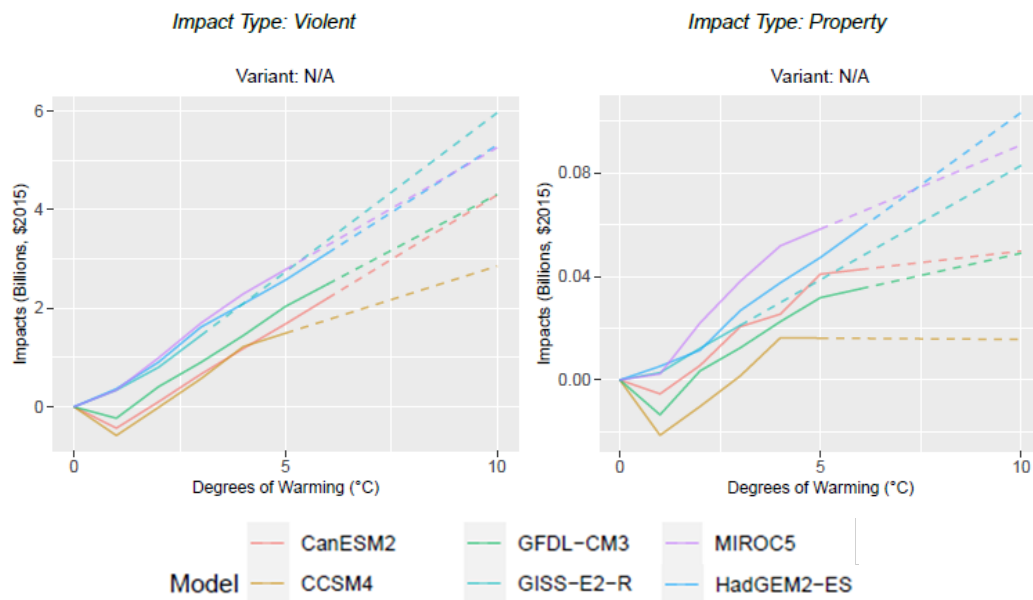
TABLE B-9. INCOMING DATA CHARACTERISTICS: CIL CRIME

Data Features	CIL Crime Attributes
Evaluated Impacts	<ul style="list-style-type: none"> Number of crimes, violent and property (physical), and damage from these crimes (economic)
Variants	<ul style="list-style-type: none"> No additional adaptation, median estimates
Data Shape	<ul style="list-style-type: none"> Year Six CMIP5 GCMs (standard CIRA set) Three variants State level
Model Type	<ul style="list-style-type: none"> Empirical
Runs Provided	<ul style="list-style-type: none"> Without socioeconomic growth and with climate change
Additional Data	<ul style="list-style-type: none"> Baseline crime rate by state Cost of crime by type
Regions and States with Impacts	<ul style="list-style-type: none"> All CONUS regions and states

For illustrative purposes, **Figure B-17** shows the resulting damages by degree of warming from violent and property crime, by GCM.

⁶¹ Corcoran, J. & Zahnow, R. (2022). Weather and crime: a systematic review of the empirical literature. *Crime Science*, 11, 16.

⁶² Heaton, P. (2010). Hidden in Plain Sight: What Cost-of-Crime Research Can Tell Us About Investing in Police, RAND Corporation. https://www.rand.org/pubs/occasional_papers/OP279.html

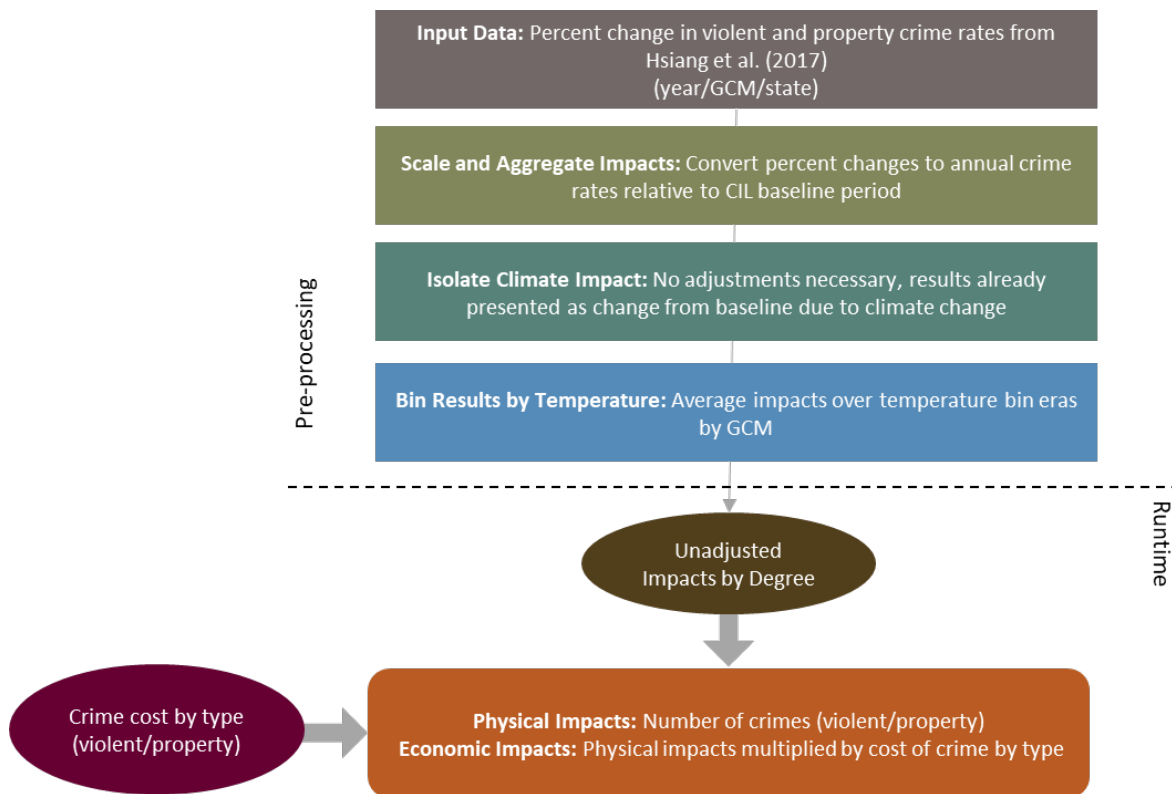
FIGURE B-17. CIL CRIME IMPACTS BY TEMPERATURE BIN DEGREE

Total impacts (billions of 2015\$) by degree ($^{\circ}\text{C}$) for each impact type, which do not vary by socioeconomic scenario or time. Extrapolated portions are shown with a dashed line. Note y-axis scales vary by plot.

Processing steps

Processing steps are shown in **Figure B-18**.

Pre-processing: The Hsiang et al. (2017) study authors provided data on the percent change in crime under RCP 8.5 by GCM, year, state, and crime type, along with baseline crime rates by state for each category of crime averaged over the 2000-2005 period. While the authors provided a full distribution of impact results, FrEDI currently only accounts for the median estimate. In the first pre-processing step, the percent changes and baseline data by state are multiplied to calculate annual changes in the number of crimes. In the second pre-processing step, the state-level annual incremental changes in crime are binned by degree of CONUS temperature change for each GCM by averaging across the 11-year windows where each GCM reaches each integer degree of CONUS warming relative to the baseline. State-specific, likelihood-weighted cost of crime estimates are derived using cost of crime data from Heaton (2010) and the provided baseline crime rate data from Hsiang et al. (2017) and input as an economic scalar in FrEDI. These cost of crime estimates are held constant for all projected years as the available documentation does not provide information on how or whether crime costs would scale with population, GDP, GDP per capita, or other socioeconomic driver data.

FIGURE B-18. CIL CRIME DATA PROCESSING FRAMEWORK

Runtime: When FrEDI is run, the pre-processed by-degree crime functions are then applied to the input temperature scenario to calculate the unadjusted annual number of crimes based on the level of warming in each year of the input scenario. Lastly, the annual damages from both types of crime are monetized by multiplying these incremental changes in crime rates by the state-specific, likelihood-weighted cost of crime economic scalar estimates.

Limitations and Assumptions

- These projections of crime rates do not account for future changes in population or other socioeconomic drivers. Because the crime rates are not scaled with socioeconomic growth, it is likely that we underestimate future impacts. For reference, the standard CIRA data inputs imply that population would grow by approximately 50%, and GDP would grow by about a factor of 5 over the 21st century.
- These projections use static values for the state-specific weighted costs of property and violent crime. It is possible that at least some components of the costs of property and violent crime could grow over time – for example a VSL for victims of murder, or the value of property damaged or stolen – but because the crime rates are aggregated, we are currently unable to assess the possible growth in these costs per crime over time.
- For further discussion of the limitations and assumptions in the underlying sectoral model, please see Hsiang et al. (2017).

Vibriosis

Summary

This sector estimates the health burden and the associated economic value in the CONUS resulting from changes in vibriosis cases projected with climate change. Vibriosis is an illness contracted through food (typically raw seafood) and waterborne exposures to various *Vibrio* species. *Vibrio* is a bacterium that is prevalent in marine environments. Warmer water temperatures increase the abundance of *Vibrio* species in saltwater environments, and warmer air temperatures can increase the likelihood that efforts to keep harvested seafood cool up to the point of consumption may fail, leading to a higher risk of *Vibrio* infection.

UNDERLYING DATA SOURCES AND LITERATURE

Sheahan, M., Gould, C.A., Neumann, J.E., Kinney, P.L., Hoffmann, S., Fant, C., Wang, X. and Kolian, M. (2022). Examining the Relationship between Climate Change and Vibriosis in the United States: Projected Health and Economic Impacts for the 21st Century. *Environmental Health Perspectives*, 130(8). <https://doi.org/10.1289/ehp9999a>

The underlying study (Sheahan et al., 2022) uses CDC data on historical *Vibrio* infections and the severity of the resulting health effects, traces the infections to likely locations of exposure, and estimates the influence of environmental factors such as sea surface temperature on infection rates. The model of infection rates is then used to develop estimates of projected cases of vibriosis for future climate change scenarios. While the route of exposure is limited to marine coastal environments, the transport of seafood across the country means that infections can occur almost anywhere. State results reported in FrEDI are based on coastal exposure locations, not locations where seafood might be consumed. Damages are based on estimates of monetized direct medical costs, lost workdays, and changes in mortality outcomes. Lost workdays are monetized through estimated daily wage rate, and mortality outcomes through VSL.

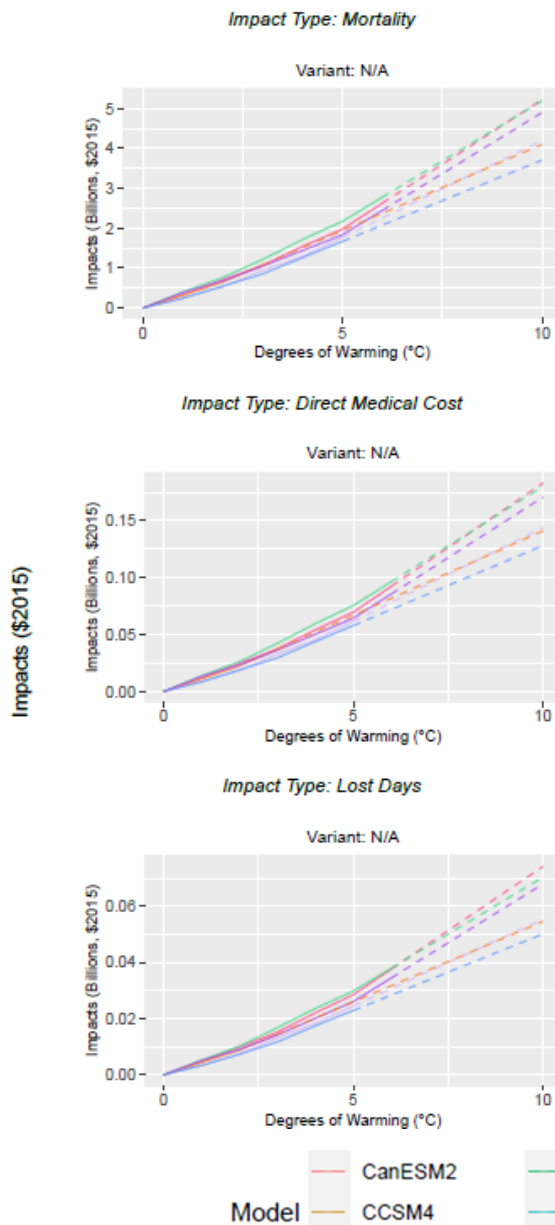
TABLE B-10. INCOMING DATA CHARACTERISTICS: VIBRIOSIS

Data Features	Vibriosis Attributes
Evaluated Impacts	<ul style="list-style-type: none"> Mortality: premature deaths (physical) and value (economic) Morbidity: direct medical costs (economic) Productivity losses: lost work days (physical) and lost wages (economic)
Variants	<ul style="list-style-type: none"> No additional adaptation
Data Shape	<ul style="list-style-type: none"> Annual Six GCMs (standard CIRA set) State level
Model Type	<ul style="list-style-type: none"> Empirical
Runs Provided	<ul style="list-style-type: none"> With climate change, no population growth Historical baseline vibriosis rates (e.g., no climate change and no population growth)
Additional Data	<ul style="list-style-type: none"> None
Regions and States with Impacts	<ul style="list-style-type: none"> Northeast (excluding VT, WV) Northwest (excluding ID) Southeast (excluding AR, KY, TN) Southern Plains (excluding KS, OK) Southwest (excluding AZ, CO, NV, NM, UT)

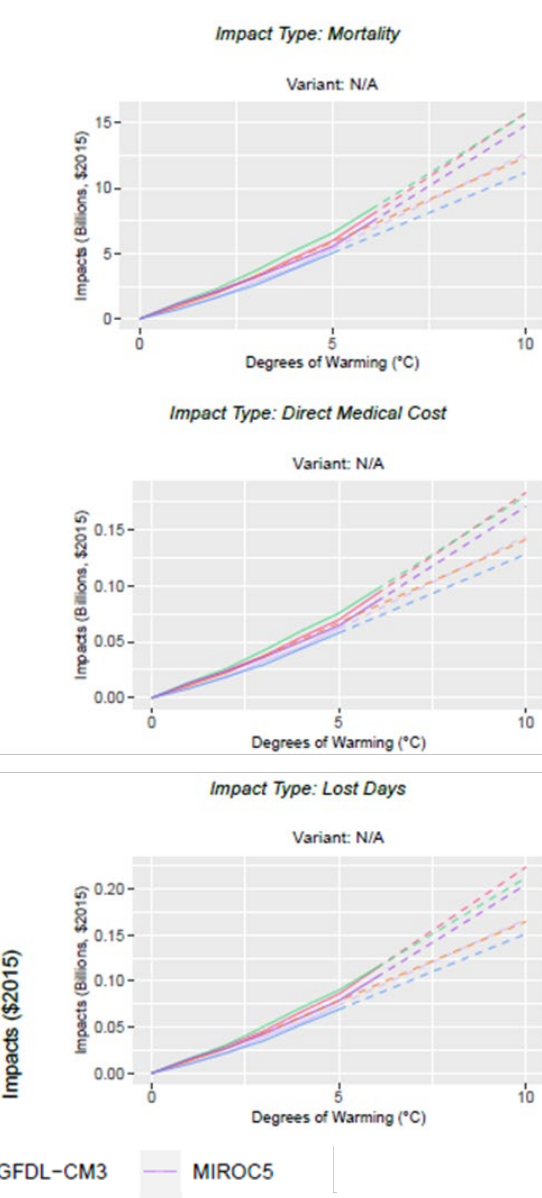
For illustrative purposes, **Figure B-19** shows the resulting damages by degree of warming for the mortality, direct medical cost, and lost workdays impact types, by GCM, calculated using 2010 (panel A) and 2090 (panel B) socioeconomics (i.e., the endpoints of the socioeconomic scenarios).

FIGURE B-19. VIBRIOSIS IMPACTS BY TEMPERATURE BIN DEGREE

A. 2010 SOCIOECONOMICS



B. 2090 SOCIOECONOMICS



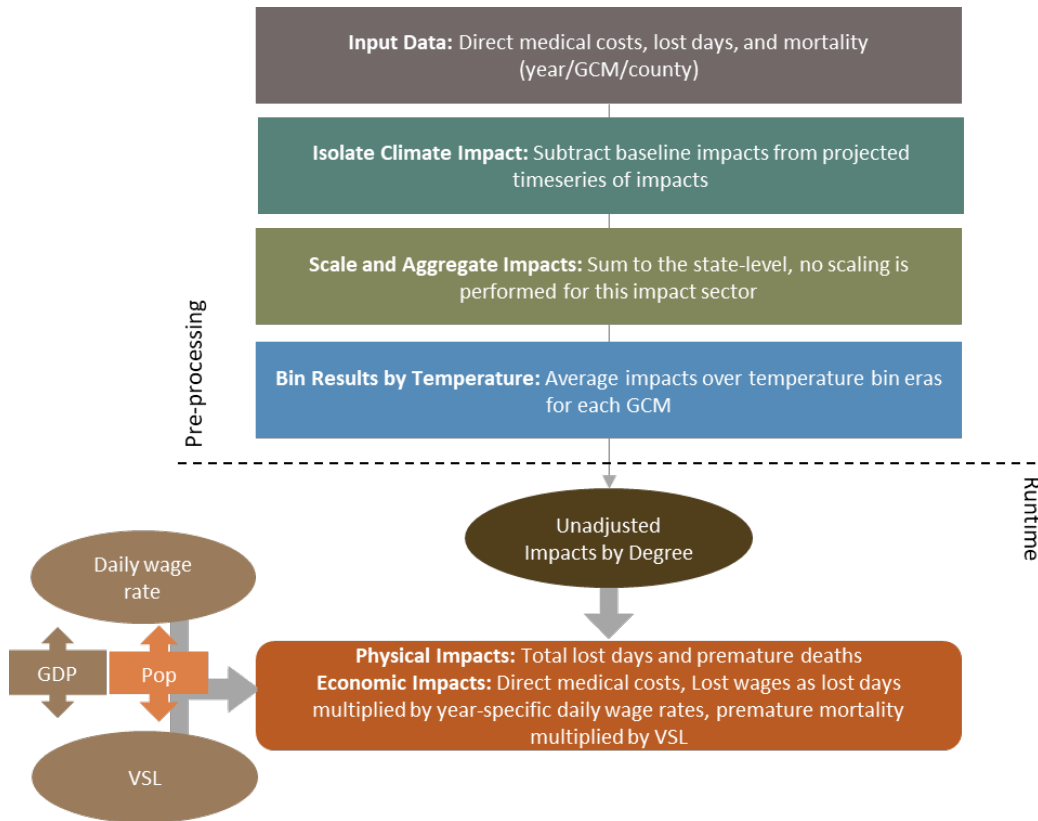
Total impacts (billions of 2015\$) by degree (°C) for each impact type for two socioeconomic snapshots (2010 and 2090 default scenarios). Extrapolated portions are shown with a dashed line. Note y-axis scales vary by plot.

Processing steps

Processing steps are illustrated in **Figure B-20**.

Pre-processing: Original data provided by the Sheahan et al. (2023) study authors include the increases in health impacts (direct medical costs, lost days, or mortality counts) for affected populations at the county level from 2006 to 2099. To isolate the climate impacts in the first pre-processing step, baseline values (provided by study authors) are subtracted from these yearly values and summed to the state level. In the next steps, state-level impacts are binned by degree of CONUS temperature change for each GCM.

FIGURE B-20. VIBRIOSIS DATA PROCESSING FRAMEWORK



Runtime: When FrEDI is run, the pre-processed by-degree impact functions are then applied to the input temperature scenario to calculate the unadjusted annual impacts based on the level of warming in each year of the input scenario. Population is not used in this calculation (see Limitations and Assumptions below). Lastly, annual mortality counts are monetized using the VSL, calculated at runtime from input GDP per capita (Eq. B-1), and lost workdays are monetized using the daily wage rate scaled by user-input GDP per capita. Direct medical costs are already in dollar values and therefore only scale by the user-input temperature scenario.

Limitations and Assumptions

- The original study does not consider population growth in future case projections because the factors that drive vibriosis do not necessarily scale with population. Therefore, this processing does not provide per capita results to allow for population scaling.

- While the original study investigated the impact of changes in sea surface temperatures (related to GCMs) and vibriosis, this tool assumes changes in atmospheric temperature serve as a proxy for changes in baseline sea surface temperatures.
- Consistent with standard EPA practice, real healthcare costs are assumed constant over time in this analysis. There is some evidence, however, that healthcare costs have risen faster than the overall rate of inflation in the recent past – if that trend were to hold true in the future, this assumption would lead to an underestimation bias in the valuation component of this analysis.
- For further discussion of the underlying sectoral model, see Sheahan et al. (2022).

Suicide

Summary

This sector estimates the impact of climate-driven changes in temperature and weather on suicide rates for the population age 5 and older across CONUS using projections based on Belova et al. (2022).

UNDERLYING DATA SOURCES AND LITERATURE

Belova, A., Gould, C.A., Munson, K., Howell, M., Trevisan, C., Obradovich, N., and Martinich, J. (2022). Projecting the Suicide Burden of Climate Change in the United States. *GeoHealth* 6, no. 5. <https://doi.org/10.1029/2021GH000580>

The causative factors driving the association between temperature and suicide are not well understood, but evidence from other countries suggest that suicide by violent means is connected to elevated temperature over a relatively longer period of time than a single heat wave (on the order of a month or more), and hypothesized factors include sociological (e.g., increased alcohol use during heat waves), biological (e.g., effects on neurotransmitters such as serotonin which affect impulsivity and aggression), and psychological (e.g., temperature links to disinhibition and increased propensity for aggression and violence) components.⁶³

Belova et al. (2022) assessed these effects using four different health impact function specifications developed primarily using results from Mullins & White (2019)⁶⁴. Per the authors' recommendation, we use results from Belova et al. (2022) averaged across the four health impact function specifications. Changes in mortality are monetized by applying the GDP per capita adjusted VSL. Additional mental health effects from climate change have been suggested in the literature, but the scope of the quantitative results in this sector is limited to mortality from suicide.

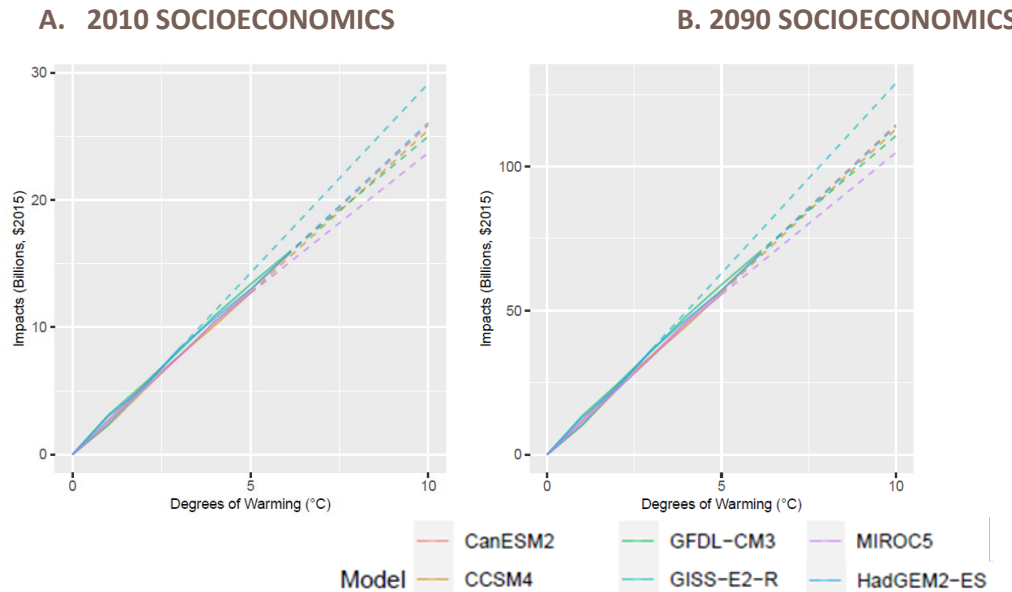
⁶³ Page, L. A., Hajat, S., & Kovats, R. S. (2007). Relationship between daily suicide counts and temperature in England and Wales. *The British Journal of Psychiatry*, 191(2), 106-112. <https://doi.org/10.1192/bjp.bp.106.031948>.

⁶⁴ Mullins, J. T., & White, C. (2019). Temperature and mental health: Evidence from the spectrum of mental health outcomes. *Journal of Health Economics* 68, 102240. <https://doi.org/10.1016/j.jhealeco.2019.102240>

TABLE B-11. INCOMING DATA CHARACTERISTICS: SUICIDE

Data Features	Suicide Attributes
Evaluated Impacts	<ul style="list-style-type: none"> Premature deaths from suicide (physical) and value of premature deaths (economic)
Variants	<ul style="list-style-type: none"> No additional adaptation
Data Shape	<ul style="list-style-type: none"> Integer degree (1-6°C) Six CMIP5 GCMs (standard CIRA set) County level Age binned (5-24, 25-64, 65+)
Model Type	<ul style="list-style-type: none"> Empirical
Runs Provided	<ul style="list-style-type: none"> With climate change, with and without population growth
Additional Data	<ul style="list-style-type: none"> Population by age bin and county
Regions and States with Impacts	<ul style="list-style-type: none"> All CONUS regions and states

For illustrative purposes, **Figure B-20** shows the resulting damages by degree of warming by GCM, calculated using 2010 (panel A) and 2090 (panel B) socioeconomic scenarios (i.e., the endpoints of the socioeconomic scenarios).

FIGURE B-20. SUICIDE IMPACTS BY TEMPERATURE BIN DEGREE

Total impacts (billions of 2015\$) by degree (°C) for two socioeconomic snapshots (2010 and 2090 default scenarios). Extrapolated portions are shown with a dashed line. Note y-axis scales vary by plot.

Processing steps

Processing steps are shown in **Figure B-21**.

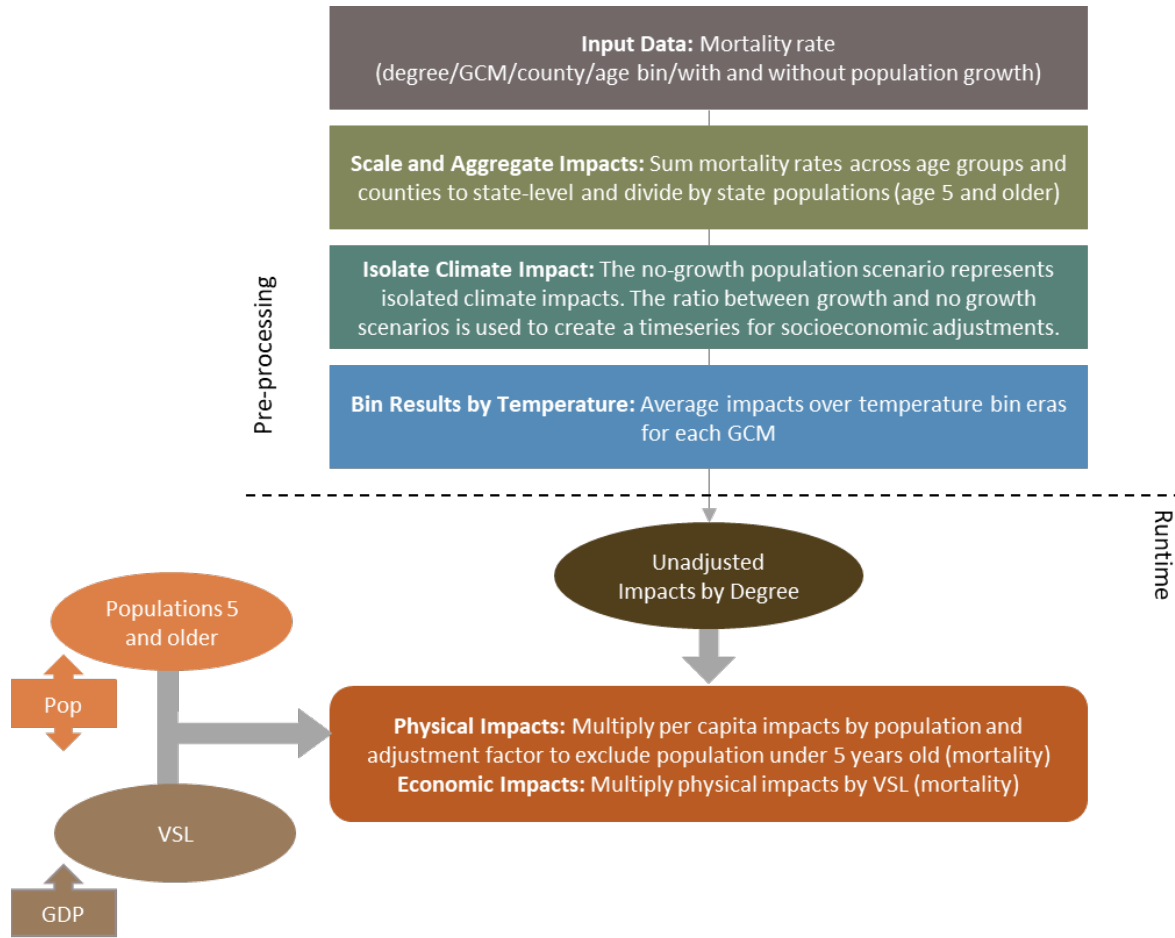
Pre-processing: The data provided by the Belova et al. (2022) study authors include baseline rates, populations, and the number of additional cases under RCP8.5 by GCM, county, age bin, and degree of warming for scenarios with and without population growth. We use the static population scenario for rate calculations and then apply scaling factors to account for demographic changes as described below. While

the authors also provided a distribution of impact results which reflects parametric uncertainty in health impact function coefficients and VSL, FrEDI currently uses point estimates rather than the results of the Monte Carlo simulation.

In the first pre-processing step, populations and incremental additional case counts are aggregated to the state level by summing across age bins and counties. The case count is then divided by the impacted population (i.e., ages 5 and older) for each state to arrive at degree-binned future marginal suicide rates. Because these rates are only based on a subset of the total population (e.g., do not include all ages), a set of scalars is calculated during pre-processing to later adjust the user-input population when FrEDI is run. These scalars are calculated as the ratio of the 5+ population to the total population using the ICLUSv2⁶⁵ projections, which is the basis of FrEDI's default population scenario and the Belova et al. (2022) analysis.

An additional set of scalars also is calculated to account for dynamic demographic changes. The mortality projections from Belova et al. (2022) represent composite rates aggregated across age bins, and the underlying analysis includes implicit assumptions about how the relative weights of these age bins (and their corresponding suicide rates) change over time. For both the static and dynamic population scenarios provided by the authors, we calculate total suicide rates at the county level by multiplying the baseline rate by the population, adding the climate-attributable additional cases, and summing across age bins. We then sum case counts and populations to the state level and divide the total case count by population for each state to arrive at degree-binned future total suicide rates. Finally, we take the ratio of the dynamic population scenario rate to the static population scenario rate. Population is the only driver that varies between these two scenarios, so the ratio of the two represents the effect of demographic change on projected suicide rates. Both sets of scalars are calculated at the state level in all years for which we received data from the authors (the integer degree arrival years for the six included GCMs) and are used during FrEDI runtime to adjust calculated impacts.

⁶⁵ Bierwagen et al., 2010; ICLUSv2, 2017 (see footnote 31)

FIGURE B-21. SUICIDE DATA PROCESSING FRAMEWORK

Runtime: When FrEDI is run, the pre-processed by-degree per capita mortality functions are then applied to the input temperature scenario to calculate the unadjusted annual per capita impacts based on the level of warming in each year of the input scenario. The total annual physical mortality counts are then calculated by applying these annual per capita rates to the input population scenario, which are then scaled to account for changes in population demographics and to only include impacts to those age 5 and older. Lastly, annual mortality counts are monetized using the VSL, calculated at runtime from input GDP per capita (Eq. B-1).

Limitations and Assumptions

- There is potential for overlap in premature mortality of any type attributable to extreme heat (addressed in the Extreme Temperature, CIL Temperature-Related Mortality, and ATS Temperature-Related Mortality sectors) and suicide mortality attributed to high heat days in this sector. For the heat event-based Extreme Temperature sector, the effect is likely to be small because the “high heat day” metrics differ substantially across the two sectors, with a different definition of the heat stressor including much lower effective threshold for high heat in the Belova et al. (2022) study used here (80°F). For the other two temperature/mortality options, the potential for overlap is greater – this is described in more detail in Section 2.2 of the main report, under the header

Aggregation of Sectoral Impacts. For this reason, the applications of FrEDI in this report take a conservative approach and incorporate a downward adjustment to the ATS Temperature-Related Mortality equal to the total mortality impact estimated for the Suicide sector, to avoid double-counting of mortality estimates.

- Based on communication with the authors of Belova et al. (2022), we use an average across the four impact function specifications here. Using an individual specification or a different subset of the four could alter estimates.
- These projections account for potential adaptation strategies only to the extent that they were implemented during the observation period of Belova et al. (2022). The potential for future adaptation efforts (e.g., expanded access to air conditioning, urban greening) and societal trends (e.g., increased recognition of mental health diagnoses and expanded access to mental health treatment) to reduce these impacts is not considered here.

Lyme Disease

Summary

This sector estimates the health burden and the associated economic value in CONUS resulting from changes in Lyme Disease cases projected with climate change. Lyme disease is an illness that can be contracted by humans when they are bitten by an *Ixodes scapularis*, commonly known as the deer tick or black-legged tick, infected with the bacterium *Borrelia burgdorferi*.

Deer ticks are commonly found in the Northeast, East Coast, and Upper Midwest of the United States. Warmer air temperatures and increased precipitation generally promote tick activity, leading to a higher risk of Lyme Disease infection, and the shift in suitable habitat for ticks changes the exposed population.

The underlying study (Yang et al., 2024) uses county-level CDC data⁶⁶ on historical Lyme Disease infections and the severity of the resulting health effects. To project future estimates of Lyme Disease infections, the authors use estimates of current rates at the county level to estimate a present-day incidence model and apply model coefficients to future bioclimatic variables, estimated future *I. scapularis* habitat suitability, and present-day land use, human population, and *B. burgdorferi* presence. Damages are based on estimates of monetized medical insurance claims from Adrión et al. (2015), which include inpatient care,

UNDERLYING DATA SOURCES AND LITERATURE

Yang, H., Gould, C. A., Jones, R., St. Juliana, A., Sarofim, M., Rissing, M., & Hahn, M. B. (2024). By-degree Health and Economic Impacts of Lyme Disease, Eastern and Midwestern United States. *EcoHealth*, 21(1), 56-70.

<https://doi.org/10.1007/s10393-024-01676-9>

Adrión, E. R., Aucott, J., Lemke, K. W., & Weiner, J. P. (2015). Health care costs, utilization and patterns of care following Lyme disease. *PloS one*, 10(2), e0116767.

<https://doi.org/10.1371/journal.pone.0116767>

⁶⁶ U.S. Centers for Disease Control and Prevention. (2022). “National Notifiable Diseases Surveillance System, Lyme Disease Surveillance Data 2008–2019.” Fort Collins, CO. CDC Division of Vector-Borne Diseases. [Dataset].; U.S. Centers for Disease Control and Prevention. (2022). “Established and reported records of *Borrelia burgdorferi* sensu stricto or *Borrelia mayonii* through Dec. 31, 2021.” <https://www.cdc.gov/ticks/surveillance/TickSurveillanceData.html>.

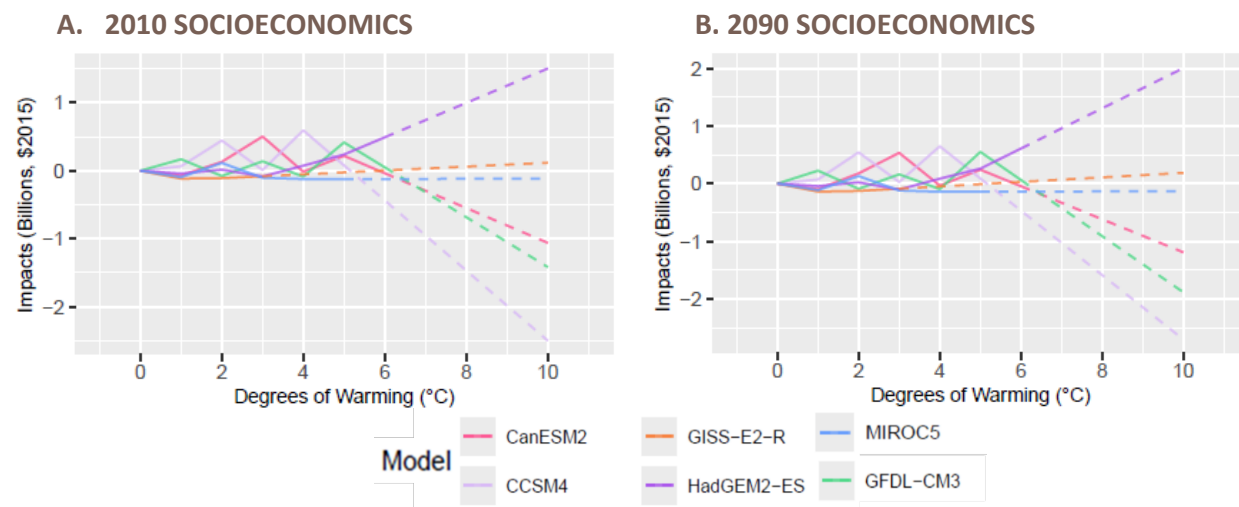
outpatient care, laboratory testing, and other expenses. Indirect costs such as lost workdays or productivity were omitted from both Adrián et al. (2015) and Yang et al. (2024).

TABLE B-12. INCOMING DATA CHARACTERISTICS: LYME DISEASE

Data Features	Lyme Disease Attributes
Evaluated Impacts	<ul style="list-style-type: none"> New Lyme Disease cases (physical) and insurance claim costs (economic)
Variants	<ul style="list-style-type: none"> No additional adaptation
Data Shape	<ul style="list-style-type: none"> Integer Degree (1-6°C) Six CMIP5 GCMs (standard CIRA set) County level
Model Type	<ul style="list-style-type: none"> Empirical
Runs Provided	<ul style="list-style-type: none"> With climate change and population growth Historical baseline
Additional Data	<ul style="list-style-type: none"> Cost of Illness
Regions and States with Impacts	<ul style="list-style-type: none"> Northeast Midwest Southeast (excluding AR, FL, GA, KY, LA, MS, SC, TN, AL)

For illustrative purposes, **Figure B-22** shows the resulting damages by degree by GCM.

FIGURE B-22. LYME DISEASE IMPACTS BY TEMPERATURE BIN DEGREE



Total impacts (billions of 2015\$) by degree (°C) for two socioeconomic snapshots (2010 and 2090 default scenarios). Extrapolated portions are shown with a dashed line. Note y-axis scales vary by plot.

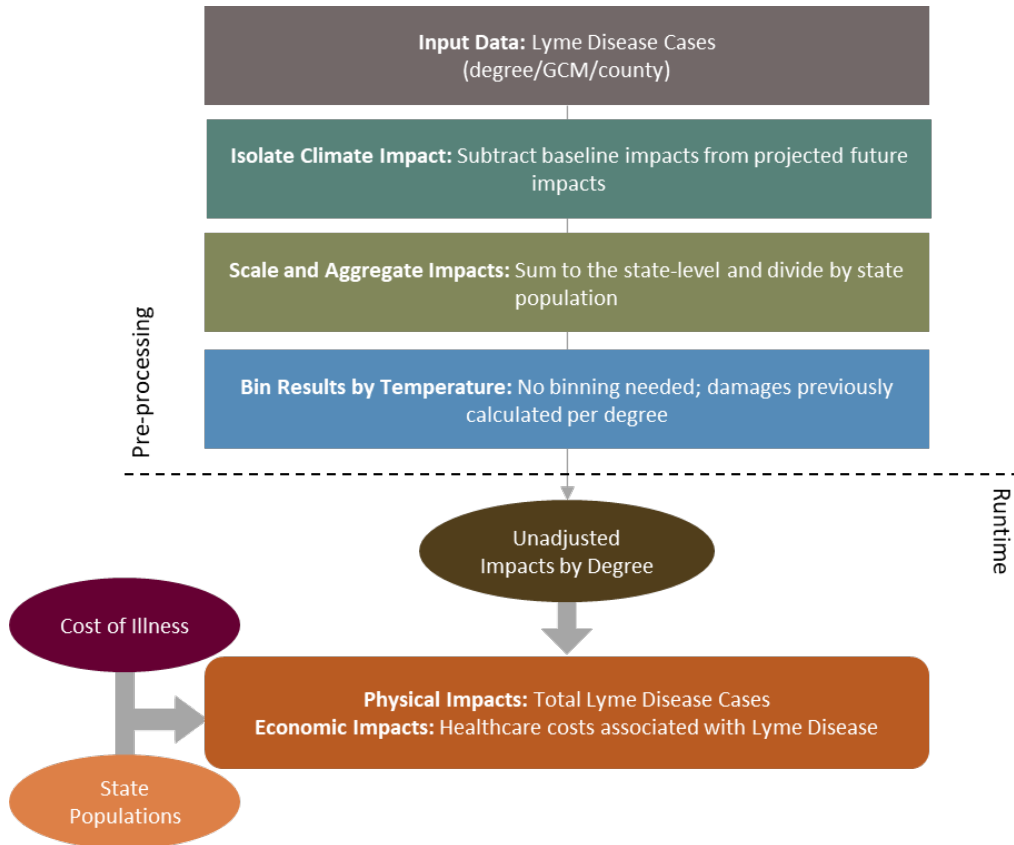
Processing steps

Processing steps are illustrated in **Figure B-23**.

Pre-processing: Original data provided by the Yang et al. (2024) study authors include projected Lyme Disease cases at the county level for integer degrees 1-6 of CONUS temperature change for each GCM. To isolate the climate impacts in the first pre-processing step, baseline values (provided by study authors) are

subtracted from these degree-binned values and summed to the state level. In the next step, net cases are divided by ICLUSv2 population projections to estimate future net Lyme Disease cases per capita.

FIGURE B-23. LYME DISEASE DATA PROCESSING FRAMEWORK



Runtime: When FrEDI is run, the pre-processed by-degree impact functions are then applied to the input temperature scenario to calculate the unadjusted annual impacts based on the level of warming in each year of the input scenario. Per capita impacts are then multiplied by the input populations by state. Lastly, Lyme Disease cases are monetized using cost of illness reported in Yang et al. (2024), which is adjusted from estimates in Adriion et al. (2015).

Limitations and Assumptions

- The analysis does not consider different subpopulations of *I. scapularis*, evolution of future subspecies, or future adaptation to tick behavior.
- The geographic region for this analysis is limited to states with historically high incidence of Lyme Disease. However, it is likely that Lyme disease risk will expand beyond these regions in the future.
- Consistent with standard EPA practice, real cost of illness is assumed constant over time in this analysis. There is some evidence, however, that healthcare costs have risen faster than the overall rate of inflation in the recent past – if that trend were to hold true in the future, this assumption would lead to an underestimation bias in the valuation component of this analysis. In addition, the study omitted indirect costs of lost workdays or productivity, and also costs for some more serious

but less common consequences of Lyme disease, such as posttreatment Lyme disease syndrome (PTLDS). The result of these limitations is an underestimate of the full costs of Lyme disease cases.

- The analysis does not consider how human behavior in response to warming temperatures may increase or decrease exposure. For example, the Outdoor Recreation sector estimates increases in time spent outdoors with warmer temperatures which may increase Lyme Disease exposure. However, increases in Lyme disease could trigger public health warnings that decrease exposure.
- For further discussion of the underlying sectoral model, see Yang et al. (2024).

B.3 Infrastructure Sectors

Coastal Properties

Summary

This sector estimates future property value damages from combined SRL and storm surge in the CONUS, attributed to climate change.

Damages are estimated for all real properties (land and structure) in all coastal counties that contain land with a hydraulic connection to the ocean and containing property that is within 20 m elevation above sea level for the year 2000. Property values for potentially vulnerable structures and land are “market adjusted” assessed values that reflect 2017 property values for 302 counties along the CONUS coast – see Neumann et al. (2021) for details. Within the model, real property values appreciate over the century by GDP per capita projections. While Lorie et al. (2020) provided details of the coastal property impact methodology for two “test areas” of the U.S., Neumann et al. (2021) applied this methodology from Lorie et al. (2020) to the full CONUS coast, while also addressing climate impacts on rail and road infrastructure.

The underlying damage simulation model includes cost estimates for no additional adaptation and two adaptation scenarios (reactive and proactive), as defined in the underlying study. Under the no additional adaptation scenario, properties are abandoned once inundated. Reactive adaptation loosely reflects structural adaptation options that can be adopted without collective action (e.g., elevation of structures and land near structures), while proactive adaptation includes consideration of options that likely require collective action (such as beach nourishment and construction of seawalls).⁶⁷ The model conducts a series

UNDERLYING DATA SOURCES AND LITERATURE

Neumann, J. E., Chinowsky, P., Helman, J., Black, M., Fant, C., Strzepek, K., & Martinich, J. (2021). Climate effects on US infrastructure: the economics of adaptation for rail, roads, and coastal development. *Climatic Change*.

<https://doi.org/10.1007/s10584-021-03179-w>

Lorie, M., Neumann, J. E., Sarofim, M. C., Jones, R., Horton, R. M., Kopp, R. E., Fant, C., Wobus, C., Martinich, J., O’Grady, M., Gentile, L. E. (2020). Modeling coastal flood risk and adaptation response under future climate conditions. *Climate Risk Management*, 29.

<https://doi.org/10.1016/j.crm.2020.100233>

⁶⁷ The underlying study (Neumann et al. 2021) outlines the logic for classifying measures as reactive or proactive. The general concept is that reactive measures are either responsive to events (without foresight about future events) or can be undertaken without coordinated action between individuals and governments. Elevation, for example, is modeled at the individual property level in response to highly localized hazards, not as a collective action of municipal governments to modify building codes.

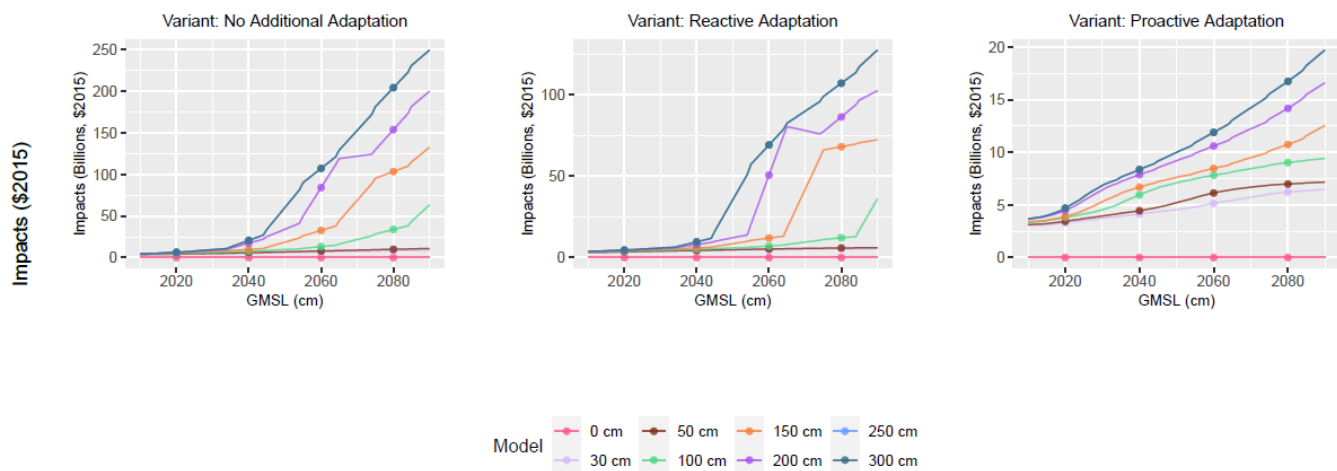
of benefit-cost calculations at the level of a 150m x 150m grid cell to assess where and when adaptation could be cost-effective in mitigating property damage due to SLR and storm surge.

TABLE B-13. INCOMING DATA CHARACTERISTICS: COASTAL PROPERTIES

Data Features	Coastal Properties Attributes
Evaluated Impacts	<ul style="list-style-type: none"> Costs of coastal property damage (economic)
Variants	<ul style="list-style-type: none"> Direct adaptation Reasonably anticipated adaptation No additional adaptation
Data Shape	<ul style="list-style-type: none"> Annual Three adaptation scenarios Six SLR scenarios County level
Model Type	<ul style="list-style-type: none"> Simulation
Runs Provided	<ul style="list-style-type: none"> With climate change, with socioeconomic growth
Additional Data	<ul style="list-style-type: none"> None
Regions and States with Impacts	<ul style="list-style-type: none"> Northeast (excluding VT, WV) Northwest (excluding ID) Southeast (excluding AR, KY, TN) Southern Plains (excluding KS, OK) Southwest (excluding AZ, CO, NV, NM, UT)

For illustrative purposes, **Figure B-24** shows the resulting damages overtime, by SLR scenario, for the three adaptation option variants included in FrEDI.

FIGURE B-24. COASTAL PROPERTIES IMPACTS BY SLR SCENARIO OVER TIME



Total impacts (billions of 2015\$) by year and variant. Note y-axis scales vary by plot.

Processing steps

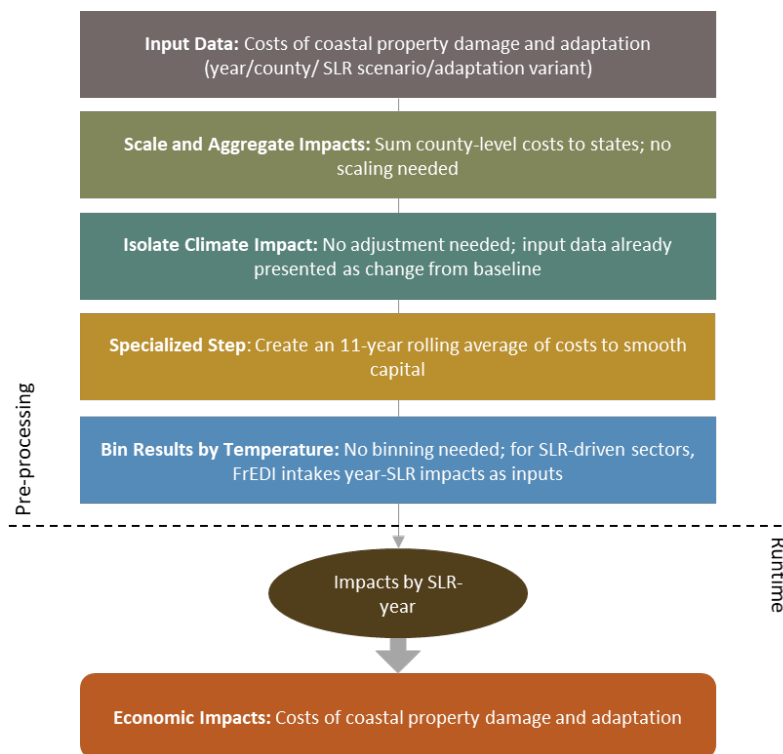
Processing steps are shown in **Figure B-25**.

Pre-processing: The study authors provided annual trajectories of property damages for each SLR scenario, year, county, and adaptation scenario. Residential and commercial properties and energy infrastructure are

considered when calculating projected damages in the underlying model. For this sector in FrEDI, the baseline is anchored at the year 2000, as the National Coastal Property Model (NCPM) starts with zero damages in this year. In the first processing step, county-level damages are summed to the state level. Annual damages are then calculated using the 11-year rolling average damages for each SLR scenario.⁶⁸

As with the temperature bin indexing, GMSL is mapped to state and local sea levels based on the localized SLR projections from Sweet et al. (2017), which include effects such as land uplift or subsidence, oceanographic effects, and responses of the geoid and the lithosphere to shrinking land ice.⁶⁹ When custom SLR scenarios are used as input in FrEDI, the relationship between GMSL and state sea levels, and ultimately state impacts, are mapped implicitly based on the underlying models. As noted in the main report text, SLR is estimated separately from a reduced complexity model that incorporates the time- and trajectory-dependent qualities of SLR response to temperature. That implies that damages should be estimated along the trajectory using both the sea level height and the year that the sea-level height is reached (and therefore, that year's implicit socioeconomics).

FIGURE B-25. COASTAL PROPERTIES DATA PROCESSING FRAMEWORK



⁶⁸ This calculation utilizes an 11-year window when five years of data are available on either side of the central year. At the beginning and end of the time series, the window tightens to preserve balance around the central year while still capturing results through 2100. The 11-year averaging technique is similar to the approach described in Appendix C for temperature binning, however since this sector is driven by SLR rather than temperature, the rolling averages are captured for every year. See Section 2.3 of the Main Text for further discussion on damage function development for SLR-driven impacts.

⁶⁹ Sweet, W., Kopp, R. E., Weaver, C. P., Obeysekera, J., Horton, R. M., Thieler, E. R., & Zervas, C. (2017). Global and Regional Sea Level Rise Scenarios for the United States (NOAA Technical Report NOS CO-OPS 083). NOAA/NOS Center for Operational Oceanographic Products and Services.

Runtime: When FrEDI is run, the damage trajectory is interpolated between the damage curves of the SLR scenarios that have the SLR heights just above and below the input scenario in each year. For example, if the SLR trajectory reaches 175cm in 2080, the damage estimate would fall between the 150cm and 200cm scenarios for that year.

Limitations and Assumptions

- Damages are limited to land and structures within the study domain (i.e., flooding impacts to structures inland of 20m elevation are not quantified), and exclude the value of public infrastructure, which was not considered in the underlying sectoral study.
- Adaptation response decisions in the coastal zone are not typically made with strict cost-benefit decision rules, particularly at the local level. Other factors may include local zoning bylaws, future land use plans, the presence of development-supporting infrastructure, or proximity to sites with high cultural value. However, the analytical framework of this coastal property model provides a simple, benefit-cost decision framework that can be consistently applied for state and national-scale analysis.
- The underlying study does not consider the effects of climate on storm surge activity (although impacts on wind damage are considered in a separate sector study included in the tool). The only non-climate change driven change to coastline considered was an increase in land and existing structure value over time.
- For further discussion of the limitations and assumptions in the underlying sectoral model see Neumann et al. (2021), Lorie et al. (2020), and U.S.EPA (2017).

Transportation Impacts from High Tide Flooding

Summary

This sector estimates the cost of delays to passenger and freight traffic on coastal roads in the CONUS that experience flooding due to combinations of high tides and SLR, as well as costs of adaptation in the form of infrastructure improvements.

UNDERLYING DATA SOURCES AND LITERATURE

Fant, C., Jacobs, J. M., Chinowsky, P., Sweet, W., Weiss, N., Martinich, J. & Neumann, J. E. (2021). Mere nuisance or growing threat? The physical and economic impact of high tide flooding on US road networks. Journal of Infrastructure Systems. [https://doi.org/10.1061/\(ASCE\)IS.1943-555X.0000652](https://doi.org/10.1061/(ASCE)IS.1943-555X.0000652)

Delay damages are in terms of passenger and freight vehicle-hours. These are monetized based on the value of travel time savings (VTTs) for passenger traffic, and the National Cooperative Highway Research Program's (NCHRP) inputs for cost of delay for freight traffic. Infrastructure improvements include building sea walls or elevating the elevation of the roadway surface. Infrastructure improvement costs include estimates of material, labor, and construction delays.

This sector in FrEDI considers three adaptation scenarios: no additional adaptation, reasonably anticipated adaptation, and direct adaptation. These adaptation scenarios differ from scenarios modeled for other infrastructure sectors. The no additional adaptation, reactive adaptation, and proactive adaptation

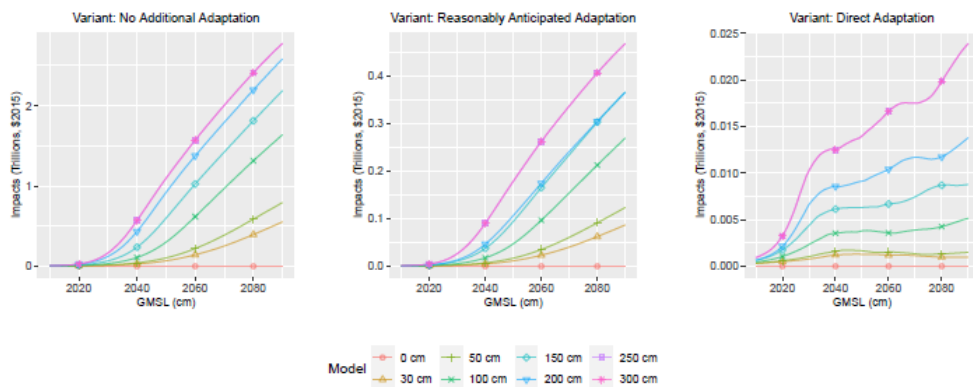
scenarios of other infrastructure sectors are based on infrastructure development for an unchanging, current, or future climate in a given model time step. For this sector, the no additional adaptation scenario estimates costs of delays associated with flooding of roadways with the assumption that drivers do not re-route and instead wait until the roadway is clear to travel. The reasonably anticipated adaptation scenario assumes drivers re-route to avoid flooded roadways, with only slight delay due to increased travel time. This scenario also includes ancillary protection; in cases where flooded roadways are near properties that would be protected by sea walls or beach nourishment, this scenario assumes those roadways would also be protected and thus no longer flood.⁷⁰ In the direct adaptation scenario, where delay costs are high enough, roadways are either protected from flooding through construction of a sea wall or road elevation.

TABLE B-14. INCOMING DATA CHARACTERISTICS: TRANSPORTATION IMPACTS FROM HIGH TIDE FLOODING

Data Features	Transportation Impacts from High Tide Flooding Attributes
Evaluated Impacts	<ul style="list-style-type: none"> Costs of delays and infrastructure improvements (economic)
Variants	<ul style="list-style-type: none"> Direct adaptation Reasonably anticipated adaptation No additional adaptation
Data Shape	<ul style="list-style-type: none"> Annual Three adaptation scenarios Six SLR scenarios County level
Model Type	<ul style="list-style-type: none"> Simulation
Runs Provided	<ul style="list-style-type: none"> With climate change, with socioeconomic growth
Additional Data	<ul style="list-style-type: none"> None
Regions and States with Impacts	<ul style="list-style-type: none"> Northeast (excluding VT, WV) Northwest (excluding ID) Southeast (excluding AR, KY, TN) Southern Plains (excluding KS, OK) Southwest (excluding AZ, CO, NV, NM, UT)

For illustrative purposes, **Figure B-26** shows the resulting damages overtime by SLR scenario for the three adaptation variants available in FrEDI.

⁷⁰ Including ancillary protection of properties with sea walls in the “reasonably anticipated” category, consistent with the underlying Fant et al. (2021) study, may seem inconsistent with the classification of sea walls as “proactive” adaptation in the coastal properties sector. As outlined in Fant et al. (2021), however, the impact of this potential inconsistency is slight - Figure 3 and accompanying text in that paper note that alternative routing reduces the no adaptation impacts by 77%, while the marginal additional impact of ancillary sea wall protection increases the total to an 80% reduction.

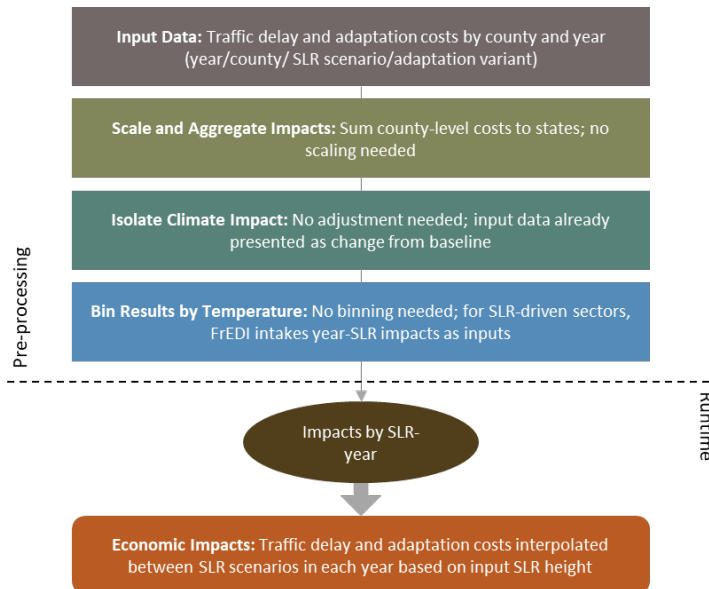
FIGURE B-26. TRANSPORTATION IMPACTS FROM HIGH TIDE FLOODING BY TEMPERATURE BIN DEGREE

Total impacts (trillions of 2015\$) by year and variant. Note y-axis scales vary by plot.

Processing steps

Processing steps are shown in **Figure B-27**.

Pre-processing: Total traffic delay and adaptation costs at the county level are provided by the Fant et al. (2021) study authors. In pre-processing step one, these total costs are aggregated to the state level. These damages are available for all SLR scenarios, year, and adaptation scenario combinations. Annual damages are then calculated using the 11-year rolling average damages for each SLR scenario.⁷¹ Similar to the Coastal Properties sector, this sector “zeroes out” in 2000, and thus has no baseline for which to adjust. This sector also relies on an interpolated damage estimation technique between results calculated in pre-processing for six SLR scenarios, as described in Section 2.3 of the Main Documentation.

FIGURE B-27. TRANSPORTATION IMPACTS FROM HIGH TIDE FLOODING DATA PROCESSING FRAMEWORK

⁷¹ This calculation utilizes an 11-year window when five years of data are available on either side of the central year (see footnote 68).

Runtime: When FrEDI is run, the damage trajectory is interpolated between the damage curves of SLR scenarios that have the SLR heights just above and below the input scenario in each year. For example, if the SLR trajectory reaches 175cm in 2080, the damage estimate would fall between the 150cm and 200cm scenarios for that year.

Limitations and Assumptions

- The underlying sectoral analysis is limited to road segments within the flood extent for the current minor flood level. This extent is expected to migrate further inland as sea levels rise. This analysis also omits consideration of impacts to underground roads.
- Flooding from rainfall or riverine flooding is not modeled and may exacerbate flood events or durations in the coastal zone if they occur simultaneously.
- Many direct adaptation options (e.g., hydrologic infrastructure) are not considered.
- The economic cost per hour of delay per passenger or freight vehicle is assumed to be constant over the century.
- For further discussion of the underlying sectoral model see Fant et al. (2021).

Rail

Summary

This sector estimates repair, equipment, and delay costs to rail infrastructure due to rail track buckling or the risk of buckling in the CONUS associated with elevated temperatures. Damages are based on costs of repair, including equipment and labor, and delay costs. These costs are then scaled using total track miles in each state of CONUS.

The analysis is completed for each of three adaptation scenarios: no additional adaptation, proactive adaptation, and reactive adaptation. The no additional adaptation scenario incorporates no speed restrictions but results in a higher risk of track buckling associated with continued use of trains during high temperature events. Track buckling events require repairs that create delays. The reactive scenario considers reduced train speeds at higher temperatures to reduce likelihood of track buckling. The proactive scenario includes installation of temperature sensors to monitor probabilities of track buckling and modify train speeds as necessary (and therefore prevent delays associated with their unexpected need for repair).

Full details of the approach, including estimation of delay costs and adaptation options, are provided in Chinowsky et al. (2019). Neumann et al. (2021) adds specification of the “no additional adaptation” scenario and provides the basis for state-level disaggregation of results for input to FrEDI.

UNDERLYING DATA SOURCES AND LITERATURE

Neumann, J. E., Chinowsky, P., Helman, J., Black, M., Fant, C., Strzepek, K., & Martinich, J. (2021). Climate effects on US infrastructure: the economics of adaptation for rail, roads, and coastal development. *Climatic Change*.

<https://doi.org/10.1007/s10584-021-03179-w>

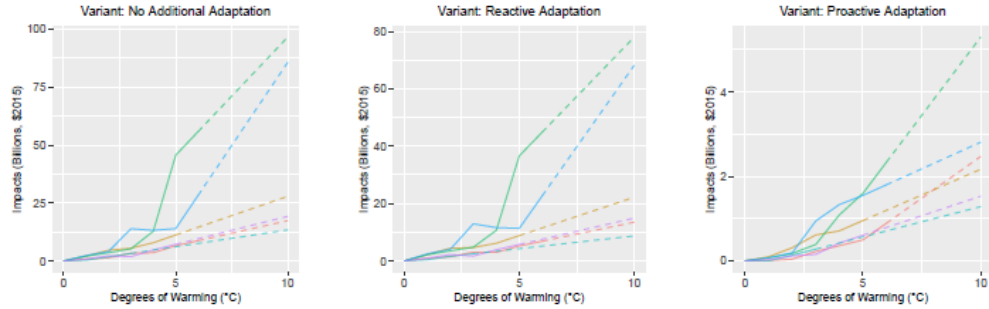
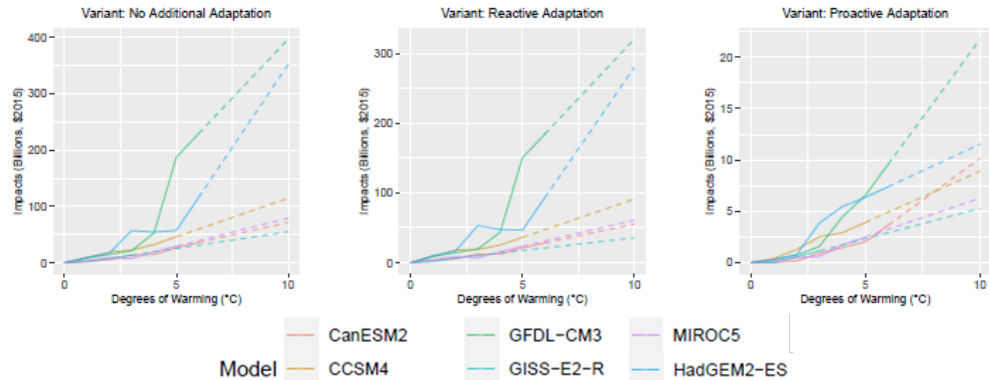
Chinowsky, P., Helman, J., Gulati, S., Neumann, J., & Martinich, J. (2019). Impacts of climate change on operation of the US rail network. *Transport Policy*, 75, 183-191.

<https://doi.org/10.1016/j.tranpol.2017.05.007>

TABLE B-15. INCOMING DATA CHARACTERISTICS: RAIL

Data Features	Rail Attributes
Evaluated Impacts	<ul style="list-style-type: none"> Rail Damage and Delay (economic)
Variants	<ul style="list-style-type: none"> No Additional Adaptation Reactive Adaptation Proactive Adaptation
Data Shape	<ul style="list-style-type: none"> Yearly projections 2006-2099 Six CMIP5 GCMs (standard CIRA set) ½ degree grid level
Model Type	<ul style="list-style-type: none"> Simulation
Runs Provided	<ul style="list-style-type: none"> With socioeconomic growth and with climate change With socioeconomic growth and without climate change (baseline runs; one baseline per adaptation scenario)
Additional Data	<ul style="list-style-type: none"> Regional rail inventory 2018 vintage ½ degree grid inventory
Regions and States with Impacts	<ul style="list-style-type: none"> All CONUS regions and states

For illustrative purposes, **Figure B-28** shows the resulting damages by degree of warming for the three adaptation scenarios, by GCM, calculated using 2010 (panel A) and 2090 (panel B) socioeconomics (i.e., the endpoints of the socioeconomic scenarios).

FIGURE B-28. RAIL IMPACTS BY TEMPERATURE BIN DEGREE**A. 2010 SOCIOECONOMICS****B. 2090 SOCIOECONOMICS**

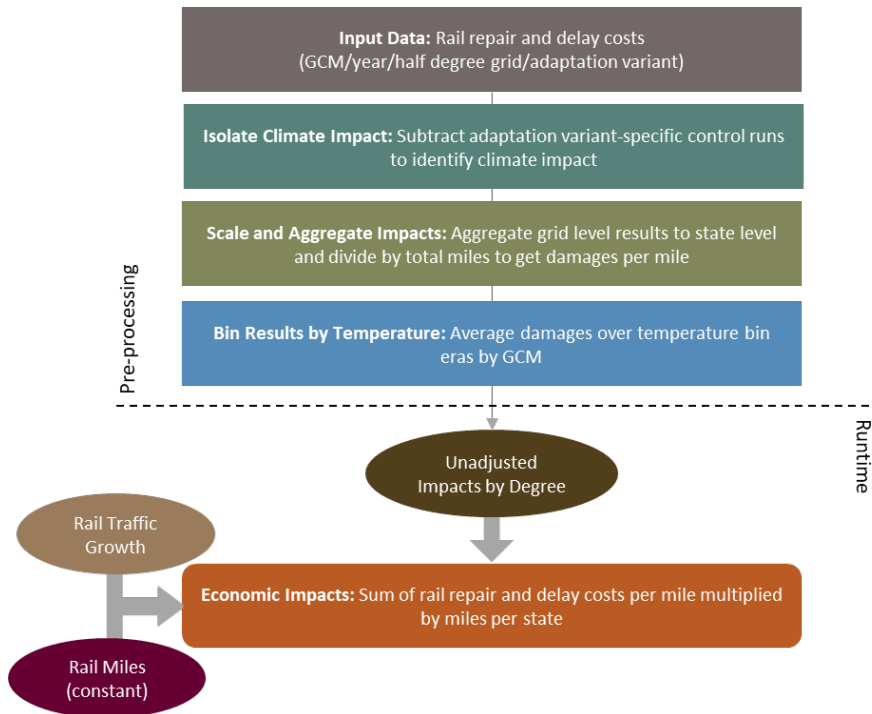
Total impacts (billions of 2015\$) by degree ($^{\circ}\text{C}$) for each variant for two socioeconomic snapshots (2010 and 2090 default scenarios). Extrapolated portions are shown with a dashed line. Note y-axis scales vary by plot.

Processing steps

Processing steps are shown in **Figure B-29**.

Pre-processing: The provided data from Neumann et al. (2021) reports damages at the Climatic Research Unit (CRU) $\frac{1}{2}$ degree grid cell level. In the first pre-processing step, baseline costs from a reference scenario (i.e., costs under a no climate change scenario that include socioeconomic growth over the century) are subtracted for all adaptation scenarios to isolate the damages just due to climate change. There are unique baselines for each of the three adaptation scenarios. Across the three baselines, each 20-year period generally displays repeating patterns of year-to-year variation at different magnitudes. Thus, we take the mean of each 20-year period and subtract from its respective years' damages to sustain general trends in the baseline without being subjected to large variance year-to-year. In the second pre-processing step, net damages and track miles are then aggregated to the state level. Damages and track miles within grids that cross state lines are distributed relative to the percentage of grid area within each state. This impact model assumes that the spatial extent and distribution of rail infrastructure remains constant across the 21st century. In the next pre-processing steps, net damages are divided by total miles of rail within a state to produce damages per mile. Rail miles per state are developed by using a 2015 vintage $\frac{1}{2}$ degree grid cell inventory⁷² to determine state share of regional inventory and applying these weights to the regional inventory within FrEDI. Lastly, resulting annual net damages per mile are binned by degree of CONUS temperature change for each GCM by averaging across the 11-year windows where each GCM reaches each integer degree of CONUS warming relative to the baseline.

FIGURE B-29. RAIL DATA PROCESSING FRAMEWORK



⁷² Bureau of Transportation Statistics (2015) National Transportation Atlas Databases – NTAD 2015.

Runtime: When FrEDI is run, the pre-processed by-degree impacts per mile functions are then applied to the input temperature scenario to calculate the unadjusted annual per mile impacts based on the level of warming in each year of the input scenario. Total damages are then calculated by applying these annual impacts per mile by the number of miles in a state, as well as a national socioeconomic growth scalar (with a 2010 base year). The scalar is calculated based on a ratio of a with and without growth scenario. Freight traffic represents 96 percent of rail traffic, and passenger traffic the remaining four percent.

Limitations and Assumptions

- The model assumes the number of rail miles is fixed and does not grow over time, though rail traffic over the existing rail network grows with a weighted average of population growth (for the passenger rail component) and economic growth (for the much larger freight rail component).
- Equipment, labor, and repair supply costs are assumed to remain constant.
- For further discussion of the limitations and assumptions in the underlying sectoral model see Neumann et al. (2021), Chinowsky et al. (2017), and U.S. EPA (2017).

Roads

Summary

This sector estimates the cost of road repair, user costs (vehicle damage), and road delays due to changes in road surface quality in the CONUS projected with climate change (specifically changes in temperature, precipitation, and flooding).

Damages are based on the cost of repairs and delays associated with either deteriorated road surfaces or road shutdowns to complete repairs, and delays are scaled by current

period traffic, which in turn is adjusted for future changes in population (described further below). The per mile impacts are then multiplied by total state road miles and adjusted to reflect the likelihood of delay mitigation as proxied by an index of road density in each $\frac{1}{4}$ degree by $\frac{1}{4}$ degree grid cell, to produce a total damage estimate in a state.

Similar to the rail and coastal properties studies, the analysis models three adaptation scenarios: no additional adaptation, proactive adaptation, and reactive adaptation. In the no additional adaptation scenario, repairs to roads are limited to historic repair budgets and damages are based on the cost of repairs to road surfaces, damage to vehicles associated with incompletely maintained roads, and delays

UNDERLYING DATA SOURCES AND LITERATURE

Neumann, J. E., Chinowsky, P., Helman, J., Black, M., Fant, C., Strzepek, K., & Martinich, J. (2021). Climate effects on US infrastructure: the economics of adaptation for rail, roads, and coastal development. *Climatic Change*.

<https://doi.org/10.1007/s10584-021-03179-w>

Neumann, J. E., Price, J., Chinowsky, P., Wright, L., Ludwig, L., Streeter, R., Jones, R., Smith, J. B., Perkins, W., Jantarasami, L., & Martinich, J. (2015). Climate change risks to US infrastructure: impacts on roads, bridges, coastal development, and urban drainage. *Climatic Change*, 131, 97-109.

<https://doi.org/10.1007/s10584-013-1037-4>

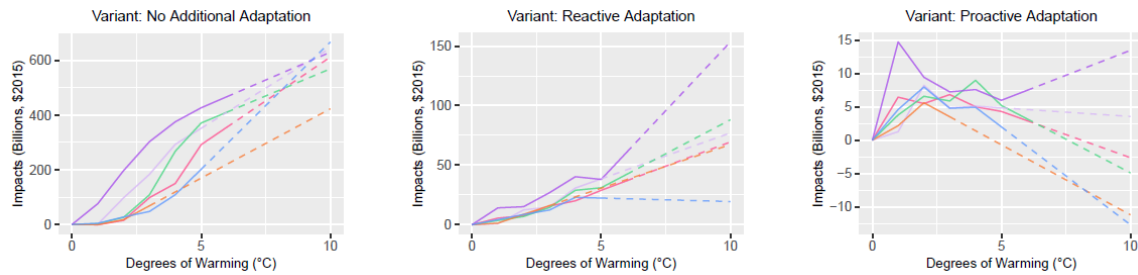
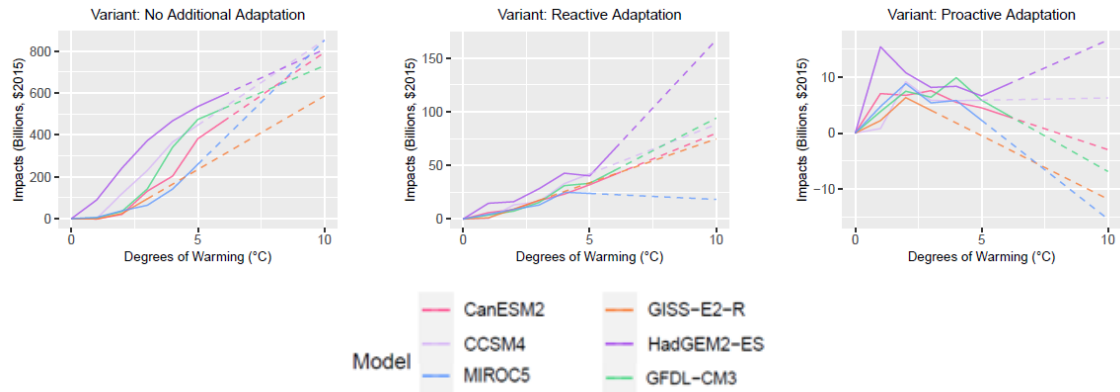
associated with repairs to road surfaces or speed limitations attributed to poorly maintained roads.⁷³ Under the reactive adaptation scenario, repair budgets are increased to repair all damages in a given year to re-establish the pre-damage level of service. In the proactive scenario, roads are pre-emptively strengthened to prevent damage with consideration of future climate changes in the design and materials used for repair. Under the reactive and proactive adaptation scenarios, damages are based on the cost of repairs to road surfaces and the delays associated with repairs or speed limitations due to poorly maintained roads. The model considers three types of environmental stressors: temperature, precipitation, and flooding. Damages differ by road surface; road surfaces are either unpaved, paved, or gravel. This impact model runs at the quarter-degree grid cell level, and each grid cell is assigned adaptation-scenario specific budget for repairs.

TABLE B-16. INCOMING DATA CHARACTERISTICS: ROADS

Data Features	Roads Attributes
Evaluated Impacts	<ul style="list-style-type: none"> Road Damage and Delay (economic)
Variants	<ul style="list-style-type: none"> No Additional Adaptation Reactive Adaptation Proactive Adaptation
Data Shape	<ul style="list-style-type: none"> Annual, 2006-2099 Six CMIP5 GCMs (standard CIRA set) ¼ degree grid level
Model Type	<ul style="list-style-type: none"> Simulation
Runs Provided	<ul style="list-style-type: none"> With socioeconomic growth and with climate change W/o socioeconomic growth and with climate change W/o socioeconomic growth or climate change (baselines; one per variant)
Additional Data	<ul style="list-style-type: none"> ¼ degree road inventory
Regions and States with Impacts	<ul style="list-style-type: none"> All CONUS regions and states

For illustrative purposes, **Figure B-30** shows the resulting damages by degree for the three adaptation scenarios, by GCM, calculated using 2010 (panel A) and 2090 (panel B) socioeconomics (i.e., the endpoints of the socioeconomic scenarios). The proactive adaptation results generally reflect a much lower damage estimate overall than no adaptation or reactive costs, but that in some scenarios the timing of those costs may be accelerated (and be triggered by relatively modest levels of warming) because of optimization of the capital cost of resilience investments and the high payoff to these investments in terms of avoiding future repairs and delays.

⁷³ The budget constraint in the no adaptation scenario can be considered a resilience threshold. For small amounts of warming, roads and their maintenance systems are adequate to meet increased stress. Once that resilience threshold is exceeded, costs increase quickly as road damage occurs.

FIGURE B-30. ROADS IMPACTS BY TEMPERATURE BIN DEGREE**A. 2010 SOCIOECONOMICS****B. 2090 SOCIOECONOMICS**

Total impacts (billions of 2015\$) by degree (°C) for each variant for two socioeconomic snapshots (2010 and 2090 default scenarios). Extrapolated portions are shown with a dashed line. Note y-axis scales vary by plot.

Processing steps

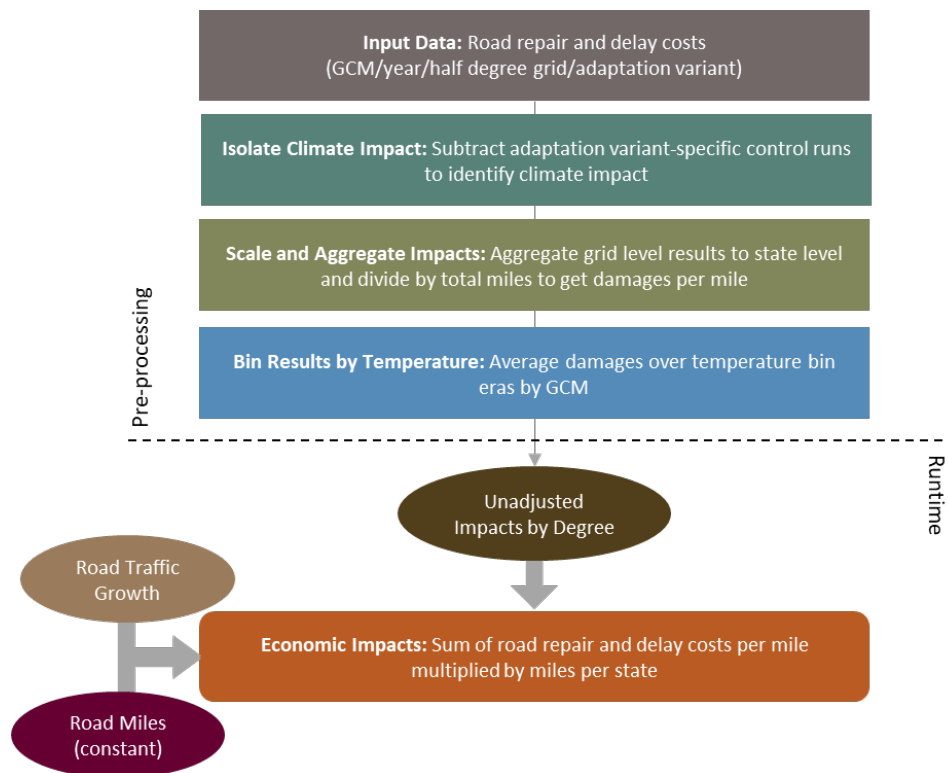
Processing steps are shown in **Figure B-31**.

Pre-processing: Quarter-degree resolution damages and road inventory data are provided by the Neumann et al. (2021) study authors and are allocated to each state. Grid cells that cross state lines are distributed proportionally by the percentage of area within each state. In the next pre-processing step, the baseline is subtracted from projected damages to isolate damages associated with climate change for each GCM, year, and adaptation scenario combination. The No Additional Adaptation and Reactive Adaptation Scenarios have the same baseline, a simple 20-year period repeated across time. We take the mean of this repeating baseline and apply it to all Reactive and No Additional Adaptation damages. The Proactive baseline is more complicated. It consists of 30 years of elevated but decreasing costs to begin the century, and from 2036 onwards is repeating 20-year period below Reactive and No Additional Adaptation. This is meant to model the high initial investments in the Proactive scenario and their resulting lower costs later in the century. We take the mean of three 10-year periods to begin the century and apply the mean of 2036-2099 to all other values. In next pre-processing step, net damages are summarized to the state level and divided by total miles of road within a state to produce damages in terms of dollars per mile. Lastly, state damages are

binned by degree of CONUS temperature change for each GCM by averaging across the 11-year windows where each GCM reaches each integer degree of CONUS warming relative to the baseline.

To account for additional repair due to increased traffic on damaged roads with increases in population, a population-dependent scalar is also calculated. The allocation of traffic by passenger and freight was not reported in the data provided by the underlying papers, and as the allocation of total damages between delay and repair cost is not provided, an aggregate scalar must be used to make the traffic adjustment. This scalar is based on the percent increase in damages across the century when the underlying model is run with population growth compared to a run with static population. There is a unique scalar for each of the three adaptation scenarios.

FIGURE B-31. ROADS DATA PROCESSING FRAMEWORK



Runtime: When FrEDI is run, the pre-processed by-degree damages per mile functions are then applied to the input temperature scenario to calculate the unadjusted annual impacts per mile based on the level of warming in each year of the input scenario. Annual damages per mile are then scaled by state-level road miles and the socioeconomic scalar to account for changes in future population. For the proactive scenario, note that because repair under this scenario strengthens road surfaces pre-emptively, before damage occurs and with a planned road closure, delay times are approximately half the projected delays for no adaptation and reactive adaptation— see Neumann et al. (2021) for details.

Limitations and Assumptions

- The model assumes a fixed capital and maintenance expense budget, which is usually exhausted at some point under the no-adaptation scenario. This time dependency of the no adaptation scenario is difficult to eliminate in the data processing steps, which could bias the estimate up or down, depending on the speed of warming relative to the underlying scenarios. This bias is expected to be relatively small and the use of GCM average results minimizes this potential bias.
- Damages to vehicles associated with incompletely maintained roads are modeled only in the no adaptation scenario; the model assumes roads are completed repaired and thus vehicles receive no damage under the reactive and proactive adaptation scenarios.
- For further discussion of the limitations and assumptions in the underlying sectoral model see Neumann et al. (2021), Neumann et al. (2015), and U.S. EPA (2017).
- There is no adjustment made to the valuation of passenger and freight delay over time. While passenger delay could be adjusted with increases in average wage rate, freight delay is a more complicated amalgamation of lost time, fuel costs, and the wage rate for drivers.

Asphalt Roads

Summary

This sector estimates the cost of asphalt road maintenance in the CONUS associated with climate change. This sector does not model any adaptation scenarios.

UNDERLYING DATA SOURCES AND LITERATURE

Underwood, B. S., Guido, Z., Gudipudi, P., & Feinberg, Y. (2017). Increased costs to US pavement infrastructure from future temperature rise. *Nature Climate Change*, 7, 704-707. <https://doi.org/10.1038/nclimate3390>

Future impacts are quantified by comparing historical asphalt grades (values associating pavement temperature and performance) and those associated with future climate projections. This analysis includes four roadway types: interstates, national routes, state routes, and local roads. Impacts are based on the cost of maintaining the standard practice of material selection for asphalt road maintenance rather than employing proactive pavement adaptation. Costs per lane mile are multiplied by total state asphalt lane miles to produce a total damage estimate in a state. This sector accounts for a subset of impacts in the FrEDI ‘Roads’ sector. Therefore, to avoid double counting, users should not add the asphalt road damages to those damages in the Roads sector. Asphalt lane miles are constant throughout the century, therefore only one set of impacts is shown in the figure.

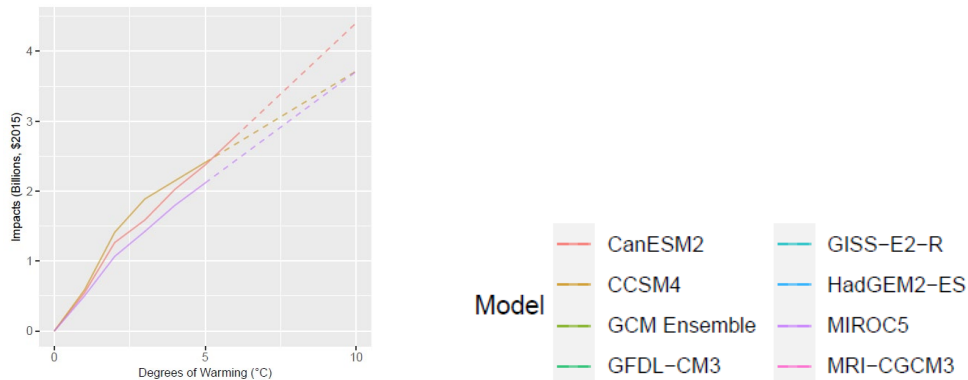
TABLE B-17. INCOMING DATA CHARACTERISTICS: ASPHALT ROADS

Data Features	Asphalt Roads Attributes
Evaluated Impacts	<ul style="list-style-type: none"> • Maintenance Costs (economic)^a
Variants	<ul style="list-style-type: none"> • No additional adaptation
Data Shape	<ul style="list-style-type: none"> • 30-year era total costs • Three CMIP5 GCMs • By weather station
Model Type	<ul style="list-style-type: none"> • Simulation

Runs Provided	<ul style="list-style-type: none"> With climate change and no socioeconomic growth
Additional Data	<ul style="list-style-type: none"> Lane Miles
Regions and States with Impacts	<ul style="list-style-type: none"> All CONUS regions and states (excluding DC)
a. Maintenance costs are meant to represent the costs of failing to update asphalt temperature grades over time.	

For illustrative purposes, **Figure B-32** shows the resulting damages by degree of warming by GCM.

FIGURE B-32. ASPHALT ROADS IMPACTS BY TEMPERATURE BIN DEGREE



Total impacts (billions of 2015\$) by degree ($^{\circ}\text{C}$), which do not vary by socioeconomic scenario or time. Extrapolated portions are shown with a dashed line.

Processing steps

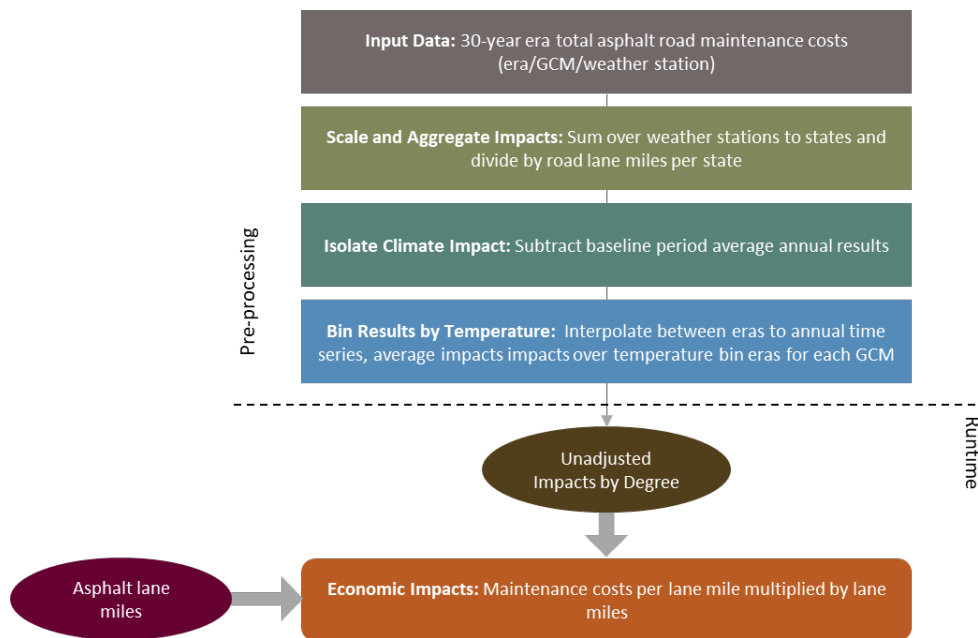
Processing steps are shown in **Figure B-33**.

Pre-processing: This study sector relies on different climate data that additionally needs to be pre-processed for this sector to be included in FrEDI. Underwood et al. (2017) selected 19 climate models from CMIP5 from the archives of the Climate Analytics Group, three of which (CanESM2, CCSM4, and MIROC5) overlap with the suite of GCMs used in FrEDI. Although Underwood et al. (2017) use the same GCMs as the typical CIRA studies, the bias correction and downscaling processes used by Climate Analytics Group differed from those used in the LOCA climate dataset (used in many of the FrEDI studies); therefore, new temperature bins are defined for the relevant new climate scenarios and related baselines. RCP8.5 results for these models are used for consistency with other FrEDI sectors. Maximum and minimum daily temperature data for these three GCMs were processed in the 30-year periods employed by the study to determine future annual temperatures associated with the era-level GCM-specific asphalt road damage estimates available from the study. The temperature hindcast was subtracted from yearly projected temperature to identify GCM-specific integer degree arrival years that were used for temperature binning of impacts for this sector.

Remaining processing steps are shown in **Figure B-33**. In the first pre-processing step, the total asphalt road maintenance costs for three 30-year eras from the Underwood et al. (2017) study are summed to the state level and divided by the number of road miles in each state to derive state-level costs per mile. These impacts are available for all GCMs and states for three eras: 2010 (2010-2039), 2040 (2040-2069), and 2070 (2070-2099), as well as a baseline era, which are assigned to 1995 (1986-2005). In the next step, baseline

impacts are subtracted from projected impacts for each GCM to arrive at maintenance costs associated with climate change for each era. Costs per mile associated with each era are then interpolated to derive annual costs, which are then binned by degree of CONUS temperature change for each GCM by averaging across the 11-year windows (as described above) where each GCM reaches each integer degree of CONUS warming relative to the baseline.

FIGURE B-33. ASPHALT ROADS DATA PROCESSING FRAMEWORK



RuntimE: When FrEDI is run, the pre-processed by-degree costs per lane mile functions are then applied to the input temperature scenario to calculate the unadjusted annual costs per lane mile based on the level of warming in each year of the input scenario. Total cost is then calculated by scaling these unadjusted results by the total lane miles in each state.

Limitations and Assumptions

- The underlying study uses a different set of climate projections (Climate Analytics Group) from most of the sectors that use LOCA, and a different baseline. While using a difference from the baseline and adjusting temperature arrival times is an attempt to correct any bias introduced, it is possible that these different climate projections and differences in the baseline create inconsistencies between this non-CIRA sector and other CIRA sectors.
- The underlying study includes a suite of 19 climate models, three of which are part of the CIRA suite of GCMs (CanESM2, CCSM4, and MIROC5). These three models reach warmer temperatures more quickly than the average across all 19 models in Underwood et al. (2017), and thus result in a higher average estimate of damages compared to the results presented in the paper. However, compared to the full suite of 38 CMIP5 GCMs, these three are close to the median 2090 temperature change.

- The model references, but does not quantify, impacts of a proactive adaptation scenario. Therefore, uncertainty exists in how the modeled maintenance costs may be reduced due to adaptive actions or technologies.
- For further discussion of the limitations and assumptions in the underlying sectoral model, see Underwood et al. (2017).

Urban Drainage

Summary

This sector estimates the costs of proactive adaptation for urban drainage systems in 100 major coastal and non-coastal cities of the CONUS to meet future demands of increased runoff associated with more intense rainfall under climate change.

Adaptive actions focus on the use of best management practices to limit the quantity of runoff entering stormwater systems and maintain current level of service (i.e., proactive adaptation to avoid damages), instead of expanding formal drainage networks of basins and conveyance systems. These best management practices generally include temporary storage above or below ground (e.g., bioswales, retention ponds), or infiltration (e.g., permeable pavement), and are based on EPA guidelines and construction cost estimates (see Price et al. (2016) for additional details).

Specifically, the analysis uses a reduced-form approach for projecting changes in flood depth and the associated costs of flood prevention under future climate scenarios, based an approach derived from EPA's Storm Water Management Model (SWMM). The approach assumes that systems are able to manage runoff associated with historical climate conditions and estimates the costs of implementing the adaptation measures necessary to manage increased runoff projected with climate change. Impacts are estimated in units of average adaptation costs per square mile for a total of 100 cities across the CONUS for three categories of 24-hour storm events (those with precipitation intensities occurring every 10, 25, and 50 years—metrics commonly used in infrastructure planning) and four future eras periods: 2030 (2020-2039), 2050 (2040-2059), 2070 (2060-2079), and 2090 (2080-2099).

UNDERLYING DATA SOURCES AND LITERATURE

Price, J., Wright, L., Fant, C., & Strzepek, K. (2016). Calibrated Methodology for Assessing Climate Change Adaptation Costs for Urban Drainage Systems. *Urban Water Journal*, 13 (4), 331-344. <https://doi.org/10.1080/1573062X.2014.991740>

Neumann, J., Price, J., Chinowsky, P., Wright, L., Ludwig, L., Streeter, R., Jones, R., Smith, J.B., Perkins, W., Jantarasami, L., and Martinich, J. (2015). Climate change risks to U.S. infrastructure: Impacts on roads, bridges, coastal development, and urban drainage. *Climatic Change*, 131, 97–109. <https://doi.org/10.1007/s10584-013-1037-4>

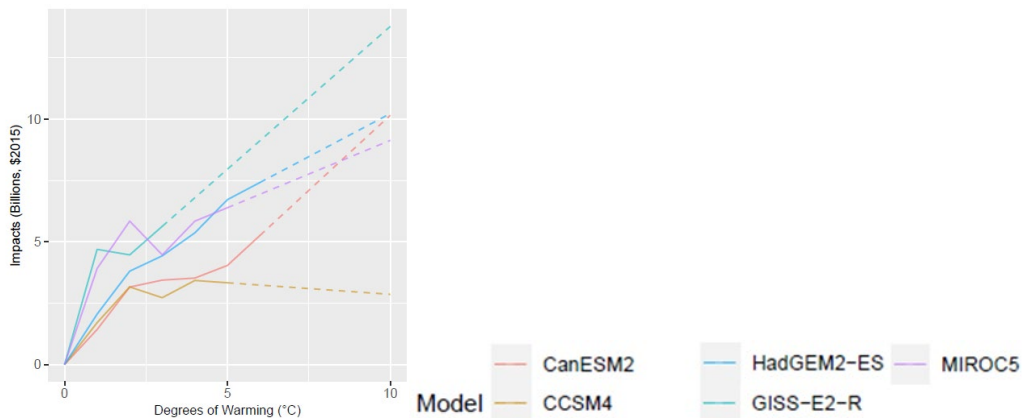
TABLE B-18. INCOMING DATA CHARACTERISTICS: URBAN DRAINAGE

Data Features	Urban Drainage Attributes
Evaluated Impacts	<ul style="list-style-type: none"> • Adaptation Costs (economic)
Variant	<ul style="list-style-type: none"> • Proactive Adaptation
Data Shape	<ul style="list-style-type: none"> • Four 20-year eras (2030, 2050, 2070, 2090) • Five CMIP5 GCMs (standard CIRA set without GFDL) • By city

Data Features	Urban Drainage Attributes
	<ul style="list-style-type: none"> • 10-year, 25-year, and 50-year storms
Model Type	<ul style="list-style-type: none"> • Simulation
Runs Provided	<ul style="list-style-type: none"> • With climate change and no socioeconomic growth
Additional Data	<ul style="list-style-type: none"> • Land area by city
Regions and States with Impacts	<ul style="list-style-type: none"> • Midwest • Northeast (excluding CT, DE, ME, NH, NJ, RI, VT, WV) • Northern Plains (excluding MT, ND, SD, WY) • Northwest • Southeast (excluding MS, SC) • Southern Plains • Southwest (excluding UT)

For illustrative purposes, **Figure B-34** shows the resulting damages by degree of warming by GCM.

FIGURE B-34. URBAN DRAINAGE IMPACTS BY TEMPERATURE BIN DEGREE



Total impacts (billions of 2015\$) by degree (°C), which do not vary by socioeconomic scenario or arrival time. Extrapolated portions are shown with a dashed line.

Processing steps

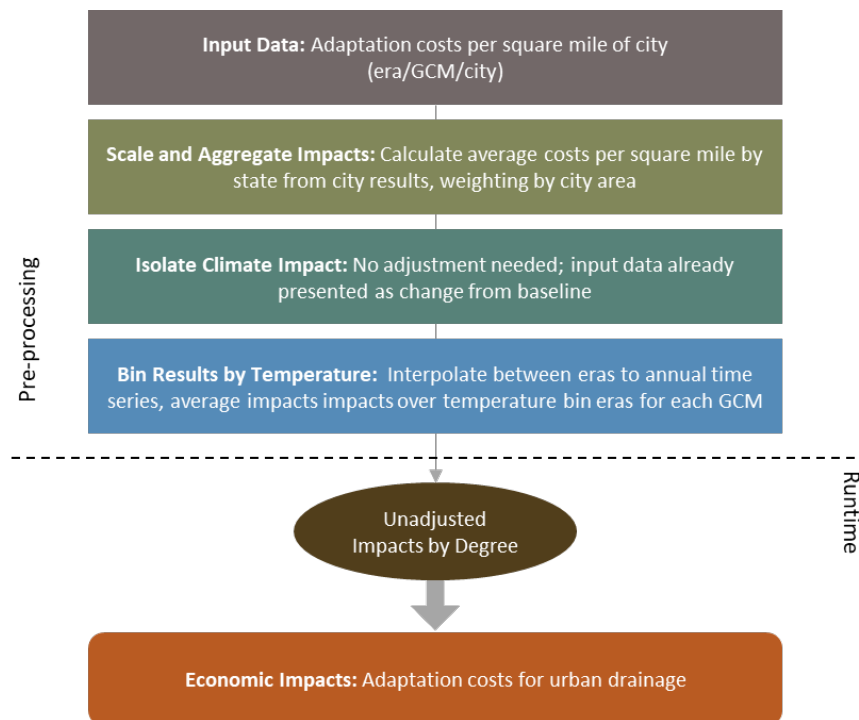
Processing steps are shown in **Figure B-35**.

Pre-processing: The adaptation costs per square mile (weighted by area) for the 50-year storm for each GCM, city, scenario, and era combination are from Price et al. (2016). In the first step, these data are aggregated to the state level.⁷⁴ Unlike most other underlying studies, the Urban Drainage study does not produce an annual time series of results, due in part to the impact of extreme events which are not well-characterized at an annual scale. Therefore, in the next step, linear interpolation is used to create an annual time series of values for each GCM, scenario, and state combination for the period 1995-2099, using the

⁷⁴ For example, for a state with 2 cities of 100 square miles each, each city's area is divided by the area sum, resulting in a proportion value of 0.5 for each city. This proportion value is then multiplied by each per-square-mile adaptation cost estimate (calculated by storm, scenario, and year) to produce a weighted average adaptation cost per square mile. The intensity/size of the 50-year storm varies with GCM, city, scenario, and era. The method yields changes in the absolute size of the storm over time and space, rather than the change in the frequency of the base period 50-year storm event.

known damage values at each of the four 20-year eras. Values are extrapolated for 2090-2099 using the linear trend observed between the 2070 and 2090 eras, and values for years prior to 2030 are estimated by using 1995 as a baseline year (i.e., impacts are assumed to be zero in 1995 and results are interpolated linearly between 1995 and 2030). Lastly, adaptation costs by state are binned by degree of CONUS temperature change for each GCM by averaging across the 11-year windows (as described above) where each GCM reaches each integer degree of CONUS warming relative to the baseline.

FIGURE B-35. URBAN DRAINAGE DATA PROCESSING FRAMEWORK



Runtime: When FrEDI is run, the pre-processed by-degree cost functions are then applied to the input temperature scenario to calculate the annual costs based on the level of warming in each year of the input scenario.

Limitations and Assumptions

- The underlying analysis assumes that the systems are able to manage runoff associated with historical climate conditions and estimates the costs of implementing the adaptation measures necessary to manage increased runoff projected with climate change.
- Inclusion of all U.S. cities with stormwater conveyance systems would provide a more comprehensive characterization of future impacts. The underlying study is limited to 100 major U.S. cities. Therefore, the current estimates included for this sector represent underestimates of potential damages.
- For further discussion of the limitations and assumptions in the underlying sectoral model see Neumann et al. (2015), Price et al. (2016), and U.S.EPA (2017).

Inland Flooding

Summary

This sector estimates the impact of riverine flooding in the CONUS attributable to climate change on property value, using the results of Wobus et al. (2021). Wobus et al. (2019), an earlier version of this research, provides more detail on the underlying CONUS-scale hydrologic modeling, while the more recent work improves aspects of the economic damage function, such as the data on affected structure values.

UNDERLYING DATA SOURCES AND LITERATURE

Wobus, C.W., Porter, J., Lorie, M., Martinich, J., & Bash, R. (2021). Climate change, riverine flood risk and adaptation for the conterminous United States. *Environmental Research Letters*. <https://doi.org/10.1088/1748-9326/ac1bd7>

Wobus, C.W., Zheng, P., Stein, J., Lay, C., Mahoney, C., Lorie, M., Mills, D., Spies, R., Szafranski, B., & Martinich, J. (2019). Projecting Changes in Expected Annual Damages From Riverine Flooding in the United States. *Earth's Future*, 7(5), 516-527. <https://doi.org/10.1029/2018EF001119>

The analysis uses change in expected annual damage (EAD) from flooding at each property in the U.S. under different temperature scenarios to value riverine flood impacts. The underlying data considers flooding for return intervals of two years through 500 years. Study authors calculate a frequency-loss curve for each property and integrate between flood frequencies of 0.0001 and 0.10 to calculate the EAD. The data excludes flooding events associated with urban drainage, quantifying only riverine floods instead. As a result, this sector does not account for all flooding events in cities and other urban areas; pluvial floods (associated with localized high rainfall events) are assessed in the Urban Drainage sector. This method estimates the baseline annual EAD using current structure characteristics (e.g., ground level floor elevation⁷⁵, replacement cost, market value), the flood depths associated with baseline conditions for varying return periods⁷⁶, and depth-damage functions available from FEMA's HAZUS documentation.⁷⁷ The underlying study model provides estimates of projected property damage at multiple spatial scales – for this work, results were provided at the Census block group level; properties were grouped by Census block group and EAD values summed under baseline and future climate scenarios. Property values are held constant over the century, and impacts are projected under a “no additional adaptation” scenario.

TABLE B-19. INCOMING DATA CHARACTERISTICS: INLAND FLOODING

Data Features	Inland Flooding Attributes
Evaluated Impacts	<ul style="list-style-type: none"> Expected annual flood damage (economic)
Variant	<ul style="list-style-type: none"> No additional adaption
Data Shape	<ul style="list-style-type: none"> Baseline Period (2001-2020)^a Integer degree (1-5°C)

⁷⁵ These characteristics were made available by the First Street Foundation. Details are provided in: First Street Foundation, 2020a. The First National Flood Risk Assessment: Defining America’s Growing Risk. Available at https://assets.firststreet.org/uploads/2020/06/first_street_foundation__first_national_flood_risk_assessment.pdf

⁷⁶ Details of the “current climate” baseline flood risk modeling: First Street Foundation, 2020b. First Street Foundation Flood Model: Technical Methodology Document. Available:

https://assets.firststreet.org/uploads/2020/06/FSF_Flood_Model_Technical_Documentation.pdf

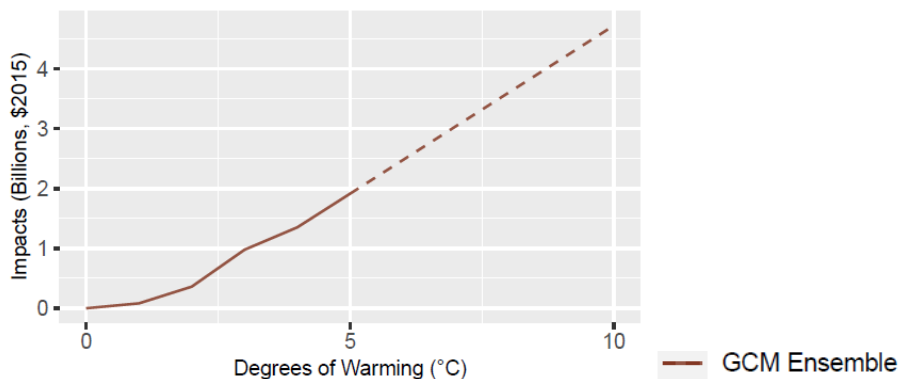
⁷⁷ FEMA, undated. Multi-hazard Loss Estimate Methodology: Flood Model Technical Manual.

https://www.fema.gov/sites/default/files/2020-09/fema_hazus_flood-model_technical-manual_2.1.pdf

Data Features	Inland Flooding Attributes
	<ul style="list-style-type: none"> • GCM Average (14 CMIP5 GCMs, including standard CIRA set) • Block Groups
Model Type	<ul style="list-style-type: none"> • Simulation
Runs Provided	<ul style="list-style-type: none"> • With socioeconomic growth and with climate change
Additional Data	<ul style="list-style-type: none"> • None
Regions and States with Impacts	<ul style="list-style-type: none"> • All CONUS regions and states
a. Baseline period is not shifted to FrEDI baseline because the damages presented are delta damage/delta temperature and damage curves are smoothed linearly.	

For illustrative purposes, **Figure B-36** shows the resulting damages by degree of warming for the average GCM ensemble.

FIGURE B-36. INLAND FLOODING IMPACTS BY TEMPERATURE BIN DEGREE



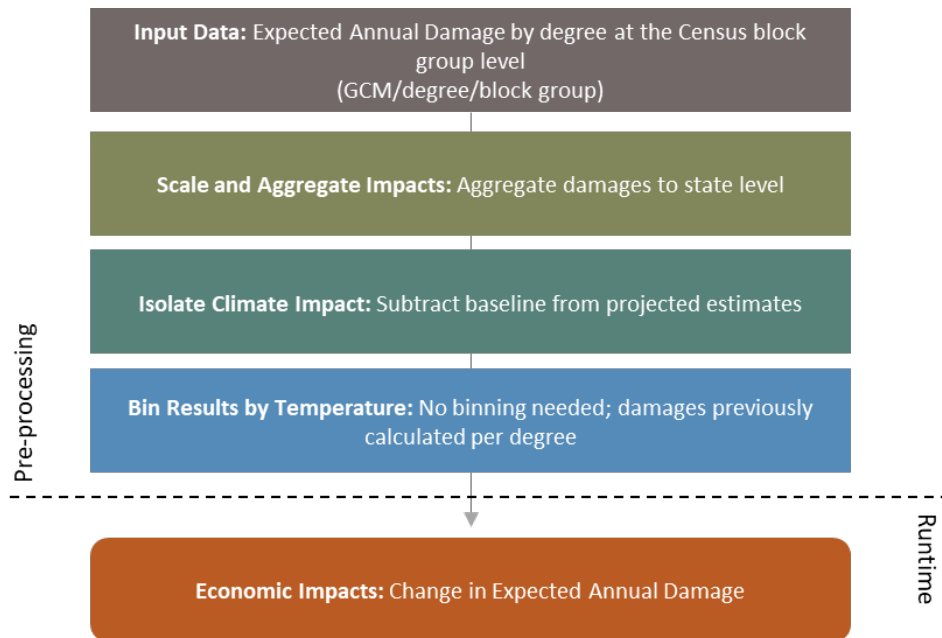
Total impacts (billions of 2015\$) by degree (°C), which do not vary by socioeconomic scenario or time. Extrapolated portions are shown with a dashed line.

Processing steps

Processing steps are shown in **Figure B-37**.

Pre-processing: Wobus et al. (2021) study authors provided damages by degree by Census block group, as well as baseline EAD for the period 2001-2020. Impacts are averaged for one “GCM Ensemble”, which includes fourteen CMIP5 models: ACCESS1-0, CanESM2, CESM1-CAM5, CMCC-CM, CSIRO-Mk3-6-0, FGOALS-g2, GFDL-CM3, HadGEM2-AO, HadGEM2-CC, HadGEM2-ES, IPSL-CM5B-MR, MIROC-ESM-CHEM, MIROC-ESM, and NorESM1-M. In the underlying study, authors use the projected hydrology for each climate model to extract an annual maximum flow timeseries for a 20-year window centered on the year that the model reaches temperature thresholds of 1°C through 5°C above the 2001-2020 baseline.

In the first pre-processing step, block group damages are summed to state damages. Next, the baseline EAD is subtracted from projected EAD by degree to isolate impacts attributable to climate change and values are deflated from 2020 dollars to 2015 dollars (FrEDI’s default).

FIGURE B-37. INLAND FLOODING DATA PROCESSING FRAMEWORK

Runtime: When FrEDI is run, the pre-processed by-degree damage functions are then applied to the input temperature scenario to calculate the total annual damages based on the level of warming in each year of the input scenario.

Limitations and Assumptions

- The analysis does not evaluate the potential for adaptation measures to mitigate flood risk at the property or community levels.
- The analysis does not account for changes in population and development within flood risk zones. Without a reasonable method to predict future floodplain development or policies governing development, these factors are held constant. The underlying analysis also holds property values constant over time – as noted in Neumann et al. (2021), there is evidence that real property values grow with changes in income (proxied by per capita GDP) over time. As a result, the inland flood risks in Wobus et al. (2021) may be underestimated.
- This analysis relates increases in CONUS temperatures to changes in economic impacts of riverine floods. While climate science indicates that warming temperatures accelerate the hydrologic cycle, which in turn increase river flows, changes in near-surface temperatures do not necessarily characterize local or regional precipitation changes, or river flows, with a consistent signal. Local precipitation changes may also be correlated with other drivers that are not necessarily well correlated with CONUS or regional scale temperature changes (e.g., the El Nino Southern Oscillation, ENSO). The study used here (Wobus et al., 2021), however, finds a monotonic trend of increases in the economic impact of floods at the CONUS scale (aggregated from the property level) as CONUS temperatures rise, supporting the relationship between CONUS temperature changes and state-level flood impacts.

- For further discussion of the underlying sectoral model see Wobus et al. (2021) and (2019).

Hurricane Wind Damage

Summary

This sector estimates the impact of changes in the frequency of hurricane strength wind damage to coastal properties in the CONUS. The results are primarily based on analysis by Dinan (2017), which projects hurricane damage from both wind and storm surge to properties in the Gulf and Atlantic coast states using a proprietary model developed by the firm Risk Management Solutions (RMS). Dinan (2017) projected changes in future hurricane frequency by hurricane category (Saffir-Simpson scale of Category 1

to Category 5) using a Monte Carlo aggregation of results from Emanuel (2013) for RCP8.5 and Knutson (2013) for RCP4.5.⁷⁸ The hurricane projections used in Dinan (2017) do not readily convert to an impact-by-degree warming indexing, so this analysis instead relies on results from more recent Marsooli et al. (2019) study which provides change in return periods, maximum wind speed, and Category 5 storm frequency for the a late century period using an updated version of the Emanuel (2013) model to project future hurricane activity by degree of warming for a set of GCMs. Further, because the detailed spatial and climate stressor results are not publicly available, we worked with Dinan, RMS, and other publicly available data to estimate damages attributable to climate change-driven changes in wind damage to properties.

UNDERLYING DATA SOURCES AND LITERATURE

Dinan, T. (2017). Projected increases in hurricane damage in the United States: the role of climate change and coastal development. *Ecol. Econ.* 138: 186–198.

<https://doi.org/10.1016/j.ecolecon.2017.03.034>

Congressional Budget Office (CBO). (2016). Potential Increases in Hurricane Damages in the United States: Implications for the Federal Budget. Washington, DC.

<https://www.cbo.gov/publication/51518>

Marsooli, R. Lin, N., Emanuel, K., Feng, K. (2019). Climate change exacerbates hurricane flood hazards along US Atlantic and Gulf Coasts in spatially varying patterns. *Nature Communications*.

<https://doi.org/10.1038/s41467-019-11755-z>

TABLE B-20. INCOMING DATA CHARACTERISTICS: HURRICANE WIND DAMAGE

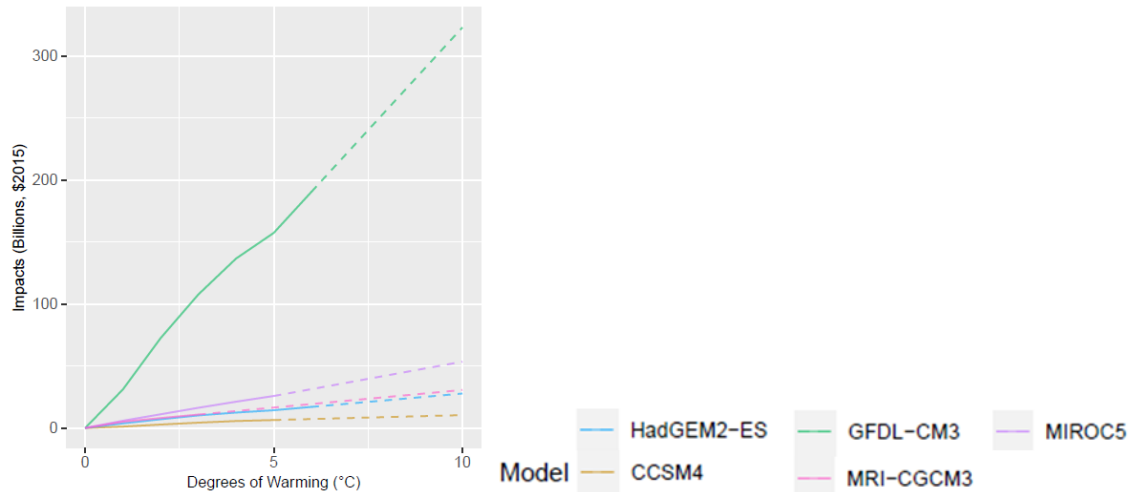
Data Features	Hurricane Wind Damage Attributes
Impact Types	<ul style="list-style-type: none"> • Cost of hurricane wind damage to coastal properties (economic)
Variants	<ul style="list-style-type: none"> • No additional adaptation
Data Shape	<ul style="list-style-type: none"> • Single values representing baseline period (1980-2005) and projection period (2070-2095) • Five CMIP5 GCMs (CCSM4, GFDL-CM3, HadGEM2-ES, MIROC5, MRI-CGCM3) • County-level
Model Type	<ul style="list-style-type: none"> • Simulation
Runs Provided	<ul style="list-style-type: none"> • With climate change and no socioeconomic growth
Additional Data	<ul style="list-style-type: none"> • None

⁷⁸ Emanuel, K., 2013. Downscaling CMIP5 climate models shows increased tropical cyclone activity over the 21st century. Proc. Natl. Acad. Sci. 110 (30), 12219–12224, and Knutson, T., et al., 2013. Dynamical downscaling projections of twenty-first-century Atlantic hurricane activity: CMIP3 and CMIP5 model-based scenarios. J. Clim. 26 (17), 6591–6617.

Data Features	Hurricane Wind Damage Attributes
Regions and States with Impacts	<ul style="list-style-type: none"> • Northeast (excluding VT, WV) • Southeast (excluding AR, KY, TN) • Southern Plains (excluding KS, OK)

For illustrative purposes, **Figure B-38** shows the resulting damages by degree by GCM.

FIGURE B-38. HURRICANE WIND DAMAGE IMPACTS BY TEMPERATURE BIN DEGREE



Total impacts (billions of 2015\$) by degree (°C), which do not vary by socioeconomic scenario or time. Extrapolated portions are shown with a dashed line.

Processing steps

Processing steps are shown in **Figure B-39**.

Pre-processing: The first pre-processing step is to collect hurricane wind damage data from Dinan (2017), county level storm surge data from the National Coastal Property Model (NCPM), and wind profile change data from Marsooli et al. (2019).

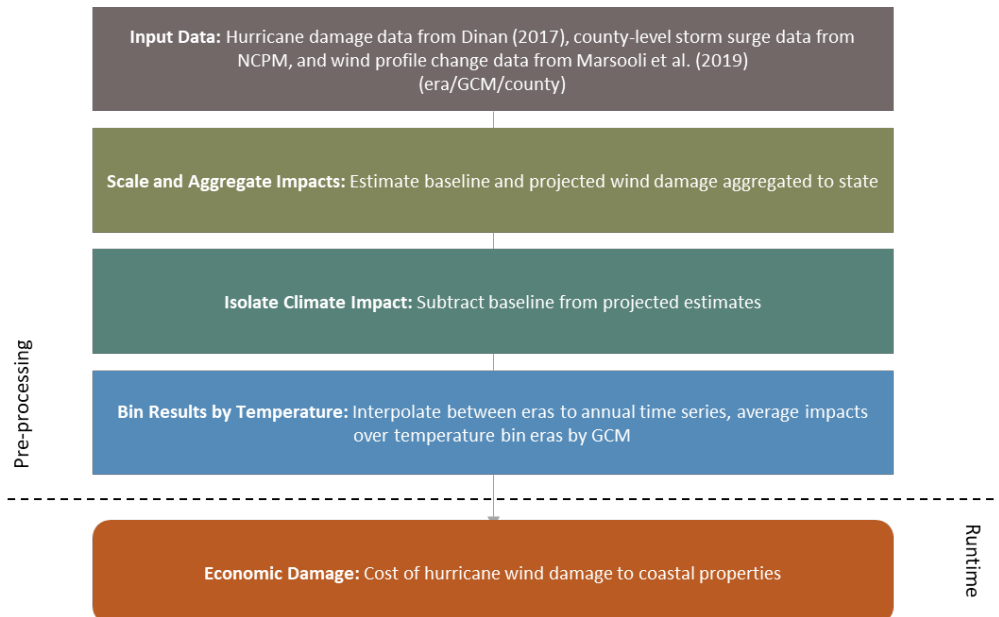
The second pre-processing step is to estimate baseline and projected wind damages from these data.

Baseline wind damage is calculated by parsing data on total hurricane damage by state from Dinan et al. (2017), reported in CBO (2016), into wind and storm surge components by state, using data on the ratio of wind to storm surge damage by state provided by the study authors (with permission from RMS). Wind damages by state are allocated to the county scale by using weights derived from the NCPM for county-level storm surge damage attributed to hurricanes in the year 2000 (base year with no SLR). This allocation method assumes that storm surge and wind damage are correlated but exclude some non-coastal inland counties which might be expected to incur wind damage (albeit with significant decay of wind speed relative to coastal counties).

Projected wind damages are then calculated using these baseline wind damages and projected wind profile changes. Wind profile changes are projected using estimates reported in Marsooli et al. (2019), which

provides gridded estimates of the max wind speed and frequency of the 90th percentile event from an ensemble of simulated tropical cyclones for the Gulf and Atlantic Coasts for both the baseline of 1980–2005 to the future period of 2070–2095. The grid-cell results are spatially reaggregated to coastal counties. The future wind damages are then projected using ratios of future damage to baseline damage for each coastal county that employ a logistic function proposed by Emanuel et al. (2012) for the baseline and five of the six GCMs evaluated in Marsooli et al. (2019).⁷⁹ Although this study uses mostly CIRA GCMs, the bias correction and downscaling processes differed from those used in the LOCA climate dataset. Therefore, new temperature bins are defined for the relevant new climate scenarios. These ratios are applied to the baseline damage estimated above, and baseline damages are subtracted to estimate future damages attributed to climate change. To interpolate between the baseline and projection, the baseline is assigned to 1986-2005 (FrEDI baseline) and the projection to 2070-2095, resulting in linear interpolation between 1995 and 2082. For extrapolation beyond 2082, the county-specific linear function is extended to 2099. Damages are then aggregated to the state level for each of the relevant GCMs and binned by degree of CONUS temperature change for each GCM by averaging across the 11-year windows (as described above) where each GCM reaches each integer degree of CONUS warming relative to the baseline.

FIGURE B-39. HURRICANE WIND DAMAGE IMPACT PROCESSING FRAMEWORK



Runtime: When FrEDI is run, the pre-processed by-degree cost of hurricane wind damage functions are then applied to the input temperature scenario to calculate the total annual costs based on the level of warming in each year of the input scenario.

The results indicate good agreement for four of the five models, with the fifth (GFDL) showing much higher damages than the other four. We considered applying skill weighting of the GCMs using weights provided in Marsooli et al. (2019) – the results using skill-weighting down-weight GFDL relative to other models,

⁷⁹ MPI excluded due to data availability issues.

reducing the mean damages across all GCMs by about one-third – but the skill weights were calculated for wind speed rather than damage (damage is a non-linear logistic function of wind speed, capped at the high end by total structure value). The non-skill weighted results are used here for consistency with other sectoral analyses.

Limitations and Assumptions

- Hurricanes are extreme events and are observed infrequently, which both limits the observed damage data on which estimates can be based and complicates estimates of projected hurricane activity. The Marsooli et al. (2019) study used here employs a well-regarded model of projected hurricane activity which provides results needed to estimate projected damages on a spatially disaggregated basis, but other models could yield different results.
- The underlying economic impact study relies on a proprietary model of hurricane wind and storm surge damages; the detailed county and scenario specific results from the model are not available for use in the Framework. The published results are therefore disaggregated from publicly available total estimates into storm surge and wind using storm surge estimates from the Coastal Properties sector. This procedure ensures that damage estimates are not double counted but introduces error and uncertainty in the estimates used here.
- Results from the underlying study were made available only at the state level, but analyses of projected storm surge damages are at the county level, and estimates of future hurricane activity are at a grid cell level. Adjustments made for spatial mismatches also introduce error and uncertainty in the estimates used here.
- This analysis interpolates linearly between the baseline period and late century (2070-2095) projection with no intermediate damage estimates, so mid-century values are less precise than other sectors.
- For further discussion of the limitations and assumptions in the underlying sectoral model see Dinan et al. (2017) and Marsooli et al. (2019).

B.4 Electricity Sectors

Electricity Demand and Supply

Summary

This sector estimates increases in system costs to the power sector in the CONUS. These system costs include capital, fuel, variable operation and maintenance (O&M), and fixed O&M.

Increased costs are based on projected changes in demand for and supply of electricity across generation types associated with changes in temperature, but also reflect projected technological change that alters relative prices for energy supply technologies in both baseline and “with climate change” projections. Effects on energy demand reflect the net impact of increased demand for residential, commercial, and industrial space cooling during summer/warmer months, and decreased demand for space heating during winter/cooler months. Effects on supply reflect the decreased production capacity of thermal power plants, and transmission capacity of the transmission system, associated with higher temperatures.⁸⁰ The complex interplay of supply and demand, coupled with forecast changes in fuel and energy production technology availability and prices, are modeled using the Global Change Assessment Model (GCAM-USA), a detailed service-based building energy model with a 50-state domain.

Costs are provided for a reference scenario, where climate is held constant to the FrEDI baseline and socioeconomic variables are dynamic, and a projection run where both climate and socioeconomic variables vary. Estimates of costs with and without climate change are provided in five-year intervals.

TABLE B-21. INCOMING DATA CHARACTERISTICS: ELECTRICITY DEMAND AND SUPPLY

Data Features	Electricity Demand and Supply Attributes
Evaluated Impacts	<ul style="list-style-type: none"> Power Sector System Costs (economic)
Variants	<ul style="list-style-type: none"> No additional adaptation
Data Shape	<ul style="list-style-type: none"> 5-year intervals 2010-2100 Six CMIP5 GCMs (standard CIRA set) State-level
Model Type	<ul style="list-style-type: none"> Simulation
Runs Provided	<ul style="list-style-type: none"> With socioeconomic growth and with climate change With socioeconomic growth and w/o climate change (reference)
Additional Data	<ul style="list-style-type: none"> None
Regions and States with Impacts	<ul style="list-style-type: none"> All CONUS regions and states

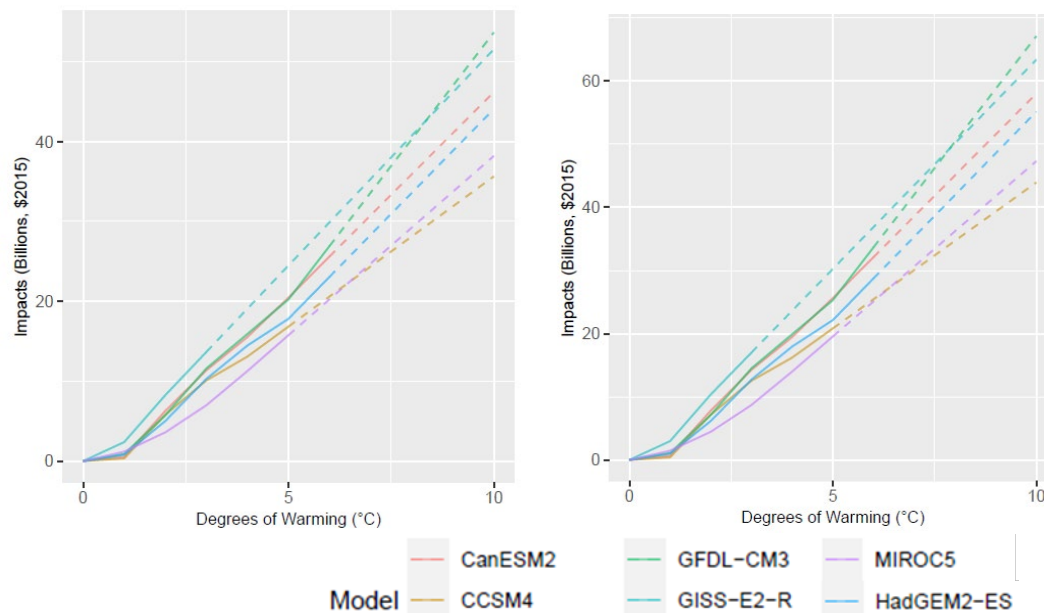
⁸⁰ Transmission system effects in this sector are separate from those modeled in the Electricity Transmission and Distribution sector. This study considers only the temperature driven changes in line ampacity, while Electricity Transmission and Distribution sector examines the vulnerability of specific other components of the transmission system to climate stress (e.g., the effect of temperature on the longevity of power transformer equipment).

UNDERLYING DATA SOURCES AND LITERATURE

McFarland, J., Zhou, Y., Clarke, L., Sullivan, P., Colman, J., Jaglom, W. S., Colley, M., Patel, P., Eom, J., Kim, S. H., Kyle, G. P., Schultz, P., Venkatesh, B., Haydel, J., Mack, C., & Creason, J. (2015). Impacts of rising air temperatures and emissions mitigation on electricity demand and supply in the United States: a multi-model comparison. *Climatic Change*, 131, 111-125. <https://doi.org/10.1007/s10584-015-1380-8>

For illustrative purposes, **Figure B-40** shows the resulting damages by degree of warming by GCM, calculated using 2010 (panel A) and 2090 (panel B) socioeconomic (i.e., the endpoints of the socioeconomic scenarios).

FIGURE B-40. ELECTRICITY DEMAND AND SUPPLY IMPACTS BY TEMPERATURE BIN DEGREE
A. 2010 SOCIOECONOMICS **B. 2090 SOCIOECONOMICS**

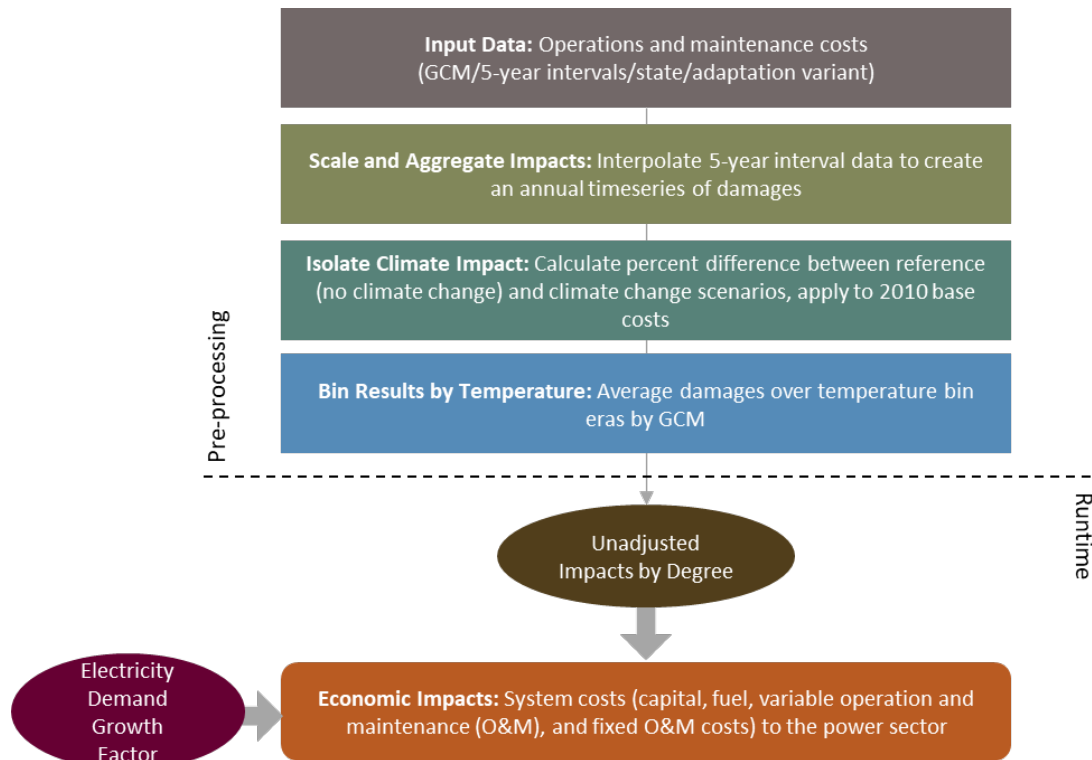


Total impacts (billions of 2015\$) by degree (°C) for two socioeconomic snapshots (2010 and 2090 default scenarios). Extrapolated portions are shown with a dashed line. Note y-axis scales vary by plot.

Processing steps

Processing steps for this sector are shown in **Figure B-41**.

Pre-processing: Data from the McFarland et al. (2015) study authors on the system costs for the power sector are provided for each GCM and a climate reference scenario for each state in 5-year intervals. In the first pre-processing step, the annual sum of power system costs (e.g., capital, fuel, variable O&M, and fixed O&M) are interpolated between the 5-year interval data for both GCM projections and the reference scenario to create an annual trajectory. Next, the percent differences between the reference scenario and the GCM projected scenarios are calculated for each state-GCM-year combination. These percentages are then multiplied by their respective 2010 reference scenario value to calculate a damage trajectory that represents climate change with no socioeconomic growth. The resulting no-growth trajectory is then binned by degree of CONUS temperature change by averaging across the 11-year windows where each GCM reaches each integer degree of CONUS warming relative to the baseline. To produce state level scalars for socioeconomic growth, each state's yearly reference scenario value is divided by its 2010 value to index the scalar to 2010.

FIGURE B-41. ELECTRICITY DEMAND AND SUPPLY DATA PROCESSING FRAMEWORK

Runtime: When FrEDI is run, the pre-processed by-degree system costs are then applied to the input temperature scenario to calculate the unadjusted annual system costs based on the level of warming in each year of the input scenario. These costs are then multiplied by the socioeconomic scalar for each given year to produce total cost estimates across the century.

Limitations and Assumptions

- Projected changes in heating degree days (HDD) and cooling degree days (CDD) are based on a temperature set-point of 65°F, a common convention that may lead to a conservative energy demand estimate.
- The temporal aggregation of the underlying electricity supply model is too coarse to assess the impact of extreme temperature events that occur on only the very hottest days of the year. As a result, the underlying study focuses on a single aspect of climate change: average ambient air temperature, and therefore omits effects of extreme temperature effects on peak demands and the loads required to meet those changes. Effects from future changes in the frequency and magnitude of extreme temperatures may stress electric power systems, and these economic risks are not captured in this study.
- The impact estimates reflect direct costs only, and do not capture how these increased costs more broadly affect consumers (consumption/welfare) or production costs in other sectors.
- For further discussion of the limitations and assumptions in the underlying sectoral model, see McFarland et al. (2015).

Electricity Transmission and Distribution Infrastructure

Summary

This sector estimates damages to the electric transmission and distribution infrastructure in the CONUS projected with climate change.

This multi-dimensional analysis considers a wide range of climate stressors, including extreme temperature, extreme rain, lightning, vegetation growth, wildfire activity, and coastal flooding. Impact receptors include transmission and distribution lines, poles/towers, and transformers.

Monetized damages for this sector are the costs of repair or replacement of damaged infrastructure. The underlying impact study estimates damages under two infrastructure system scenarios: one with expansion of infrastructure associated with demand growth, and one with static infrastructure. Increases in demand growth may be due to population growth, or increased demand expected with climatic change — in particular, warmer temperatures increase usage of air-conditioning. The model identifies changes in performance and longevity of physical infrastructure, such as power poles and transformers, and quantifies these impacts in economic terms. While certain climate stressors do cause power outages which have associated direct and indirect economic costs, these damages are not included in damage estimates.

This analysis is based on three adaptation scenarios: proactive adaptation, reactive adaptation, and no additional adaptation. Repair costs are also allocated based on the activity performed. These activities include transmission line capacity, wildfire repair, tree trimming, substation SLR, substation storm surge, wood pole decay, transmission transformer lifespan, and distribution transformer lifespan.

TABLE B-22. INCOMING DATA CHARACTERISTICS: ELECTRICITY TRANSMISSION AND DISTRIBUTION INFRASTRUCTURE

Data Features	Electricity Transmission and Distribution Infrastructure Attributes
Evaluated Impacts	<ul style="list-style-type: none"> Costs of infrastructure replacement and repair (economic)
Variants	<ul style="list-style-type: none"> Proactive adaptation Reactive adaptation No additional adaptation
Data Shape	<ul style="list-style-type: none"> Year Six CMIP5 GCMs (standard CIRA set) Three adaptation scenarios State level
Model Type	<ul style="list-style-type: none"> Simulation
Runs Provided	<ul style="list-style-type: none"> Static infrastructure with climate change
Additional Data	<ul style="list-style-type: none"> Infrastructure growth due to population change Infrastructure growth due to climate change
Regions and States with Impacts	<ul style="list-style-type: none"> All CONUS regions and states

UNDERLYING DATA SOURCES AND LITERATURE

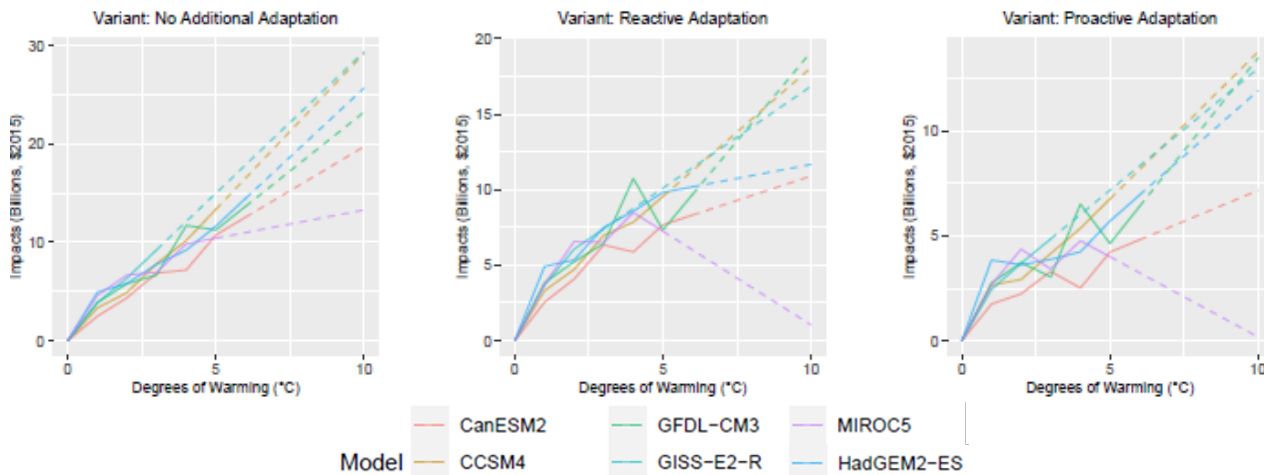
Fant, C., Boehlert, B., Strzepek, K., Larsen, P., White, A., Gulati, S., Li, Y., & Martinich, J. (2020). Climate change impacts and costs to U.S. electricity transmission and distribution infrastructure. Energy, 195.

<https://doi.org/10.1016/j.energy.2020.116899>

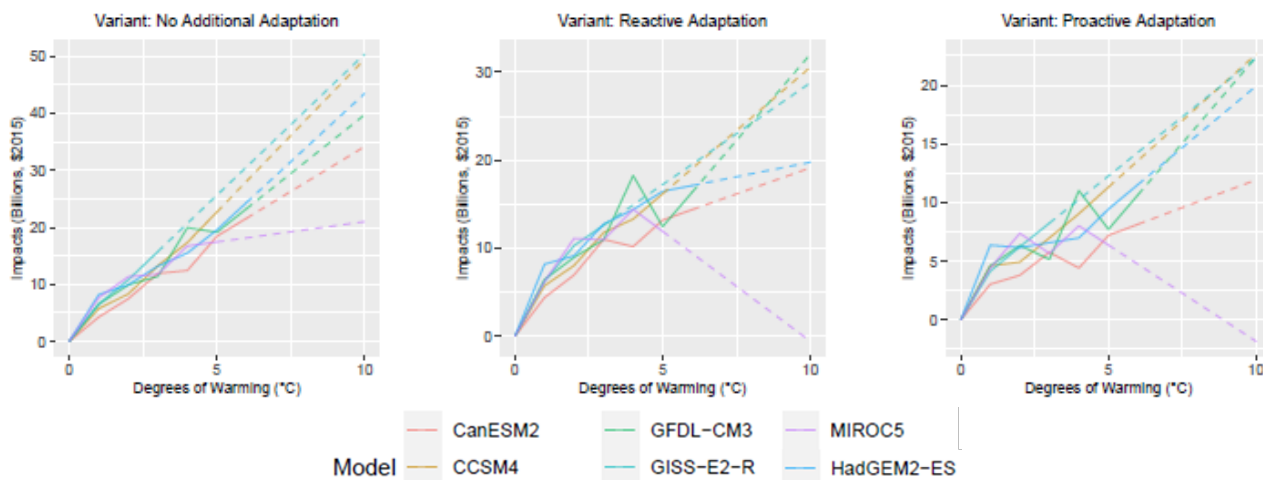
For illustrative purposes, **Figure B-42** shows the resulting damages by degree of warming for the three adaptation scenarios, by GCM, calculated using 2010 (panel A) and 2090 (panel B) socioeconomics (i.e., the endpoints of the socioeconomic scenarios).

FIGURE B-42. ELECTRICITY TRANSMISSION AND DISTRIBUTION INFRASTRUCTURE IMPACTS BY TEMPERATURE BIN DEGREE

A. 2010 SOCIOECONOMICS



B. 2090 SOCIOECONOMICS



Total impacts (billions of 2015\$) by degree (°C) for each variant for two socioeconomic snapshots (2010 and 2090 default scenarios). Extrapolated portions are shown with a dashed line. Note y-axis scales vary by plot.

Processing steps

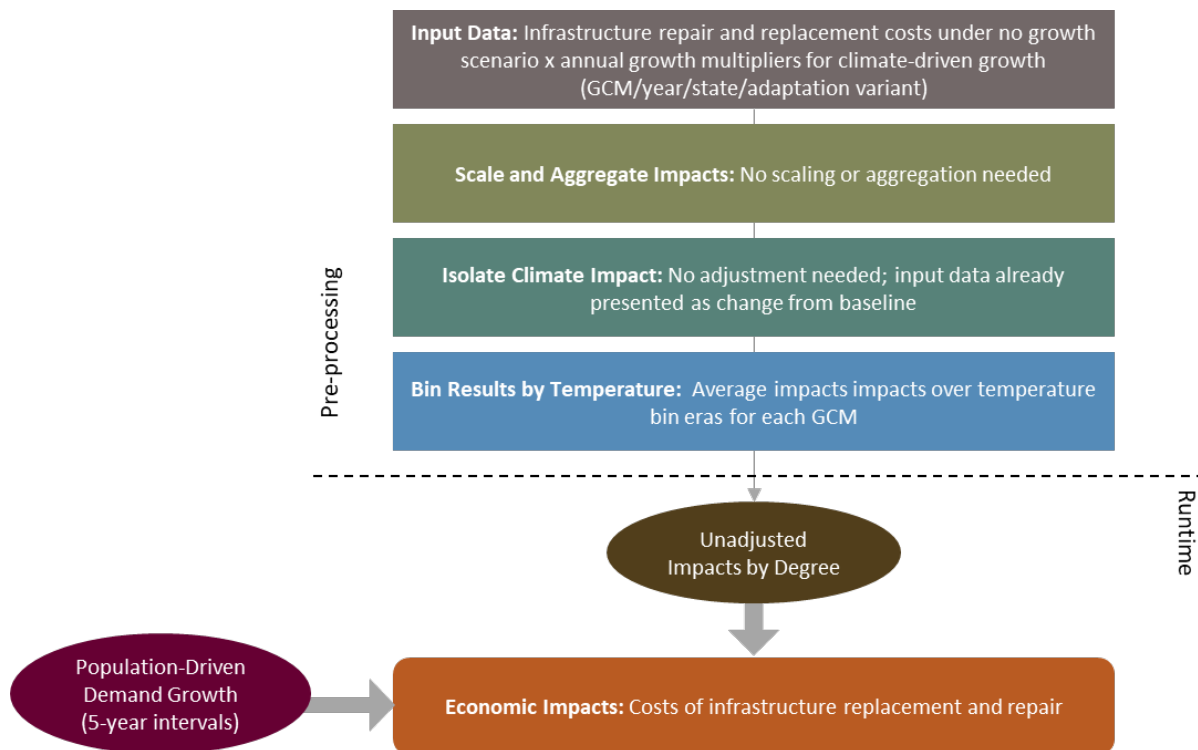
Processing steps are shown in **Figure B-43**.

Pre-processing: The underlying impact model described in Fant et al. (2020) produces annual damage estimates for each infrastructure type, state, GCM, and adaptation scenario. The underlying study grows infrastructure with electricity demand increases projected with climate change and population growth. In

the first pre-processing step, to isolate demand growth associated with warming, damages associated with static demand are scaled by growth of demand attributable to warming.

After damages associated with climate driven infrastructure growth are calculated, results are aggregated for each GCM, year, and adaptation scenario. The costs are then binned by degree of CONUS temperature change for each GCM by averaging across the 11-year windows where each GCM reaches each integer degree of CONUS warming relative to the baseline.⁸¹ One additional set of scalars is calculated and included in FrEDI to account for infrastructure expansion to respond to increased demand from population growth.

FIGURE B-43. ELECTRICITY TRANSMISSION AND DISTRIBUTION INFRASTRUCTURE DATA PROCESSING FRAMEWORK



Runtime: When FrEDI is run, the pre-processed by-degree cost functions are then applied to the input temperature scenario to calculate the unadjusted annual costs based on the level of warming in each year of the input scenario. Lastly, total annual costs are calculated by scaling the unadjusted costs by the climate-driven infrastructure growth and population-driven growth scalars. Thus, final damage estimates

⁸¹ The substation SLR and substation storm surge categories of impact were estimated in the underlying study through a custom application of the National Coastal Property Model (Neumann et al. 2021). The key climate hazard to substations is SLR, however, rather than temperature. Fant et al. (2020) used a set of SLR scenario weights by RCP (see USEPA 2017, Table 1.2, available here: <https://www.epa.gov/cira/multi-model-framework-quantitative-sectoral-impacts-analysis>) to transform the SLR trajectory based damages to substations to a 21st century damage trajectory for RCP8.5, and aggregated results with other categories of damage (e.g., impacts of temperature on transformers). FrEDI adopts the same damages aggregation procedure as the underlying paper so that all categories of damages in the resulting FrEDI damage function can be expressed as impacts-by-degree.

include expansion of electric grid infrastructure associated with a warming climate and with population growth. Because these damage estimates rely on an empirical relationship between damages with and without infrastructure growth in the underlying study's impact model, these damage estimates cannot be adjusted for custom input population trajectories.

Limitations and Assumptions

- The underlying study's impact model assumes that grid demand is controlled by population change and climatic factors; grid demand is assumed to not be influenced by economic growth. Future changes in the design and structure of electric grids are not considered in this study.
- Power outages that might be caused by the infrastructure failures modeled in this study are not estimated in the underlying study. As a result, direct and indirect costs of outages are not included.
- One of the infrastructure types (Substation Damage from SLR and Storm Surge) is not scaled by demand in the original study. Because the input data received from the authors was already aggregated across infrastructure types, all infrastructure types are scaled by demand in FrEDI. This has a minimal effect on the overall results because Substation Damage from SLR and Storm Surge accounts for the smallest portion of the damages among the final eight types considered in the original study.
- See Fant et al. (2020) for further discussion of the limitations and assumptions.

B.5 Ecosystems and Recreation Sectors

Water Quality

Summary

This sector estimates damages in terms of the change in willingness to pay to avoid changes in water quality projected with climate change. This analysis estimates climate change effects on water quality at the eight-digit Hydrological Unit Code (HUC) scale of the CONUS using the Hydrologic and Water Quality System (HAWQS) biophysical model. Damages estimated for this sector only cover the change in value of recreation opportunities (e.g., boating, fishing, swimming) due to changes in a climate water quality index developed from the HAWQS outputs and do not include the value of health effects or other amenities associated with clean water.

UNDERLYING DATA SOURCES AND LITERATURE

Fant, C., Srinivasan, R., Boehlert, B., Rennels, L., Chapra, S. C., Strzepek, K. M., Corona, J., Allen, A., & Martinich, J. (2017). Climate change impacts on US water quality using two models: HAWQS and US Basins. *Water*, 9(2), 118.

<https://doi.org/10.3390/w9020118>

Boehlert, B., Strzepek, K. M., Chapra, S. C., Fant, C., Gebretsadik, Y., Lickley, M., Swanson, R., McCluskey, A., Neumann, J., & Martinich, J. (2015). Climate change impacts and greenhouse gas mitigation effects on US water quality. *Journal of Advances in Modeling Earth Systems*, 7, 1326-1338.

<https://doi.org/10.1002/2014MS000400>

Yen, H., Daggupati, P., White, M. J., Srinivasan, R., Gossel, A., Wells, D., & Arnold, J. G. (2016). Application of large-scale, multi-resolution watershed modeling framework using the hydrologic and water quality system (HAWQS). *Water*, 8(4), 164. <https://doi.org/10.3390/w8040164>

HAWQS advances the functionality of the widely used and accepted Soil and Water Assessment Tool (SWAT), providing a platform for water quality modeling, primarily by minimizing the necessary initialization time. Originally developed by the U.S. Department of Agriculture (USDA), SWAT has been the core simulation tool for numerous U.S. national and international assessments of soil and water resources. The use of HAWQS over SWAT improves the ease of application to national scale analyses while still simulating a large array of watershed processes for a defined period of record.

The HAWQS model follows a broad modeling sequence: (1) the landscape phase, where the primary processes are climate, soil water balance, nutrient and sediment transport and fate, land cover, plant growth, farm management, and (2) the main channel phase, where the main processes are river routing, and sediment and nutrient transport through the rivers and reservoirs.

The HAWQS model projects changes in water quality parameters and simulated changes in river flow for five climate models under RCP8.5 and RCP4.5. These projections include future municipal wastewater treatment plant loadings (point source) scaled to account for population growth. Changes in overall water quality are estimated using changes in a Climate-oriented Water Quality Index (CWQI), a metric that combines multiple pollutant and water quality measures. Four water quality parameters (water temperature, dissolved oxygen, total nitrogen, and total phosphorus) are aggregated from the eight-digit

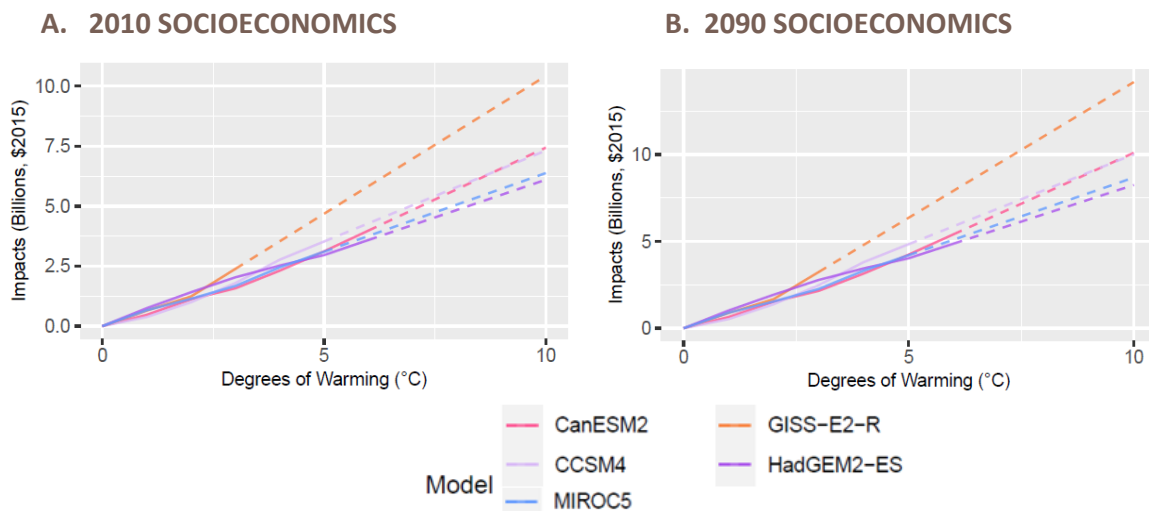
HUC level to the Level-III Ecoregions, weighted by area.⁸² Finally, a relationship between changes in the CWQI and changes in the willingness to pay for improving water quality is used to estimate the economic implications of projected water quality changes. For more information on the approach and results for the water quality sector, please refer to Fant et al. (2017), Boehlert et al. (2015), and Yen et al. (2016). Specifically, impacts are estimated in the underlying study as per capita change in the willingness to pay to improve water quality for two future eras: 2050 (2040-2059) and 2090 (2080-2099).

TABLE B-23. INCOMING DATA CHARACTERISTICS: WATER QUALITY

Data Features	Water Quality Attributes
Evaluated Impacts	<ul style="list-style-type: none"> • Willingness to pay for improved water quality (economic)
Variant	<ul style="list-style-type: none"> • No additional adaptation
Data Shape	<ul style="list-style-type: none"> • Era - 2050 (2040-2059) and 2090 (2080-2099) • Six CMIP5 GCMs (standard CIRA set) • EPA Level 3 Ecoregion
Model Type	<ul style="list-style-type: none"> • Simulation
Runs Provided	<ul style="list-style-type: none"> • With socioeconomic growth and with climate change
Additional Data	<ul style="list-style-type: none"> • State Level ICLUS Population
Regions and States with Impacts	<ul style="list-style-type: none"> • All CONUS regions and states

For illustrative purposes, **Figure B-44** shows the resulting damages by degree of warming by GCM, calculated using 2010 (panel A) and 2090 (panel B) socioeconomics.

FIGURE B-44. WATER QUALITY IMPACTS BY TEMPERATURE BIN DEGREE



Total impacts (billions of 2015\$) by degree (°C) for two socioeconomic snapshots (2010 and 2090 default scenarios). Extrapolated portions are shown with a dashed line. Note y-axis scales vary by plot.

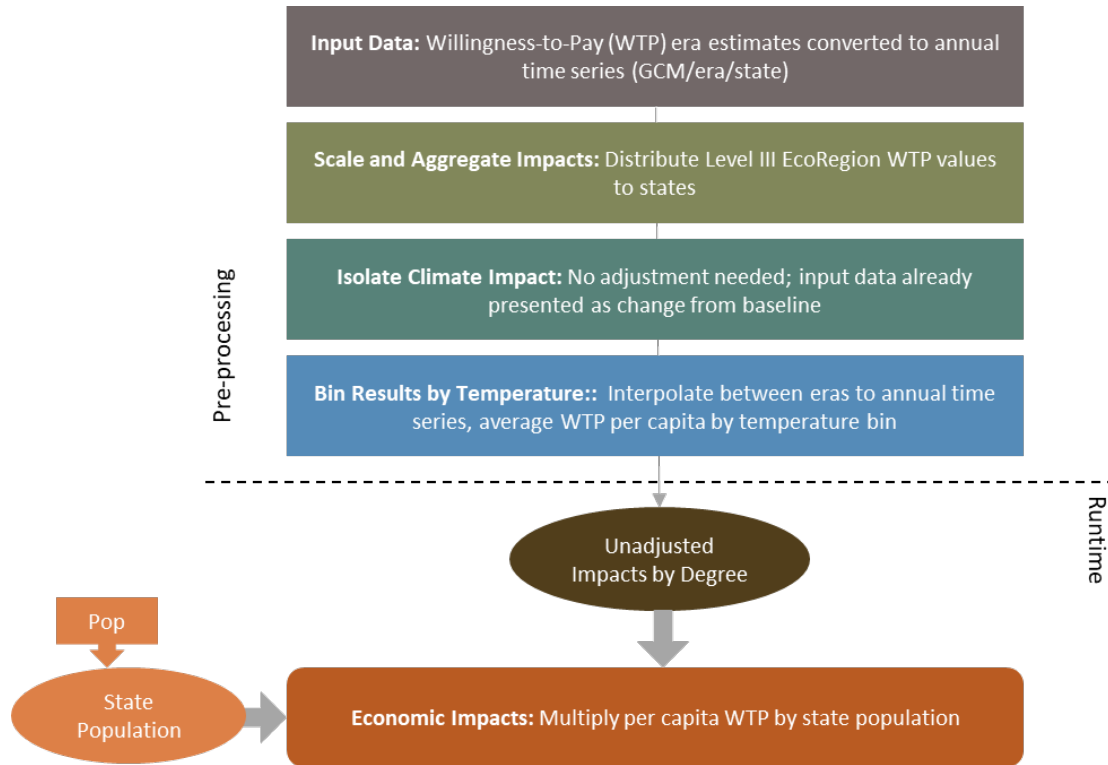
⁸² Designed to serve as a spatial framework for environmental resource management, ecoregions denote areas within which ecosystems (and the type, quality, and quantity of environmental resources) are generally similar. Ecoregions were originally created to support the development of regional biological criteria and water quality standards, and to set management goals for nonpoint source pollution.

Processing steps

Processing steps are shown in **Figure B-45**.

Pre-processing: The willingness to pay for each EPA Level 3 Ecoregion, GCM, and era combinations are from the underlying study. These climate change impacts are relative to a “control” scenario (one with socioeconomic growth and historical climate) to isolate the climate change impacts from the impacts of socioeconomic growth. In the first pre-processing step, these data are aggregated to the state level. Values are aggregated using a spatial weight, which represents a state’s contribution to the total area of an Ecoregion. Then, ICLUSv⁸³ 2050 and 2090 populations are used to calculate willingness to pay per capita. Linear interpolation is then used to create an annual time series of values for each GCM and state combination for the period 1995-2099. Values are extrapolated for 2090-2099 using the linear trend observed between 2050 and 2090, and values for years prior to 2050 are estimated by using 1995 as a baseline year; i.e., impacts were assumed to be zero in 1995 and results are interpolated linearly between 1995 and 2050. Finally, annual willingness to pay per capita rates are then binned by degree of CONUS temperature change for each GCM by averaging across the 11-year windows where each GCM reaches each integer degree of CONUS warming relative to the baseline.

FIGURE B-45. WATER QUALITY DATA PROCESSING FRAMEWORK



Runtime: When FrEDI is run, the pre-processed by-degree per capita willingness to pay functions are then applied to the input temperature scenario to calculate the unadjusted annual WTP per capita values based

⁸³ Bierwagen et al., 2010; ICLUSv2, 2017 (see footnote 31)

on the level of warming in each year of the input scenario. The total damages are then calculated by applying these annual per capita rates to the input population scenario.

Limitations and Assumptions

- Decreases in water quality projected with climate change will likely have adverse effects on human health and the environment, not represented in this section's results. For example, climate change impacts to water quality may affect ecological dynamics of freshwater systems, with cascading effects on ecosystem services and recreational opportunities.
- This analysis only considers four water quality parameters, and omits other constituents, such as sediment and heavy metals, that may be affected by changes in the climate system.
- The methods underlying the analysis do not consider the effects of climate change-induced extreme events on water quality, such as increased siltation and runoff following wildfire events.
- The analysis considers only a subset of all use/non-use values linked to water quality changes, therefore the damages reported here are likely underestimates of future impacts.
- By creating an annual time series for the period 1995 to 2100 based on values from 2050 and 2090 only, the temperature binning processing does not capture any non-linearities in the relationship between damages and temperature, particularly in the early years of the century.
- See Fant et al. (2017) and Boehlert et al. (2015) for further discussion of the limitations and assumptions.

Outdoor Recreation

Summary

This sector estimates the per capita change in number of trips and values of participation in outdoor recreation activities projected with climate change. Impacts are estimated based on an empirical relationship, developed in Willwerth et al. (2023), between weather conditions and

participation in outdoor recreation as tracked in the American Time Use Survey (ATUS) for the 17-year-period between 2003 and 2019.⁸⁴ Note: there is an alternative study that may be used to quantify impacts to “Winter Recreation”, but this “Outdoor Recreation” study is the default used in FrEDI.

This sector provides impacts across all modeled outdoor recreation activities, broken down by activity category: fishing, snow sport, water sport, and all other activities. For each category, FrEDI includes a change in number of trips and the value of the change in trips. Two scenarios are considered in this sector: No additional adaptation and adaptation. As reflected in Willwerth et al. (2023), ‘Scenario 2’ projects recreation participation using region-matched results (no additional adaptation) and ‘Scenario 3’ projects

UNDERLYING DATA SOURCES AND LITERATURE

Willwerth, J., Sheahan, M., Chan, N., Fant, C., Martinich, J., & Kolian, M. (2023). The Effects of Climate Change on Outdoor Recreation Participation in the United States: Projections for the Twenty-First Century. *Weather, Climate, and Society*, 15(3), 477-492.

<https://doi.org/10.1175/WCAS-D-22-0060.1>

⁸⁴ ATUS is a nationally representative cross-sectional survey of Americans 15+ year respondents asked to report a detailed diary of how they allocated the preceding 24-hour by activity, location, and length of time measured in minutes.

recreation participation by applying the empirical relationships developed from historical data in southern regions, where recreators are more acclimatized to warmer conditions, to all regions of CONUS, representing an approximation of acclimatization (adaptation).

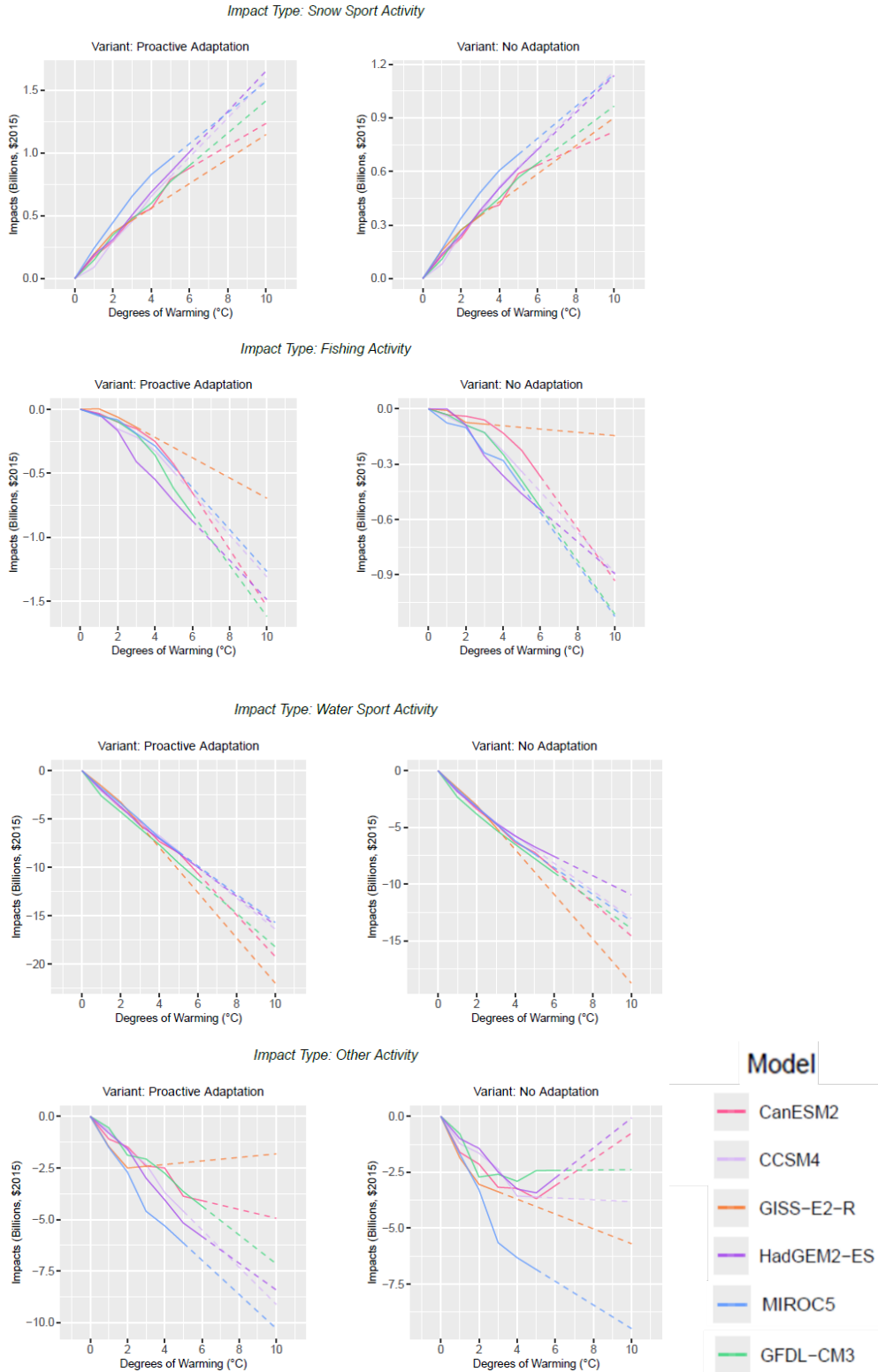
TABLE B-24. INCOMING DATA CHARACTERISTICS: OUTDOOR RECREATION

Data Features	Outdoor Recreation Attributes
Evaluated Impacts	<ul style="list-style-type: none"> Lost recreational trips for four groups of activities: fishing, snow sports, water sports, and other activities (physical) and lost value of these recreation trips taken (economic)
Variant	<ul style="list-style-type: none"> No additional adaptation Adaptation
Data Shape	<ul style="list-style-type: none"> Integer degree (1-6°C) Six CMIP5 GCMs (standard CIRA set) State level
Model Type	<ul style="list-style-type: none"> Empirical
Runs Provided	<ul style="list-style-type: none"> With climate change and no socioeconomic growth
Additional Data	<ul style="list-style-type: none"> ICLUSv2, SCORP
Regions and States with Impacts	<ul style="list-style-type: none"> All CONUS Regions and States

Damages are based on per capita change in the number of trips and the value of trips for outdoor recreation activities. For illustrative purposes, **Figure B-48** shows the resulting damages by degree of warming for each recreation impact type by GCM, calculated using 2010 (panel A) and 2090 (panel B) socioeconomics (i.e., the endpoints of the socioeconomic scenarios).

FIGURE B-46. OUTDOOR RECREATION IMPACTS BY TEMPERATURE BIN DEGREE

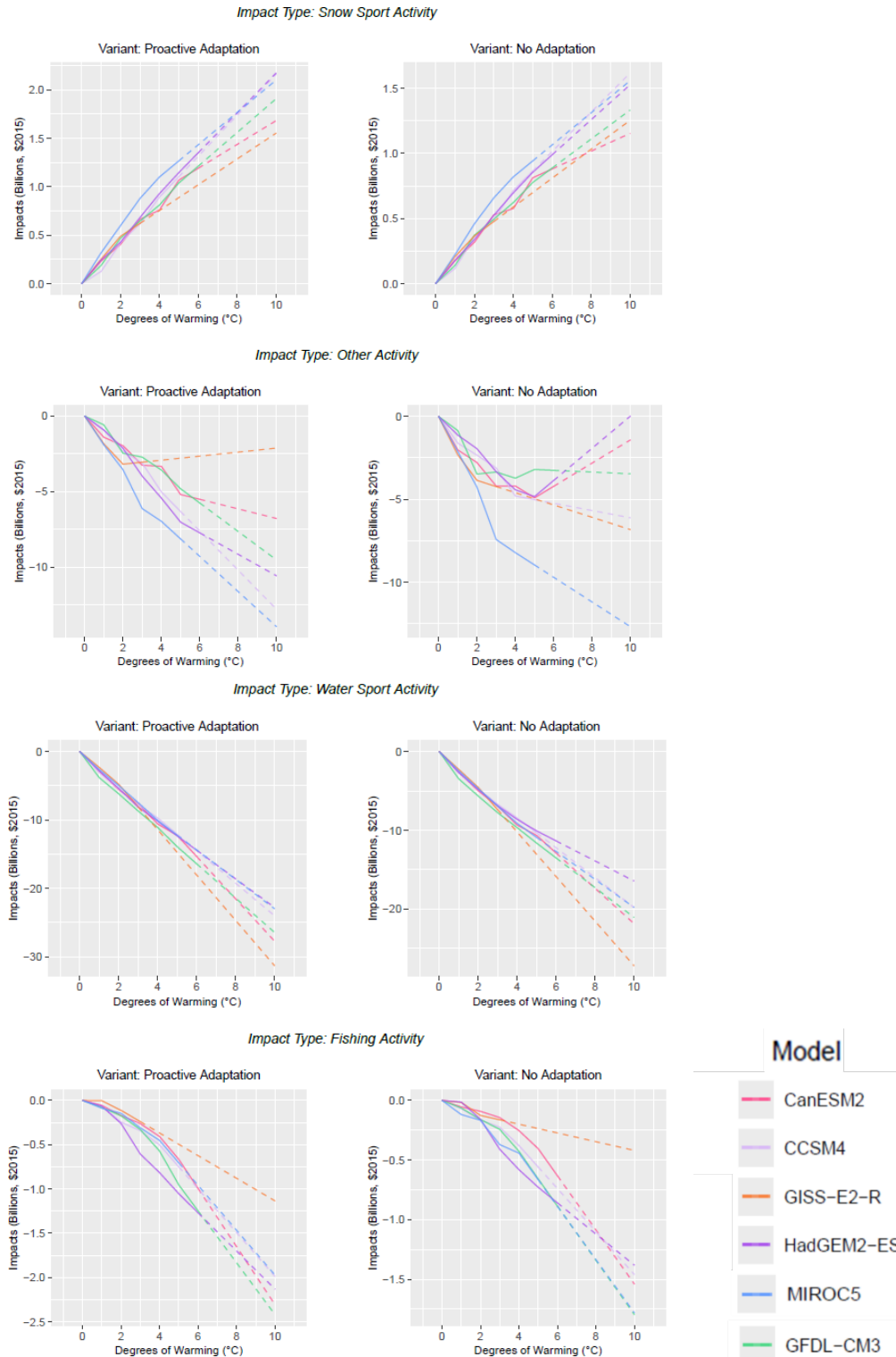
A. 2010 SOCIOECONOMICS



Model

- CanESM2
- CCSM4
- GISS-E2-R
- HadGEM2-ES
- MIROC5
- GFDL-CM3

B. 2090 SOCIOECONOMICS



Total impacts (billions of 2015\$) by degree (°C) for each impact type for two socioeconomic snapshots (2010 and 2090 default scenarios). Extrapolated portions are shown with a dashed line. Note y-axis scales vary by plot.

Model

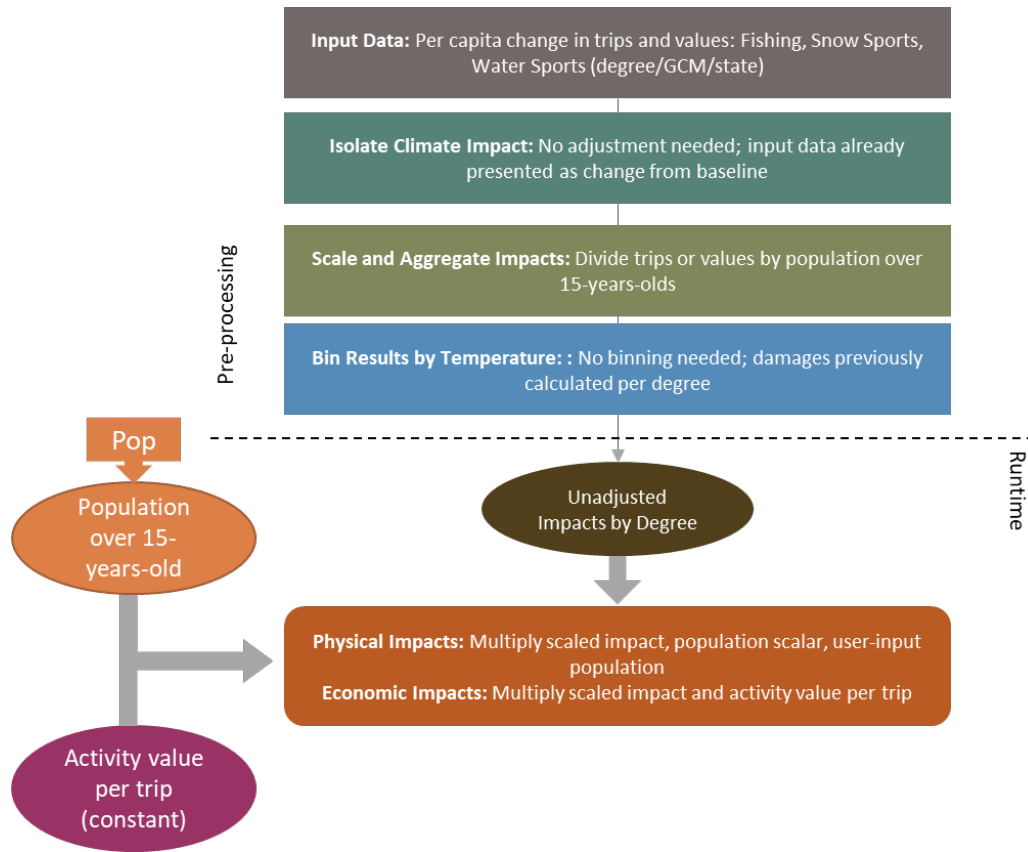
- CanESM2
- CCSM4
- GISS-E2-R
- HadGEM2-ES
- MIROC5
- GFDL-CM3

Processing steps

Processing steps are shown in **Figure B-47**.

Pre-processing: Changes in trips and values are available from Willwerth et al. (2023) by degree across outdoor recreational activities, GCM, and state. The per capita changes were calculated by dividing trips or values by the population over 15-years old (i.e. the population covered by the ATUS survey). A population scalar is calculated using the ICLUSv2 population data by state and year that represents the percent of total population over 15-years-old for use within FrEDI to adjust user population inputs to the relevant population for this sector. Changes in trips for the three specific outdoor recreation activities are valued using welfare estimates per trip from the Oregon Statewide Comprehensive Outdoor Recreation Plan (SCORP). Values for fishing, in the limited recreation set, snow sports, and water sports, in the nonlimited set, were provided from SCORP.⁸⁵ The per trip value for ‘other’ activities is a composite value specific to the state and degree of warming based on the relative change in a suite of activities tracked in ATUS. These values were adjusted to 2015\$ from 2018\$.

FIGURE B-47. OUTDOOR RECREATION DATA PROCESSING FRAMEWORK



⁸⁵ Fishing is listed in the limited recreation set with an activity-specific value from SCORP. The total change in trips is calculated and then multiplied by the totals by the activity-specific value. Water and snow sports are listed in the nonlimited set and Willwerth et al. (2023) subtracts the change in total limited activity trips from the change in all outdoor activities which results in the total change in nonlimited activities.

Runtime: When FrEDI is run, the pre-processed by-degree per capita scaled impacts are multiplied by a population scalar, user-input population, and the activity value per trip for physical impacts. For economic impacts the scaled impacts are multiplied by the activity value per trip.

Limitations and Assumptions

- In reference to Willwerth et al. (2023), the valuation methods used for nonlimited activity trips (all sports) may over- or underestimate activity day values based on the duration of participation and quality of trip.
- There are various climate stressors that are not captured in this analysis. Some relevant examples being decreased air quality, decreased water quality and harmful algal blooms. According to Willwerth et al. (2023), these stressors are predicted to decrease outdoor recreation participation, and they are not directly incorporated into the model.
- ATUS data does not provide specific location information. A respondents assigned weather may not accurately represent the conditions at the recreation site since it is not uncommon for those participating in outdoor recreation activities to travel outside of their county or states (particularly winter sport and water activities).
- For the change in trips and values specific to fishing, Willwerth et al. (2023) was unable to account for the different values associated with general fishing and cold-water fishing. Cold-water fishing for species such as trout is highly valued and vulnerable to climate change, and general fishing for warm water is less valuable and may see an increase in participation with a warmer climate.

Winter Recreation

Summary

This sector estimates lost revenue projected with climate change to suppliers of three types of winter recreation occurring at 247 sites across CONUS: alpine skiing, Nordic skiing, and snowmobiling. Note: there is an alternative study that may be used to quantify impacts to “Outdoor Recreation”, and is the default used in FrEDI.

UNDERLYING DATA SOURCES AND LITERATURE

Wobus, C., Small, E. E., Hosterman, H., Mills, D., Stein, J., Rissing, M., Jones, R., Duckworth, M., Hall, R., Kolian, M., Creason, J., & Martinich, J. (2017). Projected climate change impacts on skiing and snowmobiling: A case study of the United States. *Global Environmental Change*, 45, 1-14. <https://doi.org/10.1016/j.gloenvcha.2017.04.006>

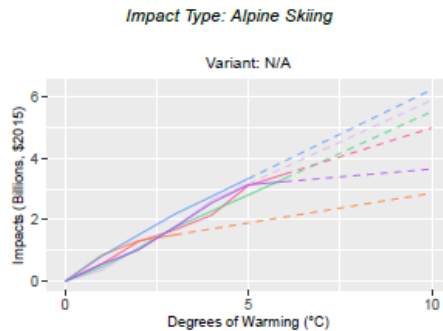
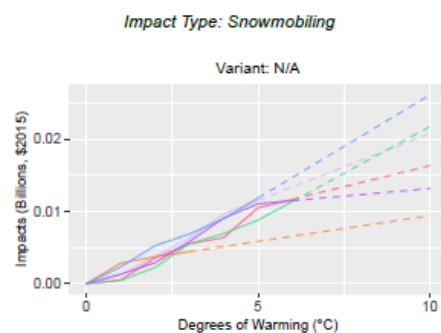
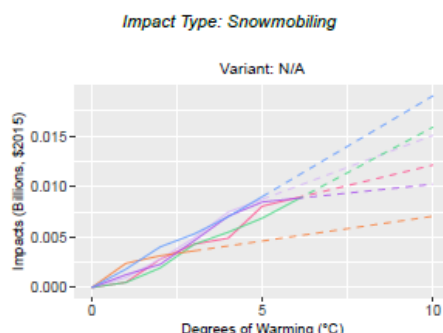
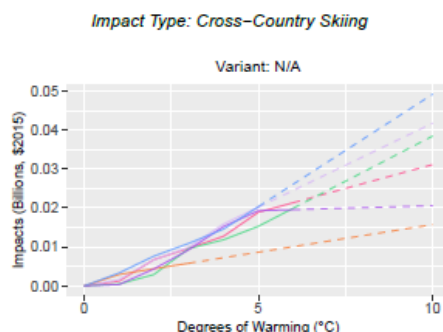
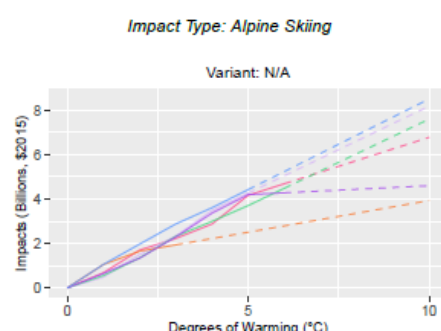
Damages are based on the number of visits to winter recreational sites, entrance fees, and state-level average ticket prices. The model described in Wobus et al., (2017) was run using both 2010 and 2090 ICLUSv2 population.

TABLE B-25. INCOMING DATA CHARACTERISTICS: WINTER RECREATION

Data Features	Winter Recreation Attributes
Evaluated Impacts	<ul style="list-style-type: none"> • Per capita cost of projected change in visits across models from baseline for three types of winter recreation activities: alpine skiing, Nordic skiing, and snowmobiling (economic)

Data Features	Winter Recreation Attributes
Variant	<ul style="list-style-type: none"> No additional adaptation
Data Shape	<ul style="list-style-type: none"> Integer degree (1-6°C) Six CMIP5 GCMs (standard CIRA set) State level (Nordic skiing and snowmobiling)/National Ski Areas Association (NSAA) regions (alpine skiing)
Model Type	<ul style="list-style-type: none"> Simulation
Runs Provided	<ul style="list-style-type: none"> With 2010 population and with climate change With 2090 population and with climate change
Additional Data	<ul style="list-style-type: none"> Average NSAA region ticket price Average per person forest rec entry fee
Regions and States with Impacts	<ul style="list-style-type: none"> Midwest (excluding IA, MO, OH) Northeast (excluding DE, DC) Northern Plains (excluding NE, ND) Northwest Southeast (excluding AL, AR, FL, GA, KY, LA, MS, NC, SC, TN) Southwest

For illustrative purposes, **Figure B-48** shows the resulting damages by degree of warming for each recreation impact type by GCM, calculated using 2010 (panel A) and 2090 (panel B) socioeconomics (i.e., the endpoints of the socioeconomic scenarios).

FIGURE B-48. WINTER RECREATION IMPACTS BY TEMPERATURE BIN DEGREE**C. 2010 SOCIOECONOMICS****B. 2090 SOCIOECONOMICS**

Total impacts (billions of 2015\$) by degree (°C) for each impact type for two socioeconomic snapshots (2010 and 2090 default scenarios). Extrapolated portions are shown with a dashed line. Note y-axis scales vary by plot.

Processing steps

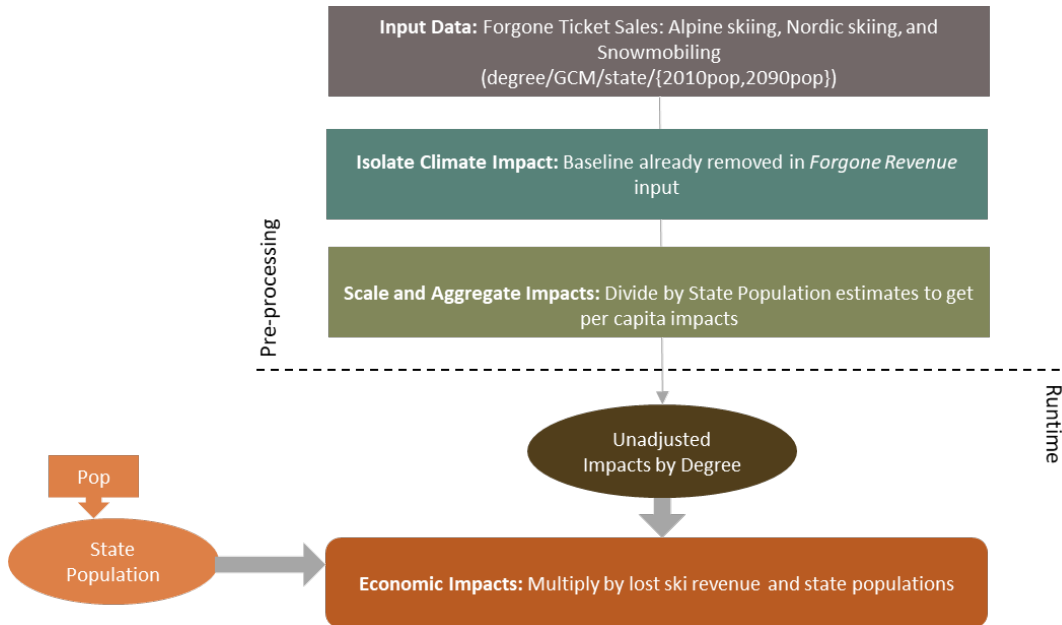
Processing steps are shown in **Figure B-49**.

Pre-processing: Lost visitation days are available from Wobus et al. (2017) by degree across recreational activities (alpine skiing, Nordic skiing, and snowmobiling), GCMs, and state, for both a 2010 and 2090 population. Climate impacts are already isolated from these data. Alpine skiing results are presented at the National Ski Areas Association (NSAA) state level, which include some states clustered in groupings of two

to three states. For these groupings comprised of multiple states, lost future visits (and associated economic impacts) are attributed to states proportionally with baseline season-ski area days (i.e. the average length of the alpine ski season in the state multiplied by the number of ski areas in the state).⁸⁶

In the last pre-processing step, both the 2010 and 2090 state estimates are divided by state population to develop per capita estimates of forgone ticket sales for the three winter activities by degree of warming.

FIGURE B-49. WINTER RECREATION DATA PROCESSING FRAMEWORK



Runtime: When FrEDI is run, the pre-processed by-degree per damage functions are then applied to the input temperature scenario to calculate the total annual lost revenue by state, GCM, and impact year.

Limitations and Assumptions

- The scope of winter recreation loss for the tool is derived only from analysis of the alpine skiing, Nordic skiing, and snowmobile sub-sectors of the industry. Potential losses to other winter recreation activities (e.g., tubing) are not quantified in this study.
- Potentially compensating adaptations from the lost opportunity to engage in winter recreation (for example, with other forms of outdoor recreation, or with indoor recreation) are not considered.
- For further discussion of the limitations and assumptions in the underlying sectoral model, see Wobus et al. (2017) and U.S.EPA (2017).

⁸⁶ One NSAA grouping (Rhode Island and Connecticut) does not have available data on baseline season-ski area days by state. For this cluster, losses are distributed between each state based on the ICLUS 2015 population.

Marine Fisheries

Summary

This sector estimates climate-driven changes in thermally available habitat for economically important commercial fish species in the CONUS based on methods described in Morley et al. (2018) and connects changes in fish species population with projected landings, valued using current ex vessel prices⁸⁷ for individual species.

UNDERLYING DATA SOURCES AND LITERATURE

Moore, C., Morley, J.W., Morrison, B., Kolian, M., Horsch, E., Frölicher, T., Pinsky, M.L., & Griffis, R. (2021). Estimating the Economic Impacts of Climate Change on 16 Major US Fisheries. *Climate Change Economics*, 12(1), 2150002.

<https://doi.org/10.1142/S2010007821500020>

Morley, J.W., Selden, R.L., Latour, R.J., Frölicher, T.L., Seagraves R.J., & Pinsky M.L. (2018). Projecting shifts in thermal habitat for 686 species on the North American continental shelf. *PLoS ONE*, 13(5), e0196127. <https://doi.org/10.1371/journal.pone.0196127>

The analysis first characterizes the potential economic impact of projected changes in the annual landings⁸⁸ of 177 commercially harvested marine species from 2021 to 2100, based on the use of five general circulation models (GCMs) to project changes in each target species' thermally available habitat within the U.S. Exclusive Economic Zone (EEZ). The Moore et al. (2021) paper from which these economic damage estimates are derived from then also includes estimates of the future welfare losses associated with changes in landings for a 16-fishery subset of fish species reflected in the estimates presented here, accounting for about 56 percent of current U.S. commercial fishing revenues. We omit consideration of the welfare estimates because they are incomplete, and instead focus on the broader "screening analysis" results from the paper.⁸⁹ The screening analysis assumes constant prices through the 21st century, however, a key limitation discussed further below. The constant price assumption means that there is no socioeconomic adjustment for this sector.

TABLE B-26. INCOMING DATA CHARACTERISTICS: MARINE FISHERIES

Data Features	Marine Fisheries Attributes
Evaluated Impacts	<ul style="list-style-type: none"> Decrease in revenue relative to baseline (economic)
Variants	<ul style="list-style-type: none"> No additional adaptation
Data Shape	<ul style="list-style-type: none"> Yearly (2006-2099) Six CMIP5 GCMs (standard CIRA set) State level
Model Type	<ul style="list-style-type: none"> Simulation
Runs Provided	<ul style="list-style-type: none"> Without socioeconomic growth and with climate change Without socioeconomic growth and without climate change (baseline)

⁸⁷ 'Ex vessel prices' are the prices catches are sold at when entering the supply chain (i.e. sale price received by anglers).

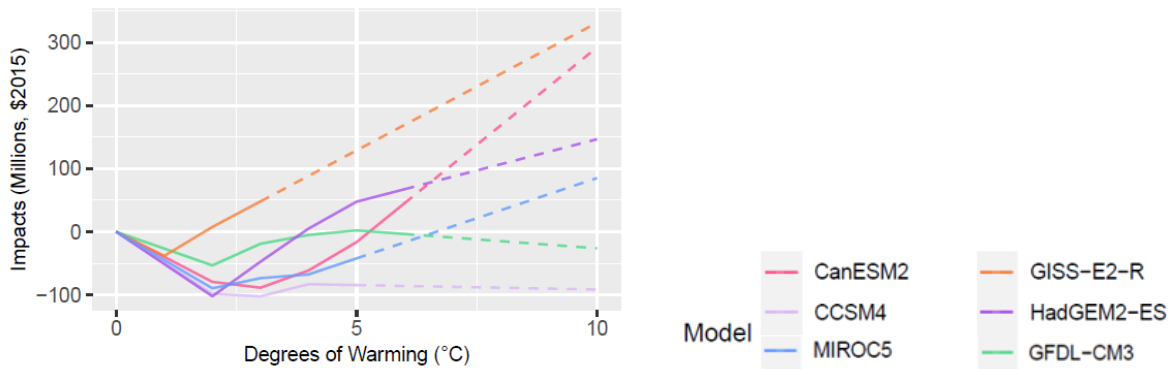
⁸⁸ 'Landings' refer to the value of all catch brought ashore.

⁸⁹ As noted in the paper, to ensure welfare assessment would be analytically tractable, the authors limited the scope to 16 species that could be equally divided into four categories, each of which would contain commodities that the consumers might consider close substitutes. Given the limited number of species the analysis could consider, the authors also chose to focus, to the extent possible, on fisheries that account for the greatest share of current ex-vessel landings. While the welfare analysis provides additional insights about the potential for market adaptation to mitigate damages through seafood consumers substituting away from fish species that might be most affected by climate change, the welfare analysis unavoidably must examine only a subset of fisheries examined in the more comprehensive screening analysis.

Data Features	Marine Fisheries Attributes
Additional Data	<ul style="list-style-type: none"> None
Regions and States with Impacts	<ul style="list-style-type: none"> Northeast (excluding DC, PA, VT, WV) Northwest (excluding ID) Southeast (excluding AR, KY, TN) Southern Plains (excluding KW, OK) Southwest (excluding AZ, CO, NV, NM, UT)

For illustrative purposes, **Figure B-50** shows the resulting damages by degree by GCM.

FIGURE B-50. MARINE FISHERIES IMPACTS BY TEMPERATURE BIN DEGREE

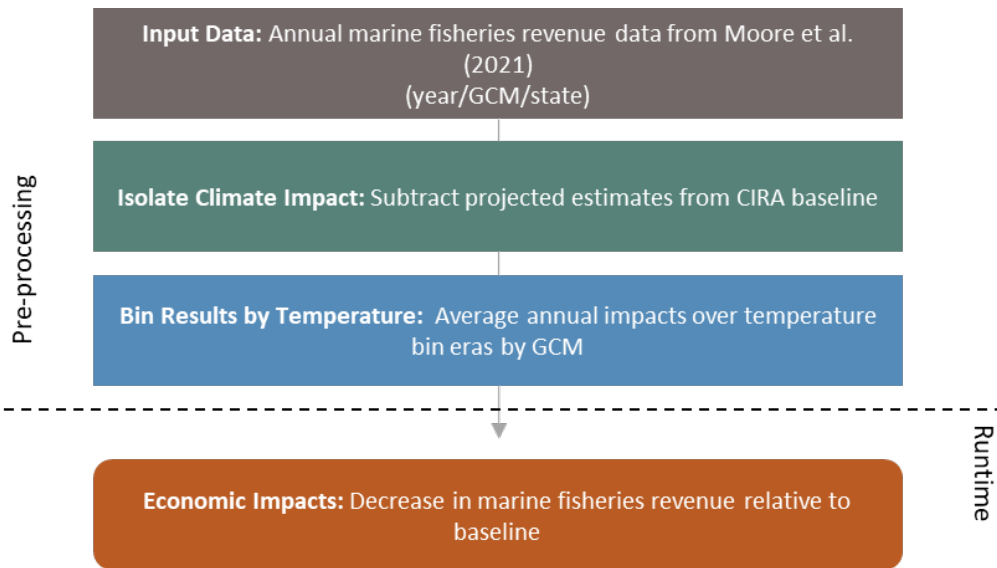


Total impacts (millions of 2015\$) by degree (°C), which do not vary by socioeconomic scenario or time. Extrapolated portions are shown with a dashed line.

Processing steps

Processing steps are shown in **Figure B-51**.

Pre-processing: Annual marine fishery revenue data were obtained from the Moore et al. (2021) study authors, by GCM and state. In the first pre-processing step, the baseline estimates are subtracted from the by year revenue data to isolate climate impacts. Results are then binned by degree of CONUS temperature change for each GCM by averaging across the 11-year windows where each GCM reaches each integer degree of CONUS warming relative to the baseline. Because the original study used a later period baseline (2006-2017), results from four of the five GCM trajectories do not have data for the one-degree warming bin. One degree bin results are therefore generated by interpolating results between the baseline (zero degree) and the two-degree bin for these four GCMs.

FIGURE B-51. MARINE FISHERIES DATA PROCESSING FRAMEWORK

Runtime: When FrEDI is run, the pre-processed by-degree lost revenue damage functions are then applied to the input temperature scenario to calculate the annual total lost revenue from marine fisheries, by GCM and state.

Limitations and Assumptions

- While the underlying study includes impacts for Southern Alaska fisheries, the analysis incorporated in FrEDI is limited to CONUS fisheries. In the 2007-2016 period, Alaska accounted for approximately one third of revenue from all fisheries, and almost 45% of the revenues from fisheries with habitat projections. The paper estimates that under RCP 8.5 climate change would reduce the annual value of ex vessel revenues by about 1.7% from baseline. These declines from baseline for Alaska fisheries are omitted from the FrEDI data, which does not include Alaska in the spatial domain.
- As noted above, Moore et al. (2021) includes a welfare analysis at national scale, for a subset of species. The results of the welfare analysis reflect both market adaptation though substitution effects, and changes in prices. The latter effect, which is characterized by large increases in ex vessel prices through the 21st century, appears to be a strong influence on the welfare estimates. Compared to the direct impacts in the screening analysis results, where prices are held constant, the welfare analysis yields results for the present value of damages that are two to three times larger, suggesting that the direct impact results incorporated in FrEDI are conservative.
- Moore et al. (2021) and Morley et al. (2018) analyses exclude many factors that may influence species abundance and commercial landings, such as potential changes in primary productivity, species interactions, population dynamics, or fisheries management. In addition, because the approach focuses on potential changes in the landings of species that are already commercially harvested, it does not account for the possibility that an increase in the abundance of other species

could lead to the development of new fisheries. This development would help offset potential losses in economic welfare attributable to a decline in the productivity of established fisheries.

- The species for which habitat projections are available account for nearly 80% of the average annual ex-vessel revenues on the East Coast. Coverage is somewhat lower in the other three regions, where the species for which habitat projections are available account for between 63% and 68% of the average annual revenue. These factors likely lead to underestimate of the total impact of climate change on fisheries.
- For further discussion of the underlying sectoral model, see Moore et al. (2021).

Marsh Migration

Summary

This sector estimates climate-driven changes in coastal wetland areas in CONUS based on methods described in Fant et al. (2022), which considers SLR, future greenhouse gas (GHG) emissions, and accretion rate uncertainty with outputs from the National Ocean and Atmospheric (NOAA) marsh migration model. The analysis considers projections of future coastal marsh area and changes in GHG sequestration for six SLR scenarios and three accretion scenarios from 2000-2100.

Economic impacts are estimated in Fant et al.

with two distinct approaches: restoration cost and ecosystem services. The ecosystem services considered are limited to coastal property protection from coastal flooding and carbon sequestration, the latter using a social cost of carbon approach.⁹⁰ ELI (2007) provides restoration costs, assigning each coastal county to one of the 17 CONUS US Army Corps of Engineers (USACE) coastal districts. Sun and Carson (2020) estimate the avoided damages to coastal property by county per unit area of wetland, and the methods employed in the EPA GHG Inventory for 1990–2019 GHG sequestration in wetlands, by type.

UNDERLYING DATA SOURCES AND LITERATURE

Fant, C., Gentile, L. E., Herold, N., Kunkle, H., Kerrich, Z., Neumann, J., & Martinich, J. (2022). Valuation of long-term coastal wetland changes in the US. *Ocean & coastal management*, 226, 106248.

<https://doi.org/10.1016/j.ocecoaman.2022.106248>

Environmental Law Institute (ELI), (2007). Mitigation of impacts to fish and wildlife habitat: estimating costs and identifying opportunities. <https://www.eli.org/research-report/mitigation-impacts-fish-and-wildlife-habitat-estimating-costs-and-identifying>

Sun, F., & Carson, R. T. (2020). Coastal wetlands reduce property damage during tropical cyclones. *Proceedings of the National Academy of Sciences*, 117(11), 5719-5725.

<https://doi.org/10.1073/pnas.1915169117>

TABLE B-27. INCOMING DATA CHARACTERISTICS: MARSH MIGRATION

Data Features	Marsh Migration Attributes
Evaluated Impacts	<ul style="list-style-type: none"> • Net marsh area lost (physical)^a • Costs of wetland area restoration (economic) • Lost value of wetland flood protection (economic)^b • Lost GHG sequestration (physical)
Variants	<ul style="list-style-type: none"> • Low accretion^c • Medium accretion^c

⁹⁰ Currently FrEDI does not include the economic value associated with carbon sequestration.

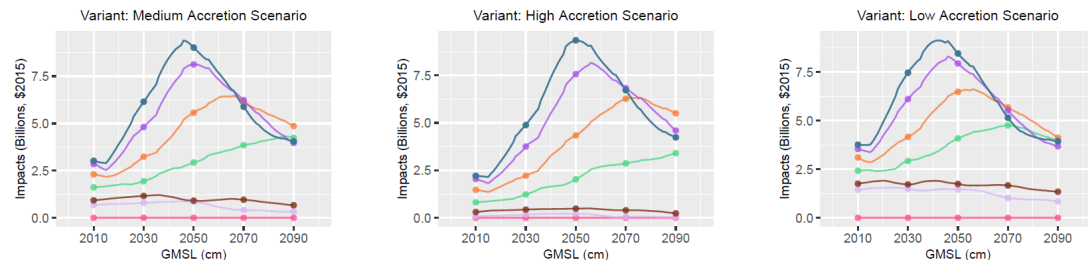
Data Shape	<ul style="list-style-type: none"> High accretion^c Annual (2000-2100) County level Six SLR scenarios Total coastal marsh area and coastal marsh net sequestration
Model Type	<ul style="list-style-type: none"> Simulation
Runs Provided	<ul style="list-style-type: none"> With socioeconomic growth and with climate change
Additional Data	<ul style="list-style-type: none"> Cost of restoration per acre^d Value of wetland area for coastal flood protection per hectare (converted to value per acre for FrEDI)^d
Regions and States with Impacts	<ul style="list-style-type: none"> Northeast (excluding VT and WV) Northwest (excluding ID) Southeast (excluding AR, KY, and TN) Southern Great Plains (excluding KS and OK) Southwest (excluding AZ, CO, NM, NV, and UT)

a. Marsh area is net of the baseline year 2000.
 b. The value of wetlands for coastal flood protection is considered an alternative valuation to restoration costs.
 c. All accretion variants represent a 'No Additional Adaptation' scenario.
 d. An average per-acre value should not be inferred across space, owing to variation in both flood protection and carbon sequestration values by location and wetland type.

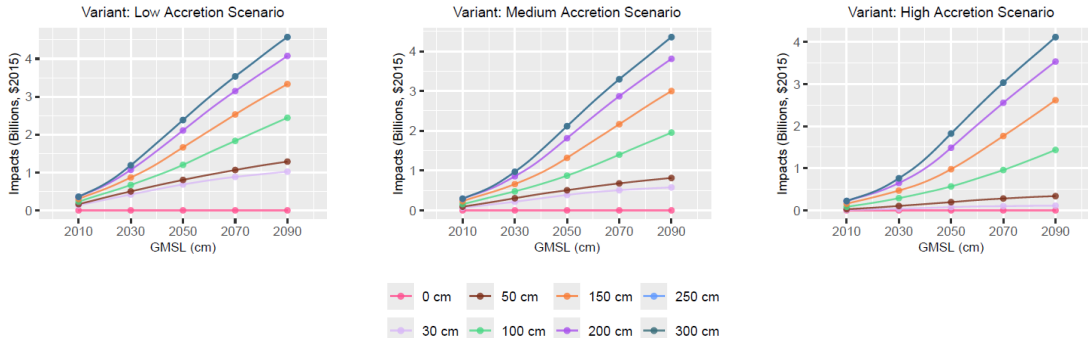
For illustrative purposes, **Figure B-52** shows the resulting damages by degree by GCM.

FIGURE B-52. MARSH MIGRATION IMPACTS BY TEMPERATURE BIN DEGREE

Impact Type: Restoration Costs



Impact Type: Property Protection Costs



Total impacts (billions of 2015\$) by year and variant. The two impact types are not additive: 'Restoration Costs' are the primary/default impact and 'Property Protection Costs' are an alternative measure. Note y-axis scale varies by plot.

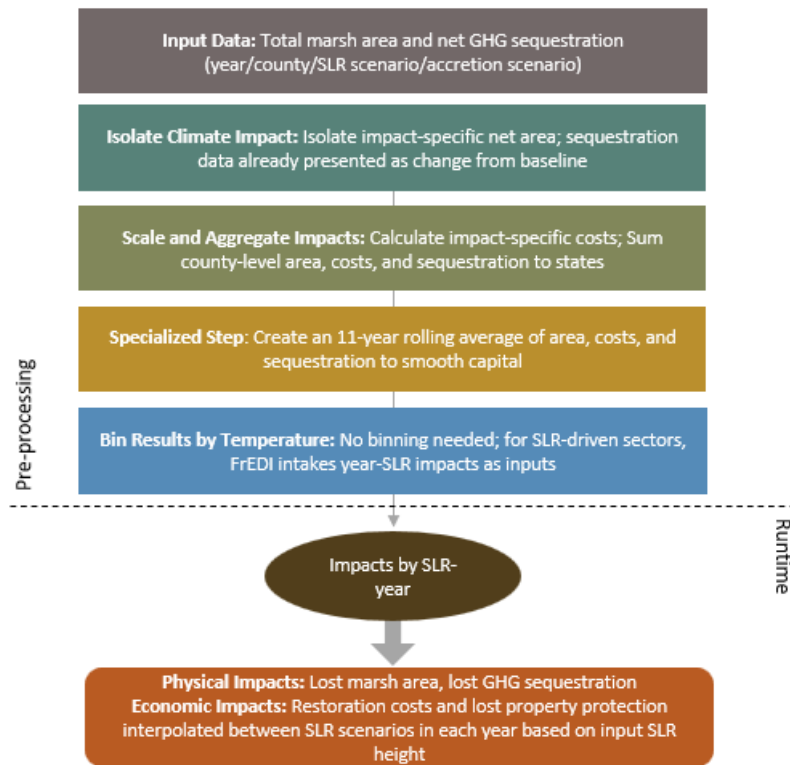
Processing steps

Processing steps are shown in **Figure B-53**.

Pre-processing: Annual projections of total marsh area and net GHG sequestration by SLR scenario and accretion scenario were obtained from the Fant et al. (2022) study authors. In the first pre-processing step, climate impacts are isolated by calculating net marsh area change by year and state. Lost benefits of wetlands for coastal flood protection are considered cumulative, continuing in perpetuity. Therefore, all county-level marsh areas in year 2000 are subtracted from the area in years 2001-2100 to produce the net area providing flood protection. Costs of restoration are only assessed relative to the previous year, and do not persist into the future. Therefore, for restoration cost purposes, net marsh area is calculated each year by subtracting the previous year's area from the annual total marsh area.

Net area is combined with county-specific area unit costs to estimate county-level costs of restoration and lost wetland-associated flood protection value. Carbon and methane sequestration were provided by the authors as net of the baseline. All impact measures (i.e., net acres, costs, and sequestration values) are summed to the state level and smoothed with 11-year rolling averages.⁹¹

FIGURE B-53. MARSH MIGRATION DATA PROCESSING FRAMEWORK



Runtime: When FrEDI is run, the damage trajectory is interpolated between the damage curves of the SLR scenarios that have SLR heights just above and below the input scenario in each year. For example, if the

⁹¹ This calculation utilizes an 11-year window when five years of data are available on either side of the central year (see footnote 68)

SLR trajectory reaches 175cm in 2080, the damage estimate would fall between the 150cm and 200cm scenarios for that year.

Limitations and Assumptions

- Valuation results should not be interpreted as a total value for wetlands lost. There are many possible marsh ecosystem services potentially amenable to valuation but which remain difficult or infeasible to quantify at regional to statewide spatial scales including carbon storage, inland flood control, water purification, recreational value (e.g., wildlife viewing), commercial and recreation fish nursery provision, and coastal storm protection.⁹²
- Valuation reflects scenarios of changes from wetlands to other land types, so it reflects net rather than gross values of coastal wetland loss.
- For further discussion of the underlying sectoral model, see Fant et al. (2022).

B.6 Labor and Learning Sector

Labor

Summary

The labor sector addresses economic damages from changes in total labor hours in CONUS projected with climate change. The analysis estimates changes in labor allocation, with both positive and negative responses in hours

UNDERLYING DATA SOURCES AND LITERATURE

Neidell, M., Graff-Zivin, J., Sheahan, M., Willwerth, J., Fant, C., Sarofim, M., & Martinich, J. (2021). Temperature and work: Time allocated to work under varying climate and labor market conditions. PLoS ONE 16(8): e0254224.

<https://doi.org/10.1371/journal.pone.0254224>

worked in weather-exposed industries (e.g., agriculture, construction, manufacturing). The study finds the relationship between temperature and hours worked is not significant during recession periods, and therefore projected losses are adjusted to account for the probability of recession. Damages are based on a physical measure of average hours worked by workers in high-risk industries, which is monetized in Neidell et al. (2021) by average wages across at-risk industries.⁹³

TABLE B-28. INCOMING DATA CHARACTERISTICS: LABOR

Data Features	Labor Attributes
Evaluated Impacts	<ul style="list-style-type: none"> • Lost hours among high-risk workers (physical) • Value of lost wages among high-risk workers (economic)
Variants	<ul style="list-style-type: none"> • No additional adaptation
Data Shape	<ul style="list-style-type: none"> • Annual • Six CMIP5 GCMs (standard CIRA set)

⁹² Flight, M. J., Paterson, R., Doiron, K., & Polasky, S. (2012). Valuing wetland ecosystem services: A case study of Delaware. *National Wetlands Newsletter*, 34(5), 16-20. <https://www.indecon.com/wp-content/uploads/flight-et-al-Wetlands-2012.pdf>

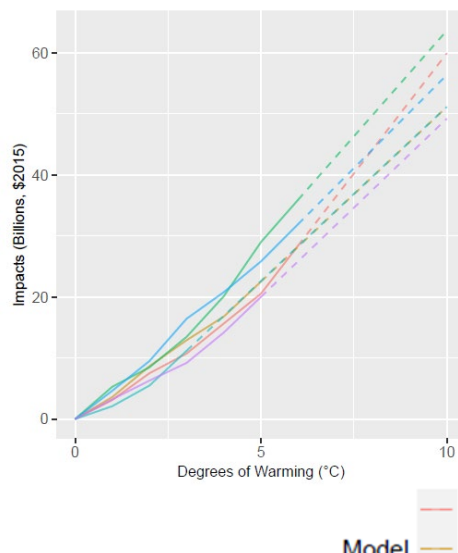
⁹³ Hourly wages are based on average wages across at-risk industries: agriculture, forestry, fishing, hunting, mining, construction, and manufacturing.

Data Features	Labor Attributes
	<ul style="list-style-type: none"> State level
Model Type	<ul style="list-style-type: none"> Empirical
Runs Provided	<ul style="list-style-type: none"> With climate change
Additional Data	<ul style="list-style-type: none"> High-risk worker population High-risk worker wage rate
Regions and States with Impacts	<ul style="list-style-type: none"> All CONUS regions and states

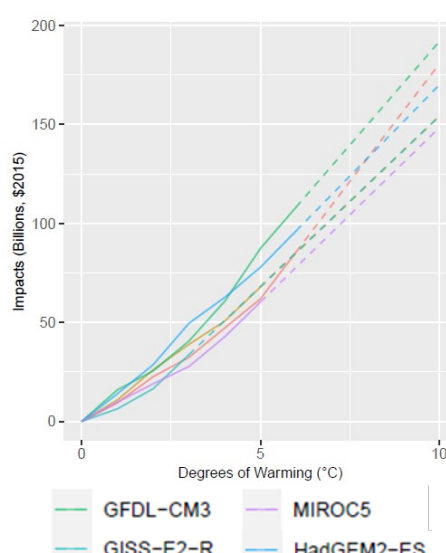
For illustrative purposes, **Figure B-54** shows the resulting damages by degree of warming by GCM, calculated using 2010 (panel A) and 2090 (panel B) socioeconomic scenarios (i.e., the endpoints of the socioeconomic scenarios).

FIGURE B-54. LABOR IMPACTS BY TEMPERATURE BIN DEGREE

A. 2010 SOCIOECONOMICS



B. 2090 SOCIOECONOMICS

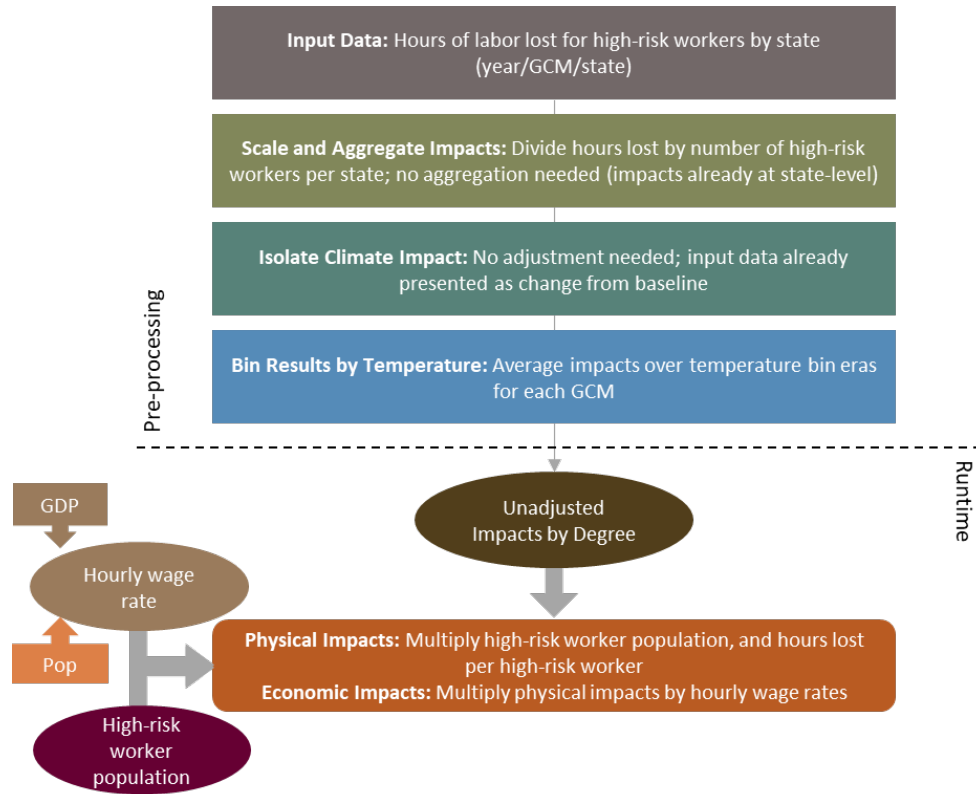


Total impacts (billions of 2015\$) by degree (°C) for each impact type for two socioeconomic snapshots (2010 and 2090 default scenarios). Extrapolated portions are shown with a dashed line. Note y-axis scales vary by plot.

Processing steps

Processing steps are shown in **Figure B-55**.

Pre-processing:Forgone labor hours for each year, GCM, and state are provided by the Neidell et al. (2021) study authors. These results already account for baseline hours lost, so no additional pre-processing is needed to isolate climate impacts. The next step divides these estimates by high-risk worker population to calculate lost hours per high-risk worker estimates. The population of high-risk workers varies by state but is assumed to remain constant over the century. Lastly, state-level lost hours per high-risk worker are binned by degree of CONUS temperature change for each GCM by averaging across the 11-year windows where each GCM reaches each integer degree of CONUS warming relative to the baseline.

FIGURE B-55. LABOR DATA PROCESSING FRAMEWORK

Runtime: When FrEDI is run, the pre-processed by-degree lost hours per high-risk worker functions are then applied to the input temperature scenario to calculate the unadjusted annual hours lost per high-risk worker based on the level of warming in each year of the input scenario. The total labor hours lost are then calculated by applying these annual rates to the number of high-risk workers in each state. Lastly, lost hours are monetized by multiplying the total annual hours lost by an average wage rate from the Bureau of Labor Statistics,⁹⁴ as is done in Neidell et al. (2021), inflated from 2010 values proportionally to GDP per capita growth. Therefore, the physical hours lost will not scale with changes in user-input population, but the monetized impacts will scale with wage rate, which is a function of user-input GDP per capita.

Limitations and Assumptions

- High-risk worker population is assumed to remain constant over the century. As discussed further in Neidell et al. (2021): “Information on the number of high-risk workers at the county level comes from the American Community Survey centered around 2010 (2008–2012 five-year estimates). We assume the number of high-risk workers will remain constant over time. This is because trends from the recent past, as well as near-term projections, suggest that while some industries defined as high-risk will

⁹⁴ U.S. Bureau of Labor Statistics. 2009. Table 2. Private industry by six-digit NAICS industry and government by level of government, 2009 annual averages: Establishments, employment, and wages, change from 2008. Available at: <https://www.bls.gov/cew/publications/employment-and-wages-annual-averages/2009/tables/private-industry-by-six-digit-naics-and-government-by-level-of-government.pdf>

reduce the number of workers they support, including agriculture and mining, and others have or will experience slight increases; on net the absolute number of high-risk workers has and is expected to remain roughly constant at least through 2029.”

- This analysis does not evaluate the potential for new adaptations (behavioral or technological) by workers or employers to mitigate the effects of extreme temperatures on labor allocation. Adaptations present in the baseline period upon which the econometric analysis is based are assumed to be part of the modeled response to future temperature changes, however, new adaptation behaviors or technology are not evaluated.
- The labor loss estimates in FrEDI are limited to impacts on the number of hours worked. Other effects such as temperature-driven reductions in productivity per hour worked and increases in morbidity due to workplace injury are not included in these estimates. Recent research in California suggests that the morbidity impacts of temperature-related workplace injuries could be significant.⁹⁵ Work-related heat mortality is captured in the temperature-related mortality estimates in other sectors in FrEDI.
- See Neidell et al. (2021) for further discussion of the limitations and assumptions.

Learning Loss

Summary

The sector estimates economic damages from heat and learning effects for high school students in CONUS projected with climate change. The analysis estimates the per capita loss in future earnings for high school students (14- to 17-year-olds) experiencing high heat during the school year for two adaptation scenarios defined by the pace of future air conditioning penetration in schools. Using historical observations, Park et al. (2020) assessed how heat impacts learning among high school students and how air conditioning in schools and homes can mitigate these effects. Learning loss is measured as changes in standardized test scores, valued as future earnings losses following the approach in Chetty et al. (2011).

EPA’s 2023 Children’s Health Report applied the historical relationships between heat and learning from Park et al. (2020) to project future learning losses (and lost future earnings) with climate change under each

UNDERLYING DATA SOURCES AND LITERATURE

Park, R. J., Goodman, J., Hurwitz, M., & Smith, J. (2020). Heat and learning. *American Economic Journal: Economic Policy*, 12(2), 306-39. <https://doi.org/10.1257/pol.20180612>

Chetty, R., Friedman, J. N., Hilger, N., Saez, E., Schanzenbach, D. W., & Yagan, D. (2011). How does your kindergarten classroom affect your earnings? Evidence from Project STAR. *The Quarterly journal of economics*, 126(4), 1593-1660. <https://doi.org/10.1093/qje/qjr041>

EPA. (2023). Climate Change and Children’s Health and Well-Being in the United States. U.S. Environmental Protection Agency, EPA 430-R-23-001. <https://www.epa.gov/cira/climate-change-and-childrens-health-and-well-being-united-states-report>

LeRoy, S., Matthews, M., & Wiles, R. (2021). Hotter Days, Higher Costs: The Cooling Crisis in America’s Classrooms. Center for Climate Integrity. <https://coolingcrisis.org/uploads/media/HotterDaysHigherCosts-CCI-September2021.pdf>

⁹⁵ Park, R. J., Pankratz, N., Behrer, A.P. (2021). Temperature, Workplace Safety, and Labor Market Inequality. IZA Discussion Paper No. 14560.

A/C adaptation scenario.⁹⁶ FrEDI's impact by degree damage functions are developed from the Children's Health Report projections, which were reviewed by the lead author of the Park et al. (2020) study and also independently peer-reviewed as part of the overall report review process, consistent with EPA's Peer Review Guidelines.

The future learning losses are estimated under two different scenarios defined in the Children's Health Report based on the penetration of A/C in schools: school A/C use consistent with historical observed (no additional adaptation) and 100% A/C coverage in schools (proactive adaptation). For the scenario with increased A/C use, damages include the cost of additional installation. A/C costs are derived from LeRoy et al. (2021), which assumes that schools will install A/C when they have greater than 32 school days above 80 degrees Fahrenheit (using climate projections from a suite of 32 CMIP5 climate models).⁹⁷ The analysis estimates installation, upgrade, and operating and maintenance costs using 30-year temperature averages around the baseline year of 1970 and two projected years (2025 and 2055) based on the number of schools in each state that are likely to reach the A/C installation temperature threshold by those projected years. For example, if a school had less than 32 school days above 80 degrees in the baseline year, but greater than 32 school days above 80 degrees in one of the projected years, then it is assumed that the school would need to install A/C by the projected year. The estimates do not provide a specific year at which a school has installed, or will install, A/C, but only that the school is assumed to have installed sometime between the baseline year and the projected year.

TABLE B-29. INCOMING DATA CHARACTERISTICS: LEARNING LOSS

Data Features	Learning Loss Attributes
Evaluated Impacts	<ul style="list-style-type: none"> • Lost future earnings (economic) • A/C installation, upgrade, and O&M costs (economic)
Variants	<ul style="list-style-type: none"> • No additional adaptation • Proactive adaptation (increased A/C penetration in schools)
Data Shape	<ul style="list-style-type: none"> • Annual (learning loss) and two eras 2025/2055 (school A/C costs) • Six CMIP5 GCMs (standard CIRA set) (learning loss) and CMIP5 GCM ensemble mean (school A/C costs) • County level (learning loss) and state level (school A/C costs)
Model Type	<ul style="list-style-type: none"> • Empirical
Runs Provided	<ul style="list-style-type: none"> • Without socioeconomic growth and with climate change
Additional Data	<ul style="list-style-type: none"> • ICLUSv2 populations by age bin
Regions and States with Impacts	<ul style="list-style-type: none"> • All CONUS regions and states

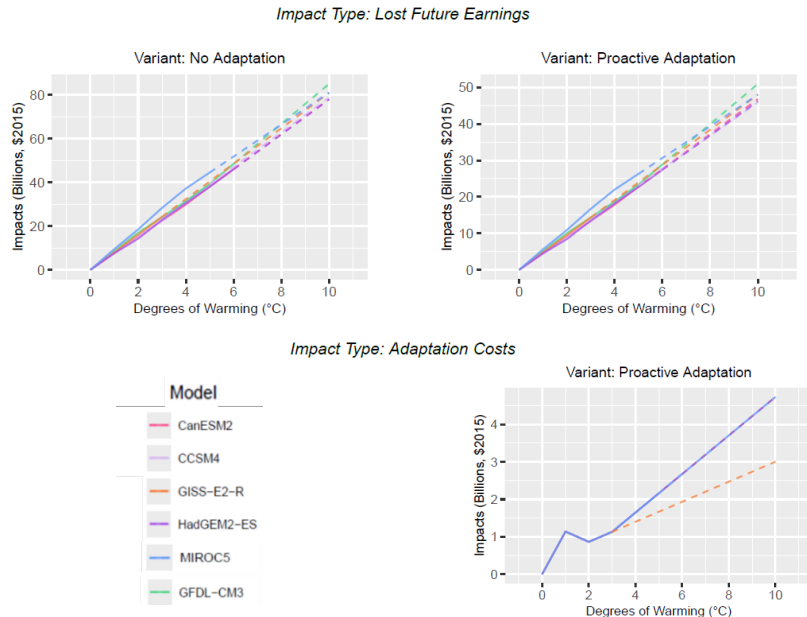
⁹⁶Future losses from the Children's Health Report include annual total future earnings losses for children aged 14-17 under a constant population scenario.

⁹⁷Leroy et al. (2021) provides capital, upgrade, and operating costs for "HVAC/cooling system" installations and upgrades, which may reflect costs that go beyond adding space cooling capacity, such as heating system upgrades. This approach reflects a trend within the industry to integrate heating and cooling systems, which is also consistent with general HVAC technology trends toward electrification of space conditioning capacity.

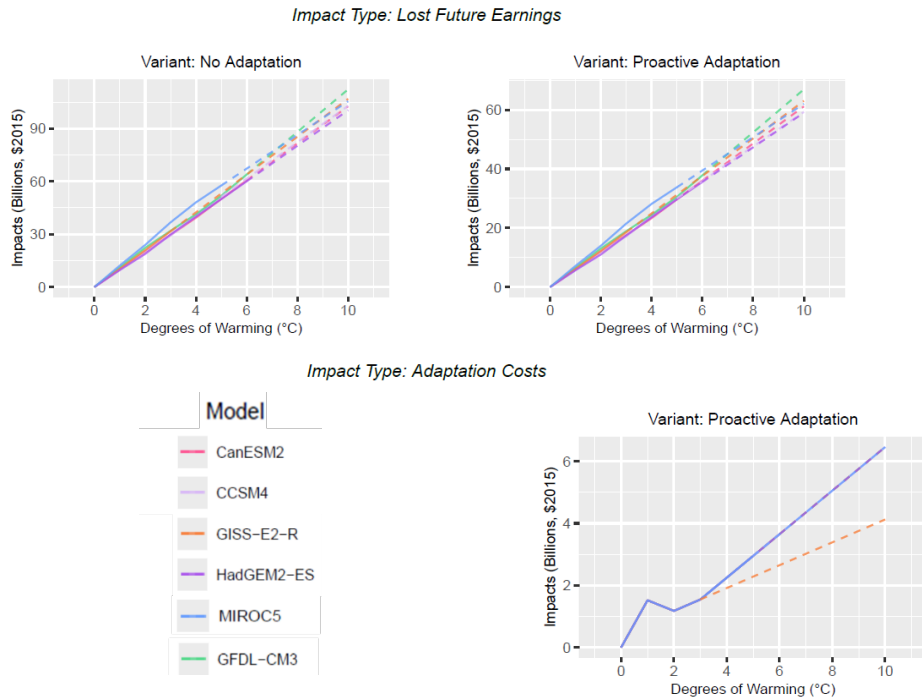
For illustrative purposes, **Figure B-54** shows the resulting damages by degree of warming by GCM, calculated using 2010 (panel A) and 2090 (panel B) socioeconomic scenarios (i.e., the endpoints of the socioeconomic scenarios).

FIGURE B-56. LOST FUTURE INCOME BY TEMPERATURE BIN DEGREE

A. 2010 SOCIOECONOMICS



B. 2090 SOCIOECONOMICS



Total impacts (billions of 2015\$) by degree ($^{\circ}\text{C}$) for each impact type for two socioeconomic snapshots (2010 and 2090 default scenarios). Extrapolated portions are shown with a dashed line. Note y-axis scales vary by plot.

Processing steps

Processing steps are shown in **Figure B-57**.

Pre-processing: Total learning loss for each scenario, year, GCM, and county were provided by the Children's Health Report authors. First, baseline damages (e.g. no climate change loss) are subtracted from the annual projections to compute net learning loss projected with climate change. Next, the net lost future earnings are summarized at the state level, by year, adaptation scenario, and GCM. Losses are divided by state-level population of high school students (14 to 17-year-olds, from ICLUSv2) to calculate lost earnings per student as the first impact type. The proactive adaptation scenario results, which were not estimated in the Children's Health Report, use results from Park et al. (2020) on the impact of school A/C in mitigating learning loss – all other steps in estimating the per student learning loss remain the same as in the no additional adaptation scenario.

The second impact type, adaptation cost, is applied to proactive adaptation, and includes the per student A/C cost. A/C costs are processed by converting the projected data from LeRoy et al. (2021) (e.g., total costs by state and total number of schools with A/C for future two eras) to incremental costs per student per degree of warming for each state. As part of FrEDI pre-processing, annual cost estimates are developed from the LeRoy et al. (2021) era-level results by interpolating the costs to a full annual series of projected costs and weighing the within-era annual trajectory by provided data on the annual and incremental number of schools that install A/C within the 30-year period around each projected year.⁹⁸ Estimates of number of schools with A/C and associated costs are then extrapolated to the year 2100 and then to six degrees of warming using the slope of each cost type between 2.5 and 3 degrees Celsius of warming.⁹⁹ The extrapolation of installation and upgrade costs is capped at the point at which the state reaches 100% A/C adoption (i.e., all schools within the state have installed or upgraded A/C), and do not account for the potential need for future replacement at the end of the A/C capital useful life (in part because it is not clear whether operating and maintenance costs incorporate a financial component for gradual replacement of capital). Therefore, operating and maintenance costs account for most of the total costs by six degrees of warming. Annual results are binned using the 11-year average around the degree of warming arrival years of the standard CIRA GCM set, then divided by the total number of students in the state to result in the per student by degree costs to be added to damages of learning loss in the proactive adaptation scenario.

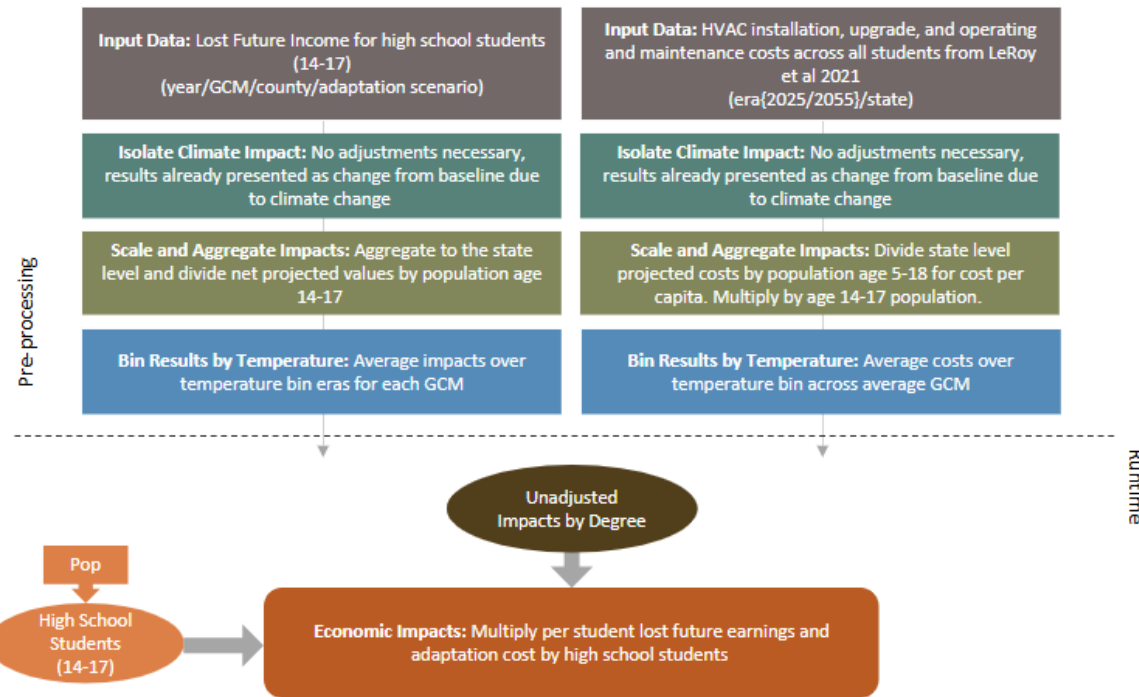
Finally, the data is temperature binned by averaging projections of annual future income lost and A/C costs across the time periods where each of the GCMs used in the underlying study reach integer degrees of CONUS warming relative to the baseline. We also calculate a scalar using the ICLUSv2 population data by

⁹⁸ Installation and upgrade costs interpreted as the total investment between 2010 and 2039 (for year 2025) and 2010 and 2069 (for 2055). 2025 estimates are subtracted from 2055 to identify the costs incurred from 2040-2069.

⁹⁹ LeRoy et al. (2021) climate projections use RCP 4.5, which reaches 3° C of warming by 2100. We extrapolate to 6° C of warming by taking the slope of each cost between 2.5 and 3° C and adding to the costs at 3° C. In addition, LeRoy et al. (2021) did not provide estimates for New Hampshire or Vermont schools. For these states, we used per student costs for Maine by year and the number of school age children for NH and VT to infer A/C installation costs for these two states.

state and year that represents the percentage of total population that is 14-17 years-old for use within FrEDI to adjust user population inputs to the relevant population for this sector.

FIGURE B-57. HEAT AND LEARNING DATA PROCESSING FRAMEWORK



Runtime: When FrEDI is run, the pre-processed by-degree learning losses and A/C costs per student functions are applied to the input temperature scenario to calculate the unadjusted annual future income lost per student, based on the level of warming in each year of the input scenario. The total learning loss and A/C cost are calculated by applying these annual rates to the number of high school students in each state (the proportion of population in high school multiplied by total population, by state and year).

Limitations and Assumptions

- This analysis focuses on future learning losses caused by heat and does not consider the potential effects of cold weather. As Park et al. (2020) found no evidence that extreme cold impacts learning, all estimates in this study exclude any learning losses that could be attributed to cold temperatures.
- This study employs predefined adaptation scenarios rather than accounting for the variability and nuances of real-world adaptation, where responses to extreme heat and air conditioning usage might fall between these scenarios. It does not model optimal adaptation behaviors, where individuals dynamically adjust to daily occurrences of extreme heat. Instead, it simulates two distinct and fixed adaptation scenarios to explore potential outcomes under different levels of adaptation.
- School calendars vary significantly across the country, so this analysis uses start and end dates provided by the study authors to align the date range with local school schedules, ensuring that only time spent in school is considered. This assumes school calendars will remain unchanged in the future.
- For further discussion of the underlying model, see Park et al. (2020), LeRoy et al. (2021), and EPA (2023).

B.7 Agriculture Sector

CIL Agriculture

Summary

This sector estimates the impact of climate change on agricultural yields of key crops across all of CONUS. The Climate Impact Lab (CIL) Agriculture projections are drawn from functions estimating the effects of changes in temperature, precipitation, and CO₂ fertilization on yields of cotton, maize, soybean, and wheat. Temperature and precipitation response functions for wheat are based on research from Hsiang et al. (2013), and functions for cotton, maize, and soybean are drawn from Schlenker and Roberts (2009). CO₂ fertilization response functions for all four crops are based on estimates from McGrath and Lobell (2013).¹⁰⁰

UNDERLYING DATA SOURCES AND LITERATURE

Hsiang, S., Kopp, R., Jina, A., Rising, J., Delgado, M., Mohan, S., Rasmussen, D.J., Muir-Wood, R., Wilson, P., Oppenheimer, M., Larsen, K., and Houser T. (2017). Estimating economic damage from climate change in the United States, *Science*, 356, 1362–1369. <https://doi.org/10.1126/science.aal4369>

Hsiang, S., Lobell, D., Roberts, M., and Schlenker, W. (2013). Climate and Crop Yields in Australia, Brazil, China, Europe and the United States. <https://doi.org/10.2139/ssrn.2977571>

McGrath, J.M. and Lobell, D.B. (2013). ‘Regional disparities in the CO₂ fertilization effect and implications for crop yields’, *Environ. Res. Lett.*, 8, 014054. <https://doi.org/10.1088/1748-9326/8/1/014054>

Schlenker, W. and Roberts, M.J. (2009). ‘Nonlinear temperature effects indicate severe damages to U.S. crop yields under climate change’, *Proc. Natl. Acad. Sci. U.S.A.*, 106, 15594–15598. <https://doi.org/10.1073/pnas.0906865106>

USDA NASS Quick Stats. <https://quickstats.nass.usda.gov/>

Hsiang et al. (2017) use these functions to project future impacts on yields by GCM and RCP through the 21st century. Economic damages are based on changes from regional baseline production value averaged over 1990-2000 drawn from the USDA National Agricultural Statistics Service’s (NASS) Quick Stats database. The currently available results include adaptation strategies only to the extent that they have been previously implemented in the study area. We anticipate that future revisions of FrEDI may incorporate a “with adaptation” variant that includes modelling of future adaptation behaviors and technologies specifically for maize.

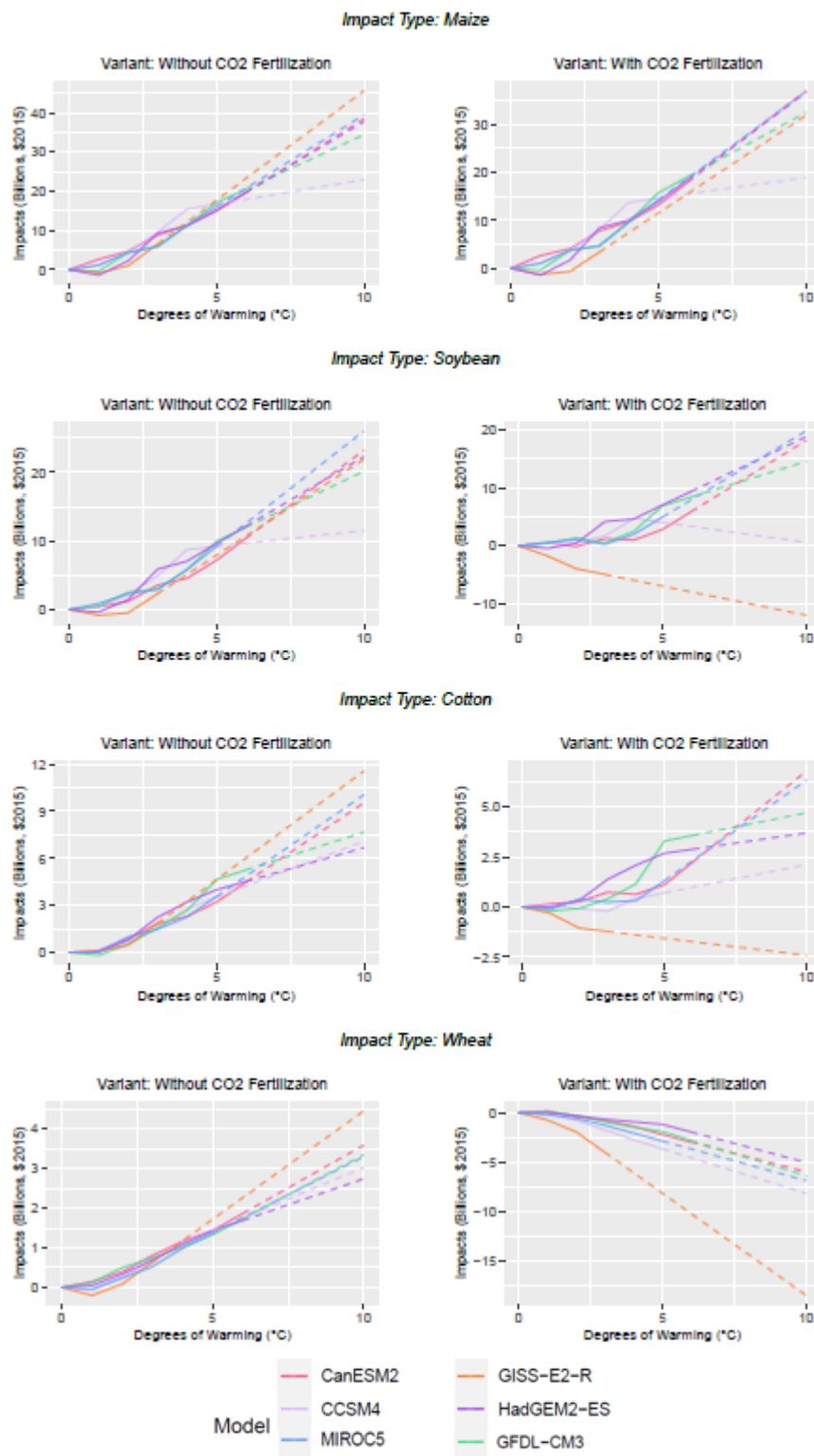
TABLE B-30. INCOMING DATA CHARACTERISTICS: CIL AGRICULTURE

Data Features	CIL Agriculture Attributes
Evaluated Impacts	<ul style="list-style-type: none"> • Lost production value (economic)
Variants	<ul style="list-style-type: none"> • With CO₂ Fertilization • Without CO₂ Fertilization
Data Shape	<ul style="list-style-type: none"> • Annual • Two variants • Four impact types • Six CMIP5 GCMs (standard CIRA set)

¹⁰⁰ The online version of McGrath and Lobell (2013) includes a link to Rosenthal and Tomeo (2013) and implies that Rosenthal and Tomeo “corrects” McGrath and Lobell (2013). In fact Rosenthal and Tomeo (2013) is a complementary Perspective (commentary) article to McGrath and Lobell (2013), and does not provide any results.

Data Features	CIL Agriculture Attributes
Model Type	<ul style="list-style-type: none">• State level• Empirical
Runs Provided	<ul style="list-style-type: none">• With climate change
Additional Data	<ul style="list-style-type: none">• Baseline production values
Regions and States with Impacts	<ul style="list-style-type: none">• Midwest• Northeast (excluding CT, DC, ME, MA, NH, RI, VT)• Northern Plains• Northwest• Southeast• Southern Plains• Southwest

For illustrative purposes, **Figure B-58** shows the resulting damages by degree of warming for each impact type and for both variants (left and right plots), by GCM.

FIGURE B-58. CIL AGRICULTURE IMPACTS BY TEMPERATURE BIN DEGREE

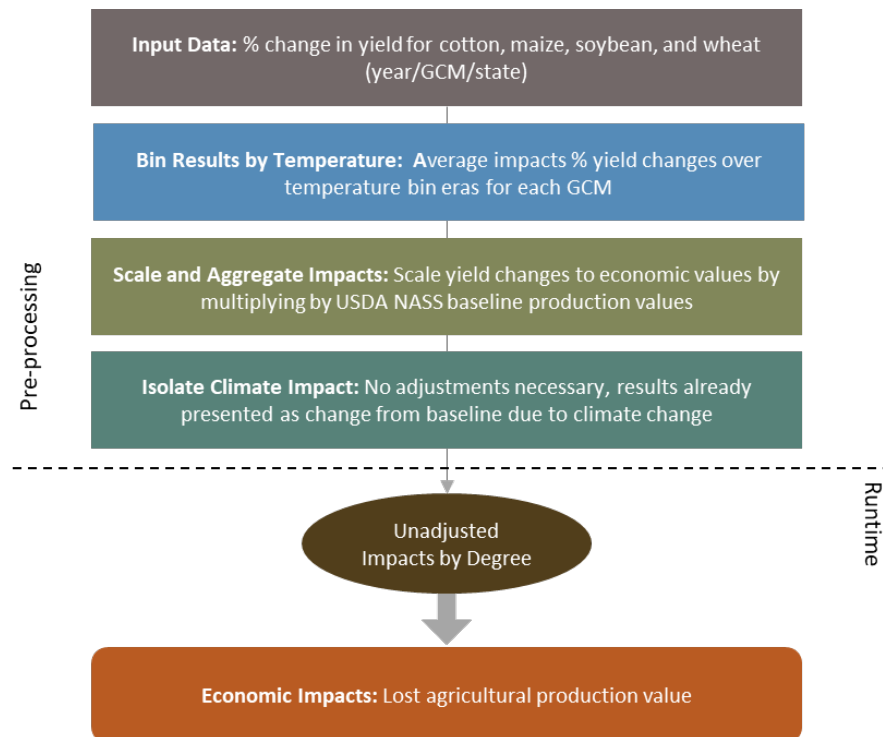
Total impacts (billions of 2015\$) by degree (°C) for each impact type and variant. Extrapolated portions are shown with a dashed line. Note y-axis scale varies by plot.

Processing steps

Processing steps are shown in **Figure B-59**.

Pre-processing: The Hsiang et al. (2017) study authors provided the percent change in yields relative to baseline for each crop under RCP8.5, by GCM, year, and state for the 2001-2099 period. The authors provided a distribution of results, but this version of FrEDI uses only the median estimates. In the first pre-processing step, the annual yield changes are binned by degree of CONUS temperature change for each GCM.¹⁰¹ In the second and final processing step, state-level percent changes in yield by degree are scaled by state-level baseline production values from USDA NASS to give economic damage estimates.

FIGURE B-59. CIL AGRICULTURE DATA PROCESSING FRAMEWORK



Runtime: When FrEDI is run, the pre-processed by-degree percent changes in production value functions are then applied to the input temperature scenario to calculate the annual percent changes in production value based on the level of warming in each year of the input scenario.

Limitations and Assumptions

- The economic impacts presented are directly proportional to the underlying physical impacts and do not incorporate market effects on price due to projected changes in supply. For this reason, we

¹⁰¹Agricultural yields are impacted by a wider set of climate variables than temperature, such as precipitation patterns, which are implicitly captured in the annual results from the underlying studies, and used in the temperature binning approach to create sectoral damage functions indexed to CONUS warming levels. See Appendix C for more discussion of non-temperature climate variables.

may underestimate future impacts. Work by Beach et al. (2015)¹⁰² suggests that climate change may cause increases in crop prices, which supports the conclusion that we underestimate impacts.

- This study takes incomplete account of the impact of future potential changes in crop technology, energy and land use policies, and other interactions that could affect market outcomes. For the most part, these important factors affecting agricultural yield are not directly tied to changes in climate but could be components of an adaptative response as climate change unfolds.
- The underlying study also omits some important aspects of climate change impacts to agriculture not directly tied to yield effects, including damages from extreme weather events, wildfire, and changes in weeds, pests, disease, and O₃ damage. Collectively, these effects would likely result in larger yield losses than those estimated here.
- For further discussion of the underlying sectoral model, please see Hsiang et al. (2017).

Forestry Loss

Summary

This sector estimates the impact of climate change on net economic welfare in the U.S. forestry sector. Baker et al. (2023) combines bottom-up estimates of forest productivity responses to climate inputs with dynamic economic modeling of the U.S. forest sector using the FASOM-GHG (Forestry and Agricultural Sector Optimization Model - Greenhouse Gas) intertemporal dynamic optimization model of the U.S. land use sectors. The forestry sector component of the FASOM model maximizes consumer and producer surplus measures and represents physical resource constraints and heterogeneity in forest productivity by site class, forest type, and region. The model yields a dynamic simulation of prices, production, management, and consumption.

Baker et al. (2023) present future consumer and producer surplus by standard CIRA GCM and Shared Socioeconomic Pathway (SSP) to consider multiple climate and socioeconomic futures. Between the SSP2

UNDERLYING DATA SOURCES AND LITERATURE

Baker, J. S., Van Houtven, G., Phelan, J., Latta, G., Clark, C. M., Austin, K. G., Sodiya, O. E., Ohrel, S. B., Buckley, J., Gentile, L. E., & Martinich, J. (2023). Projecting US forest management, market, and carbon sequestration responses to a high-impact climate scenario. *Forest policy and economics*, 147, 102898.

<https://doi.org/10.1016/j.forpol.2022.102898>

Hauer, M. (2021). Population projections for all U.S. counties by age, sex, and race controlled to the Shared Socioeconomic Pathways. <https://doi.org/10.17605/OSF.IO/9YNFC>

KC, S., & Lutz, W. (2014). The human core of the shared socioeconomic pathways: Population scenarios by age, sex and level of education for all countries to 2100. *Global Environmental Change*, 42, 181–192.

<https://doi.org/10.1016/j.gloenvcha.2014.06.004>

Cuaresma, J. C. (2015). Income projections for climate change research: A framework based on human capital dynamics. *Global Environmental Change*, 42, 226–236.

<https://doi.org/10.1016/j.gloenvcha.2015.02.012>

¹⁰² Beach, R., Y. Cai, A. Thomson, X. Zhang, R. Jones, B. McCarl, A. Crimmins, J. Martinich, J. Cole, and B. Boehlert, 2015: Climate change impacts on US agriculture and forestry: benefits of global climate stabilization. *Environmental Research Letters*, **10**, doi: 10.1088/1748-9326/10/9/095004.

and SSP5 variants, SSP5 represents conditions with higher income and population growth, and therefore substantially higher demands for softwood lumber (associated mainly with new housing construction).

TABLE B-31. INCOMING DATA CHARACTERISTICS: FORESTRY LOSS

Data Features	Forestry Loss Attributes
Evaluated Impacts	<ul style="list-style-type: none"> • Lost total surplus (economic)
Variants	<ul style="list-style-type: none"> • SSP2^b • SSP5^b
Data Shape	<ul style="list-style-type: none"> • 5-year periods from 2015-2095 • Six CMIP5 GCMs (standard CIRA set) • Producer Surplus: FASOM Region^a, Consumer Surplus: CONUS
Model Type	<ul style="list-style-type: none"> • Simulation
Runs Provided	<ul style="list-style-type: none"> • With socioeconomic growth and with climate change • With socioeconomic growth and without climate change
Additional Data	<ul style="list-style-type: none"> • Custom temperature trajectory • Forest productivity by ownership type^c • Mill production 1993-2023^d • Forest area cover by ownership type^e • Value added components forestry industry^f • Population projections by SSP scenario • GDP per capita projections by SSP scenario
Regions and States with Impacts	<ul style="list-style-type: none"> • All CONUS regions and states

a. The District of Columbia is not assigned a FASOM region. We include it with Maryland in the Northeast Region.

b. All SSP variants represent a 'No Additional Adaptation' scenario.

c. Oswalt, S. N., Smith, W. B., Miles, P. D., Pugh, S. A. (2019). Forest Resources of the United States, 2017: a technical document supporting the Forest Service 2020 RPA Assessment. Gen. Tech. Rep. WO-97. Washington, DC: U.S. Department of Agriculture, Forest Service, Washington Office. 223 p.

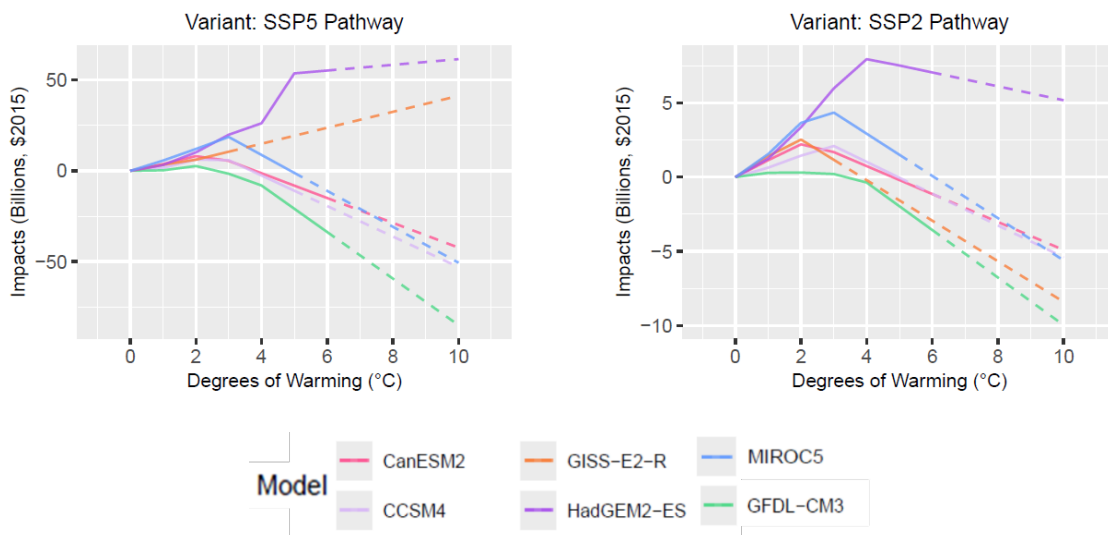
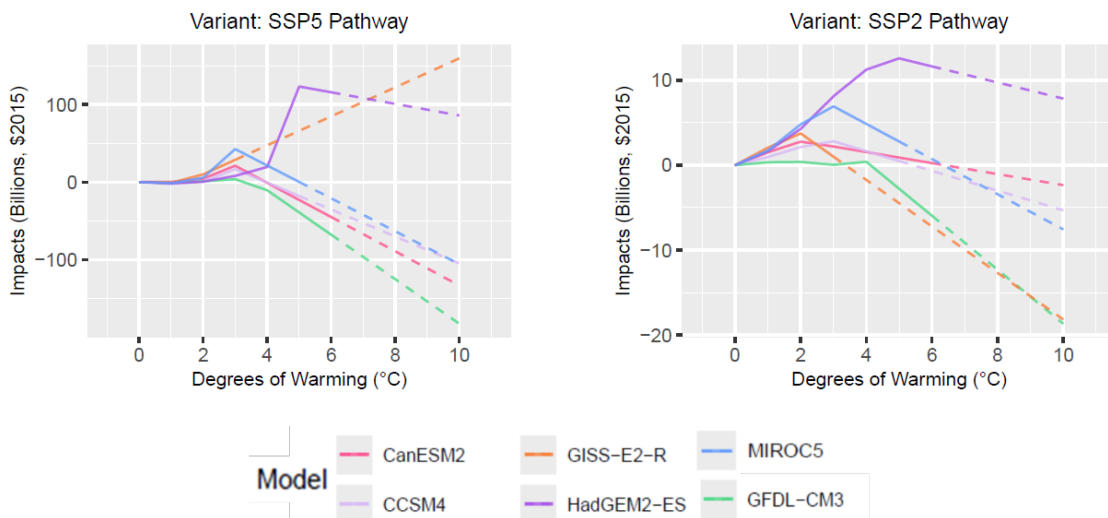
<https://doi.org/10.2737/WO-GTR-97>

d. USDA Forest Service Research and Development Branch. (2023). Timber Products Output [Dataset; Interactive Reporting Tool]. Forest Inventory and Analysis (FIA) Program. <https://research.fs.usda.gov/products/dataandtools/tools/timber-products-output-tpo-interactive-reporting-tool>

e. USDA Forest Service, FIA. (2024) Forest Inventory EVALIDator web-application, Version 2.1.2. St. Paul, MN: U.S. Department of Agriculture, Forest Service, Northern Research Station. <https://apps.fs.usda.gov/fiadb-api/evaluator>

f. Bureau of Economic Analysis (BEA), U.S. Department of Commerce. (2017). Industry Economic Accounts [Dataset]. BEA.

For illustrative purposes, **Figure B-60** shows the resulting damages by degree of warming for both variants (left and right plots), by GCM.

FIGURE B-60. FORESTRY IMPACTS BY TEMPERATURE BIN DEGREE**A. 2010 SOCIOECONOMICS****B. 2090 SOCIOECONOMICS**

Total impacts (billions of 2015\$) by degree (°C) for each impact type and variant. Extrapolated portions are shown with a dashed line. Note y-axis scales vary by plot.

Preprocessing Steps

Processing steps are shown in **Figure B-61**.

Pre-processing: Consumer (CS) and Producer (PS) Surplus projections were obtained from the Baker et al. (2023) authors by GCM, SSP scenario, and 5-year period. CS was provided at the CONUS level, and PS was provided at the FASOM Region level (i.e., regions that together make up CONUS). A no climate change baseline scenario was provided alongside the six GCMs for each SSP and 5-year period.

First, the 5-year estimates of CS and PS are interpolated to produce an annual trajectory from 2015-2095 and extrapolated for the full range of required years¹⁰³ and CS and PS are disaggregated to the state level. CS is disaggregated from CONUS to state using SSP-specific projections of population at the state level from Hauer (2021).¹⁰⁴ PS, is provided by FASOM Region (which do not align directly with state boundaries), therefore, PS is disaggregated to the county level and re-aggregated to the state level. Disaggregation to the county level is based on a set allocation weights that account for county-level processing capacity and forest supply (70% and 30% of the allocation weight, respectively, based on processing and timber supply contributions to total value added from BEA (2017)).

- Mill Capacity (70% of the allocation weight): A county's share of total FASOM Region mill production determines its processing weight. Mill production by county is determined as the annual average mill production by county from the Timber Products Output (TPO) survey data from USDA Forest Service Research and Development Branch (2023).¹⁰⁵
- Forest Supply (30% of the allocation weight): A county's share of total FASOM Region forest supply determines its supply weight. Forest supply is determined by the ratio of timber supplied to total forest area (forest productivity) by ownership type (public or private) and Resource Planning Act (RPA) region from Oswalt et al. (2019), and forest area cover by county and ownership type from USDA Forest Service (2024). Forest productivity is converted from RPA region to FASOM region and multiplied by forest area cover to give forest supply by county and ownership type. County-level forest supply is combined across ownership types.

Using the combined supply-processing weight, PS is disaggregated to the county level and aggregated to the state level. At the state level, PS and CS are combined to determine total surplus by state, climate scenario, and SSP scenario. Total surplus is divided by SSP-specific GDP per capita projections, used in Baker et al. (2023), to isolate changes in surplus from socioeconomic growth.¹⁰⁶ Net surplus is determined by subtracting GCM-specific surplus from no climate change surplus in the same year within an SSP scenario. To further isolate the effects of climate, within an SSP scenario, net surplus is divided by the percent change in the no climate scenario in year x from 2015 to form scaled impacts, which the Baker et al. (2023) authors consider the projection base period. This ratio forms the variant, or SSP-specific, damage adjustment scalar.

¹⁰³ Temperature binning required estimates for 2013-2098. Extrapolation to earlier before 2015 is defined such that the with and without climate change scenarios are equal in the baseline year (1995) for each SSP, GCM, and county. Years after 2095 are extrapolated by extending the rate of change observed in 2090 to 2095.

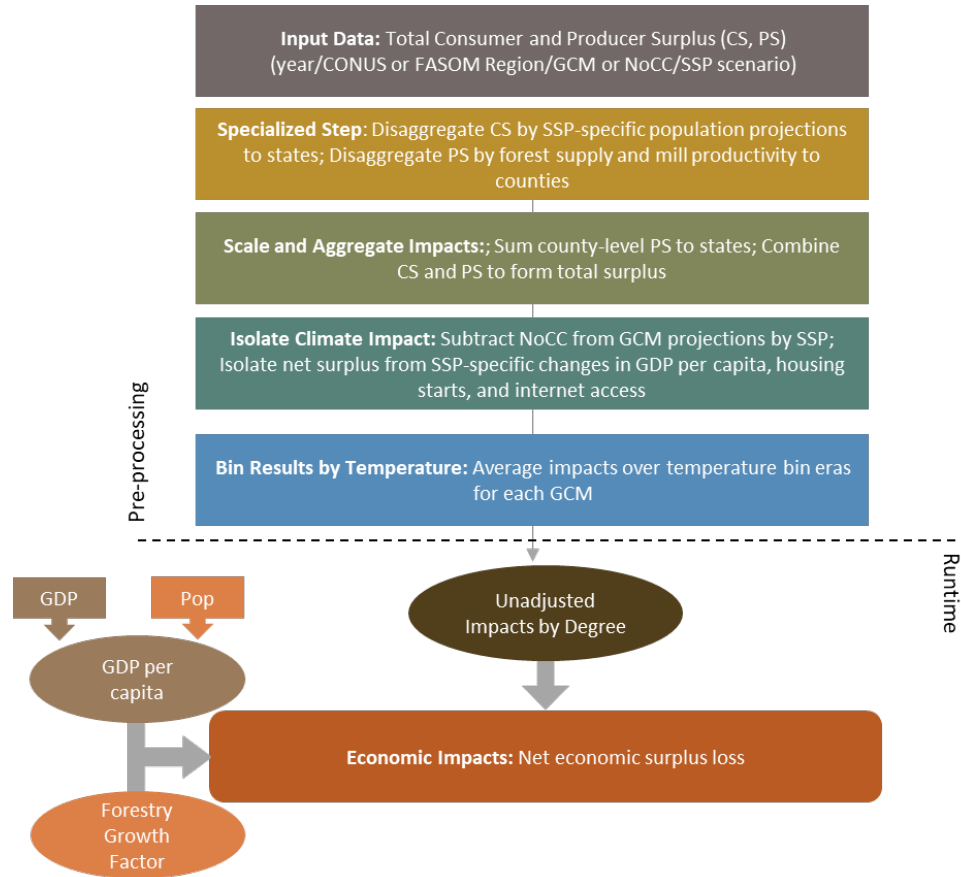
¹⁰⁴ Population projections span 2020-2100 in 10-year periods, so intermediate years are estimated by interpolating. Years before 2020 are estimated by interpolating between 2020 projections from Hauer (2021) and 2010 Census populations

¹⁰⁵ The TPO database is built on an annual survey of timber mills from 1993-2023, which does not include every mill in every year. Instead, each county's average production across each year of its survey inclusion is considered.

¹⁰⁶ GDP and population projections are from Cuaresma (2015) and KC & Lutz (2014) respectively. Both projections are reported by the International Institute for Applied Systems Analysis (IIASA). The IIASA also hosts GDP projections from the Organization for Economic Cooperation and Development (OECD) and the Potsdam Institute for Climate Impact Research (PIK), but we choose to use projections of GDP and population from the same source (IIASA). Baker et al. (2023) does not specify which SSP-specific GDP and population projections are used.

Finally, annual SSP and state specific scaled impacts are degree binned according to a custom temperature trajectory provided by the authors of Baker et al. (2023). To capture periods of high variance late in the century, a half degree bin is included for all GCMs that reach an additional half degree of warming (GISS-E2-R, HadGEM2-ES, and GFDL-CM3).

FIGURE B-61. FORESTRY LOSS DATA PROCESSING FRAMEWORK



Runtime: When FrEDI is run, net economic surplus isolated from non-climate related temporal changes is combined with GDP per capita and the damage adjustment scalar.

Limitations and Assumptions

- We report a combined change in PS and CS surplus; however, each of the two components of total surplus follow very different trends over time and across SSPs. FrEDI currently does not model the two individually; however, information on the relative contribution of each to total change in surplus can be found in Baker et al. (2023).
- Economic surplus does not include a valuation of changes in carbon sequestration.
- For further discussion of the limitations and assumptions in the underlying sectoral model, see Baker et al. (2023).

APPENDIX C | IMPACTS-BY-DEGREE AND TEMPERATURE BINNING METHODOLOGY

This appendix provides additional detail on the impacts-by-degree and temperature binning approaches that form the basis of the FrEDI framework (C.1), sensitivities of some of the underlying assumptions (C.2), and a discussion of CMIP6 GCMs (C.3).

C.1 Impacts-By-Degree

An ‘impacts-by-degree’ approach quantifies climate-related impacts as a function of future warming. By providing impact estimates for a given amount of warming, regardless of when the warming occurred or which climate model or scenario was used to develop the estimate, the ‘by-degree’ approach allows for increased comparability between independent climate impact studies and flexibility to facilitate custom scenario analysis. This complements more traditional scenario-based approaches, which instead quantify future climate change impacts associated with a specific set of emissions or concentration scenarios. The impacts-by-degree approach has been widely used in previous scientific assessments for quantifying and communicating impacts at distinct levels of warming, including by the National Research Council (NRC) Climate Stabilization Targets assessment¹⁰⁷, IPCC 1.5 degree assessment¹⁰⁸, and 5th U.S. NCA¹⁰⁹.

In FrEDI, by-degree damage functions are used to relate sectoral impacts to integer degrees of warming at the CONUS level. Average CONUS warming (as compared to average warming at the global level) was chosen, because domestic impacts will be more directly related to local temperatures. While average CONUS warming is used as the climate-driver within FrEDI, the impacts data from the underlying studies are associated with a much richer set of climate variables and greater spatial variation. Therefore, while each damage function is indexed to specific degrees of CONUS warming, the total impacts to each sector will also account for changes in precipitation, extreme heat days, freeze/thaw patterns, temperature patterns, and other climate variables present in and specific to the GCMs used in each sectoral impact study. As an example of these patterns, **Figure C-1** shows the spatial variation in annual average temperature (panel A) and percent change in precipitation (panel B) at 2° C of CONUS warming relative to the 1986-2005 FrEDI baseline across the six GCMs from the 5th Coupled Model Intercomparison Project (CMIP5). The limitation of this approach is that these patterns in climate variables and how they relate to

¹⁰⁷ National Research Council (2011) Climate stabilization targets: emissions, concentrations, and impacts over decades to millennia. The National Academies Press, Washington, DC. <https://doi.org/10.17226/12877>

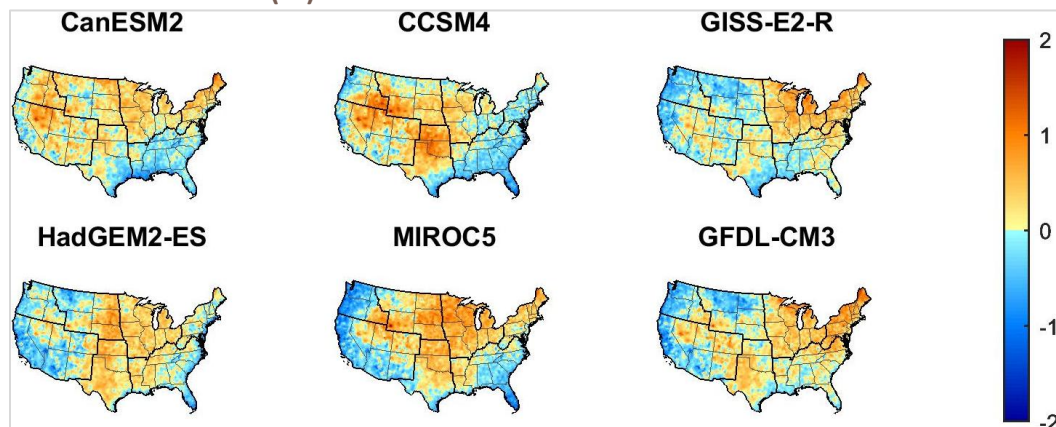
¹⁰⁸ IPCC (2018) Summary for policymakers. In: Masson-Delmotte V, Zhai P, Pörtner H-O, Roberts D, Skea J, Shukla PR, Pirani A, Moufouma-Okia W, Péan C, Pidcock R, Connors S, Matthews JBR, Chen Y, Zhou X, Gomis MI, Lonnoy E, Maycock T, Tignor M, Waterfield T (eds) Global warming of 1.5°C. An IPCC Special Report on the impacts of global warming of 1.5°C above pre-industrial levels and related global greenhouse gas emission pathways, in the context of strengthening the global response to the threat of climate change, sustainable development, and efforts to eradicate poverty. World Meteorological Organization, Geneva, Switzerland, p 32

¹⁰⁹ USGCRP, 2023: Fifth National Climate Assessment. Crimmins, A.R., C.W. Avery, D.R. Easterling, K.E. Kunkel, B.C. Stewart, and T.K. Maycock, Eds. U.S. Global Change Research Program, Washington, DC, USA.

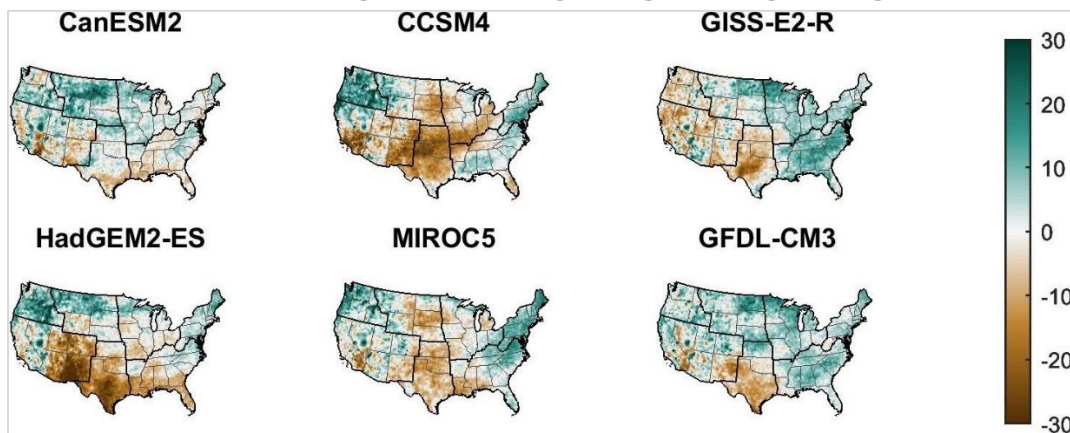
average CONUS warming are specific to each GCM. This could have implications for the resulting sectoral impacts if the user provides input data derived from a scenario or from a GCM that has, for example, a different distribution of precipitation across states or a different distribution of extreme high and low temperature days than the GCMs that were considered in the studies used to develop the impact functions.

FIGURE C-1. GRIDDED TEMPERATURE AND PRECIPITATION PATTERNS AT TWO DEGREES OF WARMING

A. DIFFERENCE IN TEMPERATURE (°C)



B. PERCENT DIFFERENCE IN TOTAL PRECIPITATION



Maps of the spatial patterns of climate changes at 2°C of warming. The upper six maps show the difference between a homogeneous 2°C CONUS temperature change and the actual mean temperature change projected by the six CMIP5 models used across a number of underlying sectoral impact models in the 11-year temperature bin at 1/16th degree. The lower six maps show the percentage change in precipitation during the 11-year binning window relative to the historical period (1986–2005) for the six models. Seasonal patterns may differ from the 11-year mean.

To develop these types of damage functions, ‘Temperature Binning’ is the process of translating annual climate change impact data into an impacts-by-degree framework (Sarofim et al., 2021).¹¹⁰ In this Documentation, ‘temperature binning’ specifically refers to the process of averaging projections of annual sectoral impact data from each of the underlying studies across the time period where each of the underlying GCMs reach integer degrees of CONUS warming relative to the baseline. The main purpose of

¹¹⁰ Sarofim, M. C., Martinich, J., Neumann, J. E., Willwerth, J., Kerrich, Z., Kolian, M., ... & Hartin, C. (2021). A temperature binning approach for multi-sector climate impact analysis. Climatic change, 165(1), 22.

using binning windows rather than a single year is to smooth out interannual variability. This is like the time-shift approach of Tebaldi et al. (2020) and the time-slice approach of Schleussner et al. (2016).¹¹¹

In FrEDI, an 11-year window is selected for each temperature ‘bin’ or ‘era’ as a way to balance between smoothing out interannual variability in the climate projections and keeping the windows small enough that all years within the window are representative of each degree of warming (see sensitivity analysis below). Shorter windows have increased noise from year-to-year temperature variability, however, longer windows, such as 30-year periods that are often used to establish a climatology, would cause inconsistencies near the end or the beginning of the timeseries. For example, the first degree of warming is often within the first 10 years of the projection and could not be captured with a 30-year window. In addition, since the average impacts across all years in the defined window are attributed to the integer degree of warming, the longer the window, the larger the potential difference between the impacts across these years. Therefore, a window that is too large could also cause a bias in the average impact assigned to the degree of warming if the impacts don’t scale linearly with temperature in the underlying data. An 11-year window is chosen to keep the window relatively tight to minimize these potential impacts.

As an illustration of these temperature ‘bins’, **Figure C-2** shows an example of the 11-year window (and the central ‘arrival’ year) where different CMIP5 GCM’s reach 1 to 6° C of CONUS warming under an example RCP8.5 scenario. The models shown are the six CMIP5 GCMs that are used in many of FrEDI’s underlying sectoral impact studies. For example, the GFDL-CM3 model is projected to reach 2° C of CONUS warming between 2027 and 2037 (centered on 2032) and 6° C between 2082 and 2092 (centered on 2087). In contrast, the GISS-E2-R model is only projected to reach 3° C of warming before 2090.

FIGURE C-2. INTEGER DEGREE ARRIVAL WINDOWS AND YEARS FOR SIX CMIP5 GCMS

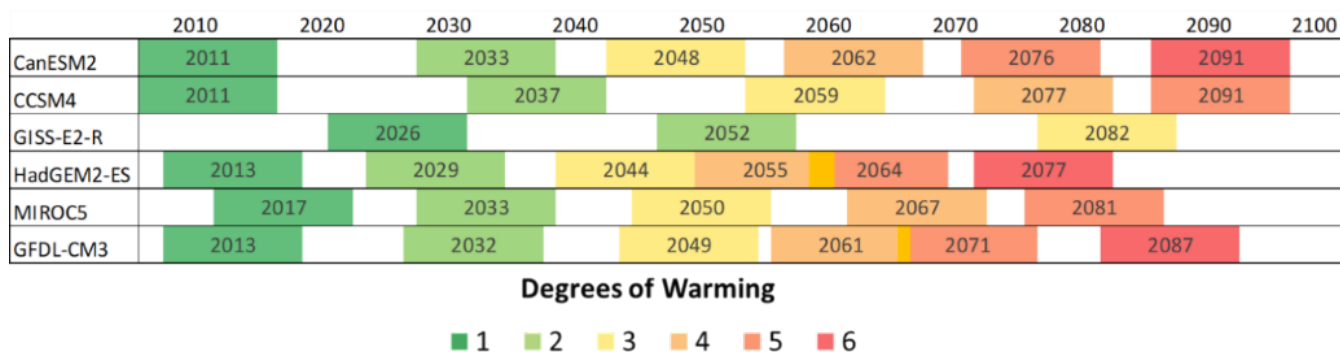
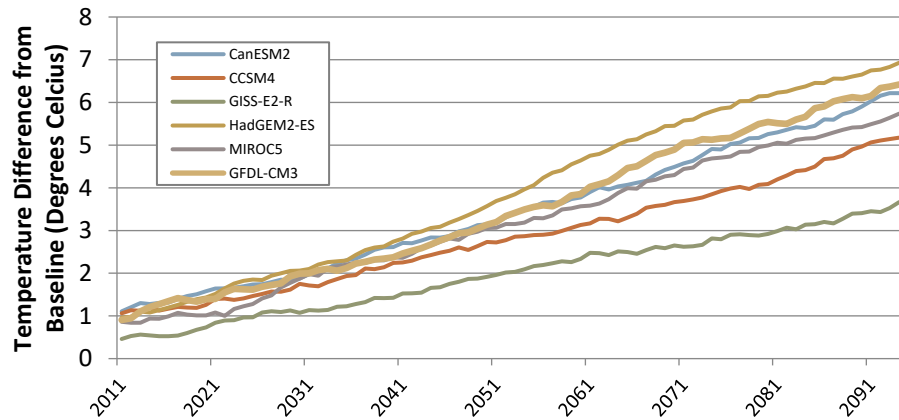


Illustration of arrival windows of each integer CONUS degree of warming for RCP8.5 in six CMIP5 GCMs. Arrival years, or the year at which the 11-year moving average reaches the given integer, are listed in each bin. The six CMIP5 represent many of the studies included within FrEDI. Figure reproduced from Sarofim et al., 2021.

¹¹¹ Tebaldi, C., Armbruster, A., Engler, H. P., & Link, R. (2020). Emulating climate extreme indices. *Environmental Research Letters*, 15(7), 074006 and Schleussner, C. F., Lissner, T. K., Fischer, E. M., Wohland, J., Perrette, M., Golly, A., ... & Schaeffer, M. (2016). Differential climate impacts for policy-relevant limits to global warming: the case of 1.5 C and 2 C. *Earth system dynamics*, 7(2), 327-351.

As an additional example, **Figure C-3** shows a time series of these same arrival times as an 11-year moving average of the CONUS temperature change relative to the 1986-2005 baseline.

FIGURE C-3. CONUS DEGREES OF WARMING WITH 11-YEAR MOVING AVERAGE



Annual degrees of warming (C) from 1986-2005 average baseline for CONUS after an 11-year moving average is applied.

To investigate the sensitivity of the arrival year to the choice of an 11-year moving average, as opposed to a shorter or longer period, the following tables indicate how the arrival years would differ for a 5-year window (**Table C-1**) or a 15-year window (**Table C-2**). As shown, in most cases, arrival years only differ by one to three years and differences are greater for the 5-year window than the 15-year window.

TABLE C-1. DIFFERENCE IN ARRIVAL TIMES FOR A 5-YEAR WINDOW

Differences between arrival times (years) if a 5-year window is used compared to an 11-year window.

GCM (CMIP5)	Difference between arrival times for a 5-year window (years)					
	1 Deg	2 Deg	3 Deg	4 Deg	5 Deg	6 Deg
CanESM2	2	1	0	3	1	1
CCSM4	2	1	3	2	1	N/A
GISS-E2-R	3	1	3	N/A	N/A	N/A
HadGEM2-ES	1	3	1	1	0	1
MIROC5	3	3	1	0	0	0
GFDL-CM3	1	3	0	1	3	1

TABLE C-2. DIFFERENCE IN ARRIVAL TIMES FOR A 15-YEAR WINDOW

Differences between arrival times (years) if a 15-year window is used compared to an 11-year window.

GCM (CMIP5)	Difference between arrival times for a 15-year window (years)					
	1 Deg	2 Deg	3 Deg	4 Deg	5 Deg	6 Deg
CanESM2	2	2	1	2	1	0
CCSM4	2	0	1	0	0	N/A
GISS-E2-R	1	0	0	N/A	N/A	N/A
HadGEM2-ES	0	0	0	0	1	0
MIROC5	2	0	0	1	0	N/A
GFDL-CM3	0	0	0	0	2	1

In FrEDI, as described in Appendix B, temperature binning is applied in the pre-processing stages of the FrEDI framework (i.e., listed as ‘Bin Results by Temperature’ in Appendix B flow diagrams) to derive the GCM and state-specific ‘by-degree’ damage functions from the time series of impact data from each underlying sectoral study. These functions are created by determining the average impacts (from each GCM and in each state) that are associated with the arrival window where the GCMs used in the underlying study reaches each integer degree of CONUS warming (via an 11-year moving average). During runtime, FrEDI calculates impacts using each of the GCM-specific damage functions, which users can then average during post-processing. If users are instead interested in results from a subset of GCMs with specific climate patterns or warming level, users could alternatively select FrEDI results based on that subset of GCMs. For example, if there is interest in the implications of a relatively wet future, an analysis using the CMIP5 CanESM2 GCM, the wettest of the ensemble, could provide insights.

Additional background on the temperature binning methodology can be found in Sarofim et al. (2021).

C.1 Sensitivity to GHG emissions scenarios

Related to the discussion above, patterns of climate variables (such as temperature and precipitation) and other non-climate stressors are implicitly accounted for in the by-degree CONUS damage functions. However, these patterns vary by GCM and may also vary across different climate scenarios (e.g., RCPs or SSPs). As the underlying studies used to derive damage functions within FrEDI are typically based on results from a small number of GHG emission scenarios, it is important to understand the sensitivity of the estimated impacts to this process of calibrating the damage function to a single scenario—i.e., would the impacts at each degree of warming be significantly different if derived from two different GHG emissions scenarios? For example, there could be potential bias in the damage function calibration approach because

of the land-sea warming differences between higher and lower GHG scenarios or other potential differences (Herger et al. 2015).¹¹²

To test this sensitivity of the damage function calibration, the remainder of this section presents impact function data derived from the RCP8.5 scenario compared to data derived from the RCP4.5 scenario, which is a lower emissions alternative to RCP8.5.

First, **Table C-3** shows the difference in arrival years between the two RCP scenarios for each GCM. As anticipated, each of the select CMIP5 GCMs reach 1 degree of warming in similar years for the two RCP scenarios, but the arrival years start to diverge at higher levels of warming. For example, the CanESM2 model does not warm more than 3°C by the end of the century under the RCP4.5 scenario (compared to the 6°C of warming in RCP8.5), and the arrival year for 3°C is also much later (2067 vs. 20480). Differences in arrival years between the RCP scenarios for each GCM are expected, and the assumption underlying the temperature binning approach is that the projected impacts at each degree of warming (e.g., 3°C) are similar in each GCM, regardless of the input scenario.

TABLE C-3. ARRIVAL YEARS OF CONUS INTEGERS OF WARMING, BY GCM AND GHG EMISSIONS SCENARIO

Arrival years (i.e. the year in which the 11-year average CONUS temperature reaches integers of warming compared to the 1986-2005 baseline period) through 2100. 2095 is the last possible arrival year due to the 11-year window (2090-2100).

GCM (CMIP5)	RCP	Degrees of Warming (°C, CONUS)					
		1	2	3	4	5	6
CanESM2	4.5	2013	2029	2067	-	-	-
	8.5	2011	2033	2048	2062	2076	2091
CCSM4	4.5	2046	-	-	-	-	-
	8.5	2011	2037	2059	2077	2091	-
GISS-E2-R	4.5	2038	-	-	-	-	-
	8.5	2026	2052	2082	-	-	-
HadGEM2-ES	4.5	2015	2037	2052	-	-	-
	8.5	2013	2029	2044	2055	2064	2077
MIROC5	4.5	2012	2037	2079	-	-	-
	8.5	2017	2033	2050	2067	2081	-
GFDL-CM3	4.5	2017	2029	2055	-	-	-
	8.5	2013	2032	2049	2061	2071	2087

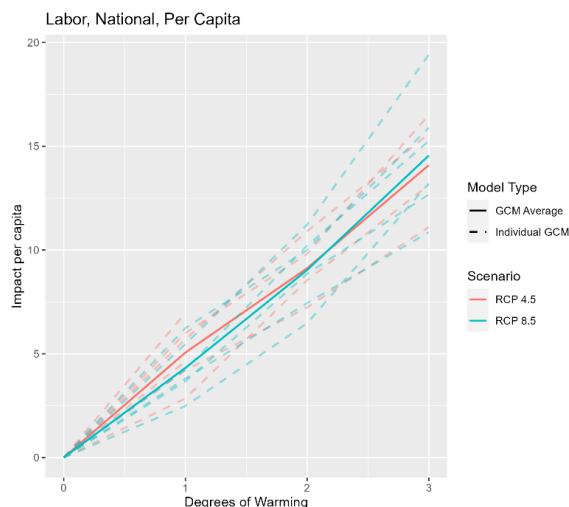
To test this underlying assumption, **Figure C-4** and **Figure C-5** show the by-degree damage functions by GCM and RCP for the FrEDI Labor and Roads sectors. These specific sectors were chosen because the original underlying studies included impact results associated with both the RCP4.5 and RCP8.5 scenarios. These sectors also cover multiple underlying damage mechanisms. For example, the impacts in the Labor

¹¹² Herger, N., B. M. Sanderson, and R. Knutti (2015), Improved pattern scaling approaches for the use in climate impact studies, *Geophys. Res. Lett.*, 42, 3486–3494, doi:10.1002/2015GL063569

sector are largely driven by changes in temperature, while the impacts in the Roads sector are implicitly related to both temperature and precipitation changes.

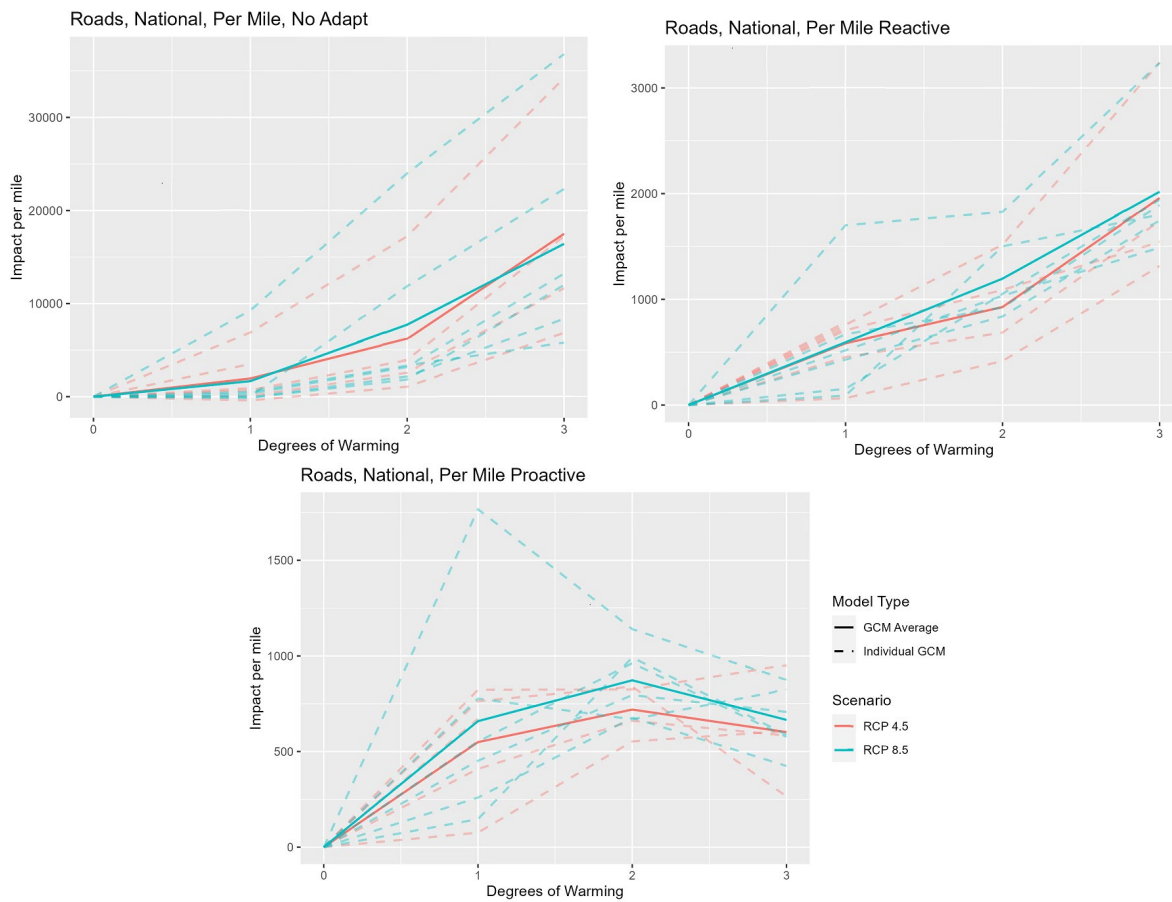
This comparison is run through 3° C of warming, which is the maximum level of warming reached this century in RCP4.5. These figures show that while there is some variation between the functions within this temperature range, there is no clear directional bias that would suggest that damage functions derived from annual impact data based on the RCP8.5 scenario would systematically result in higher (or lower) impacts compared to those based on RCP4.5 data. For example, the RCP4.5-based damage function (averaged across GCMs) is larger than the RCP8.5-based function up to 2° C of warming for Labor, as well as above temperatures of 2.6° C for Roads (no additional adaptation variant). In addition, the magnitude of variation across GCMs for each RCP is larger than the variation across RCPs for each GCM, indicating that in the range of temperature where warming levels overlap (i.e., 0-3° C), the process of deriving impact-by-degree damage functions using a temperature binning approach is robust to the GHG emissions scenario used in the underlying study. This result is generally consistent with previous external studies that also found the sensitivity to GHG emission scenarios is lower than other sources of uncertainty. For example, Tibaldi et al., 2020 showed that the “time-shift” approach (similar to temperature binning) had emulation errors smaller than the natural variability of the models across many key metrics.¹¹³

FIGURE C-4. LABOR SECTOR IMPACT BY DEGREE FUNCTION COMPARISON: RCP8.5 VS. RCP4.5



Impacts by degree functions for the Labor sector using results generated in the underlying study under RCP4.5 (red) vs RCP8.5 (blue), for six CMIP5 GCMs. GCM averages represented by solid lines.

¹¹³ Tebaldi, C., Armbruster, A., Engler, H. P., & Link, R. (2020). Emulating climate extreme indices. Environmental Research Letters, 15(7), 074006.

FIGURE C-5. ROADS SECTOR IMPACT BY DEGREE FUNCTION COMPARISON: RCP8.5 VS RCP4.5

Impacts by degree functions for the Roads sector using results generated in the underlying study under RCP4.5 (red) vs RCP8.5 (blue), for six CMIP5 GCMs. GCM averages represented by solid lines.

C.2 Sensitivity to GCM selection and CMIP6 Recommendations

As described in the previous section, many of the studies underlying the FrEDI impact functions (published before 2023) rely on data from CMIP5 GCMs. As detailed in the 2017 CIRA report appendix¹¹⁴, five CMIP5 GCMs were selected (with a sixth added later), based on their availability of downscaled data, their span of temperature and precipitation trends within the United States, their independence from each other, and measures of their quality. Not all studies underlying FrEDI, however, have used data from the same CMIP5 GCMs. For example, the climate-driven air quality impact analysis from Fann et al., (2021)¹¹⁵ relied on two different CMIP5 GCMs, which were selected because they had previously been dynamically downscaled for use in the atmospheric chemistry impact model. In addition, new impact studies incorporated into future version of FrEDI will likely be based on the more recent CMIP6 GCM data.

¹¹⁴ https://www.epa.gov/sites/default/files/2021-03/documents/cira2.0_technicalappendixfornc4.pdf section A.4.1.

¹¹⁵ Fann NL, Nolte CG, Sarofim MC, Martinich J, Nassikas NJ. Associations Between Simulated Future Changes in Climate, Air Quality, and Human Health. *JAMA Netw Open*. 2021;4(1):e2032064. doi:10.1001/jamanetworkopen.2020.32064

There are currently several dozen GCMs developed and maintained by government and academic institutions around the world. Each GCM uses different mechanisms and parameterizations to represent the climate system. While the FrEDI by-degree framework allows for the flexible incorporation of impact analyses based on any GCM, there are still distinct advantages to relying on a consistent set of GCMs. For example, the use of consistent GCMs enables the sum of impacts across impact categories within a single model, economies of scale (e.g., if a research group has already downloaded and worked with a given GCM's data), and clear communication of results (such as the 2017 CIRA report). Therefore, the question arises as to which (and how many) GCMs should be used to inform a single climate impact analysis project.

Key considerations for GCM selection include:

- model quality
- model independence
- availability of models in key downscaling datasets¹¹⁶

As described in this section, we conducted a meta-analysis of available GCM data to inform a selection of recommended CMIP6 GCMs for future impact studies. We recommend the following seven CMIP6 GCMs for use in future analyses of climate-driven impacts to the U.S.:

- GFDL-ESM4
- ACCESS-CM2
- MPI-ESM1-2-HR
- NorESM2-MM
- EC-Earth3-Veg
- MRI-ESM2-0
- BCC-CSM2-MR

In addition to these seven GCMs, the FGOALS-f3-L and GISS-E2-1-G models also meet the criteria for quality and independence, but not the availability of downscaled data. For many models, multiple ensemble members with different starting conditions are also available - for consistency, we recommend selecting the first ensemble member (r1i1p1f1).

GCM Selection Criteria Details

First and foremost, researchers should use the GCMs best suited for their purpose. However, if there are no strong differentiating factors between GCMs for a given analysis, the criteria discussed here will aid in selecting GCMs that are generally of good quality, independent from each other, and available in the most used statistical downscaling datasets (see downscaling section below).

Quality

To assess GCM quality, we conducted a review of the peer-reviewed literature, published as of March 2025, that analyzed the ability of multiple CMIP6 GCMs to reproduce historical observed data at either

¹¹⁶ The temporal frequency and spatial resolution of GCM projections will vary depending on the application and may need to be downscaled to a higher resolution to more appropriately capture the resulting impacts.

the global or U.S./North American scale. Eight studies were identified and are listed in **Table C-4**, along with a summary of the geographic scope of the comparison, comparison metrics, and number of GCMs considered in each. These studies each evaluated anywhere between 12 and 37 different GCMs, with a total of 50 unique GCMs being analyzed by at least one study. All studies limited the pool of GCMs to those that were part of CMIP6. CMIP6 is the compilation of outputs of the most recent generation of climate models that were used to inform the 2021 IPCC 6th assessment report.

Of the GCMs analyzed, each study ranked the GCM quality based on its ability to reproduce historical observations. Each study considered a different number of variables by which to measure the GCM performance, ranging from the GCM's ability to reproduce historical temperature and precipitation in the CONUS¹¹⁷, to comparing performance across more than 60 metrics¹¹⁸. Each study then ranked the GCMs from highest to lowest based on these performance metrics (results described below in the summary section).

TABLE C-4. PEER-REVIEWED STUDIES THAT COMPARED MULTIPLE CMIP6 GCMs

Study	Geographic Scope of the Comparison	Study Comparison Metrics	Number of GCMs Compared
Brunner et al. (2020) ¹¹⁹	Global	temperature, temperature variability, sea level pressure & variability, temperature trend	33
Ashfaq et al. (2022)	CONUS	66 metrics – including temperature, precipitation (seasonal, diurnal, max, min), frost days, ENSO, PDO, NAO, SLP ^a , winds, geopotential height	37
Zhang et al. (2022) ^{b,120}	N. America	18 variables: including surface temperature and precipitation, air temperature, wind fields, specific humidity, and geopotential height at 4 pressure levels.	35
Almazroui et al. (2021) ^c	CONUS	temperature, precipitation	31
Chen et al. (2020) ¹²¹	Global, land area only	Daily max/min temperature, 20 mm precipitation days, max 5-day consecutive precipitation, consecutive dry days	12
Abdelmoaty et al (2021) ^{d,122}	Global, land area only	Daily annual max precipitation	34

¹¹⁷ Almazroui et al. 2021 Projected Changes in Temperature and Precipitation Over the United States, Central America, and the Caribbean in CMIP6 GCMs. *Earth Syst Environ* 5, 1–24: <https://link.springer.com/article/10.1007/s41748-021-00199-5>

¹¹⁸ Ashfaq et al. 2022 Evaluation of CMIP6 GCMs over the CONUS for downscaling studies. *Journal of Geophysical Research: Atmospheres*, 127, <https://agupubs.onlinelibrary.wiley.com/doi/full/10.1029/2022JD036659>

¹¹⁹ Brunner, L., Pendergrass, A. G., Lehner, F., Merrifield, A. L., Lorenz, R., and Knutti, R.: Reduced global warming from CMIP6 projections when weighting models by performance and independence, *Earth Syst. Dynam.*, 11, 995–1012, <https://doi.org/10.5194/esd-11-995-2020>, 2020.

¹²⁰ Zhang, MZ., Xu, Z., Han, Y. et al. Evaluation of CMIP6 models toward dynamical downscaling over 14 CORDEX domains. *Clim Dyn* 62, 4475–4489 (2024). <https://doi.org/10.1007/s00382-022-06355-5>

¹²¹ H Chen, J Sun, W Lin, H Xu, Comparison of CMIP6 and CMIP5 models in simulating climate extremes, *Science Bulletin*, Volume 65, Issue 17, 2020, <https://doi.org/10.1016/j.scib.2020.05.015>.

¹²² Abdelmoaty et al. 2021 Biases Beyond the Mean in CMIP6 Extreme Precipitation: A Global Investigation. *Earth's Future*: <https://doi.org/10.1029/2021EF002196>

Study	Geographic Scope of the Comparison	Study Comparison Metrics	Number of GCMs Compared
DiLuca et al. (2020) ¹²³	Global, land area only	Cold & hot extreme temperatures: annual cycle, diurnal cycle, synoptic variability, seasonal variability	28
Kim et al. (2020) ¹²⁴	Global, land area only	20-year return of warmest day & coldest night, annual max daily precipitation	32

^a ENSO: El Niño-Southern Oscillation, PDO: Pacific Decadal Oscillation, NAO: North Atlantic Oscillation, SLP: sea level pressure
^b Study only provided numerical rankings for the best 15 models in any region. We assigned all the other models evaluated in the study a ranking of 16.
^c Study determined that nine of the GCM studies had a bias for emulating historical precipitation of greater than 1.5 standard deviations. Of the remaining 22 GCMs, nine were identified as performing better than the others based on the temperature and precipitation metrics. The nine best GCMs were assigned a rank of 4.5, the next thirteen a rank of 10, and the remaining nine a rank of 22. Data from Figure 6b of the paper was not used due to a mismatch between labels and the data: the authors did not respond to inquiries regarding the figure.
^d A mismatch between the labels and the data was identified in Figure 7 of this study. Upon request, the authors provided a corrected version of the figure which was then used to determine rankings.

Independence

The concept of ‘model independence’ refers to the similarity between the output of two GCMs, given a specific input forcing scenario. This metric can range from 0, suggesting the GCMs are indistinguishable from each other, to values greater than 1, indicating a high level of independence between the two GCMs. In addition to quantitative metrics, independence can also be assessed by other qualitative factors, such as the country or organization that developed and maintains each GCM. For example, models developed by similar organizations or countries may use similar modules, parameterizations, or mechanisms for specific aspects of the climate system (e.g., the atmospheric chemistry scheme), which can reduce their independence. Therefore, to reflect some of the uncertainty in the climate system, impact analyses should ideally consider GCMs with a high level of independence from each other. Three of the GCM assessment studies in Table C-4 (Brunner et al., (2020), Zhang et al., (2022), and Ashfaq et al. (2022)) included analyses of model independence, but used different variables by which to measure independence. For example, Brunner et al. (2020) calculated generalized distances between the 33 GCMs they considered, based on horizontally resolved temperatures and sea level pressure climatologies. In contrast, Zhang et al. (2022) used a clustering analysis based on climatological means and interannual variability of seven variables for the 15 best models in the North American domain. Alternatively, Ashfaq et al. (2022) included a chart showing models that had cosine similarity scores greater than 0.8 (where any GCM pair has a score of at least 0.51). These studies revealed important similarities between some of the top performing GCMs, such as between multiple NorESM2 and GFDL GCMs, as discussed further in the recommendations section below.

¹²³ A. Di Luca, A. J. Pitman, & R. de Elía (2020). Decomposing temperature extremes errors in CMIP5 and CMIP6 models. *Geophysical Research Letters*, 47, e2020GL088031. <https://doi.org/10.1029/2020GL088031>

¹²⁴ Y-H Kim, S-K Min, X Zhang, J Sillmann, M Sandstad, Evaluation of the CMIP6 multi-model ensemble for climate extreme indices, *Weather and Climate Extremes*, 2020, <https://doi.org/10.1016/j.wace.2020.100269>.

Availability in Downscaling Datasets

Due to computational limitations, GCMs are often run at lower spatial and temporal resolution than is useful to resolve regional and local impacts. Therefore, downscaling and bias correction of the raw GCM data to a higher spatial and temporal resolution is necessary for driving many climate impact analyses. One downscaling approach is based on statistical methods that use the relationships between GCM outputs and historical observed local climate data to create higher-resolution projections. Downscaling processes are computationally expensive and require expertise in working with GCM output and meteorological variables.

LOCA2 and STAR-ESDM¹²⁵ are two external datasets that are readily available and include the statistically downscaled output from multiple GCMs. The LOCA2 and STAR-ESDM datasets were also used to inform the U.S. 5th NCA. Therefore, due to the importance of using high-resolution climate data, we favorably ranked GCMs that already have downscaled data available in the LOCA and STAR datasets¹²⁶. However, not all output variables from each GCM have been downscaled in these datasets, and some of those may be necessary for specific impact studies (e.g., winds are necessary for driving atmospheric chemistry models to analyze future climate impacts on air quality, and statistical approaches to downscaling generally cannot produce the necessary wind fields).

Other considerations

While this appendix recommends seven CMIP6 GCMs based on model quality, independence, and downscaling availability, there are other factors that could be considered. We discuss three of those factors here: consideration of model climate sensitivity in GCM selection, whether agreement between models and historical observations increases confidence in future projections, and the evaluation of downscaled datasets separate from the evaluation of the parent GCM.

The IPCC has produced a best estimate and a likely range of climate sensitivities. For some applications, it would make sense to choose a set of GCMs where half were below and half were above the best estimate, and where most fell within the likely range. This could be an important consideration for creating a set of model projections that produce a range of future temperatures consistent with the IPCC assessed climate sensitivities. Due to the larger number of GCMs emerging from CMIP6 that have a high climate sensitivity, these higher sensitivity GCMs are sometimes down-weighted such that the ensemble of GCMs match the IPCC best estimate (see Tokarska et al. 2(020)¹²⁷, Table S1, for a set of TCR and ECS estimates for CMIP6 models). However, because FrEDI is built around the by-degree framework, a selected model subset does not need to be weighted according to future temperature. As described in Section 3 in the main documentation, global temperature projections are created using reduced complexity climate models such as FaIR, Hector, or MAGICC, and then the damage functions

¹²⁵ STAR refers to the STAR-ESDM or Seasonal Trends and Analysis of Residuals, Empirical-Statistical Downscaling Model. LOCA refers to the Localized Constructed Analogs downscaling product.

¹²⁶ The list of models included in each dataset was taken from Ullrich et al. (2023).

¹²⁷ KB Tokarska et al. Past warming trend constrains future warming in CMIP6 models. Sci. Adv. 6, eaaz9549(2020). DOI:10.1126/sciadv.aaz9549

developed from the more sophisticated GCMs are used in that probabilistic context. There is still a question of whether some aspects of climate change that are correlated with climate sensitivity: e.g., patterns of temperature change or precipitation per degree global warming that differ between high sensitivity models and low sensitivity models. In the absence of evidence of this kind of correlation of by-degree patterns with climate sensitivity, we did not include this consideration in our criteria.

For the last two decades, there has been active discussion in the climate modeling community about the value of using model agreement with observations to inform model selection. For example, Knutti et al. (2010)¹²⁸ stated that, “It is thus unclear by how much the confidence in future projections should increase based on improvements in simulating present-day conditions.” This is relevant to the goal of this appendix to select a set of GCMs based on model quality. However, more recently, Brunner et al. (2020) used a “perfect model” to demonstrate that weighting GCMs by quality and independence does improve their ability to match the ‘perfect model’ that was held out of the testing set and compared against. This analysis by Brunner et al. (2020) provides evidence that recommending a set of GCMs based on quality and independence does have value. In addition (relevant to the prior paragraph’s discussion of climate sensitivity), the Brunner et al. (2020) analysis also shows that weighting by model quality and independence leads to a lower mean climate sensitivity than in the original dataset.

We are not aware of any large-scale assessments of individual LOCA2 or STAR-ESDM downscaled GCM output. Ullrich et al. (2023)¹²⁹ compares the downscaled models to observed data but does not show how well they replicate trends from the GCM projections. Baek et al. (2024) did compare LOCA and STAR projections from eight different GCMs to the raw GCM data as well as to dynamically downscaled data, and found that both datasets, but particularly LOCA2, dampen future intensification of frontal precipitation that is seen in the underlying GCM and the dynamically downscaled projections. However, Baek et al., (2024) did not provide relative rankings of the different statistically downscaled GCMs, and with only eight GCMs analyzed, this analysis would not support a larger selection of models. Therefore, the quality and independence criteria are based on analyses of the GCMs themselves, and not the downscaling products thereof.

Model Analysis Summary

In this analysis, we considered the quality and independence results from eight GCM assessment studies, as well as the availability of downscaled data in the LOCA2 and STAR-ESDM. As listed in **Table C-5**, we recommend using seven CMIP6 GCMs to inform future sectoral impact analyses (i.e., the underlying studies used to develop FrEDI impact functions). This is meant to be a recommendation, not a requirement. The recommended models have been chosen because of their ability to match historical observations across a range of common metrics – however, there are other metrics not considered here which might be of more interest for some applications (e.g., emulation of Arctic sea ice). As noted above, dynamical downscaling

¹²⁸ Knutti, R., R. Furrer, C. Tebaldi, J. Cermak, and G. A. Meehl, 2010: Challenges in Combining Projections from Multiple Climate Models. *J. Climate*, 23, 2739–2758, <https://doi.org/10.1175/2009JCLI3361.1>.

¹²⁹ Ullrich, P. Validation of LOCA2 and STAR-ESDM Statistically Downscaled Products, Lawrence Livermore National Laboratory, 2023. <https://www.osti.gov/servlets/purl/2202926>

may also produce outputs that are not available from statistical downscaling, such as wind fields, and so applications that require those outputs would be constrained in choice of GCM by which models have been dynamically downscaled. To understand the influence of natural variability, using multiple ensemble members of a single GCM might also be desirable. Depending on computational constraints, researchers may be limited to using fewer than seven GCMs. Absent these considerations, the seven recommended GCMs provide a good range of quality, independence, and availability.

TABLE C-5. RANKED LIST OF THE 7 RECOMMENDED (RED AND SHADED) AND TOP 21 CMIP6 GCMS

GCM	Average Quality Rank ^a	Count ^b	Model Independence ^c	Model Availability ^d
GFDL-ESM4	4.5	7	Developed in the US	✓
GFDL-CM4	6.1	5	similar to GFDL-ESM4	
AWI-CM-1-1-MR	7.1	5	similar to MPI-ESM1	not in STAR
ACCESS-CM2	7.5	7	Developed in Australia	✓
HadGEM3-GC31-MM	7.8	4	Similar to ACCESS	not in STAR
MPI-ESM1-2-HR	8.0	8	Developed in Germany	✓
FIO-ESM-2-0	8.7	3	similar to NorESM2	not in LOCA or STAR
NorESM2-MM	8.9	7	Developed in Norway	✓
CMCC-CM2-HR4	10.7	1	only evaluated in one study	Not in LOCA or STAR
MRI-ESM2-0	11.0	8	Developed in Japan	✓
CAMS-CSM1-0	11.0	4	similar to EC Earth	not in LOCA or STAR
EC-Earth3-Veg	11.4	6	Developed in Europe	✓
SAMO-UNICON	11.6	5	similar to NorESM2	not in LOCA or STAR
CESM2-WACCM	11.9	4	similar to NorESM2	not in LOCA or STAR
FGOALS-f3-L	12.5	7	unique model ‘family’ (China)	not in LOCA or STAR
MPI-ESM1-2-LR	12.8	7	similar to MPI-ESM1-2-HR	✓
BCC-CSM2-MR	13.2	7	Developed in China	✓
CESM2	13.9	4	similar to NorESM2	not in LOCA or STAR
NorESM2-LM	14.1	6	similar to NorESM2-MM	✓
GISS-E2-1-G	14.4	4	unique model family ^e (US)	not in LOCA or STAR
EC-Earth3	14.5	7	similar to EC-EARTH3-Veg	✓

^a Average rank across the studies that assessed GCM quality (see Table C-4). For example, the GFDL-ESM4 GCM was considered in 7 of the 8 studies, and on average, was ranked as the 4.5th best performing model in each study

^b The number of assessment studies that included the GCM (out of 8).

^c The country of development (for the seven selected models), the model that it is similar to, if it is in a ‘unique model family’ (i.e., if it is independent from the seven selected models)

^d Whether the GCM output has been downscaled and is included in the STAR and LOCA datasets.

For an assessment of quality, we averaged the GCM rankings from each assessment study to derive an overall average ranking for each GCM (listed in **Table C-5**). Of the 50 unique GCMs considered in the eight studies, 21 GCMs had an average ranking better than 15. The seven recommended GCMs each had an average rank between 4.5 and 13.2. Since alternative averaging schemes could be used (e.g., by giving more weight to studies that include more GCMs, studies that had more diverse metrics, or studies that focused on the CONUS), we conducted a sensitivity analysis where we dropped out one study at a time and found that none of the seven recommended GCMs had a ranking worse than 14.4 and did not increase in

average ranking by more than 1.8. Therefore, the model selection process is likely robust with regard to the selected quality weighting scheme.

For an assessment of independence, we considered the independence results from the three relevant assessment studies, including the model family and country of development. GCMs were considered similar to each other if they had generalized distances of less than 0.75 (from Brunner et al., (2020)). Zhang et al. (2022) showed that SAM0-UNICON (not included in Brunner et al., (2020)) was similar to NorESM2-MM. Ashfaq et al., (2022) confirmed that NorESM2-MM and NorESM2-LM were similar, and that GFDL-CM4 and GFDL-ESM4 were similar (these pairs were not included in Brunner et al., (2020) or Zhang et al., (2022)). Of the seven recommended GCMs, each had generalized distances of more than 0.75 from each other, were developed by different countries, and are considered different model families.

For an assessment of the availability of downscaled data, we assessed whether the GCM output had been downscaled and included in the LOCA2 or STAR-ESDM statistically downscaled datasets. All seven recommended GCMs are included in both these datasets.

Additional Recommendations for Using GCM Data in U.S. Climate Impact Analyses

Using the entire time-period (e.g., 1986-2100) as inputs to a climate impact analysis will preserve flexibility. If computational resources are limited, researchers can calculate average U.S. temperatures to develop the integer degree ‘arrival window’ (as described in Section C.1). **Figure C-6** shows the arrival windows for five of the seven recommended CMIP6 GCMs using an example Shared Socioeconomic Pathway. For example, ACCESS-CM2 reaches 2°C above the baseline by 2034 and 6°C of warming by 2090. All five CMIP6 GCMs shown in **Figure C-7** reach at least 4°C by 2100, with one reaching 5°C and two reaching 6°C. FrEDI uses the baseline period of 1986-2005, but for discussion of impact results, it may sometimes be better to use the most recent historical time period supported by the data underlying the analysis.

FIGURE C-6. BY-DEGREE ARRIVAL YEAR WINDOWS FROM CMIP6 GCMS

A. CONUS ARRIVAL WINDOWS

	2015	2025	2035	2045	2055	2065	2075	2085	2095	2105
ACCESS-CM2		2017		2034		2052	2065	2078	2090	
EC-Earth3-Veg			2024		2042	2056	2069	2081	2090	
GFDL-ESM4			2025		2049		2071		2088	
MPI-ESM1-2-HR			2021		2053	2068		2083		
NorESM2-MM			2023		2042	2063		2079	2094	

B. GLOBAL ARRIVAL WINDOWS

	2015	2025	2035	2045	2055	2065	2075	2085	2095	2105
ACCESS-CM2			2022		2046	2062	2077		2090	
EC-Earth3-Veg				2030		2052	2068		2084	
GFDL-ESM4				2037		2063			2085	
MPI-ESM1-2-HR				2033		2062		2084		
NorESM2-MM				2036		2062		2082		



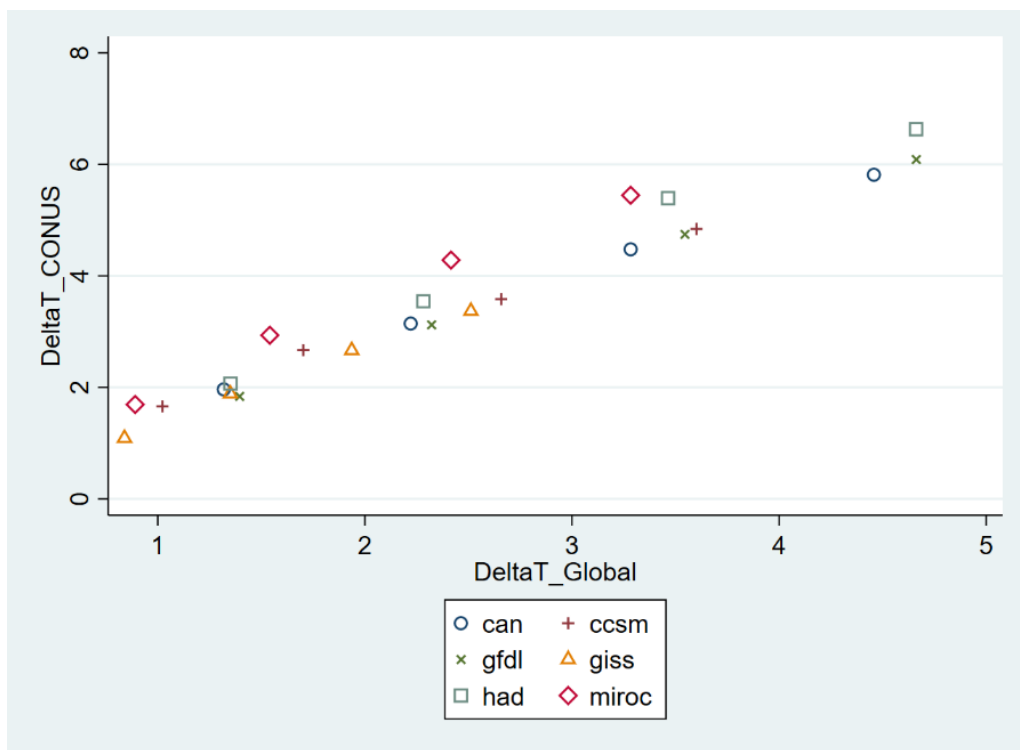
Illustration of arrival windows of each integer CONUS degree of warming (panel A) and global degree of warming (panel B) for SSP5-8.5 in five CMIP6 GCMs. Arrival years, or the year at which the 11-year moving average reaches the given integer, are listed in each bin. This SSP scenario is chosen only to illustrate the concept of an arrival window.

APPENDIX D | METHODS DETAILS

D.1 Global to CONUS Temperature Translation

FrEDI was designed with the flexibility to generate impact estimates from either global or CONUS temperature input data. To accomplish this, FrEDI contains a translation function, derived from global and CONUS temperatures from six CMIP5 GCMs used in many of FrEDI's underlying damage functions. **Figure D-1** plots the CONUS versus global average temperatures as a function of the six CMIP5 GCMs (from RCP8.5), where each point represents an era (i.e., 2030, 2050, 2070, 2090). All temperature changes presented are relative to the 1985-2006 baseline period.

FIGURE D-1. CONUS VS. GLOBAL TEMPERATURES BY CMIP5 GCM



Global and CONUS temperatures for six CMIP5 GCMs, from RCP8.5, where each data point represents average temperatures during an era of warming.

The relationship between CONUS and global temperatures is relatively stable across GCMs and over time, which allows for the development of a generalized relationship between global and CONUS temperature anomalies. The coefficients of this equation are in **Table D-1**.¹³⁰

¹³⁰ RCP8.5 is used in this analysis for consistency with the use of RCP8.5 to define impacts by degree, however the relationship is stable across RCPs. Rerunning the regression estimate in Table D-1 with both RCP8.5 and RCP4.5 yields a coefficient of 1.444 (compared to 1.421 using only RCP8.5).

TABLE D-1. CONUS TO GLOBAL TEMPERATURE TRANSLATION COEFFICIENT ESTIMATES

Regression estimates relating CONUS and global temperature changes, relative to a 1986-2005 baseline.

	ΔT_{CONUS}
ΔT_{GLOBAL}	1.421 *** (0.000)
R-squared	0.990
Adjusted R-squared	0.990
N	24

Standard errors listed below coefficients, in parentheses. * p<0.05; ** p<0.01; *** p<0.001

These coefficients are used to translate global temperature inputs into CONUS temperatures, however if a user inputs CONUS temperatures, the inverse of the formula can also be used to generate global temperatures.

In general, relative to global temperatures, the use of CONUS temperatures in FrEDI reduces scatter, improves fit, and allows better emulation of GCMs that might not have been used to generate the sector-specific damage functions. However, there are some sectors where an impact may be better associated with global rather than CONUS temperatures. For example, in the case where the impacts are a function of large-scale weather patterns or ocean circulation changes. Additionally, if global temperatures are input to FrEDI rather than CONUS temperatures, the translation from global to CONUS temperatures is fixed and does not take into account how that relationship might vary by GCM and over time, for example with stabilization.

D.2 Calculation of global mean sea level

If a user provides FrEDI with an input temperature trajectory, but does not provide a custom sea-level rise trajectory, FrEDI calculates the projected sea-level rise at runtime from input amount of input temperature change. To calculate global mean sea level from global mean temperature, FrEDI uses a semi-empirical sea level model from Kopp et al., 2016.¹³¹ This model relates the rate of global mean SLR ($dh(t)/dt$) to global mean temperature at time $T(t)$, an equilibrium temperature $T_e(t)$, and a small residual trend arising from the long-term response to earlier climate change $\emptyset(t)$, relative to 2000 using equation 10 from Kopp et al., (2016).

$$\frac{dh(t)}{dt} = a * (T(t) - T_e(t)) + \emptyset(t) \quad (\text{Equation D-1})$$

In the equation above, $T_e(t)$ and $\emptyset(t)$ are functions of time, where:

¹³¹ Kopp, R. E., Kemp, A. C., Bittermann, K., Horton, B. P., Donnelly, J. P., Gehrels, W. R., ... & Rahmstorf, S. (2016). Temperature-driven global sea-level variability in the Common Era. *Proceedings of the National Academy of Sciences*, 113(11), E1434-E1441.

$$\frac{dT_e(t)}{dt} = \frac{(T(t) - T_e(t))}{\tau_{\alpha_1}} \quad (\text{Equation D-2})$$

$$\frac{d\phi(t)}{dt} = \frac{-\phi(t)}{\tau_{\alpha_2}} \quad (\text{Equation D-3})$$

The parameter values are estimated from the probability distributions of the semiempirical model parameters in Figure S5, and Dataset S1j, focusing on the posterior distribution calculated with the Mann et al., (2009) temperature data set.¹³² We use the median parameter values across the distributions for this calculation. We used HadCrUT4 to determine the appropriate temperature offset between the actual temperature and the equilibrium temperature in 2000.

TABLE D-2. PARAMETER VALUES FROM KOPP ET AL., 2016, MEDIAN AND 5TH AND 95TH PERCENTILES.

Parameter	Value	Units
$\phi(2000)$	0.14 (0.05, 0.29)	mm/yr
τ_{α_1}	174 (87, 366)	Year
τ_{α_2}	4175 (1140, 17670)	Year
a	4.0 (3.2, 5.4)	mm/yr/K
$T_e(2000)$	-0.05 (-0.12, 0.07)	K

Future versions of FrEDI may use several different approaches for addressing uncertainty. Some of these approaches include: using the parameter distributions in S1j using a Monte Carlo approach to sample the parameters distributions provided in Kopp et al., (2016), Mann et al., (2009), and Marcott et al., (2013)¹³³; calibrating $T_e(2000)$ and alpha parameters to emulate the range of SLR from AR6; and examine low-probability high impact outcomes such as the SLR projection including ice sheet instability from AR6 or the higher Sweet et al. (2017) scenarios.¹³⁴ Some approaches (such as using the normal distributions for parameters or the alternate parameter set calibrated against Marcott et al. (2013)) will be straightforward, but others may be more challenging to implement. The semi-empirical approach was not designed to incorporate future SLR processes that were not observed in historical data such as ice sheet instability and may not be accurate for multi-century applications. However, users can supply FrEDI with exogenous global mean SLR scenarios instead of calculating them from global mean temperature.

¹³² Mann, M. E., Zhang, Z., Rutherford, S., Bradley, R. S., Hughes, M. K., Shindell, D., ... & Ni, F. (2009). Global signatures and dynamical origins of the Little Ice Age and Medieval Climate Anomaly. *science*, 326(5957), 1256-1260.

¹³³ See previous references and Marcott, S. A., Shakun, J. D., Clark, P. U., & Mix, A. C. (2013). A reconstruction of regional and global temperature for the past 11,300 years. *science*, 339(6124), 1198-1201.

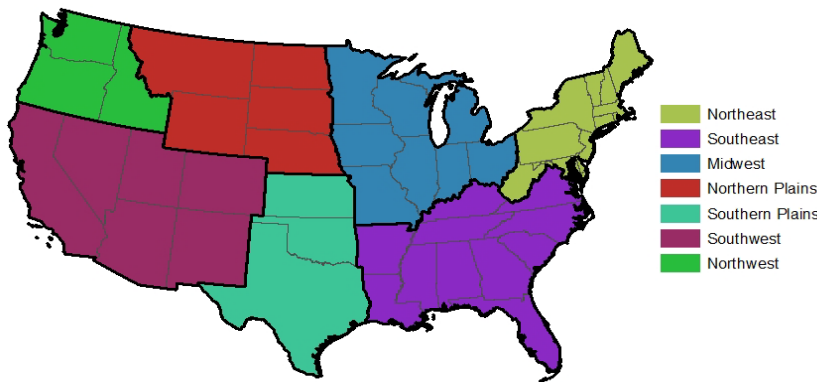
¹³⁴ Sweet, W. V., Horton, R., Kopp, R. E., LeGrande, A. N., Romanou, A. (2017). Climate Science Special Report: Fourth National Climate Assessment, Volume I. U.S. Global Change Research Program.

APPENDIX E | SOCIAL VULNERABILITY MODULE

E.1 Overview

The main purpose of this module is to integrate the underlying data and analytical approach from EPA's Social Vulnerability Report¹³⁵ (hereafter referred to as the SV report) into the FrEDI tool. This allows users to explore how the impacts of climate change will be distributed among four population groups of concern: (1) individuals with low income (below two times the national poverty line), (2) those identifying as Black, Indigenous, or people of color (BIPOC)¹³⁶, (3) those that are without a high school diploma, and (4) those that are 65 years of age or older. Analyzing impacts and disproportionality for specific racial and ethnic populations (e.g., Black or African American, Hispanic, Asian, etc.) within the BIPOC group has also been incorporated into the FrEDI module, consistent with data presented in the SV Report. In contrast to the main sector calculations in FrEDI, the SV module estimates impacts for seven CONUS regions, to maintain consistency with the methodology in EPA's peer-reviewed SV Report. The regions used are defined in the 4th and 5th U.S. NCA (see **Figure E-1**).

FIGURE E-1. NCA REGIONS (SPATIAL LEVEL OF SV MODULE OUTPUTS)



Map of seven NCA regions.

E.2 Features of the module

The SV module assesses the disproportionate impacts of climate change under any user-defined scenario of temperature change across select sector categories. For inclusion in this module, the underlying sector study must first meet specific qualifications for technical feasibility:

¹³⁵ <https://www.epa.gov/cira/social-vulnerability-report>

¹³⁶ Consistent with other EPA reports, FrEDI-SV uses the abbreviation "BIPOC" (for Black, Indigenous, and people of color) to refer to individuals identifying as Black or African American; American Indian or Alaska Native; Asian; Native Hawaiian or Other Pacific Islander; and/or Hispanic or Latino. It is acknowledged that there is no 'one size fits all' language when it comes to talking about race and ethnicity, and that no one term is going to be embraced by every member of a population or community. The use of BIPOC is intended to reinforce the fact that not all people of color have the same experience and cultural identity. This report therefore includes, where possible, results for individual racial and ethnic groups. The SV report referred to this group as the "minority" category. The category title has been updated here.

1. **Fine spatial scale:** At least county-level results but preferably census tract.
2. **Physical impacts:** Easily converted to “physical” impacts per population unit or as a non-monetary impact metric (for example, rates per 100,000 for health impacts or damage ratios for flooding damage), ideally avoiding economic impacts because the burden of the same monetary cost can be realized differently across individuals with, for example, different levels of income.

The sectors included in FrEDI-SV are listed in **Table E-1**, which also lists the impact estimated and whether a variant is included for that sector. The sectors included in FrEDI-SV are from EPA’s SV Report and are a subset of sectors in the main FrEDI domain.

TABLE E-1. SECTORS CURRENTLY IMPLEMENTED IN FREDI-SV

EPA SV Report Sector	Corresponding FrEDI-SV Impact Type	FrEDI-SV Metric of Impact	Incoming Spatial Scale	Default Adaptation scenario
Air Quality and Health	Air quality and new asthma cases (PM _{2.5} only)	New childhood asthma cases (age 0-17)	Tract	No Additional Adaptation
	Air quality and premature mortality (PM _{2.5} only)	Premature mortality (over age 65 only)	Tract	No Additional Adaptation
Extreme Temperature and Health ^a	Extreme temperature and mortality	Premature mortality (all ages)	Tract	No Additional Adaptation
Extreme Temperature and Labor	Extreme temperature and labor	Work hours lost	Tract	No Additional Adaptation
Temperature/Precip. and Traffic ^b	Roads: Temp/Precip and traffic	Hours of traffic delay	Tract	No Additional Adaptation
Coastal Flooding and Traffic	Transportation impacts from high tide flooding	Hours of traffic delay	Tract	Reasonably Anticipated Adaptation
Coastal Flooding and Property	Coastal flooding and property	Individuals threatened with total property loss	Block Group	No Additional Adaptation

a. Based on the Mills et al. (2014) Extreme Temperature study.
b. The impact of temperature and precipitation on road integrity and delays is not included in the main text of the social vulnerability report, but the method and results are described in detail in Appendix G of that report.

Briefly, the FrEDI-SV module uses damage functions (i.e., physical impacts by CONUS half-degree temperature increment) at the census tracts or block group level for each sector, which are derived from the same “main FrEDI” sectoral analyses but limited to selected physical impacts. The impact metrics used in the SV module are always physical measures, which are not always included in the main FrEDI code. For example, for the Coastal Flooding and Property category, the physical impact metric, individuals threatened with total property loss, aligns with the impact metric included in the SV report. In contrast, the Coastal Property impact metric used elsewhere in FrEDI is total monetized property damage or loss. The physical metric used in FrEDI-SV is designed to consider the likelihood of permanent home loss through repeated flood episodes causing damage and serves as an indicator of the most severe impacts of coastal flooding. Total property loss can be triggered by intense and repeated damage from storm surge or by permanent inundation from SLR. Main FrEDI identifies the annual expected damages to residential structures within a

block group, and the property loss scenario considers properties which reach the 10 percent annual expected damage threshold – that is, total home loss is expected within a decade. This aligns with the assumption for a threat of abandonment in the underlying sector study for coastal property.¹³⁷ Nonetheless, both the FrEDI and FrEDI-SV metrics are derived from the same underlying National Coastal Property Model runs included in the published and peer-reviewed Neumann et al. (2021).

The FrEDI-SV module also relies on demographic population information. While the SV Report did not consider population growth, total national population growth projections are included in the FrEDI-SV module so that it is consistent with the impacts derived from main FrEDI. The relative percent of each population group in each census tract are taken from current demographic patterns from the U.S. Census American Community Survey (ACS) dataset (2014-2018) (accessed via the IPUMS platform).¹³⁸ In the FrEDI-SV module, current demographic patterns are applied to projections of total national population growth (from ICLUS) and are held constant overtime because robust and long-term projections for local changes in demographics are not readily available. Therefore, FrEDI-SV does not consider how changes in future demographic patterns in the U.S. could affect risks to these populations.

As shown in **Table E-1**, the FrEDI-SV module is also designed with the capability to assess the impacts across different adaptation scenarios in each sector. The default adaptation assumption considered for most of the sectors in the FrEDI-SV module is a ‘no additional adaptation’ scenario, which current adaptation responses and human acclimatization to hazards are incorporated in the projection, but no additional planned adaptation investments are modeled beyond those already in place. For transportation impacts from high tide flooding, a “reasonably anticipated” adaptation scenario is used as the default, which incorporates virtually costless and autonomous adaptation actions. As with the main FrEDI module, the ability to incorporate damage functions under different adaption assumptions depends on the data available in the underlying studies. Alternative adaptation scenarios in FrEDI-SV currently include proactive adaptation scenarios for both roads and coastal property. In cases where alternative adaptation scenarios are included, which apply to sectors in the last three rows of **Table E-1**, those results are directly reported along with the default assumptions from the FrEDI-SV module.

E.3 Approach

This section summarizes the overall methodology of the FrEDI-SV module.

¹³⁷ Neumann, J. E., Chinowsky, P., Helman, J., Black, M., Fant, C., Strzepek, K., & Martinich, J. (2021). Climate effects on US infrastructure: the economics of adaptation for rail, roads, and coastal development. *Climatic Change*.

<https://doi.org/10.1007/s10584-021-03179-w>

¹³⁸ This analysis relied on the IPUMS platform to download ACS data through its National Historical Geographic Information System (NHGIS). The NGHIS codes are provided in Table 3, Appendix C of the SV Report. For the IPUMS platform see Manson S, Schroeder J, Van Riper D, Kugler T, and Ruggles S. IPUMS National Historical Geographic Information System: Version 15.0 American Community Survey 2014-2018a. Minneapolis, MN: IPUMS. 2020.

<http://doi.org/10.18128/D050.V15.0>. The NGHIS field codes in Table 3 are unique to IPUMS – ACS table numbers differ from the field codes shown in the SV report, but the data are identical.

Like the main FrEDI module, a series of pre-processing steps are first used to incorporate the underlying peer-reviewed studies from the SV report into a series of impact-temperature damage functions at the census tract level. In contrast with the main FrEDI module, which uses a database of state-aggregated impact-temperature functions from (mainly) six individual CMIP5 GCMs, the FrEDI-SV module uses impact-temperature relationship derived from the average across the six CMIP5 GCMs. This significantly reduces the processing time and database file size to compensate for the increased spatial detail in this module.

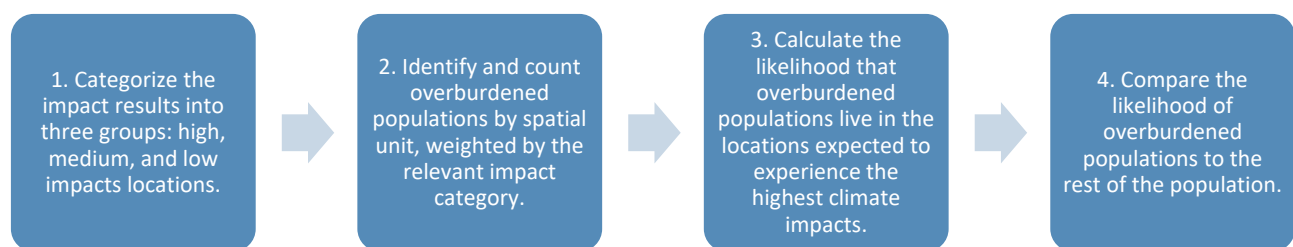
When run in R, the FrEDI-SV module then uses this database of damage functions in the following steps:

1. Determine the physical impacts per population at the census tract level for each year of the input temperature and population trajectories. With this, the R-code uses a linear interpolation between half degrees¹³⁹ of warming.
2. Calculate aggregate impacts and populations at the regional and CONUS levels each year, for both the population groups of concern and reference populations. This is done by weighting the impacts at the census tract or block group by the respective population groups. This is where we apply county-level population projections by applying county-level growth ratios to census tract or block group populations.
3. Calculate the variables used to calculate the disproportionality metrics (e.g., difference in risk, with and without adaptation (if available)), as used in EPA's SV Report and described in detail in the following section.

E.4 Disproportionality, difference in risk calculation

The following text provides additional detail about the steps taken to calculate the disproportionate risks (or difference in risk) of those currently living in a location that is projected to experience the largest impacts from climate change. **Figure E-2** provides a visual representation of these steps. **Table E-2** shows an example of each calculation step. All four steps are completed within the FrEDI-SV module during runtime, rather than in pre-processing of underlying study results – this is one reason that FrEDI-SV requires longer runtimes relative to the main FrEDI module.

FIGURE E-2. STEPS FOR ASSESSING THE DISPROPORTIONALITY OF IMPACTS ON SPECIFIC POPULATIONS



¹³⁹ In contrast, the main FrEDI module linearly interpolates between integer degrees of warming.

Step 1: Categorize the annual spatial impact data into three groups: high, medium, and low impact locations.

We use the annual impacts per population (relative impacts or rates) associated with the input temperature and population trajectories to categorize the annual spatial climate impacts (by Census tracts or block groups) into three evenly sized groups, called terciles. The focus of this risk analysis is on the composition of populations found in the ‘high impact’ group because we are attempting to identify cases where specific populations are more likely to currently live in areas that will experience the largest impacts from climate change. The spatial resolution of the analysis varies by sector (e.g., census tract or block group), but is consistent within each sector. For coastal properties and high tide flooding, we only consider populations that live in coastal areas exposed to the coastal hazards of sea-level rise or storm surge during the 21st century projection period – we do not include inland areas.

Step 2: Identify and count specific populations by location. As discussed in the SV report, while we cannot observe exactly which individuals are exposed to the relevant climate hazard, we can overlay the impacts and population groups by location. For demographic patterns, we rely on data from the American Community Survey (2014-2018) at the Census tract or block group (see Section E.6) to (1) count the number of individuals in each population group of concern (sv_group) relative to reference population and then (2) weight the proportions by relevant exposed population for each climate hazard (e.g., children aged 0-17 years for childhood asthma). In the absence of projections describing how detailed demographics will shift over the century, we assume the relative distribution of overburdened to non-overburdened populations is fixed at 2014-2018 levels.

Step 3: Calculate the likelihood that populations live in the locations expected to experience the highest climate impacts. After identifying the total populations of interest (and remaining populations) living in each ‘high impact’ area in Steps 1 and 2, we calculate the likelihood of living in a high impact location, relative to the reference domain, for both the population of interest and the reference population.

Step 4: Compare the likelihoods of population groups of concern and reference populations. Relative likelihoods are calculated by comparing likelihoods that populations of interest are living in high impact areas compared to their reference population. These likelihoods relative to the reference population are calculated at the national and NCA region level. The likelihood measures are separately calculated for each social vulnerability metric and sector, for each year of the temperature and population trajectories. These likelihood metrics can be interpreted as the degree to which climate impacts disproportionately affect population groups of concern relative to each reference population.

TABLE E-2. EXAMPLE CALCULATION OF DISPROPORTIONATE IMPACTS ON A POPULATION EACH YEAR

Step	Example Results and Values
1. Identify high impact areas for each specific sector and each year	<ul style="list-style-type: none"> The result is an allocation of census tracts into high, medium, and low impact groupings, with the same number tracts in each grouping. For example, the total population experiencing a sectoral impact in a given year is 115 million across all three impact groupings: <ul style="list-style-type: none"> 22 million people in specific group of concern 93 million people in reference population

2. Identify specific populations within 'high impact' areas for each sector and year	<ul style="list-style-type: none"> Populations living within high impact census tracts for a specific sector in a given year: <ul style="list-style-type: none"> 3.5 million people in group of concern 14 million are in the reference population
3. Calculate the likelihood of living in a high impact area for each sector and year	<ul style="list-style-type: none"> Likelihood of living in high impact area for a specific sector in a given year: <ul style="list-style-type: none"> $3.5/22 = 0.16$: likelihood individuals in specific group are living in high impact areas $14/93 = 0.15$: likelihood individuals in the reference population are living in high impact areas
4. Compare likelihoods of each population group for each sector and year	<ul style="list-style-type: none"> Group of concern likelihood / reference population likelihood = $0.160/0.15 = 1.09$. $1.09 - 1 = 9\%$ difference in risk

E.5 Calculating impacts and rates by population groups

The previous section provides the method for estimating likelihood ratios, the first of three results metrics generated by FrEDI-SV. Below is the process for estimating the 1) impacts (e.g., case counts) and 2) impact rates for population groups of concern and reference populations for each temperature scenario. These metrics are calculated using a weighted average impact for the CONUS and for each region. In this case, "pop_weights" are the fraction of the population that are impacted in each region. For example, people that are 17 or younger make up the childhood asthma population, so a weight is applied that reflects the portion of the population at age 17 or younger. The equations below are for impacts by tract, which applies to most sectors, but some sectors (coastal properties, for example) include impacts by census block group.

Total impacts by tract: Multiply impact by weighted populations in each population

$$\text{impacts_sv_tract} = \text{rate_tract} * \text{sv_population_tract} * \text{pop_weights}$$

$$\text{impacts_ref_tract} = \text{rate_tract} * \text{ref_population_tract} * \text{pop_weights}$$

Total impacts by region: Sum impacts for each region (and CONUS) and each population

$$\text{impacts_sv_region} = \text{Sum}(\text{impacts_sv_tract})$$

$$\text{impacts_ref_region} = \text{Sum}(\text{impacts_ref_tract})$$

Average rates by region and CONUS

$$\text{Impact_sv_region} = \text{impacts_sv_region} / (\text{sv_population_region} * \text{pop_weights})$$

$$\text{Impact_ref_region} = \text{impacts_ref_region} / (\text{ref_population_region} * \text{pop_weights})$$

Total avoided cases for sv group, in scenario with policy action relative to baseline

$$\text{Avoided_cases_sv_region} = \text{impacts_sv_region_policy} - \text{impacts_sv_region_baseline}$$

E.6 Demographic data

Analyses in the FrEDI-SV module rely on demographic data from the five-year 2014-2018 ACS. Where available, data are collected at the block group level or the census tract level. We rely on the IPUMS¹⁴⁰ platform to download ACS data through its National Historical Geographic Information System (NHGIS).

Population groups of concern include:

- **Low Income:** populations living in households that have an aggregate income that is at most, twice the poverty threshold. ACS definitions for poverty thresholds are not geographically differentiated but do vary by household composition. Additional information on the definition of poverty thresholds can be found on the Census website.¹⁴¹ In the SV module we aggregate the estimates of population living in those households that fall into income to poverty threshold ratios below two.
- **BIPOC (ACS and the SV Report both use the term “Minority”):** The ACS provides race and ethnicity information at the block group level. We define BIPOC as all racial and ethnic groups except white, non-Hispanic. The module relies on total population and white, non-Hispanic population to calculate BIPOC population at the block group spatial scale.
- **No High School Diploma:** The ACS tracks information on educational attainment – we consider populations without a high school diploma to be an overburdened demographic. To estimate the number of people per block group with an educational credential of less than a high school diploma or equivalent, we rely on educational attainment data for the population 25 years and older.
- **65 and Older:** We use age demographic information from the ACS to determine 65 and older populations at the block group level by aggregating population estimates for age groups provided by the ACS counting people 65 and older.

E.7 Outputs and Visualization

FrEDI-SV regional outputs (defined in **Table E-3**) can be used to assess: 1) absolute impacts on population groups of concern; 2) differences in risks (or exposure to hazards) across populations (a measure of disproportionality); and 3) the relative rates of impacts across different populations. Uses of FrEDI-SV could also include a comparison of disproportionality across multiple scenarios, such as a user-defined baseline and a GHG mitigation policy scenario. Examples are shown in Section 3 and discussed below.

TABLE E-3. FREDI SV MODULE OUTPUT DATA DICTIONARY

Variable	Description
svGroupType	Population group of concern category (e.g., ‘sv_’) or racial/ethnic group (e.g., ‘race_’)
driverUnit	Units of climate driver (centimeters of SLR or degrees Celsius of temperature)
driverValue	Value of climate driver relative to baseline
year	Year

¹⁴⁰ IPUMS had previously been an acronym for Integrated Public Use Microdata Series, but not all of the data it accesses is public or is microdata, so since 2016 it has been known only by its acronym.

¹⁴¹ <https://www.census.gov/topics/income-poverty/poverty/guidance/poverty-measures.html>

Variable	Description
impPop_ref	Number of impacted people in the reference population. Counts people who both live in a region where climate damages are assessed for the sector and fall into the population assessed by the sector (Labor: high-risk workers, Air Quality - Premature Mortality: age 65+, Air Quality - Childhood Asthma: age 17 and under, Coastal Properties: residents of the coastal zone, High Tide Flooding and Traffic: residents of the coastal zone, Extreme Temperature: residents of 49 CONUS urban centers including 91 counties included in the underlying study, Mills et al. (2014), Roads: all people).
impPop_sv	Number of impacted people in the population group of concern. Counts people who both live in a region where climate damages are assessed for the sector and fall into the population assessed by the sector (Labor: high-risk workers, Air Quality - Premature Mortality: age 65+, Air Quality - Childhood Asthma: age 17 and under, Coastal Properties: residents of the coastal zone, High Tide Flooding and Traffic: residents of the coastal zone, Extreme Temperature: residents of 49 CONUS urban centers including 91 counties included in the underlying study, Mills et al. (2014), Roads: all people).
impact_ref	Total impact in the reference population (childhood asthma cases, mortality, hours of labor lost, hours of delay, or number of individuals threatened with total property loss, depending on sector)
impact_sv	Total impact in the population group of concern (childhood asthma cases, mortality, hours of labor lost, hours of delay, or number of individuals threatened with total property loss, depending on sector)
national_highRiskPop_ref	Number of impacted people in the reference population living in tracts in the highest tercile of impacts nationally (subset of impPop_ref)
national_highRiskPop_sv	Number of impacted people in the overburdened population living in tracts in the highest tercile of impacts nationally (subset of impPop_sv)
regional_highRiskPop_ref	Number of impacted people in the reference population living in tracts in the highest tercile of impacts regionally (subset of impPop_ref)
regional_highRiskPop_sv	Number of impacted people in the overburdened population living in tracts in the highest tercile of impacts regionally (subset of impPop_sv)
aveRate_ref	Impacts per person or per 100k people (depending on the sector) for the reference population
aveRate_sv	Impacts per person or per 100k people (depending on the sector) for the overburdened population
scenario	Name of user-provided climate scenario
variant	Adaptation scenario variant (e.g. with adaptation or without adaptation)

First, the FrEDI-SV outputs can be used to assess the risks (defined as the likelihood of living in areas projected to experience the largest impacts from climate change) for each population group of concern relative to those of the national impacted population, as follows:

$$\text{Difference in Risk} = \left(\frac{\text{national_highRiskPop}_{sv}/\text{national_highRiskPop}_{ref}}{\text{impPop}_{sv}/\text{impPop}_{ref}} \right) - 1 \quad (\text{Equation E-1})$$

These results are shown in the top panels of Figure 9 in the main documentation and can be interpreted as: A specific population group (sv) is x% more likely to live in a location that is projected to experience the greatest impacts of climate change compared to the reference population.

Outputs from FrEDI-SV can also be used to assess the relative rates of impacts between different population groups or individuals of different races and ethnicities, as well as differences in impact rates. These types of analyses can be done by comparing the ‘aveRate_sv’ and ‘aveRate_ref’ outputs for each group and sector from the SV module, which can be equivalently calculated from the impact [sv or ref]/impPop_[sv or ref] variables. Example results from this type of calculation are shown in the bottom panels of Figure 9.

To apply this calculation to a mitigation scenario and to calculate the relative benefits that will be experienced by different population groups, follow Equation E-2.

$$\text{Benefits Relative to the Ref. Population} = \frac{\text{baselineScenAvgRate}_{\text{SV}} - \text{policyScenAvgRate}_{\text{SV}}}{\text{baselineScenAvgRate}_{\text{ref}} - \text{policyScenAvgRate}_{\text{ref}}} \quad (\text{Equation E-2})$$

To calculate the extent to which disproportionate impacts may be exacerbated or mitigated under a temperature mitigation scenario, follow Equation E-3.

$$\text{Change in Disproportional Impacts for Each Group between a Baseline and Policy Scenario} = \frac{\text{baselineScenAvgRate}_{\text{SV}}}{\text{baselineScenAvgRate}_{\text{ref}}} - \frac{\text{policyScenAvgRate}_{\text{SV}}}{\text{policyScenAvgRate}_{\text{ref}}} \quad (\text{Equation E-3})$$

Example results from these types of analyses are shown in Figure 20 of the main documentation.

E.8 Comparison of FrEDI-SV to Underlying EPA (2021) SV Report

As noted in Section E.1, the FrEDI-SV module is based on methods and data developed for EPA's peer-reviewed Social Vulnerability Report.¹⁴² To ensure that the module produces results consistent with those in the SV Report, we show results here from the FrEDI-SV module, that has been run with similar inputs to those used in the SV Report.

The cross-consistency test presented here focuses on the Air Quality – Childhood Asthma sector results.

Table E-4 provides a comparison of one of the FrEDI-SV metrics, the total impacts in terms of cases of childhood asthma diagnoses, at two degrees of warming (as an example scenario). As shown in the table, the differences between FrEDI-SV results and those presented in the SV Report are 10% or less in most regions. These small differences are largely driven by two factors:

1. Warming arrival time. Impacts in The SV Report were reported for degrees of mean global warming, while FrEDI-SV calculates impacts based on mean CONUS warming. **Table E-4** includes a comparison between the number of new childhood asthma diagnoses per year from climate-driven changes in air quality, predicted at 2°C global warming (SV Report) and the best match of 2°C global to CONUS warming (FrEDI-SV). Differences in arrival time (i.e., year where 2°C is reached) between the global and CONUS projections cause minor discrepancies between the two impact estimates.
2. Changes in the distribution of sub-regional populations overtime. The SV Report used static population from the Bureau of the Census ACS, centered on 2016 at the spatial scale appropriate for each sector (county, tract, etc.). FrEDI-SV, however, uses user-supplied regional population projections and disaggregates them to the county level using ratios calculated from ICLUSv2 projections (to downscale to state from region and then to county from state). These county-level ratios change over time with the ICLUS projections. The county populations are then further disaggregated to the tract level using static current-day ratios calculated from the same ACS data used in the SV report (tract/county). This second set of ratios is static over time.

¹⁴² <https://www.epa.gov/cira/social-vulnerability-report>

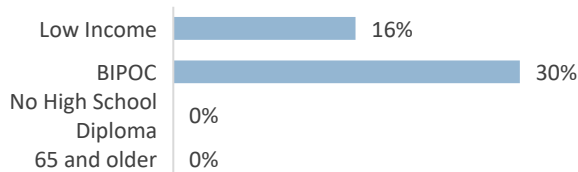
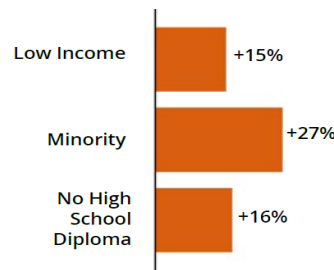
TABLE E-4. COMPARISON OF PROJECTED CHANGES IN ANNUAL CHILDHOOD ASTHMA DIAGNOSES DUE TO CLIMATE-DRIVEN EFFECTS ON PM2.5

Comparison of results from FrEDI-SV¹⁴³ (FrEDI-SV below) to those in EPA's SV report (SV Report – Table 3.3 on page 26), for 2°C of global warming (GMAT). Absolute differences between the estimates is also shown.

Region	Number of New Childhood Asthma Diagnoses Per Year		
	2 Degree FrEDI-SV	2 Degree SV Report	Difference
Midwest	-1,100	-1,100	0
Northeast	520	450	70
Northern Plains	-69	-75	6
Northwest	120	130	10
Southeast	1,900	2,000	100
Southern Plains	50	40	10
Southwest	1,000	1,000	0
National Total	2,500	2,500	0

All estimates rounded to two significant figures.

Figure E-3 shows the comparison of the *difference in risk* for those overburdened populations currently living in a location projected to experience large changes in climate-driven changes in air quality at two degrees warming, relative to their reference populations. The results show good but not exact replication, owing to the previously mentioned differences in county and tract level populations. Differences between the results for the No High School Diploma category highlight a difference in methodological choice rather than a replication error. In FrEDI-SV, because the calculations for this endpoint measure impacts on children, the 65 and Older and No High School diploma groups are omitted. In the SV Report, the 65 and Older category was omitted, but the No High School Diploma category result was reported and discussed as a potential indicator of household overburdened status.

FIGURE E-3. COMPARISON OF DIFFERENCE IN RISK FOR CHILDHOOD ASTHMA DIAGNOSES DUE TO CLIMATE-DRIVEN EFFECTS ON PM2.5
A. FREDI-SV

B. SV REPORT


Comparison of results from FrEDI-SV¹⁴⁴ to those in EPA's SV report (Figure 3.4 on page 27), for 2°C of global warming.

¹⁴³ The SV Module has not changed since FrEDIv3.4; these results are expected to hold in more recent versions.

¹⁴⁴ *Ibid*

These tests highlight the population-driven differences discussed above. However, additional offline tests of FrEDI with external population inputs do provide an exact replication with the SV Report values, therefore confirming that while FrEDI-SV module uses the same treatment of regional population projections as the main module, it is consistent with the effect and relative patterns/magnitudes between regions and across scenarios when comparing to the SV report.

E.9 Guidance on interpreting results

While there is a growing body of literature revealing the abundance of historical and current disproportionate impacts from climate-driven hazards, FrEDI-SV does not include these historical (baseline) disproportionate impacts. FrEDI estimates the impacts of climate change relative to a baseline. In that process, the historical (or baseline) impacts are effectively a starting point for incremental analysis and are controlled for in the projection results. The FrEDI-SV module also follows this approach, focusing on the disproportionality of climate change impacts relative to the baseline impacts. In doing so, the historical disproportionality of impacts has also been removed and is not the focus of the module. For example, it has been shown that low-income communities are more at risk of both riverine (inland) and coastal flooding (e.g., Wing et al. 2022¹⁴⁵). The impacts evaluated in FrEDI-SV for flood risk to homes (both inland and coastal) exclude these historical disproportionate impacts by subtraction, and instead focus on where flood risks are increasing or decreasing compared to historical risk, and by how much. While baseline conditions can have an impact on the vulnerability to changes in flood risk, (e.g., a home in the current floodplain is more vulnerable to increases in flood occurrence or magnitude than a home outside the floodplain), changes in climatic conditions drive the *direction* (positive or negative) as well as magnitude of future change in flood risk.

For this reason, we encourage users of FrEDI-SV to carefully examine the absolute risk results for the scenarios applied in the module, as well as the incremental changes in risk, at both the national and regional scale, to best understand the dynamics of how risks to specific populations change over time. Careful consideration of the full range of results from FrEDI-SV can enhance the interpretation of results for policy analysts and decision-makers as well as for external and public constituencies who may be key audiences for these analyses.

¹⁴⁵ Wing, O.E.J., Lehman, W., Bates, P.D. et al. Inequitable patterns of US flood risk in the Anthropocene. Nat. Clim. Chang. 12, 156–162 (2022). <https://doi.org/10.1038/s41558-021-01265-6>

APPENDIX F | CONCENTRATION-DRIVEN MODULE

This section describes the optional module within the FrEDI framework that allows users to assess additional impacts from changes in atmospheric GHG concentrations. This module will continue to be updated as new information becomes available. The current module calculates the changes in health impacts associated with changes in exposure to ozone that is produced from methane in the atmosphere.

F.1 Overview and Background

The purpose of this module is to integrate the underlying data and analytical approach from previously published peer-reviewed literature on the impacts associated with changes in atmospheric concentrations of GHGs into FrEDI. This module (hereafter referred to as the ‘concentration-driven module’ or ‘FrEDI-GHG’) is driven by changes in GHG concentrations, rather than by changes in temperature or sea-level rise. This approach complements main FrEDI damages and allows users to explore how additional GHG-related impacts will be distributed across the CONUS.¹⁴⁶ While the FrEDI-GHG methodology may be updated in the future to include additional GHG-related impacts as new information becomes available, this section describes the first concentration-driven impacts integrated into this module, which are the health-related damages associated with exposure to ozone (O_3) produced from changes in atmospheric methane.

Methane is an important pollutant because of its contribution to global warming and to the chemical formation of tropospheric O_3 , which has direct impacts on human health, agriculture, and ecosystems. FrEDI-GHG currently estimates health impacts associated with O_3 concentrations resulting from changes in methane concentrations (and methane emissions, either globally or in the U.S.).

Methane's 12-year lifetime is much longer than the hour-to-week lifetimes of most other O_3 precursors. Therefore, methane becomes relatively well-mixed in the atmosphere and O_3 production from methane's oxidation contributes to “background” levels of O_3 , rather than localized production. While localized O_3 production is an important consideration for regional air pollution mitigation policies, the U.S. EPA has long recognized that methane mitigation is a poor candidate for addressing local air quality problems. Since 1977, EPA has exempted methane from the definition of “volatile organic compound” on the grounds that methane has “negligible photochemical reactivity.” (40 CFR 51.100(s)(1), 2023)¹⁴⁷; “Recommended Policy on Control of Volatile Organic Compounds,” (42 Fed. Reg. 35314, 8 July 1977)¹⁴⁸. As a result, EPA does not regulate methane as part of its programs to implement the national ambient air quality standards for O_3 . The health effects of O_3 , however, are determined by total tropospheric concentrations, which are a combination of local/regional O_3 production and the global background. In contrast to localized O_3 , changes in background O_3 concentrations occur on time scales similar to methane's lifetime (e.g., ~12 years), are

¹⁴⁶ Results from FrEDI-GHG are also available for Alaska and Hawaii

¹⁴⁷ 40 CFR 51. 100 (s)(1). (2023). <https://www.ecfr.gov/current/title-40/chapter-I/subchapter-C/part-51/subpart-F/section-51.100>.

¹⁴⁸ 42 Fed. Reg. 35314. (1977). <https://www.govinfo.gov/content/pkg/FR-1977-07-08/pdf/FR-1977-07-08.pdf>.

relatively insensitive to specific locations where emission changes occur, and have been shown to respond linearly to changes in methane (e.g., West et al., (2006)¹⁴⁹). Therefore, this module has been developed to capture the effects of changing background O₃ concentrations resulting from changes in methane, which serves to complement the existing climate-driven impacts within the FrEDI package.

F.2 Approach

This section provides a summary of the methodology behind the FrEDI-GHG module.

The methane-O₃-health impacts within FrEDI-GHG currently include mortality and select morbidity endpoints associated with changes in O₃ exposure. As described in Section F.3, both the mortality and morbidity estimates in FrEDI-GHG rely on a reduced form damage function approach developed by McDuffie et al. (2023)¹⁵⁰, which relates changes in methane concentrations, O₃ production, population exposure, and health risks. For mortality, this function uses the O₃ respiratory-related mortality relative risk function from the Global Burden of Disease.¹⁵¹ For respiratory morbidity impacts, the reduced-form model is adapted to use health impact functions of new childhood asthma cases from Tetreault et al. (2016)¹⁵² and Emergency Department (ED) visits for all-ages from Mar and Koenig (2009).^{153,154} The resulting timeseries of health impacts can be (optionally) combined with results from FrEDI's climate-driven impact sectors. In the future, additional impacts can be added as new peer-reviewed information becomes available.

As input, FrEDI-GHG accepts population at the state level, U.S. GDP, a timeseries of changes in global methane concentrations (derived from changes in national or global methane emissions¹⁵⁵) relative to the baseline, and (optionally) a timeseries of changes in total NO_x emissions at the national level.¹⁵⁶ When run with these inputs, FrEDI-GHG outputs 1) annual state-level premature mortality, valued using the same Value of Statistical Life (VSL) approach used in the main climate-driven FrEDI sectors (see Section B.2 for

¹⁴⁹ West, J. J., Fiore, A. M., Horowitz, L. W., & Mauzerall, D. L. (2006). Global health benefits of mitigating ozone pollution with methane emission controls. *Proceedings of the National Academy of Sciences of the United States of America*, 103(11), 3988–3993. <https://doi.org/10.1073/pnas.0600201103>

¹⁵⁰ McDuffie, E. E., Sarofim, M. C., Raich, W., Jackson, M., Roman, H., Seltzer, K., Henderson, B. H., Shindell, D. T., Collins, M., Anderton, J., Barr, S., & Fann, N. (2023). The Social Cost of Ozone-Related Mortality Impacts From Methane Emissions. *Earth's Future*, 11(9), e2023EF003853. <https://doi.org/10.1029/2023EF003853>

¹⁵¹ Murray, C.J., Aravkin, A.Y., Zheng, P., Abbafati, C., Abbas, K.M., Abbasi-Kangevari, M., Abd-Allah, F., Abdelalim, A., Abdollahi, M., Abdollahpour, I. and Abegaz, K.H., 2020. Global burden of 87 risk factors in 204 countries and territories, 1990–2019: a systematic analysis for the Global Burden of Disease Study 2019. *The Lancet*, 396(10258), pp.1223-1249. [https://doi.org/10.1016/S0140-6736\(20\)30752-2](https://doi.org/10.1016/S0140-6736(20)30752-2)

¹⁵² Tetreault, et al., (2016) (see footnote 46)

¹⁵³ Mar, T.F., J.Q. Koenig. 2009. Relationship between visits to emergency departments for asthma and ozone exposure in greater Seattle, Washington. *Annals of Allergy, Asthma & Immunology*, Vol. 103(6):474-479.

¹⁵⁴ ED visits are modeled for two age groups: 0-17 and 18-99. In contrast to the Air Quality, Southwest Dust, and Wildfire sectors in main FrEDI, FrEDI-GHG includes hospitalization costs for ED visits for both children and adults and does not include impacts from lost-school days.

¹⁵⁵ When starting with emission changes, users can input these emission scenarios into a simple climate model, like FaIR, to derive trajectories of atmospheric methane concentrations (as described in Section 3 of the main documentation).

¹⁵⁶ Alternatively, users may provide a timeseries of changes in O₃ concentrations by state and year instead of changes in methane concentrations and NO_x emissions.

further details on the VSL), and 2) annual state-level childhood new asthma cases and ED visits, monetized using results from U.S. EPA's BenMAP, which estimates human health impacts and economic value of air quality changes in the atmosphere.

F.3 Module Details and Underlying Data

The FrEDI-GHG module relies on a number of underlying peer-reviewed studies and datasets. This section describes these data and the pre-processing used to adapt these studies for integration into FrEDI-GHG.

Methane-Ozone Health

The FrEDI-GHG module currently assesses the health impacts associated with changes in exposure to O₃ that is produced from atmospheric methane. As described in McDuffie et al. (2023), increases in atmospheric methane concentrations lead to higher levels of global background O₃ in the troposphere, and result in increased O₃ attributable respiratory-related health outcomes. The sensitivity of O₃ production to changes in methane varies geographically, and depends on local emissions of other O₃ precursors, as well as local and regional meteorological patterns. The susceptibility of a given population to increased O₃ exposure also depends on factors impacting mortality and morbidity rates, such as total population and age, while the economic valuation also depends on socioeconomic conditions and how these may change in the future. These impacts within FrEDI-GHG are calculated by adapting the reduced form damage function developed by McDuffie et al. (2023) (mortality) and applying the Tetreault et al. (2016) and Mar and Koenig (2009) health impact functions (morbidity) to the McDuffie et al. (2023) damage function.

IMPACT FUNCTION: METHANE OZONE MORTALITY

McDuffie et al. (2023) uses a series of previously published models and data to determine the relationships between methane concentrations, O₃ formation, population characteristics, and excess respiratory mortality at the national-level, for all world countries. Using this relationship, the authors developed a reduced form model that relates changes in methane concentrations to excess national-level mortality for a reference scenario. When provided with alternative inputs for methane concentrations, population, or GDP, the reduced form model can then be used to scale this reference case to estimate the new level of excess mortality in any custom scenario based on these new conditions.

For FrEDI-GHG, this reduced form model (see **Eq. F-1**) was modified to work at the state level¹⁵⁷, for consistency with FrEDI's other climate-driven impact sectors.

$$ExcessMort_{t,s,g} = ExcessMort_{0,s,g} \times MortRatio_{0,s} \times \frac{Pop_{t,s}}{Pop_{0,s}} \times \frac{RespMortRate_t \times MortRatio_{t,s}}{RespMortRate_0 \times MortRatio_{0,s}} \times \frac{\frac{\Delta O_3}{\Delta CH_4}_{s,g} \times CH_4Conc_t}{\frac{\Delta O_3}{\Delta CH_4}_{s,g} \times CH_4Conc_0} \times \frac{NO_xScalar_{t,g}}{NO_xScalar_{0,g}} \quad (Eq. F-1)$$

In Eq. F-1., *ExcessMort* (units = number of deaths) is the premature mortality from O₃ for each year (*t*), state (*s*), and GCM (*g*). *MortRatio* is the ratio of the state level background mortality rate to the national

¹⁵⁷ McDuffie et al. (2023) has global coverage but is limited to the U.S. in FrEDI-GHG, for alignment main FrEDI. The methodology could be extended to calculate impacts globally.

average background mortality rate in year (t) and state (s).¹⁵⁸ $RespMortRate$ is the background U.S. incidence of respiratory mortality each year (t). Pop is the total population each year (t) in each state (s). $\Delta O_3 / \Delta CH_4$ is the change in O_3 concentration per change in methane concentration for each state (s) and GCM (g), while $CH_4 Conc$ is the scenario-specific change in methane concentrations in year (t). The previous two terms are used to calculate the change in O_3 concentrations ($\Delta O_3 Conc_{t,s,g}$) in each year (t), state (s), and for each GCM (g) associated with a particular change in methane concentration. Lastly, $NO_x Scalar$ is the (optional) modifier on methane-produced O_3 due to national-scale NO_x emissions in each year (t) and GCM (g) (see more in Section F.4). In each term in Eq. F-1, the reference case is $t=0$.

To integrate the mortality function into FrEDI-GHG, pre-processing steps are used to first calculate the reference excess mortality ($ExcessMort_{0,s,g}$) using the same conditions and underlying datasets as used in McDuffie et al. (2023): a scenario with a defined pulse of methane (275 million metric tons, or about 100 ppbv, in the year 2020, tracked over the course of the methane perturbation) and global gridded O_3 response surfaces from five GCMs from the UNEP/CCAC global methane assessment¹⁵⁹ are used to estimate timeseries of changes in O_3 concentrations ($\Delta O_3 Conc_{0,s,g}$) for each state. Mortality is then calculated for these O_3 changes using U.S. EPA's BenMAP tool and national background respiratory mortality rates from the International Futures (IFP) project¹⁶⁰. Changes in mortality are then valued using the VSL.

IMPACT FUNCTION: METHANE OZONE MORBIDITY- NEW CASES OF CHILDHOOD ASTHMA
 FrEDI-GHG includes two morbidity endpoints: new cases of childhood asthma and all-age ED visits. The projections rely on health impact functions from external epidemiological studies, then follow the process of the reduced-form model from McDuffie et al. (2023) to determine morbidity impacts for relative changes in methane O_3 concentration throughout CONUS.

The reduced form model used in FrEDI-GHG for **new cases of childhood asthma** is as follows:

$$NewAsthma_{t,s,g} = NewAsthma_{0,s,g} \times \frac{Pop_{t,s} \times 017factor_{t,s}}{Pop017_{0,s}} \times \frac{\frac{\Delta O_3}{\Delta CH_4}_{s,g} \times CH_4 Conc_t}{\frac{\Delta O_3}{\Delta CH_4}_{s,g} \times CH_4 Conc_0} \times \frac{NO_x Scalar_{t,g}}{NO_x Scalar_{0,g}} \quad (\text{Eq. F-2})$$

In **Eq. F-2**, $NewAsthma$ (units = number of new cases) is the onset of new asthma cases from O_3 for each year (t), state (s), and GCM (g). Pop is the total population each year (t) in each state (s). $pop017$ is the total

¹⁵⁸ State rates are available in BenMAP through 2060 after which we hold the ratio of state to national rates constant at 2060 ratios. State specific mortality rates are not available for Alaska and Hawaii, therefore these states are assigned a ratio of 1 (i.e. assigned the national average mortality rate). This equation includes two offsetting MortRatio_{0,s}, however both are presented in the equation for clarity in the mechanics of the function.

¹⁵⁹ United Nations Environment Programme and Climate and Clean Air Coalition. (2021). *Global methane assessment: Benefits and costs of mitigating methane emissions*. United Nations Environment Programme.

<https://www.unep.org/resources/report/global-methane-assessment-benefits-and-costs-mitigating-methane-emissions>

¹⁶⁰ International Futures (IFs) modeling system. *International futures (IFs) modeling system Version 7.88*. Pardee Center for International Futures, Josef Korbel School of International Studies, University of Denver.
<https://korbel.du.edu/pardee/international-futures-platform/download-ifs>

population ages 0 to 17 in each year (t) and each state (s). The $017factor$ is the proportion of the total population that is in the 0 to 17 age group in each year (t) and in each state (s). The rest of the formula follows the same calculations as Eq. F-1. In each term in Eq. F-2, the reference case is again $t=0$.

To integrate new asthma cases into FrEDI-GHG, pre-processing steps are used to first calculate the reference new asthma cases ($NewAsthma_{0,s,g}$), using BenMAP and the health impact epidemiological function for this endpoint¹⁶¹, for the same methane scenario and conditions as that used in McDuffie et al. (2023) as described above. This calculation also requires adjusting BenMAP populations to reflect the RFF-SP population aged 0-17 and baseline new asthma cases (which are calculated as 1-% of population with asthma, from “National Incidence and Prevalence” 2021¹⁶², multiplied by the baseline rate of asthma incidence from Winer et al. 2012¹⁶³).

New childhood asthma cases are then valued using Appérée et al. (2024)¹⁶⁴, which estimates the mean value of a statistical case of childhood asthma using a marginal willingness to pay per year over a ten-year period. This value reflects the amount a parent is willing to pay to reduce the risk of their child developing a new case of chronic asthma. The mean value of a statistical case of asthma that we apply, is the U.S. specific recommended value of \$637,041 (in 2015\$), which is scaled with the change of GDP per capita relative to 2010, and a 0.06 income elasticity. This value is also used for childhood asthma cases described for the Climate-Driven Changes in Air Quality, Wildfire, and Southwest Dust sectors in Appendix B.2

IMPACT FUNCTION: METHANE OZONE MORBIDITY- CHILD AND ADULT ED VISITS

The reduced form model used in FrEDI-GHG for asthma-related **child and adult ED visits** is as follows:

$$AdultEDasthma_{t,s,g} = AdultEDasthma_{0,s,g} \times \frac{Pop_{t,s} \times 1899factor_{t,s}}{Pop1899_{0,s}} \times \frac{\frac{\Delta O_3}{\Delta CH_4}_{s,g} \times CH_4Conc_t}{\frac{\Delta O_3}{\Delta CH_4}_{s,g} \times CH_4Conc_0} \times \frac{NO_xScalar_{t,g}}{NO_xScalar_{0,g}} \quad (\text{Eq. F-3})$$

$$ChildEDasthma_{t,s,g} = ChildEDasthma_{0,s,g} \times \frac{Pop_{t,s} \times 017factor_{t,s}}{Pop017_{0,s}} \times \frac{\frac{\Delta O_3}{\Delta CH_4}_{s,g} \times CH_4Conc_t}{\frac{\Delta O_3}{\Delta CH_4}_{s,g} \times CH_4Conc_0} \times \frac{NO_xScalar_{t,g}}{NO_xScalar_{0,g}} \quad (\text{Eq. F-4})$$

Eq. F-3 and Eq. F-4 follow the same steps as Eq. F-2. In Eq. F-3, *ExcessAdultEDasthma* (units = number of Adult ED visits) is the visits to the ED by adults aged 18 to 99 for asthma-related causes. Following the same ideology as Eq. F-2, *Pop1899* is the population aged 18 to 99 in each year (t) and each state (s), and *1899factor* is the proportion of the total population that is in the 18 to 99 age group in each year (t) and in each state (s). *ExcessChildEDasthma* (units = number of Child ED visits) in Eq. F-4 is the visits to the ED by children aged 0 to 17 for asthma-related causes.

¹⁶¹ Tetreault et al. (2016) (see footnote 46)

¹⁶² Sacks et al. (2018) (see footnote 30)

¹⁶³ Winer, R. A., Qin, X., Harrington, T., Moorman, J., & Zahran, H. (2012). Asthma Incidence among Children and Adults: Findings from the Behavioral Risk Factor Surveillance System Asthma Call-back Survey—United States, 2006–2008. *Journal of Asthma*, 49(1), 16–22. <https://doi.org/10.3109/02770903.2011.637594>

¹⁶⁴ Appérée et al. (2024) (see footnote 21)

During the pre-processing steps, the reference adult and child ED visits ($AdultED_{asthma_{0,s,g}}$, $ChildED_{asthma_{0,s,g}}$) are calculated using BenMAP, health impact epidemiological function for this endpoint¹⁶⁵, and the same methane scenario and conditions as that used in McDuffie et al. (2023). This reference run relies on the RFF-SP populations broken down by relevant age group. Baseline incidence of ED visits (another necessary input to the health impact function) is derived from the BenMAP Dataset “Other Incidence” 2014,¹⁶⁶ which aggregates health care databases at the state-level to form the Healthcare Cost and Utilization Project (HCUP).¹⁶⁷ HCUP provides information on primary diagnosis, age, and categorization of hospital admission (ED, trauma, urgent care, newborn, etc.), which BenMAP calculates to county-level hospitalization counts by age and health endpoint.

ED visit valuation is averaged across two studies of the cost per ED visit due to asthma. Smith et al. (1997)¹⁶⁸ report the average cost per visit to the hospital for treating asthma, for the approximate 1.2 million asthma-related visits in 1987 to get a cost of \$533.69 (in 2015\$). Stanford et al. (1999)¹⁶⁹ builds on Smith et al. to consider costs or charges by the patient and/or third-party payer for asthma treatments in the ED. Both values are averaged for a value of \$490.11 (2015\$) per ED visit. The valuation used here is consistent with EPA (2023), as well as two other CIRA sector studies (Wildfire and Southwest Dust) which averaged the two values.¹⁷⁰ ED visit valuation is not scaled with GDP per capita or income elasticity. This valuation is also used in the Climate-Driven Changes in Air Quality sector in Appendix B.2.

Methane Ozone Health Underlying Datasets

Table F-1 summarizes the datasets underlying the methane-ozone health impact functions described in Eqs. F-1-4. These datasets are used in the pre-processing steps to derive the impacts in the reference scenario that is scaled to calculate projected impacts during runtime. Compared to the data used in McDuffie et al., (2023), the only adaptation made during pre-processing is the addition of the morbidity endpoints, and that BenMAP is re-run using state-level population data (vs. national population) to derive the reference excess values at the state-level, rather than at the national-level as was done in the original study.

TABLE F-1. DATASETS USED IN THE PRE-PROCESSING FOR THE METHANE-OZONE HEALTH IMPACTS

Dataset	Description	Source(s)	Used in Mortality Analysis	Used in Morbidity Analysis
UNEP/CCAC Global Methane Assessment	Ozone response ratios (e.g. change in O_3 per change in methane) at the half degree resolution, for five GCMs	UNEP/CCAC. (2021). (see footnote 159)	Y*	Y*
Global Burden of Disease (GBD) mortality relative risk coefficient for O_3 exposure	Relative risk coefficient of 1.06 for the log-linear health impact function relating to change in O_3 exposure and mortality	Murray et al. (2020). (see footnote 151)	Y*	

¹⁶⁵ Mar and Konig 2009 (see footnote 153)

¹⁶⁶ Sacks et al. (2018) (see footnote 30)

¹⁶⁷ HCUP provides information on primary diagnosis, age, and categorization of hospital admission (ED, trauma, urgent care, newborn, etc.) which BenMAP calculates to county-level hospitalization counts by age and health endpoint.

¹⁶⁸ Smith, et al. (1997) (see footnote 22)

¹⁶⁹ Stanford, et al. (1999) (see footnote 23)

¹⁷⁰ See footnote 24

Dataset	Description	Source(s)	Used in Mortality Analysis	Used in Morbidity Analysis
New childhood asthma relative risk coefficient for O ₃ exposure	Health impact function of children diagnosed with asthma (via discharged hospital visit or two physician claims for asthma within a 2-year period) considering annual O ₃ levels at their place of birth	Tetreault et al. (2016) (see footnote 46)		Y
Relative risk coefficient ED visits due to ozone concentrations	Health impact function of all-age ED visits for a 0 through 5-day lag due to changes in 1-hour and 8-hour maximum ambient air pollutant concentrations during warmer months from 1998 to 2002	Mar & Koenig (2009). (see footnote 153)		Y
Resources for the Future Socioeconomic Projections (RFF-SPs)	1,000 probabilistic projections of country-level populations and background all-cause mortality rates, 2020-2300, by age and sex	Rennert et al. (2022) (see footnote 183); Raftery, A. E., & Ševčikova, H. (2023). (see footnote 184)	Y*	
BenMAP all-cause mortality rates	County level mortality rates aggregated to the state level, 2020-2060 ¹⁷¹ .	Sacks et al. (2018) (see footnote 30)	Y	
International Futures Project (IFP) respiratory mortality ratio	All-cause and respiratory mortality projections by country, age, and year	<i>International futures (IFs) modeling system Version 7.88.</i> (see footnote 160)	Y*	
Baseline Incidence Rate of Asthma Cases	Annual rate of new asthma diagnosis by age bin	Winer et al. (2012) (see footnote 163)		Y**
BenMAP prevalence of asthma	Asthma prevalence rates by year and age bin; Calculate the population at risk of receiving a new asthma case to apply to Winer et al. 2012 formula by calculating input population * (1-% of population with asthma).	Sacks et al. (2018) (see footnote 30)		Y**
BenMAP baseline annual ED Visits	County-level ED visit counts by age and health endpoint using a collection of health care databases developed through the Federal-State-Industry partnership HCUP.	Sacks et al. (2018) (see footnote 30)		Y**
Gridded Population of the World (GPW) population distribution	Population distribution at the half degree resolution	<i>Gridded population of the world, version 4 (GPWv4)</i> ¹⁷²	Y*	Y*

*Dataset also used in McDuffie et al. (2023).
 **Dataset used in the underlying reference case run however because projected values are not available, the ratio term would cancel out in the reduced form function (i.e., reference case values = projection values) and it is therefore omitted.

¹⁷² Center for International Earth Science Information Network - CIESIN - Columbia University. (2018). *Gridded population of the world, version 4 (GPWv4): Population count, revision 11, Palisades*. NASA Socioeconomic Data and Applications Center (SEDAC). <https://doi.org/10.7927/H4JW8BX5>

Methane Ozone Health - Additional Function Details

NO_x ADJUSTMENT FUNCTION

As described in McDuffie et al., (2023), the efficiency of O₃ production from methane ($\frac{\Delta O_3}{\Delta CH_4}_{S,g}$ in Eqs. F-1-4)

is sensitive to (or modified by) the presence of other O₃ precursors, such as nitrogen oxides (NO_x), CO, or volatile organic compounds (VOCs). GCM simulations conducted by the UNEP/CCAC Methane Assessment Report (which formed the basis of the McDuffie et al. (2023) results) previously showed that the O₃ response efficiency was more sensitive to changes in NO_x emissions than to changes in VOCs or CO. The study also derived a NO_x-specific modification factor, shown in Eq. F-5, which defines a logarithmic relationship between NO_x emissions and changes to the O₃ response. The slope and intercept values reported in the UNEP/CCAC report are specified by country and GCM.¹⁷³

$$NO_xScalar_{t,g} = \frac{\Delta O_3 (pptv)}{CH_4 (ppbv)} = \frac{1000(\text{slope} \times \ln(NO_x) + \text{intercept})}{556} \quad (\text{Eq. F-5})$$

This relationship shows that as NO_x emissions are reduced, O₃ production will become more NO_x limited (or VOC saturated) and methane will have a smaller impact on O₃ production. Therefore, the final term in Eq. F-1 can be used to modify the amount of methane-O₃ production in each state by a ratio of the change in the level of U.S. NO_x emissions relative to the emission levels in the original UNEP/CCAC simulations.

In FrEDI-GHG, users can provide a timeseries of annual NO_x emissions (in Megatonnes/year) which, through Eq. F-5, is converted to an annual O₃ production response factor per ppbv of methane (referred to as $NO_xScalar_{t,g}$ in Eq. F-1). As shown in Eq. F-1, the ratio of this user-defined scenario response factor compared to the response factor for the reference scenario (which assumes annual NO_x emissions of 10.53Mt/year in the US, following the UNEP/CCAC scenario), is used to modify the amount of O₃ produced per change in methane in each state. If the user does not provide a NO_x emissions trajectory, the module assumes that NO_x levels stay constant at the UNEP/CCAC reference level, creating a NO_x ratio of one, or no adjustment to the methane-O₃ response ratios. Incorporation of this modification allows users to adjust the amount of anticipated O₃ health effects based on anticipated changes in NO_x emissions.¹⁷⁴

F.4 Running FrEDI-GHG

The FrEDI-GHG module is run within the FrEDI R package (<https://github.com/USEPA/FrEDI>).

Inputs

To calculate the methane-ozone-health impacts for a user-defined scenario, FrEDI-GHG requires user input a timeseries of changes in methane concentration, relative to a 1986 to 2005 baseline, and also accepts as

¹⁷³ FrEDI-GHG currently uses a single value for the U.S., averaged across all 5 GCMs in the underlying study (slope = -1.12 and intercept = -0.49), though GCM-specific values are available and could be added in future revisions.

¹⁷⁴ This modification is currently limited to using national-level slope and intercept values from the UNEP/CCAC assessment; the sensitivity of ozone production will vary spatially based on local abundances of both NOx and other ozone precursors.

optional inputs national GDP, state or U.S.-level population, and national NO_x emissions.¹⁷⁵ Detailed specifications for these inputs are as follows:

- **Primary inputs:**

- **Change in Methane Concentration.** Timeseries of changes in global methane concentrations relative to the 1986 to 2005 baseline. Methane concentrations (which are likely coming from a reduced complexity climate model that converts U.S. or global methane emissions into global concentrations), should be input in parts per billion by volume (ppbv). FrEDI-GHG accepts values from 2010-2300.¹⁷⁶ The user can input any intervals of data, and the model will interpolate to the annual level, as needed. If methane concentrations are not provided, the module includes default methane concentrations representing an SSP245 scenario.^{177,178}
- **NO_x Emissions (Optional).** Timeseries of absolute total U.S. NO_x emissions, in megatons (or million metric tonnes) per year (Mt/year). As with methane concentrations, the module interpolates and extrapolates from any provided datapoints. If NO_x emissions are not provided, the module assumes constant NO_x emissions level matching the reference run (10.53 Mt/year).
- **GDP and Population (Optional).** As is the case in main FrEDI, users can input national GDP and/or state or U.S.-level populations. See Section 2.4 of the main Technical Documentation for discussion of FrEDI's default GDP and population projections.

- **Alternative inputs:**

- **Change in Ozone Concentration.** If the user has data on O₃ concentration by state from an analysis external to the module, the user may directly provide changes in O₃ concentrations in parts per billion by volume (ppbv) relative to a 1986 to 2005. To avoid potential double counting of O₃ mortality between this module and the Air Quality sector in main FrEDI, all direct changes in ozone concentration inputs should only reflect the influence of methane concentration on background O₃ formation and exclude any impacts of temperature or other precursor changes on O₃ formation. User-input changes in O₃ concentrations supersede any user-supplied values for methane concentrations and NO_x emissions. Because user-inputs are not expected to align with the GCMs used in the underlying analysis, excess mortality (*ExcessMort_{O₃,g}*) is averaged across GCMs for custom O₃ inputs.

¹⁷⁵ If the user does not provide the optional inputs, the module uses the FrEDI default population and GDP scenarios and the reference case NO_x emissions (resulting in no adjustment based on NO_x emissions in the scenario run).

¹⁷⁶ FrEDI-GHG runs through 2100 by default, but includes an option for users to select any end year through 2300.

¹⁷⁷ Default methane concentrations are not currently consistent with the default temperature scenario in main FrEDI. The user should supply a consistent set of climate and GHG scenario inputs if combining main FrEDI and FrEDI-GHG results.

¹⁷⁸ Zebedee Nicholls, & Jared Lewis. (2021). Reduced Complexity Model Intercomparison Project (RCMIP) protocol (v5.1.0) [Data set]. Zenodo. <https://doi.org/10.5281/zenodo.4589756>

Runtime Processes

OVERVIEW

When FrEDI-GHG is run, user inputs will first be applied to Eqs. F-1-4. There are several supporting variables in these equations that depend on specific user inputs, and are therefore calculated during runtime. These variables are described in **Table F-2**. These variables, along with Eqs. F-1-4, are then used to calculate the excess premature respiratory-related mortality, new cases of childhood asthma, and number of adult and child asthma-related ED visits for each GCM, year, and state associated with the input methane and (optional) socioeconomic conditions.

TABLE F-2. FREDI-GHG: METHANE OZONE HEALTH INPUT SUMMARY

Variable	Reference Case (t=0)	Scenario Run (t)	Mortality Analysis	Morbidity Analysis
Population ($Pop_{t,s}$)	Population from the RFF-SP mean scenario in 2020, distributed to states using the GPW gridded population map.	User input total population at the state or national level. If the user provides a national level population (including Alaska and Hawaii), FrEDI allocates population to states based on the proportion of population by state in ICLUSv2 population, the FrEDI default scenario, in each year.	Y	Y
Background incidence of respiratory mortality ($RespMortRate_t$)	All-cause mortality rate from the RFF-SP mean scenario in 2020, multiplied by the percent of deaths related to respiratory conditions from IPF , by age, at the country level by year.	No user input required. Background all-cause mortality rates are calculated at runtime (see details below)	Y	
Adjustment for state level background mortality rates ($MortRatio_{t,s}$)	All-cause mortality rate from BenMAP in 2020, aggregated to the state level and applied to the <i>RespMortRate</i> to adjust national-level background mortality to state level.	All-cause mortality rate from BenMAP by year, aggregated to the state level and applied to the <i>RespMortRate</i> to adjust national-level background mortality to state level. Values available from BenMAP for 2020 to 2060, and held at 2060 levels for all later years.	Y	
Population factors ($017factor$, $1899factor$)	Proportion of the population in either the 0 to 17 or 18 to 99 year old age group of the total population in 2020 at t=0.	Proportion of the population in either the 0 to 17 or 18 to 99 age group of the total population in each year of the projection to account for demographic composition over the course of the century and held constant at 2100 for any future levels.		Y
Change in ozone concentrations per change in methane	GCM-specific ozone response ratios at the half degree horizontal resolution from the UN/CCAC Global Methane Assessment. Results at half degree grid cell in BenMAP are converted to state level for FrEDI using an area-weighted	No user input required. Scenario runs use the same O_3 response ratios (e.g., O_3/CH_4) as the reference case, unless modified by changes in NO_x emissions (see above)	Y	

Variable	Reference Case (t=0)	Scenario Run (t)	Mortality Analysis	Morbidity Analysis
concentration ($\Delta O_3 / \Delta CH_{4s,g}$)	average. O_3 concentrations are measured as the maximum daily summertime 8-hour average exposure (MDA8).			
Change in methane concentration ($CH_4 Conc_t$)	Methane concentration resulting from the McDuffie et al. (2023) methane pulse (275 million metric tons, or about 100 ppbv) in 2020.	User input timeseries of changes in methane concentration at the CONUS level relative to a 1986 to 2005 baseline average, in parts per billion by volume (ppbv). ¹⁷⁹	Y	
NO _x emissions influence on ozone formation ($NOxScalar_{t,g}$)	Total U.S. baseline NO _x emissions (10.5 million metric) entered in the country-specific NO _x function from the UN/CCAC Global Methane Assessment (see details below).	User input NO _x emissions (mt/year) entered in the country-specific NO _x function from the UN/CCAC Global Methane Assessment (see details below). ¹⁸⁰	Y	

Lastly, the calculated annual timeseries of physical health impacts are monetized to project total annual impacts in \$2015 USD by impact type, year, state, and GCM¹⁸¹. Premature mortality is monetized using the VSL, new asthma cases are monetized using the value of a statistical case, and asthma-related ED visits are monetized using hospitalization costs.

ADDITIONAL DETAILS - AUTOMATIC CALCULATION OF BACKGROUND MORTALITY RATES

As shown in Eq. F-1, to project future excess respiratory-related mortality rates for a custom scenario ($ExcessMort_{s,g,t}$), the reduced form model also requires additional information on the background respiratory mortality rates in the U.S. and how these are expected to change over time ($RespMortRate_t$). Background mortality rate projections are not always readily available to accompany specific population projection data. Therefore, to ease the burden on the user, instead of requiring users to input background respiratory mortality rates that correspond to the input population scenarios, FrEDI-GHG calculates (during runtime) the associated background respiratory mortality rates in each year associated with the user input population trajectory. This approach is a departure from the original study modeled in McDuffie et al. (2023) in which background respiratory mortality rates were calculated for each specific population scenario assessed in that study.

In FrEDI-GHG, to relate U.S. population to respiratory mortality rates we first use relationships between population and all-cause mortality rates derived from the 10,000 probabilistic scenarios in RFF-SP

¹⁷⁹ Alternatively, users can directly input a change in O_3 concentrations from methane emissions calculated outside of the module. User-provided changes in O_3 concentrations are provided per state-GCM-year combination and should reflect changes relative to the 1986 to 2005 baseline era.

¹⁸⁰ If the user inputs changes in O_3 concentrations instead of changes in methane concentrations, the module will not accept a NO_x emission input.

¹⁸¹ As is the case in the main FrEDI function, the income elasticity used to calculate VSL over the timeframe of the analysis is set at a default value of 1, though the user can set any custom value.

dataset.¹⁸² As described previously in Rennert et al., 2021¹⁸³, the RFF-SP population projections are defined by the UN projections from 2020-2100¹⁸⁴, extended to 2300 based on input from a panel of expert reviewers. In this dataset, population is a function of fertility rates, all-cause mortality rates, and net migration, where the former two components are a function of the population age structure (mortality is projected based on life expectancy at birth).

In a pre-processing step, we derive a log-linear relationship between the probabilistic population estimates and all-cause mortality rates in the U.S. in each of the RFF-SP population projections for each year through 2300.¹⁸⁵ By defining the change in relationship each year, we capture changing age distributions over time, which is particularly important in the mid- to late-21st century, as shown in **Figure F-1**, during which a shift in population age structure results in shifts in all-cause mortality rates. **Figure F-2** shows the fit of the log-linear function in select decades spanning the analysis timeframe¹⁸⁶, which are stored in FrEDI-GHG and used during runtime to calculate the background all-cause mortality rates associated with the user-defined input population scenario. As shown in Figure F-2, population in each year are inversely correlated with mortality rate as increases in all-cause mortality rates drive decreases in total population. All-cause mortality rates are converted to respiratory mortality rates using the IFP respiratory mortality ratio (described in Table F-1). Lastly, national background respiratory mortality rates are adjusted to the state level by applying a ratio of the state-level background all-cause mortality rate to the national all-cause mortality rate using BenMAP data (described in Table F-1). While there are uncertainties introduced in this mortality estimation approach, this methodology reproduces the results from the original McDuffie et al. (2023) reference scenarios to within 5% and serves to minimize the inputs required by the user.

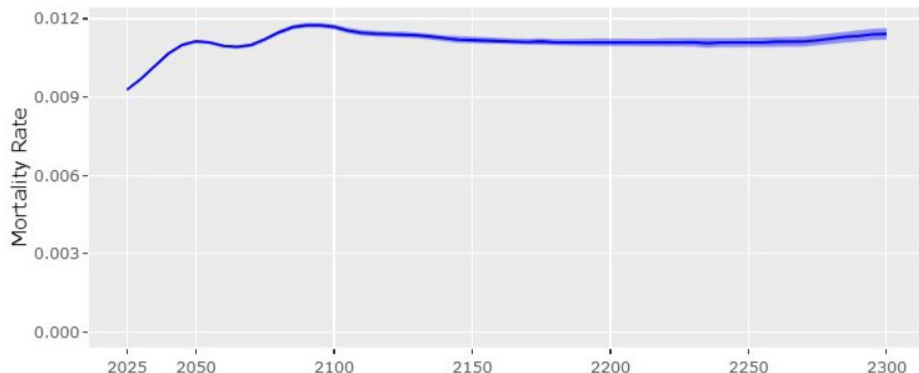
¹⁸² Rennert, K., Prest, B. C., Pizer, W., Newell, R. G., Anthoff, D., Kingdon, C., et al. (2022). Resources for the Future Socioeconomic Projections (RFF-SPs) (Version 5) [Data set]. Zenodo. <https://doi.org/10.5281/zenodo.6016583>

¹⁸³ Rennert, K., Prest, B.C., Pizer, W.P., Newell, R.G., Anthoff, D., Kingdon, C., Rennels, L., Cooke, R., Raftery, A.E., Ševčíková, H., & Erickson, F. (2021). The social cost of carbon: Advances in long-term probabilistic projections of population, GDP, emissions, and discount rates. Resources for the Future Working Paper 21-28.

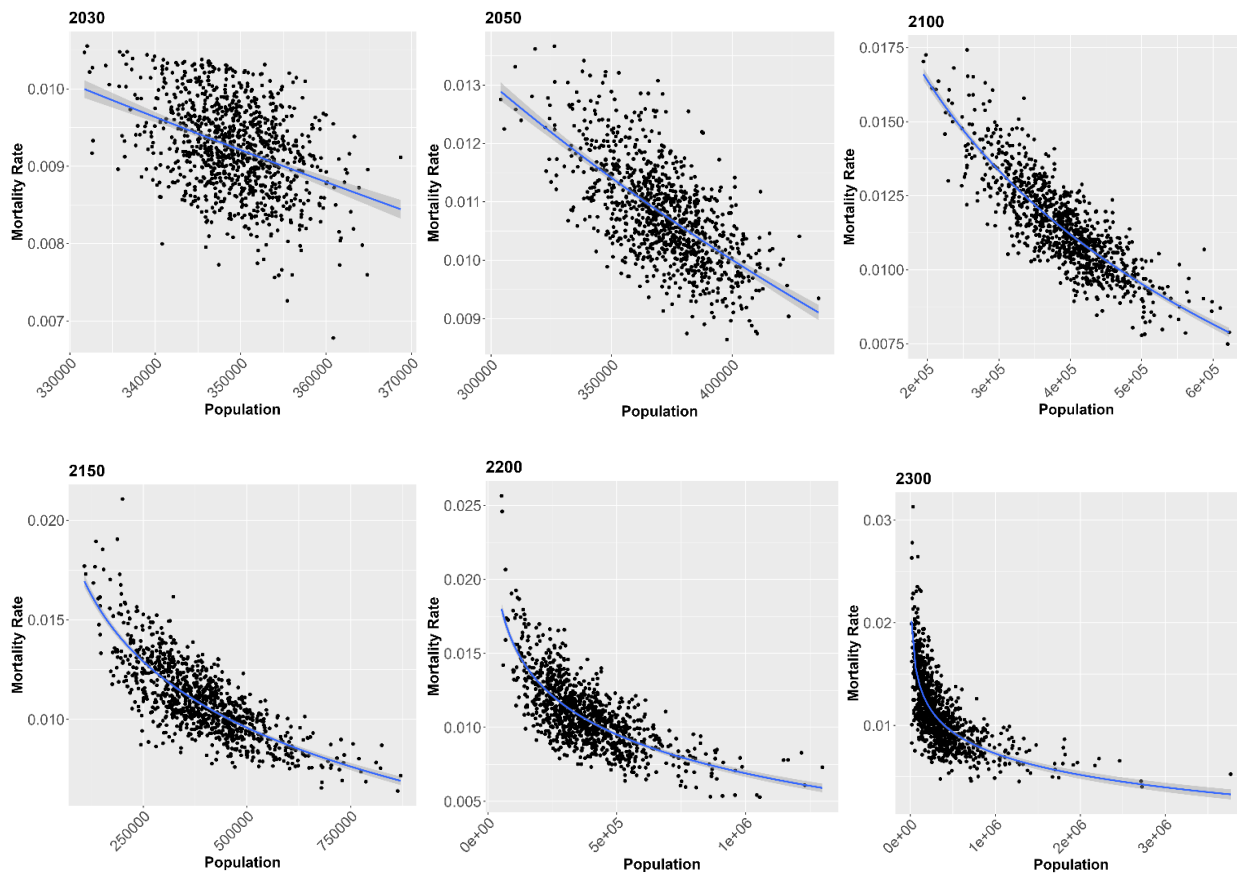
¹⁸⁴ Raftery, A. E., & Ševčíkova, H. (2023). Probabilistic population forecasting: Short to very long-term. *International Journal of Forecasting*, 39(1), 73–97. <https://doi.org/10.1016/j.ijforecast.2021.09.001>

¹⁸⁵ We use the defined log-linear relationship for 2021 (the first year in the dataset with 1,000 probabilistic projections) to estimate the underlying all-cause mortality rates for all years prior to 2021 in the module. The RFF-SP projections are provided for every five years; the coefficients in the log-linear relationship are interpolated for intervening years.

¹⁸⁶ The fit improves over time as other drivers of population size, such as variation in migration or birth rate, converge to assumed rates. Over time, the projected all-cause mortality rate most closely defines the projected population size.

FIGURE F-1. ALL-CAUSE MORTALITY RATE BY YEAR FOR THE RFF-SP MEAN SCENARIO

All cause mortality rate (deaths per 100,000 people) by year in the U.S. across the RFF-SP scenarios, through 2300. The RFF-SPs include 1,000 probabilistic scenarios of future socioeconomic inputs. The mean scenario (dark blue line) is surrounded by the 95th percent confidence interval.

FIGURE F-2. ALL-CAUSE MORTALITY RATE AND POPULATION BY YEAR FOR SELECT DECADES

All-cause mortality rate (deaths per 100,000 people) as correlated with population estimates in the U.S. across the RFF-SP scenarios for select years. Each data point represents a single scenario. The blue line represents the log-linear best fit used to calculate all-cause mortality rates with FrEDI for a user input population in the given year. All-cause mortality rates are converted to respiratory mortality rates for use in Eq. F-1 using the IFP respiratory mortality ratios (described in Table F-1).

F.4 Limitations and Uncertainty

This module provides an efficient means to calculate the additional impacts associated with changes in GHG concentrations. There are, however, several limitations and uncertainties to consider given the reduced form nature of the module.

- Ozone formulation is influenced by other atmospheric conditions beyond methane concentrations and national-level NO_x emissions, which are not accounted for in this module, including other O₃ precursors and more detailed temporal and spatial differences in O₃ production chemistry and emission sources.
- There is uncertainty in the estimation of background respiratory mortality from a user-input population. As shown in Figure F-2, there is substantial variation in mortality for a given national population, even within each year. The employed method of calculating mortality rates does not account for the specific demographics (e.g. age structure) in the user input population scenario.
- Several key inputs in the analysis are defined at the country level (e.g. respiratory mortality as a proportion of all-cause mortality rates, NO_x adjustment function coefficients) which will not capture variation across states in FrEDI beyond the extent to which it is reflected in current state- and county-level spatial O₃ patterns used to calibrate the methane-O₃-mortality effect. Where possible, state level data has been incorporated (for example, the state-level mortality ratios to scale national average mortality rates to state level rates).
- The morbidity analyses do not incorporate changes in baseline rates (i.e. changes in rates of ED visits or childhood asthma incidence) over time due to non-methane related O₃ formation causes. Data from the CDC on rates of childhood asthma prevalence from 2001 to 2021¹⁸⁷ shows relatively constant rates (7.7 percent in 2001 and 2021, with a range of 7.0 to 8.5 percent), suggesting this omission is likely have a limited effect on the results.
- For additional limitations impacts, see the Air Quality sector in Appendix B.2.
- For more limitations on the underlying reduced form model, see McDuffie et al. (2023).

F.5 Comparison of FrEDI-GHG to Underlying Studies

To ensure that the FrEDI-GHG module produces mortality results consistent with those in McDuffie et al. (2023), we ran the FrEDI-GHG module with similar inputs to those used in the McDuffie et al. (2023) study. This section provides a comparison of the results.

McDuffie et al. (2023) estimate premature mortality globally, by country, associated with a 275 million metric ton (or ~100 ppbv) methane emissions pulse in the year 2020. This estimation uses the atmospheric perturbation lifetime of methane of 11.8 years from the IPCC AR6 (Szopa et al., 2021)¹⁸⁸ and the methane

¹⁸⁷ <https://www.cdc.gov/asthma/nhis/default.htm>

¹⁸⁸ Szopa, S., Naik, V. S., Adhikary, B., Artaxo, P., Bernsten, T., Collins, W. D., et al. (2021). Short-lived climate forcers.

In *Climate change 2021: The physical science basis. Contribution of working Group I to the sixth assessment report of the intergovernmental panel on climate change.* (pp. 817–922). Cambridge University Press. <https://doi.org/10.1017/9781009157896.008>

mass to mixing ratio (Tg/ppbv) conversation factor from Prather et al. (2012)¹⁸⁹ to develop a timeseries of methane concentrations associated with this 2020 pulse. The central McDuffie et al. (2023) results use the baseline NO_x concentrations (i.e. no NO_x adjustment factor) and GDP, population, and baseline mortality inputs from the mean RFF-SP scenario. We run FrEDI with the same timeseries of methane concentrations, no NO_x factor, and mean RFF-SP socioeconomic inputs, except for baseline mortality rates, which are calculated within FrEDI-GHG during runtime.

McDuffie et al. (2023) authors shared annual results of total deaths, specifically in the U.S., for purposes of this comparison. **Table F-3** presents the results of this comparison for the 5-GCM average. Across all years, differences are less than 6%, with a difference of less than 2% in most of the years tested.¹⁹⁰ Table F-3 presents the GCM average, however the results are relatively consistent across individual GCMs (the maximum percent difference across individual GCMs is 6.0% in 2020 for GFDL-CM3). The replication results do not show a clear directional bias in the FrEDI-GHG estimates and generally reproduce the original results within an acceptable threshold of differences.

TABLE F-3. FREDI-GHG REPLICATION OF MCDUFFIE ET AL. (2023)

Comparison of attributable U.S. death estimates from McDuffie et al. (2023) and FrEDI-GHG when run with the same input parameters (methane concentration, NO_x emissions, GDP, and population). Results are presented for the 5-GCM average.

	2020	2025	2030	2035	2040	2050	2060	2070	2080	2090	2100
ΔMethane (ppbv)	100	65.46	42.85	28.05	18.36	7.87	3.37	1.44	0.62	0.27	0.11
Attributable Deaths (U.S., annual, GCM average)											
McDuffie et al. (2023) ^a	503.1	372.0	272.9	198.3	141.3	66.4	29.8	13.8	6.5	3.0	1.3
FrEDI-GHG	530.7	361.3	265.9	193.9	138.8	66.9	29.6	13.7	6.4	3.0	1.3
Differences (FrEDI-GHG minus McDuffie et al. (2023))											
Difference in Deaths (#)	27.5	-10.8	-7.1	-4.4	-2.5	0.4	-0.2	-0.2	-0.1	0.1	0.0
Difference in Deaths (%)	5.5%	-2.9%	-2.6%	-2.2%	-1.7%	0.7%	0.8%	1.1%	1.5%	1.8%	-2.8%
a. The published paper only reports global results, but U.S. results were provided by the McDuffie et al. (2023) authors for purposes of this comparison.											

The morbidity outcomes from FrEDI-GHG do not have an analogous set of published results calculating impacts for a particular methane emissions scenario to compare to. As an alternative, we validated the results by comparing to results from the Children's Health Report (EPA, 2023), which published projected child ED visits from O₃ concentration changes due to increased temperatures. While this is an inexact comparison due to differences in populations and O₃ measures, standardizing ED visits by population and O₃ concentration (i.e., incidence per child per change in O₃ [ppbv]) yields a less than 10% difference in the

¹⁸⁹ Prather, M. J., Holmes, C. D., & Hsu, J. (2012). Reactive greenhouse gas scenarios: Systematic exploration of uncertainties and the role of atmospheric chemistry. *Geophysical Research Letters*, *39*(9), L09803. <https://doi.org/10.1029/2012GL051440>

¹⁹⁰ Small variations are expected due to the use of state level background mortality rates in the FrEDI run (where the methods have been adapted for state level results) versus the national level background mortality rates in the McDuffie et al. (2023) run (where the results were calculated at the national level, globally).

results.¹⁹¹ This comparison shows an acceptable threshold of differences and provides confidence in the method applied to calculate the morbidity endpoints for methane-ozone.

F.5 Guidance on Interpreting Results

FrEDI-GHG currently assesses the respiratory-related mortality and morbidity effects of methane-induced changes in O₃ concentration. When calculated using a consistent set of inputs, users can directly aggregate these annual concentration-driven results (both physical and economic impacts) with the climate-driven impacts derived from main FrEDI. In this case, users should consider using FaIR or a similar reduced complexity climate model to calculate both the temperature and methane concentration changes from the same emission trajectory.

Although main FrEDI includes a ‘Climate-Driven Changes in Air Quality’ sector, which specifically measures impacts associated with O₃ concentrations, results from the main FrEDI function and from FrEDI-GHG are additive. The Air Quality sector in main FrEDI accounts for the influence of increased temperatures on O₃ concentrations, not the additional impact from changes in methane, as is measured in this module. However, there is still the potential for synergistic effects between methane concentration changes, temperature changes, and O₃ that are not captured here: e.g., changes in climate will change the relationship between methane and O₃, and changes in background methane concentrations will change the relationship between temperature and O₃. See Section 3 in the Main Technical Documentation for an example where impacts are aggregated across multiple FrEDI modules.

Streamlined Policy Benefits Calculation

As described in Section 3, the impacts of a specific GHG emissions policy can be calculated in FrEDI-GHG by comparing the impacts from a reference scenario to a policy scenario and calculating the difference. Because the impact function used in FrEDI-GHG is linear, users can either follow the same process (which may have advantages when the methane module is run in conjunction with main FrEDI), or users can directly enter the differences in methane concentrations (or O₃ concentrations) between the two scenarios as the inputs to this module calculate the impacts in a single run. The streamlined process assumes that all other inputs (i.e., NO_x concentrations, population, and GDP) remain constant between the two scenarios.

¹⁹¹ Scaling results per capita controls for first-order population differences; however, differences in the age bin composition within the 0 to 17 year-old population results in different background ED visit rates between the two analyses.

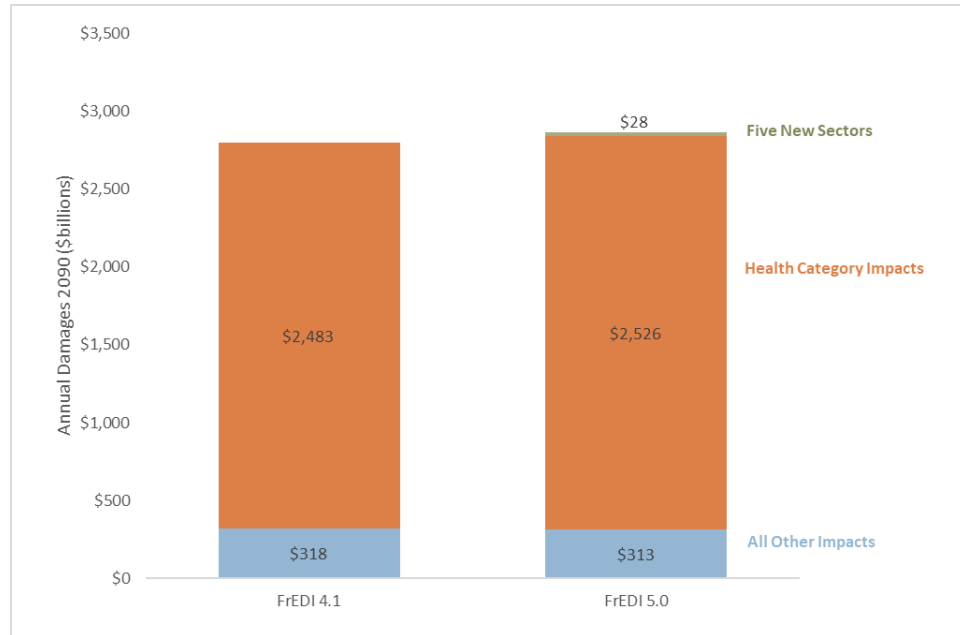
APPENDIX G | UPDATE REVISION LOG

This revision log provides a list of changes made to the documentation since publication of the FrEDI Technical Documentation (EPA 430-R-24-001).

TABLE G-1. FREDI DOCUMENTATION REVISION LOG

Revision Date	Location of Revision in Documentation	Brief Description of Change and Rationale
2025	Section 2, Section 3, Appendix B	Added five new sectors: Lyme Disease, Outdoor Recreation, Marsh Migration, Learning Loss, and Forestry Loss. See Figure G-1 for net added damages in 'Five New Sectors' and reduction in 'All Other Impacts' as the Winter Recreation sector is no longer considered a primary sector (now replaced by new sector Outdoor Recreation).
	Section 2, Section 3, Appendix B	Added new childhood asthma morbidity endpoints to Climate-driven Changes in Air Quality, Southwest Dust, and Wildfire (see change in value for 'Health Category Impacts' in Figure G-1).
	Section 2, Section 3, Appendix F	Added discussion and results of the peer-reviewed FrEDI-GHG module
	Appendix C	Discussion of CMIP6 models

FIGURE E-1. COMPARISON OF 2090 ANNUAL DAMAGES FOR GCAM REFERENCE SCENARIO (\$BILLIONS)



Annual damages in 2090 by FrEDI version, for temperature changes from the GCAM reference scenario (ESC3) with FrEDI default GDP and populations. Damages here reflect the default climate-related damages currently included within FrEDI and include the post-processing step of subtracting the value of mortality from Suicide from the Temperature Mortality results. This does not provide a comprehensive accounting of all climate-related damages to the U.S. This figure will be updated with comparisons to the current version as new code versions are released.